Available online at www.sciencedirect.com
ScienceDirect
Coordination Chemistry Reviews 252 (2008) 1871–1995
COORDINATION CHEMISTRY REVIEWS
www.elsevier.com/locate/ccr

Review

Advances in acyclic compartmental ligands and related complexes

P.A. Vigato, S. Tamburini *

Istituto di Chimica Inorganica e delle Superfici, CNR, Area della Ricerca, C.so Stati Uniti 4, 35127 Padova, Italy

Received 20 March 2007; accepted 29 October 2007
Available online 4 November 2007

Contents

Abstract

Symmetric and asymmetric compartmental acyclic Schiff bases and their reduced polyamine analogues have been considered; they have been classified according to their synthetic procedures, i.e. the condensation ratio between the formyl (or keto) and amine precursors, as [1 + 1] acyclic, [1 + 1] asymmetric end-off, [1 + 2] or [2 + 1] symmetric end-off, [2 + 1] or [1 + 2] side-off asymmetric and [3 + 1] or [1 + 3] systems. Their preparation has been reviewed, together with the physico-chemical and structural properties arising from the different synthetic reactions. The influence of their symmetric or asymmetric nature, their planar or three-dimensional structure on the possibility to obtain the same or different recognition processes at the two adjacent chambers were evaluated. The magneto-structural correlations of the homo- and hetero-dinuclear or -polynuclear complexes, together with the photochemical and photophysical properties resulting from these specific recognition processes, were also considered. The use of specific linkers, capable of forming oligomeric or polymeric complexes or unusual structures (as helicates) with the consequent modification of their properties (especially the magnetic interaction between the metal ions), is also reported. The design and diversification of the two adjacent sites, aimed at enhancing the ability of these ligands to act as selective transfers of specific cations, anions or salts across liquid membranes is considered and the results obtained are adequately discussed. Finally, the specific reactivity and catalytic properties of these systems are discussed.

Keywords: Compartmental ligands; Symmetric acyclic ligands; Asymmetric acyclic ligands; Schiff bases; Dinuclear complexes; Polynuclear complexes

1. Introduction

Many variously shaped polydentate chelating ligands has been prepared in the past and successfully used in the selective coordination of metal ions. The properties arising from this aggregation were investigated in detail by different physico-chemical procedures and adequately reviewed [1–18].

These systems were acyclic or cyclic in nature, planar or tridimensional in their framework, this depending on the designed structure (discrete, ordered, porous, helicoidal, 1D, 2D or 3D polymeric, etc.) to which they give rise, the specific functions they must perform or the peculiar properties they must achieve.

* Corresponding author. Tel.: +390498295963; fax: +390498702911.
E-mail address: tamburini@icis.cnr.it (S. Tamburini).

0010-8545/$ – see front matter © 2007 Elsevier B.V. All rights reserved.
doi:10.1016/j.ccr.2007.10.030

Compartmental ligands, i.e. compounds with two (or more) coordination chambers in close proximity, represented a relevant evolution, owing to their capability of providing different, well selective recognition of charged and/or neutral species at their adjacent chambers. These systems quite often are Schiff bases (or the related reduced derivatives), obtained by condensation of appropriately designed and prepared formyl- (or keto-) and primary amine precursors. The synthesis and the properties of these ligands and related complexes have been reviewed up to 2002 [18]. Furthermore, a more recent paper reviewed the results published on related macrocyclic compartmental systems up to 2005 [19]. Here we report the most recent results achieved with the acyclic compartmental systems which have been classified into [1 + 1] acyclic, [1 + 1], [1 + 2] or [2 + 1] end-off, [2 + 1] or [1 + 2] side-off and [3 + 1] or [1 + 3] polypodal systems according to Scheme 1.

The [1 + 1] acyclic ligands are obtained by reaction of one equivalent of formyl- or keto-derivative with an equimolar amount of a primary amine. Several of these precursors, except those containing additional donor groups at the appropriate positions (i.e. 3-methoxy-3-ethoxy-, 2-hydroxybenzaldehyde, 3-formylsalicylic acid), are not strictly compartmental; nevertheless, they can serve as dinucleating or polynucleating ligands through their phenolate and alcoholate oxygen atoms. More rel-

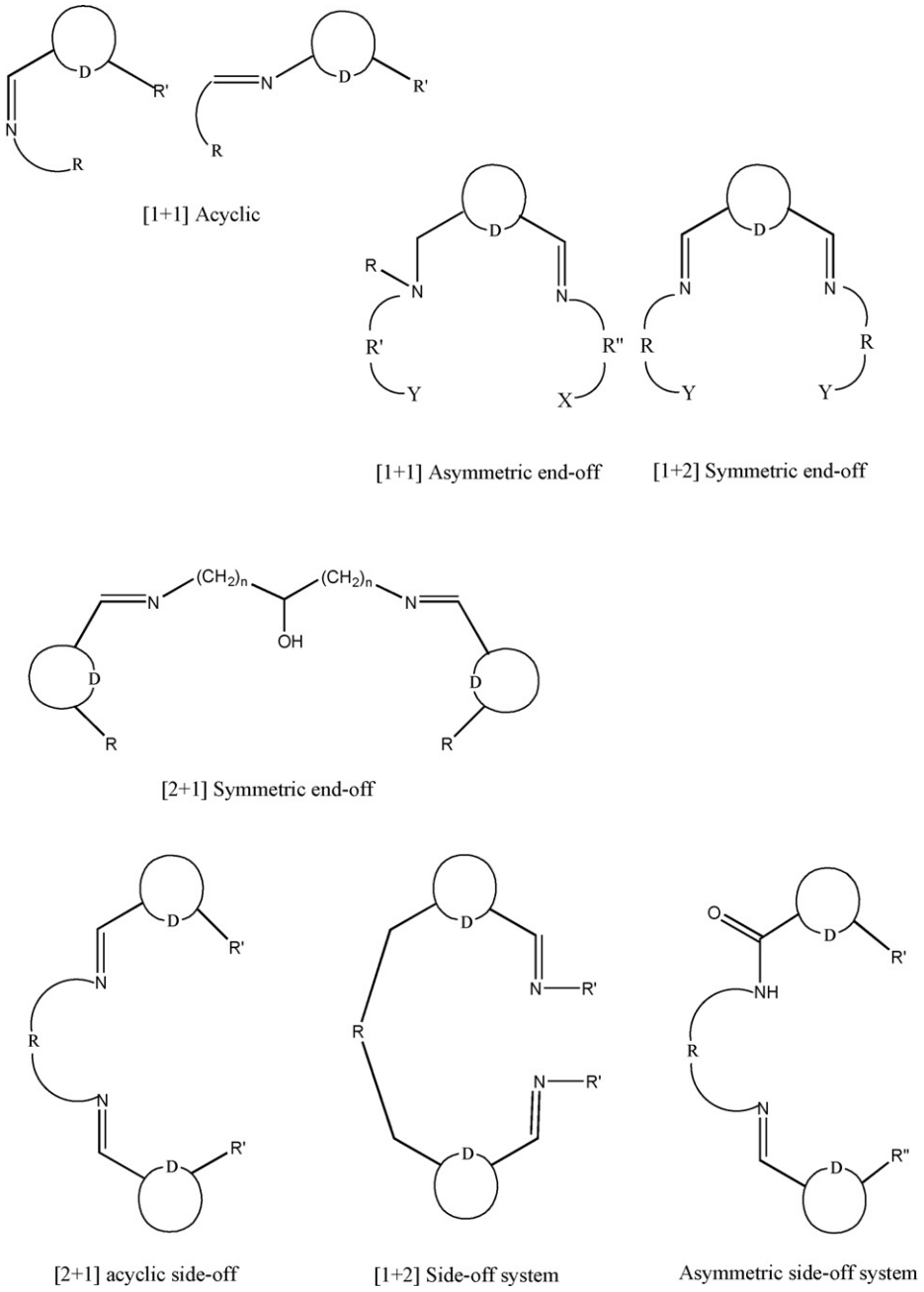

Scheme 1. A schematic representation of the examined ligands.

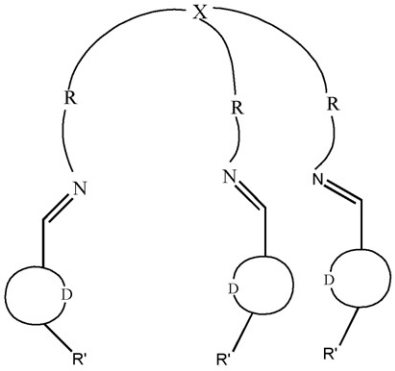

[3+1]

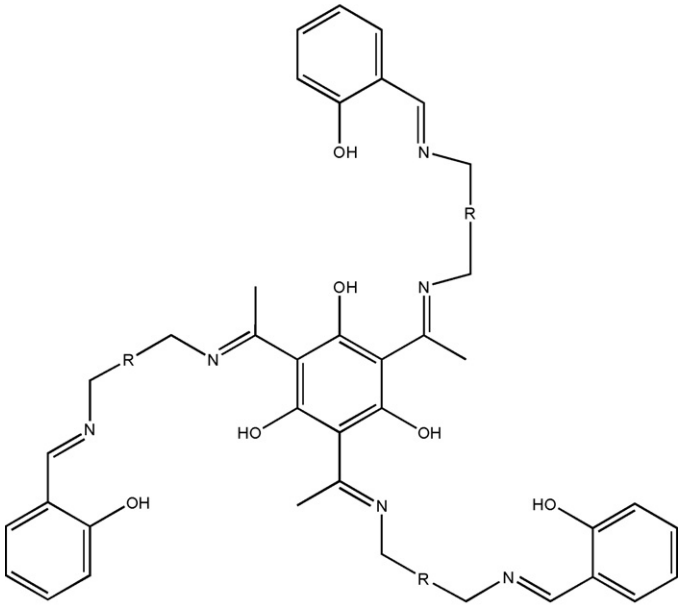

[1+3]

Scheme 1. (*Continued*).

evant,, through quite specific self-assembling reactions, they can give rise to hetero-polynuclear systems capable of acting as single molecule magnets (SMM). Some examples are reported which demonstrate that preorganization of the ligand, as occurs in the compartmental systems, although quite useful, is not a necessary requisite for obtaining organized polynuclear systems. Self-organization of different, organic and inorganic components can produce quite sophisticated supramolecular architectures. When the formyl- or the amine-precursors contain an additional pendant group with donating atoms, this condensation reaction gives rise to [1 + 1] asymmetric end-off ligands, which contain two adjacent dissimilar coordination chambers appropriately designed to verify the different stereochemistry and properties of the dinuclear complexes obtained according to the coordination moiety of the two chambers. Thus, these ligands were progressively modified in order to provide [5 + 5], [5 + 6], [6 + 5] and [6 + 6] adjacent chambers and to verify the parameters affecting the stereochemistry of the resulting complexes.

The [1 + 2] end-off ligands, mainly symmetric, derive from the condensation of one equivalent of a suitable diformyl precursor with two equivalents of a functionalized amine while the [2 + 1] end-off ligands originate from the reaction of two equivalents of the desired formyl derivative with one equivalent of a diamine bearing a bridging group (mainly a –OH group) between the two primary aminic functions.

The [2 + 1] side-off ligands originate from the reaction of two equivalents of a formyl-precursor, bearing an additional donor group at the three-position with one equivalent of a suitable diamine while the [1 + 2] side-off ligands are obtained by condensation of one equivalent of the appropriate functionalized diformyl precursor with two equivalents of a primary monoamine derivative.

Finally the [3 + 1] polypodal ligands derive from the condensation of a formyl derivative with the triamines $(NH_2)(CH_2)_nN[(CH_2)_nNH_2](CH_2)_nNH_2$ ($n = 2$ or 3), $N(C_6H_4NH_2)_3$ or $C_6H_3(C{\equiv}CC_6H_4NH_2)_3$ in a 3:1 molar

ratio. Quite interesting, the two chambers of these ligands can give rise to a site migration of specific metal ions (i.e. a lanthanide ion) from the outer to the inner coordination chamber, generating a molecular metal ion movement inside the ligand, which depends on the pH of the solution. Also relevant is the capability of these ligands to form heterodinuclear lanthanide(III) complexes, only with specific LnLn′ couples, thus furnishing an example of lanthanide ion discrimination on the basis of the ionic radius. Similarly the [1 + 3] polypodal ligands derived from the reaction of one equivalent of a suitable triformyl- or triacetyl-derivative with three equivalents of a diamine of the type NH_2–R–NH_2; the further condensation at the free NH_2 groups of the resulting Schiff bases with a formyl derivative (i.e. salicylaldehyde) can give rise to the designed ligand.

Further synthetic details of these ligands and related complexes will be given in the appropriate section of the review.

In the related metal complexes the group D reported in Scheme 1 provides an endogenous bridge (i.e. –OH, –SH, –N=N–, =N–NH–); a further exogenous bridge may be provided by a mono- or bidentate anion. The chains R, R^I or R^{II} can contain additional donor atoms (NH, S, O, P, etc.) producing a multiplicity of different compartments.

The complexation with weakly or non-coordinating anions can favor hydrolysis of the Schiff bases. And the resulting formyl precursor acts as ligand, quite often giving rise to quite sophisticated complexes. To avoid these problems the Schiff bases have been reduced to the corresponding polyamine derivatives, less sensitive to hydrolysis and more flexible. These reduced compounds contain NH groups which may be further functionalized by appropriate synthetic procedures. Noticeably, in the presence of metal ions, these amine derivatives can be reoxidized to the related Schiff bases and some explanatory examples are reported in the text.

The experimental conditions are also relevant: Some Schiff bases really form but, on heating, they evolve into more complex systems. Some explanatory examples are reported in the text especially in the section dedicated to [2 + 1] side-off systems. Furthermore, the presence of secondary amine groups close to the imine group of the Schiff bases favors a cyclisation reaction with the formation of one or more dihydroxy benzoimidazole rings which can easily be oxidized to the corresponding benzoimidazole rings.

These acyclic ligands have been used for the generation of compounds with specific spectroscopic and magnetic properties. Complexes containing magnetic metal centers exhibit magnetic properties which are not simply the sum of those of the individual ions surrounded by their nearest-neighbor ligands; these properties result from both the nature and the magnitude of the interactions between the metal ions within the molecular unit. Using compartmental ligands, dinuclear complexes can be synthesized where the two metal centers, if paramagnetic, can interact with each other through the endogenous and/or the exogenous bridges in a ferromagnetic or antiferromagnetic way. By changing the type of ligand, the distance between the two chambers and/or the paramagnetic centers, it is possible to vary considerably the magnetic interaction, and particular complexes are good models for the fabrication of molecular ferromagnets.

Furthermore, the specific recognition processes occurring at the two chambers, especially when strongly asymmetric ligands (especially with the end-off or side-off ones) are used, can confer peculiar optical properties; the resulting systems can be the necessary molecular components in the fabrication of quite efficient optical devices (for instance, simultaneous presence of an appropriate organic moiety acting as an antenna toward the lanthanide ion through an energy transfer process, and emission at different wavelengths, red-shift of the bands in consequence of complexation, etc.).

Very efficient catalytic processes, arising from the simultaneous presence of two (or more) equal or different metal ions inside an appropriate organic framework, very interesting in processes of industrial or biological relevance as oxidation, reduction, polymerization or hydrolysis of organic substrates, have been proposed. In particular, oxidation of substituted catechol to the corresponding quinone, polymerization of olefins (norbornene by Pd_2 complexes, ε-caprolactone, D,L-lactide, etc.), reduction of aldehydes to the corresponding alcohols, H_2O_2 disproportionation (especially by polynuclear manganese complexes), activation of small molecules, benzene hydroxylation (especially by di- or polynuclear copper complexes), amide formation by hydrolysis of nitriles by Pd_2 complexes, hydrolysis of phosphoric esters and DNA phosphodiesters cleavages, etc. are mentioned in the following sections.

Furthermore, preorganization is necessary, when specific salt recognition must be achieved; this is particularly relevant in the selective transport and separation of cations and the related anions across liquid membranes, quite important in hydrometallurgy. Acyclic side-off ligands containing additional functionalizations (i.e., bearing protonable groups) have demonstrated their potential in the transport from a feeding to a receiving water solution across an organic medium of metal sulfates (especially nickel(II) over copper and cobalt(II) sulfate).

When the self-condensation reactions are not feasible, these ligands can be obtained by template procedure which directly gives the designed complexes. Metal ion self-assembly processes are of paramount relevance in the evolution of single systems into supramolecular architectures. In addition to this structural role, the metal ion exerts a functional role in determining new physico-chemical properties. In the development of this chemistry engineering exo-dentate ligands (spacers or linkers) connect dinuclear entities (nodes) influencing the structural and functional properties of the single components. By this procedure tetranuclear or polynuclear systems have been prepared from both homo- and heterodinuclear complexes, d,d- and especially d,f-complexes with end-off and side-off ligands. The 3d, 4f-complexes are particularly interesting since the metal ions interact selectively with the different spacers, generating porous molecular materials, single molecule magnets or single chain magnets. The role of the metal ion is quite important in determining the reaction pathway; the ligand:metal ratio is also quite relevant in the formation of dinuclear or polynuclear species and examples of these different pathways are reported in this review. In addition, a role in directing these reactions is also played by

the anions, especially when they act as exogenous bridges. These exogenous bridges can contain two neutral or anionic functionalities (pyridine or carboxylic groups) separated by appropriate spacers. This hence can allow the dinuclear species to evolve into polynuclear ones.

The stoichiometry of the reaction is also relevant in determining the stereochemistry of the resulting complexes. A large amount of metal ions with respect to the ligand tends to form polynuclear aggregates. Furthermore, MLn or M_2Ln_2 complexes can be obtained by varying the stoichiometry of the reactants, the amine, the solvent and the temperature reaction.

Moreover, the prepared complexes can undergo transmetalation reactions when reacted with a different metal salt; this synthetic procedure allows the formation of not otherwise accessible complexes. Template and transmetalation reactions quite often give rise to the designed complexes in high yield and in a satisfactory purity grade. Thus, the large actinide ions quite often transmetalate the transition metal ions from the related mononuclear complexes giving rise to quite complicated polynuclear entities. Also the reverse, although much less frequently, was observed: thus the cobalt(II) ion substituted the lanthanide(III) ion from the outer O_2O_2 chamber of heterodinuclear MLn complexes with side-off ligands forming the related MCo species.

Finally, the acyclic ligands can be functionalized by inserting appropriate groups in the aliphatic and/or aromatic chains of the formyl- or keto- and amine precursors. Following this strategy, reactive groups for well defined supports (i.e. $–Si(OR)_3$ for activated silica) can be introduced at the periphery of the coordinating moiety, making their link to these supports quite feasible. Heterogeneous catalysts or modified surfaces, bearing well-defined molecular assemblies have been prepared following these synthetic strategies [20–26].

2. Aim of the review

This article reviews the most interesting results published in the last years up to 2006 on the basic and applied aspects related to the acyclic compartmental ligands and their mononuclear, homo- and hetero-dinuclear or -polynuclear complexes. The design and synthesis, the physico-chemical properties, the magneto-structural correlations, the reactivity and catalytic activities of these systems have been examined. The ligands, symmetric or asymmetric in nature, generally derive from the self-condensation or template synthesis of appropriately designed formyl- and amine-precursors. By these procedures [1 + 1], [1 + 2] or [2 + 1] planar and [3 + 1] or [1 + 3] polypodal

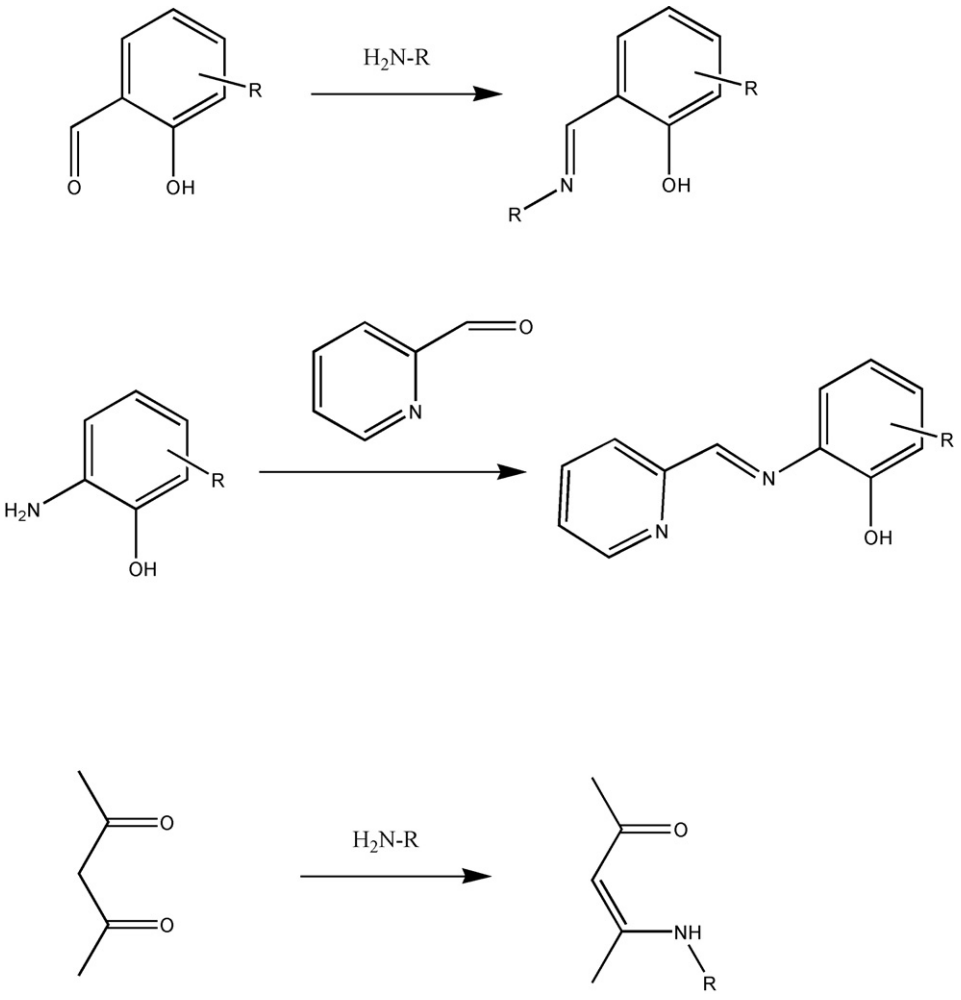

Scheme 2. Synthetic pathways of the [1 + 1] acyclic ligands.

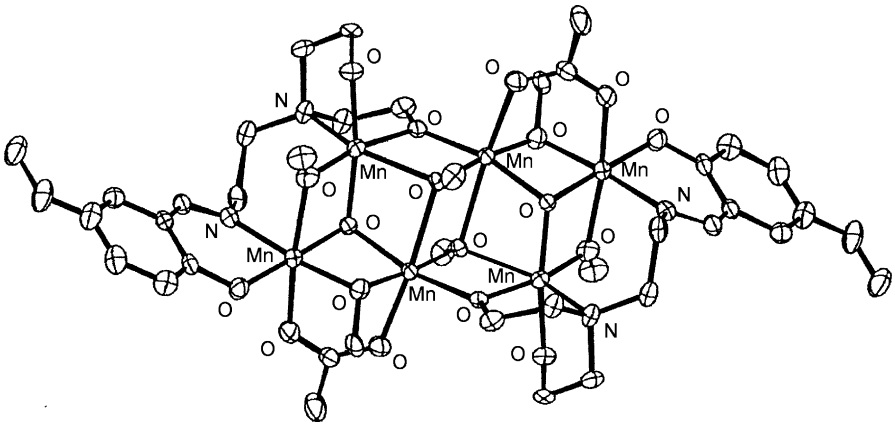

Fig. 1. Structure of $[Mn_6(\mathbf{1a})_2(O)_2(CH_3COO)_2(CH_3O)_6]$.

systems have been obtained and the review has been ordered accordingly to the increasing complexity of the obtained Schiff bases. Attention was devoted to the systems derived from the reduction of the iminic groups of these compartmental Schiff bases; the coordinating ability of these polyamine derivatives and the physico-chemical properties of the resulting complexes have been considered and reviewed in the appropriate sections.

3. [1 + 1] Acyclic systems

The phenolic oxygen atoms of the Schiff bases, obtained by reaction of equimolar amounts of substituted salicylaldehyde or β-diketones with monoamines (NH_2–R) or substituted aminophenol with aldehyde (Scheme 2), can act as bridging groups giving rise to dinuclear or polynuclear entities.

In a recent review [19] it was reported that the Schiff bases H_3-**1a**···**H_3**-**1d** react with manganese(II) acetate tetrahydrate under anaerobic conditions to give $[Mn_2^{II}(\mathbf{L})(CH_3COO)(solv)]_n$ (solv = CH_3OH, H_2O), as indicated by EPR spectra [27] and, under aerobic conditions, $[Mn_6^{III}(\mathbf{L})_2(O)_2(CH_3COO)_2(CH_3O)_6]$ (Fig. 1), where the six octahedral manganese ions, distributed in two μ-oxo-centered trinuclear arrays, give rise to antiferromagnetic interactions [28]. Under similar anaerobic conditions $[Mn_4(\mathbf{2})_2(CH_3COO)_4(CH_3OH)_2]$, $[Mn_4(\mathbf{3})_2(CH_3COO)_4(CH_3OH)_2]$, and $[Mn_4(H\text{-}\mathbf{4})_2(CH_3COO)_4(CH_3OH)_2]$ have been synthesized where, according to magnetic and EPR spectra, an overall antiferromagnetic coupling of the manganese(II) ions in the solid state and in solution occurs [28,29].

In $[Mn_4(\mathbf{2})_2(CH_3COO)_4(CH_3OH)_2]$ (Fig. 2) the two $[\mathbf{2}]^{2-}$ ligands coordinate to the two outer N_2O_3 trigonal bipyramidal manganese ions through two nitrogen and one oxygen atom and to the two inner, O_6 distorted octahedral manganese ions through three oxygen atoms. The four acetate ligands bridge the inner and the outer manganese ions. The Mn···Mn distances are 3.413 Å and 3.297 Å. The arrangement of the four manganese ions is chair like [29].

More recently, Schiff bases derived from the [1 + 1] condensation of aldehydes or ketones with primary amines, bearing additional groups, and the related reduced polyamine derivatives have been successfully used in the synthesis of polynuclear complexes, upon coordination with appropriate metal ions.

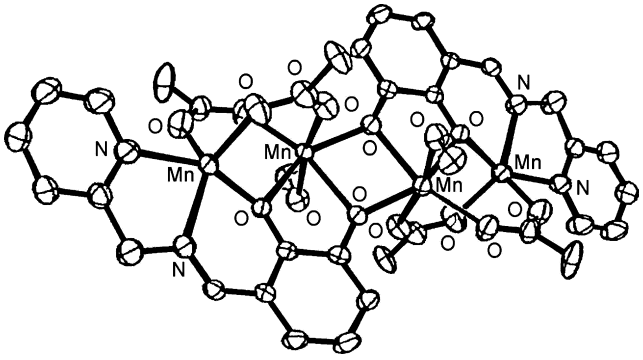

Fig. 2. Structure of $[Mn_4(\mathbf{2})_2(CH_3COO)_4(CH_3OH)_2]$.

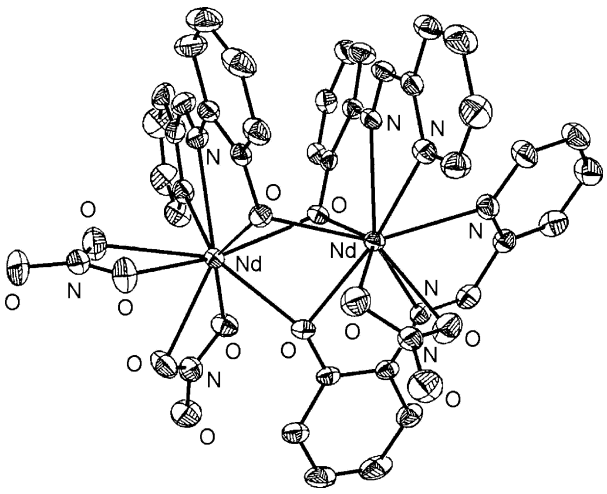

Fig. 3. Structure of $[Nd_2(\mathbf{5a})_3(NO_3)_3]$.

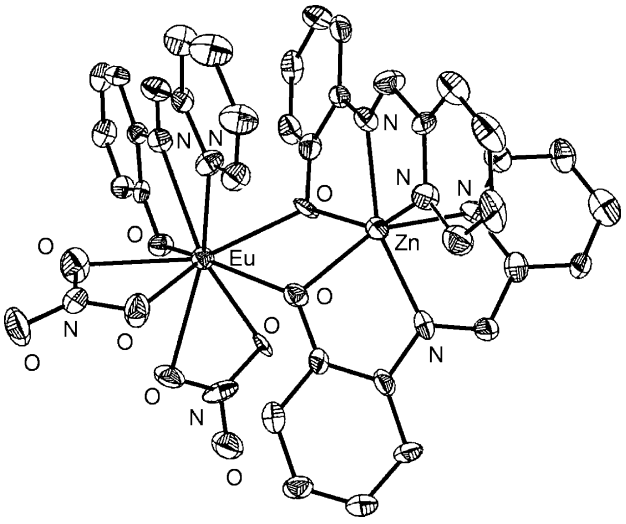

Fig. 4. Structure of [EuZn(**5a**)$_3$(NO$_3$)$_2$].

H-**5a**, derived from the condensation of 2-aminophenol and 2-formylpyridine, forms [Ln$_2$(**5a**)$_3$(NO$_3$)$_3$] with most lanthanide(III) ions but also [EuDy(**5a**)$_3$(NO$_3$)$_3$] and [ZnEu(**5a**)$_3$(NO$_3$)$_2$]. In the isostructural [Ln$_2$(**5a**)$_3$(NO$_3$)$_3$] (Ln = Nd^{III}, Eu^{III}, Dy^{III}) the two nine coordinate lanthanide ions are bridged by the phenolate oxygen atoms of three [**5a**]$^-$ ligands: one lanthanide ion is coordinated by two [**5a**]$^-$ ligands and one nitrate ion, while the other lanthanide ion binds to one ligand [**5a**]$^-$ and two nitrate ions (Fig. 3). In [ZnEu(**5a**)$_3$(NO$_3$)$_2$] the europium(III) ion is again nine coordinate, while the zinc(II) ion is six coordinate in a distorted octahedral geometry (Fig. 4). Quantum mechanical calculations indicate that the formation of the ZnEu heterodinuclear complex is slightly favored energetically over the Eu$_2$ homodinuclear complex [30].

In [Mn$_3$(**5a**)$_2$(CH$_3$COO)$_4$(H$_2$O)$_2$] and [Mn$_3$(**5b**)$_2$(CH$_3$COO)$_4$ (CH$_3$OH)$_2$], prepared by H-**5a** or H-**5b** and Mn(CH$_3$COO)$_2$·2H$_2$O, the two terminal N$_5$O octahedral manganese(II) ions and the central O$_6$ distorted octahedral manganese ion are linked by four acetate and two phenolate oxygen bridges. The intra- and inter-molecular Mn···Mn separations are 3.417 Å and 6.834 Å for [Mn$_3$(**5a**)$_2$(CH$_3$COO)$_4$(H$_2$O)$_2$] and 3.523 Å and 7.046 Å for [Mn$_3$(**5b**)$_2$(CH$_3$COO)$_4$ (CH$_3$OH)$_2$] (Fig. 5). A relatively weak intramolecular antiferromagnetic interaction between the manganese(II) ions was observed in these complexes [31].

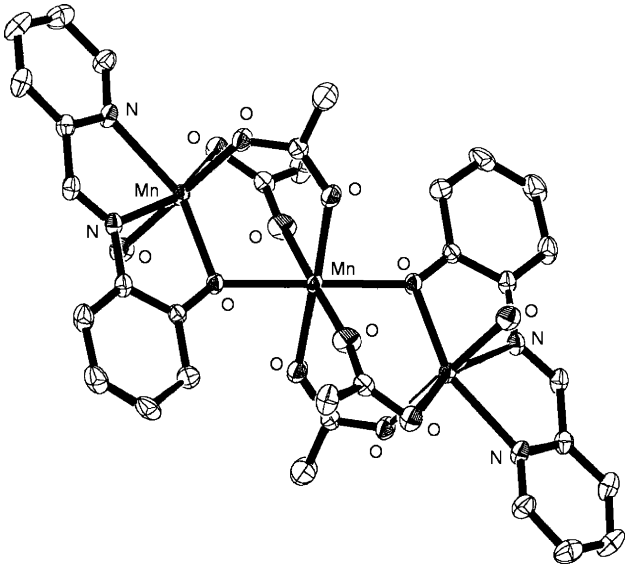

Fig. 5. Structure of [Mn$_3$(**5a**)$_2$(CH$_3$COO)$_4$(H$_2$O)$_2$].

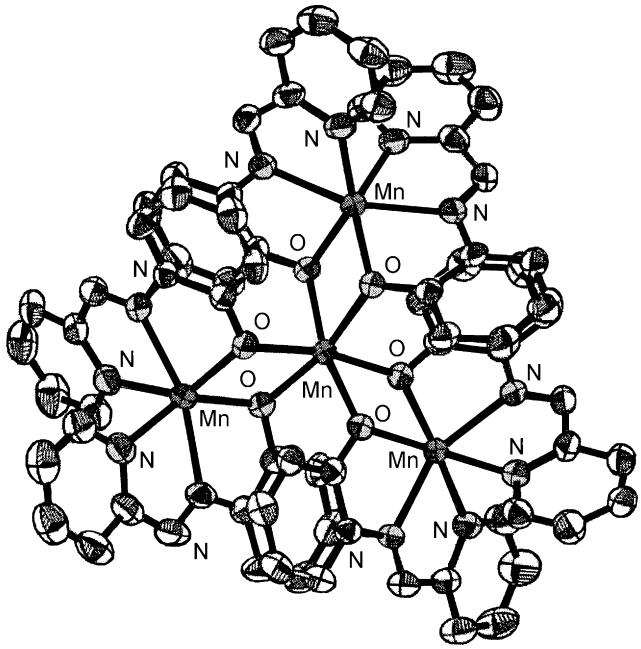

Fig. 6. Structure of [Mn$_4$(**5a**)$_6$]$^{2+}$.

H-**5a** and [Mn(acac)$_2$] form both [Mn(**5a**)$_2$]·4H$_2$O and [Mn$_4$(**5a**)$_6$](BPh$_4$)$_2$ [32]. In the tetramanganese(II) complex the three outer metal ions exhibit equivalent N$_4$O$_2$ distorted octahedral environments while the fourth manganese(II) ion is in a O$_6$ coordination geometry. The average Mn···Mn distance is 3.310 Å (Fig. 6) [32].

H-**6** is oxidized to H-**5c** upon coordination with Zn(CH$_3$COO)$_2$·2H$_2$O and forms [Zn$_3$(**5c**)$_2$(CH$_3$COO)$_4$]. One phenolate oxygen and two acetate oxygen atoms bridge

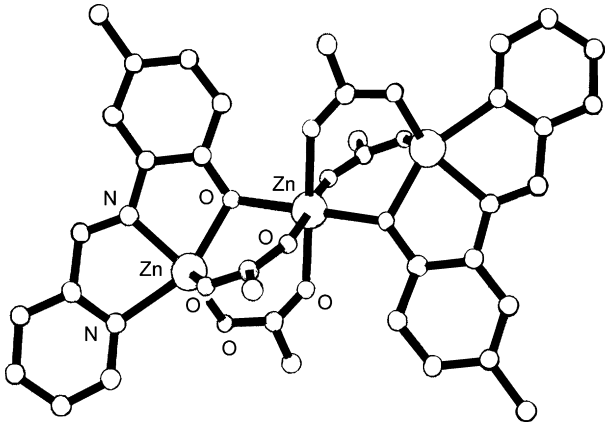

Fig. 7. Structure of [Zn$_3$(**5c**)$_2$(CH$_3$COO)$_4$].

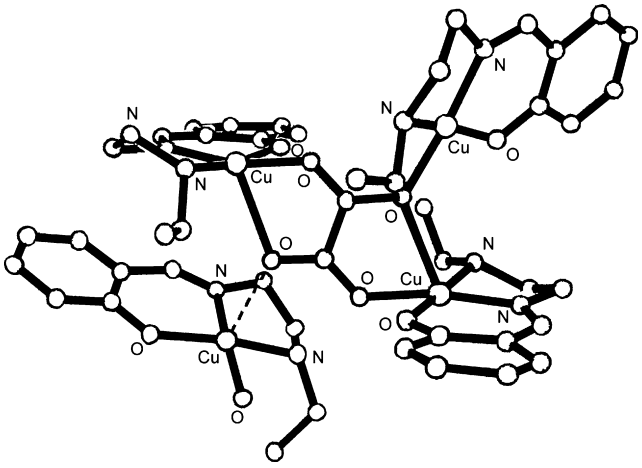

Fig. 8. Structure of $\{[Cu_3(\mathbf{7})_3(\mu_3\text{-}C_2O_4)][Cu(\mathbf{7})(H_2O)]\}^{2+}$.

each N_2O_3 distorted trigonal bipyramidal external zinc(II) ion and the central O_6 octahedral zinc(II) ion. The intramolecular Zn···Zn distance is 3.355 Å (Fig. 7) [33].

In $\{[Cu_3(\mathbf{7})_3(\mu_3\text{-}C_2O_4)][Cu(\mathbf{7})(H_2O)](ClO_4)_2\}\cdot 0.5H_2O\cdot 0.5\,CH_3OH$, derived from the reaction of H-**7** with $Cu(ClO_4)_2\cdot 6H_2O$ and $K_2[Cu(C_2O_4)]\cdot 2H_2O$, the three copper(II) ions are bridged by an oxalate group to form an asymmetric unit with one short (3.871 Å) and two long Cu···Cu distances (5.597 and 5.079 Å). One copper(II) ion has a N_2O_2 distorted square planar geometry, while the other two copper(II) ions are in a N_2O_3 square pyramidal environment (Fig. 8) [34]. An overall antiferromagnetic coupling operates between the copper(II) ions within the trinuclear copper(II) unit originated by the ferromagnetic ($J = 1.48\,cm^{-1}$) interaction between the copper(II) ions via the oxalate bridge and the antiferromagnetic ($J' = -12.82\,cm^{-1}$) interaction between the copper(II) ions via the single oxygen atom bridge in the $[Cu_3(\mathbf{7})_3(\mu_3\text{-}C_2O_4)]^+$ cation [34].

H-**8** and $Ni(CCl_3COO)_2$ produce $[Ni_2(\mathbf{8})_2(\mu\text{-}CCl_3COO)(CCl_3COO)(CH_3OH)]$ with the two metal(II)

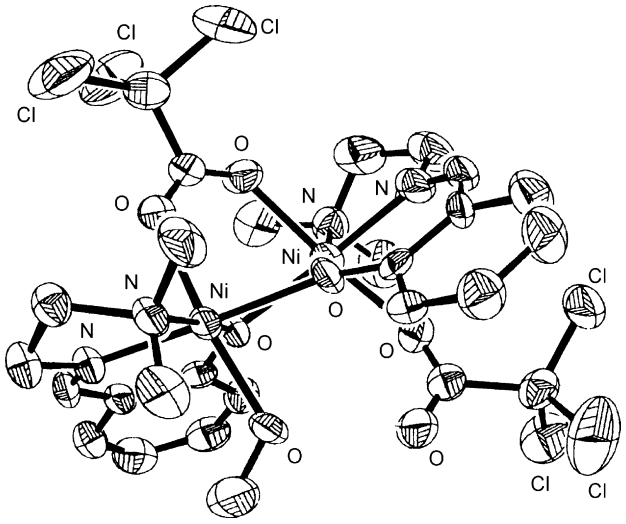

Fig. 9. Structure of $[Ni_2(\mathbf{8})_2(\mu\text{-}CCl_3COO)(CCl_3COO)(CH_3OH)]$.

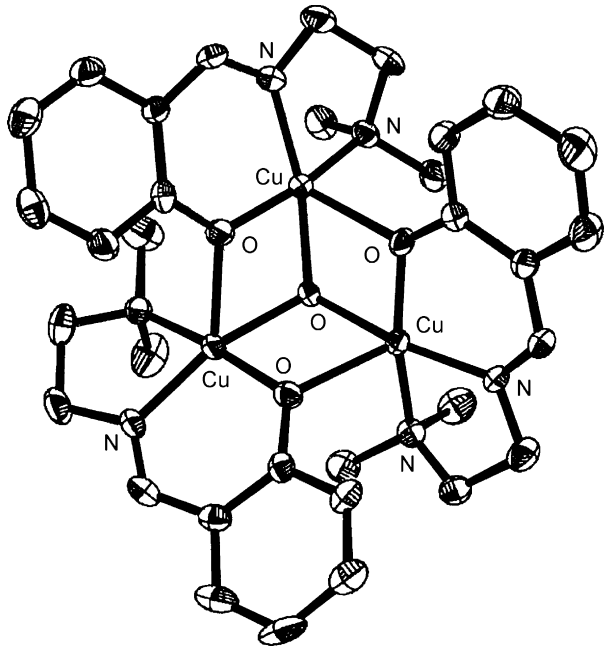

Fig. 10. Structure of $[Cu_3(\mathbf{8})_3(\mu\text{-}OH)]^{2+}$.

ions, 3.058 Å apart, in different distorted octahedral O_4N_2 environments. In one nickel(II) ion, two oxygen atoms, one from a monodentate trichloroacetate and the other from a bridging trichloroacetate group are in apical position, whereas in the other nickel(II) ion one oxygen atom comes from bridging trichloroacetate group and other oxygen atom comes from a methanol molecule (Fig. 9) [35].

The condensation of *N*,*N*-dimethylethylenediamine with salicylaldehyde or acetylacetone, using $Cu(ClO_4)_2\cdot 6H_2O$ as templating agent in the presence of base, affords the isostructural complexes $[Cu_3(\mathbf{8})_3(\mu_3\text{-}OH)](ClO_4)_2\cdot 1.5H_2O$ and $[Cu_3(\mathbf{9})_3(\mu_3\text{-}OH)](ClO_4)_2\cdot 1.5H_2O$, respectively, which contain a partial cubane Cu_3O_4 core. The basal plane of the square pyramidal copper centers comprises two nitrogen atoms and an oxygen atom from the tridentate ligand $[\mathbf{8}]^-$ or $[\mathbf{9}]^-$ and the hydroxy OH^-, while oxygen atom of the ligand completes the coordination sphere in the apical site. The average Cu···Cu distance is 3.210 Å (Fig. 10). While $[Cu_3(\mathbf{8})_3(\mu_3\text{-}OH)](ClO_4)_2\cdot 1.5H_2O$ exhibits a ferromagnetic interaction between the copper(II) ions ($J = 7.83\,cm^{-1}$), $[Cu_3(\mathbf{9})_3(\mu_3\text{-}OH)](ClO_4)_2\cdot 1.5H_2O$ shows an antiferromagnetic interaction ($J = -2.40\,cm^{-1}$) [36,37].

The employment of $CuCl_2\cdot 2H_2O$ instead of $Cu(ClO_4)_2\cdot 6H_2O$ results in the formation of the 1D chain complex $\{[Cu_3(\mathbf{8})_2(Cl)_3(H_2O)_2](Cl)\cdot 3.5H_2O\}_n$. The subsequent replacement of the bridging chloro ligands by azido groups yields, depending upon the used solvents, $[Cu_3(\mathbf{8})_2(N_3)_4(DMF)_2]$, $[Cu(\mathbf{8})(N_3)(DMF)]_n$, and $\{[Cu(\mathbf{8})(N_3)]\cdot[Cu(\mathbf{8})(N_3)]\}_n$ [38].

In the chain complex $\{[Cu_3(\mathbf{8})_2(Cl)_3(H_2O)_2](Cl)\cdot 3.5H_2O\}_n$ two copper(II) ions are five coordinate in slightly distorted square pyramidal geometry while the third one is six coordinate in an elongated octahedral environment. Within the trimeric

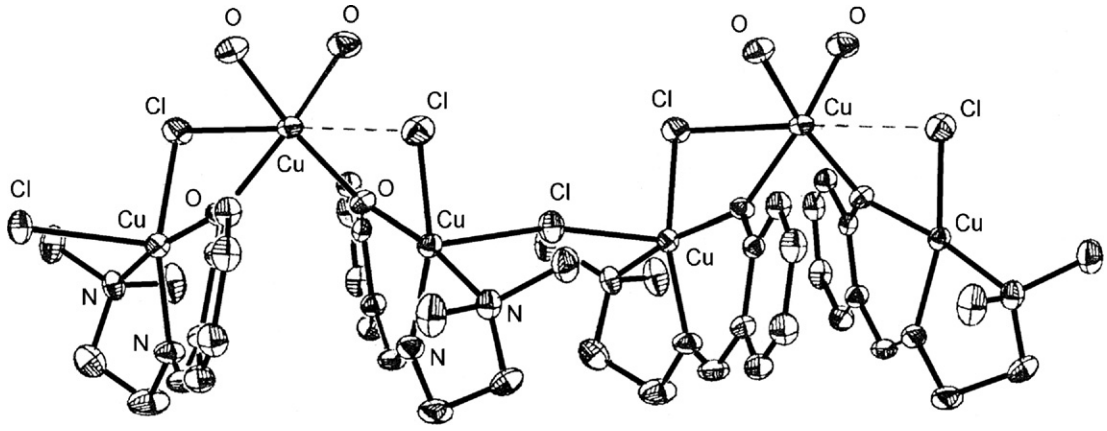

Fig. 11. Structure of $\{[Cu_3(\mathbf{8})_2(Cl)_3(H_2O)_2]^+\}_n$.

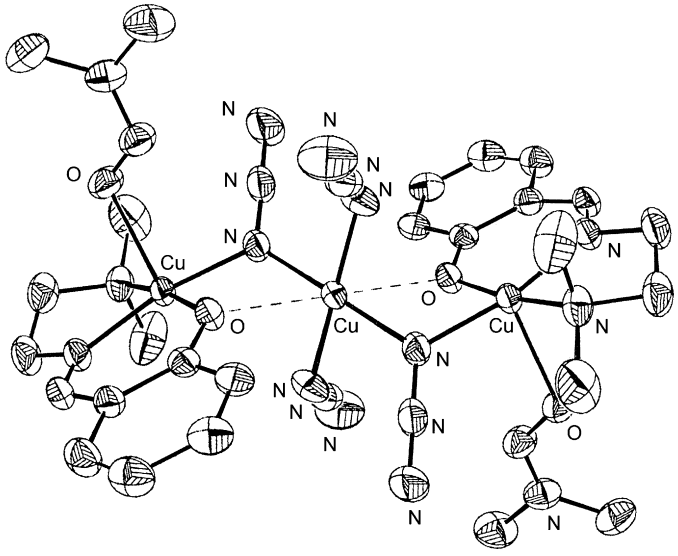

Fig. 12. Structure of $[Cu_3(\mathbf{8})_2(N_3)_4DMF)_2]$.

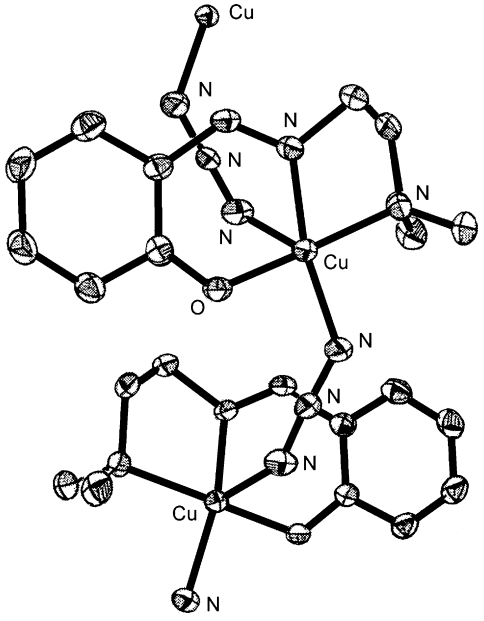

Fig. 13. Structure of $[Cu(\mathbf{8})(N_3)(DMF)]_n$.

cation, the Cu···Cu distances are similar, 3.257 Å and 3.223 Å, while the intertrimer Cu···Cu separation is 5.161 Å (Fig. 11) [38].

$[Cu_3(\mathbf{8})_2(N_3)_4(DMF)_2]$ contains one central octahedral six coordinate and two terminal square pyramidal five coordinate copper(II) ions bridged by two end-on azido ligands (Fig. 12) [38], while the structure of $[Cu(\mathbf{8})(N_3)(DMF)]_n$, consists of end-to-end azido-bridged 1D infinite chains where each slightly distorted square pyramidal copper ion is coordinated by a $[\mathbf{8}]^-$ and two azido ligands. The intrachain Cu···Cu distance is 5.530 Å, while the closest interchain Cu···Cu distance is 7.671 Å (Fig. 13) [38].

$\{[Cu(\mathbf{8})(N_3)]_n{\cdot}[Cu(\mathbf{8})(N_3)]\}$ contains 1D chains, similar to that of $[Cu(\mathbf{8})(N_3)(DMF)]_n$, with discrete $\{Cu(\mathbf{8})(N_3)\}$ monomers beside the chains, where the copper ion is square planar. The intrachain Cu···Cu distance is 5.392 Å [38].

The overall magnetic behaviour of $[Cu_3(\mathbf{8})_2(H_2O)_2(Cl)_3](Cl){\cdot}6H_2O$ corresponds to a weak antiferromagnetic coupled system ($J = -4.89\,cm^{-1}$) while in $[Cu_3(\mathbf{8})_2(N_3)_4(DMF)_2]$ a ferromagnetic coupling between the adjacent copper(II) ions occurs ($J = 32.6\,cm^{-1}$). Intrachain ferromagnetic interactions ($J = 6.7\,cm^{-1}$, $zJ' = -1.3\,cm^{-1}$ and $J = 6.64\,cm^{-1}$, $zJ' = -0.30\,cm^{-1}$, respectively) operate in$[Cu(\mathbf{8})(N_3)(DMF)]_n$ and $\{[Cu(\mathbf{8})(N_3)]{\cdot}[Cu(\mathbf{8})(N_3)]\}$ [38].

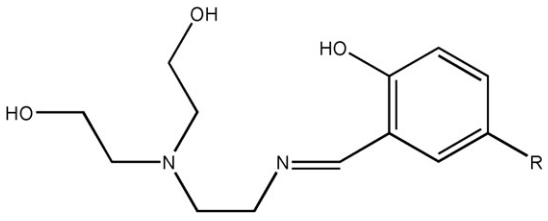

	R
H_3-**1a**	OCH_3
H_3-**1b**	Cl
H_3-**1c**	Br
H_3-**1d**	H

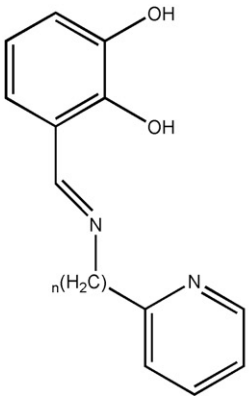

	n
H_2-**2**	1
H_2-**3**	2

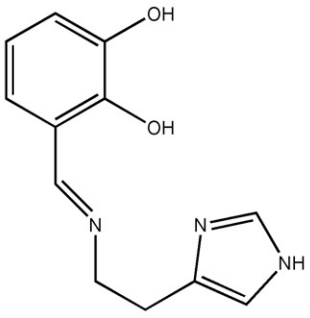

H_3-**4**

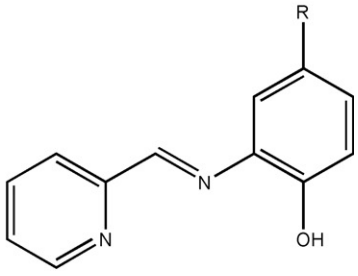

	R
H-**5a**	H
H-**5b**	Cl
H-**5c**	CH_3

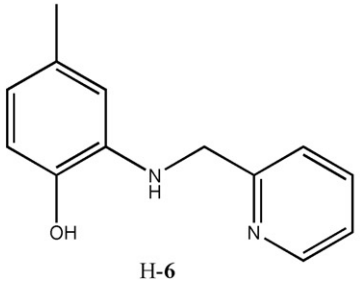

H-**6**

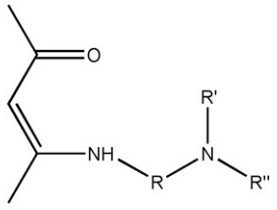

	R	R'	R''
H-**9**	CH_2CH_2	CH_3	CH_3
H-**10**	$CH_2C(CH_3)_2CH_2$	H	H
H-**11**	$CH_2CH(CH_3)$	H	H
H-**12**	CH_2CH_2	H	C_2H_5
H-**13**	CH_2CH_2	H	CH_3

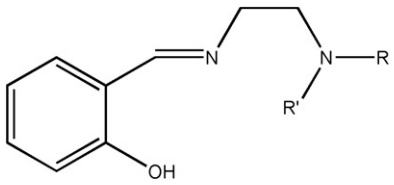

	R	R'
H-**7**	H	C_2H_5
H-**8**	CH_3	CH_3

H-**10**, H-**11**, H-**12**, H-**13**, H-**13a** and H-**13b**, on treatment with $Cu(ClO_4)_2{\cdot}6H_2O$ and $N(C_2H_5)_3$, yield $[Cu_3(\mathbf{L})_3(OH)](ClO_4)_2$, whereas H-**13c** hydrolyses under the same reaction conditions. In these complexes, $[Cu_3(\mathbf{L})_3(\mu_3\text{-}OH)]^{2+}$ is comprised of three $\{Cu(\mathbf{L})\}$ subunits, held together by the oxygen atom of a single, triply bridging hydroxo group, coordinated to each of the three square pyramidal copper centers, and by the three bridging carbonyl oxygen atoms, each of them from a different ligand molecule. The Cu···Cu distances are in the range 3.164–3.329 Å (Fig. 14) [39]. Magnetic data indicate an antiferromagnetic coupling constant in all these complexes with a $J = -66.7\,cm^{-1}$ for $[Cu_3(\mathbf{10})_3(OH)](ClO_4)_2$, $J = -36.6\,cm^{-1}$ for $[Cu_3(\mathbf{11})_3(OH)](ClO_4)_2$, $J = -24.5\,cm^{-1}$ for $[Cu_3(\mathbf{12})_3(OH)](ClO_4)_2$, $J = -14.9\,cm^{-1}$ for $[Cu_3(\mathbf{13})_3(OH)](ClO_4)_2$, $J = -25.6\,cm^{-1}$ for $[Cu_3(\mathbf{13a})_3(\mu_3\text{-}OH)](ClO_4)_2$ and $J = -11.2\,cm^{-1}$ for $[Cu_3(\mathbf{13b})_3(\mu\text{-}OH)](ClO_4)_2$. EPR spectra at low temperature show the existence of spin frustration in $[Cu_3(\mathbf{12})_3(OH)](ClO_4)_2$, $[Cu_3(\mathbf{13})_3(OH)](ClO_4)_2$ and $[Cu_3(\mathbf{13a})(\mu\text{-}OH)](ClO_4)_2$ [39].

The ability of [1 + 1] Schiff bases or ketimines to self assemble in the presence of different metal ions into clusters with particular magnetic properties (i.e. the capability to behave as single molecule magnet) was proved with H_2-**13d**, which is known to give cubane-like clusters with copper(II) salts and a

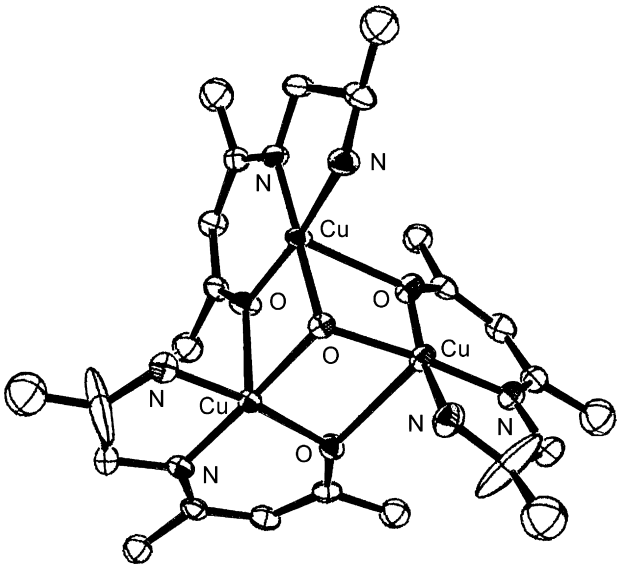

Fig. 14. Structure of $[Cu_3(\mathbf{11})_3(\mu_3\text{-OH})]^{2+}$.

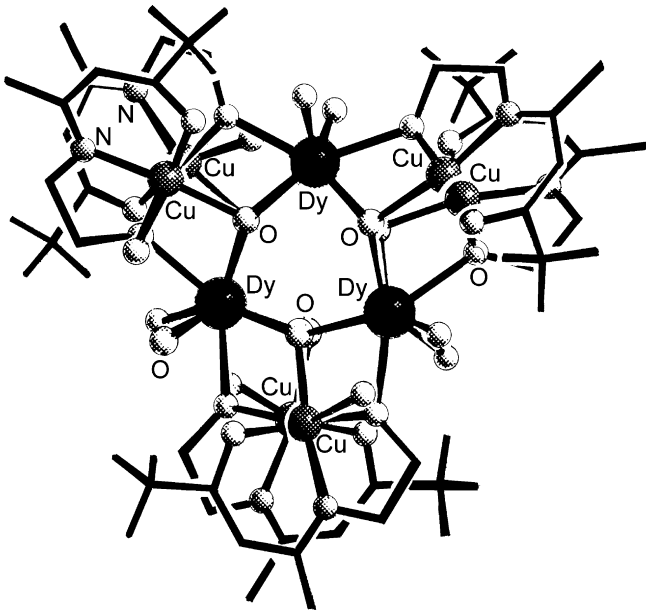

Fig. 15. Structure of $[Dy_3Cu_6(\mathbf{13d})_6(\mu\text{-OH})_6(\mu\text{-}H_2O)_{10}]^{3+}$.

family of heteronuclear $Ln_3^{III}Cu_6^{II}$ clusters in a one-pot reaction of $CuCl_2$ and $Ln(ClO_4)$ [39].

$[Dy_3Cu_6(\mathbf{13d})_6(\mu_3\text{-OH})_6(\mu\text{-}H_2O)_{10}](Cl)_2{\cdot}ClO_4$ is built from three dysprosium(III) ions arranged in a triangular fashion with $\{Cu_2(\mathbf{13d})_2\}$ units on each edge of the triangle. Six alkoxo oxygen atoms of the deprotonated ligands $[\mathbf{13d}]^{2-}$ and six OH groups bridge the different metal ions in a μ_3-fashion. The six OH groups connect the dysprosium(III) ions within the triangular framework $\{Dy_3(OH)_6\}$ and with the copper(II) ions of adjacent $\{Cu_2(\mathbf{13d})_2\}$ units. One alkoxo bridge connects the copper(II) ions within the $\{Cu_2(\mathbf{13d})_2\}$units and the second bridge with adjacent dysprosium(III) ions. The three dysprosium(III) ions, with a Dy···Dy distance in the range 3.788-3.820 Å, have the same eight coordinate environment. The Cu···Cu distances of the six, five coordinate copper(II) ions are in the range 3.138–3.195 Å. Moreover, four copper(II) ions have an additional weakly coordinated water molecule in the sixth position to form an elongated octahedron (Fig. 15). The complex exhibits hysteretic behavior of the magnetization and frequency dependence of the ac susceptibility typical of single molecule magnet. The ground spin state of the Dy_3Cu_6 complex is expected to be $S=3$ with an anisotropy barrier of 25 K associated with a slow zero-field relaxation and a large coercive field [39].

H-**14**, when mixed in the dark with $Cu(NO_3)_2{\cdot}3H_2O$ in the presence of NaOH, yields $[Cu(H\text{-}\mathbf{14})(\mathbf{14})](NO_3){\cdot}H_2O$, where a square pyramidal metal ion and one $-CH_2NH(CH_3)_2$ protonated pendant arm occur. This complex, when exposed to light in CH_2Cl_2, turns into $[Cu(\mathbf{15})_2][Cu_3(\mathbf{15})_6](Cl)_8{\cdot}4H_2O$. In $[Cu(\mathbf{15})_2]$ the copper ion is square planar while in $[Cu_3(\mathbf{15})_6]^{6+}$ the trinuclear copper ions are in a linear fashion, held together by μ-phenoxo bridges, with the central copper ion in a distorted octahedral geometry and the two terminal copper ions in an environment intermediate between square pyramidal and trigonal bipyramidal (Fig. 16) [40].

Condensation of *n*-alkanoylhydrazines with salicylaldehyde affords H_2-**16a**···H_2-**16f**, which form $[Cu_2(\mathbf{L})_2]$ with copper(II) acetate and $[Cu(H\text{-}\mathbf{L})(Cl)(H_2O)]{\cdot}xH_2O$ (H_2-**L** = H_2-**16a**···H_2-**16d**) or $[Cu_2(H\text{-}\mathbf{L})_2(Cl)_2]$ (H_2-**L** = H_2-**16e**, H_2-**16f**) with copper(II) chloride. In $[Cu_2(H\text{-}\mathbf{16a})_2(Cl)_2]$ the distorted square pyramidal copper(II) ions are 3.039 Å, apart. A strong antiferromagnetic coupling was found for $[Cu_2(H\text{-}\mathbf{L})_2(Cl)_2]$ ($-2J = 466\text{–}477\ cm^{-1}$) and for $[Cu_2(\mathbf{L})_2]$ ($-2J = 170\text{–}243\ cm^{-1}$) [41].

H-**17**, synthesized by 4-methyl-2-aminopyridine and salicylaldehyde, reacts with $Cu(CH_3COO)_2{\cdot}H_2O$ to form

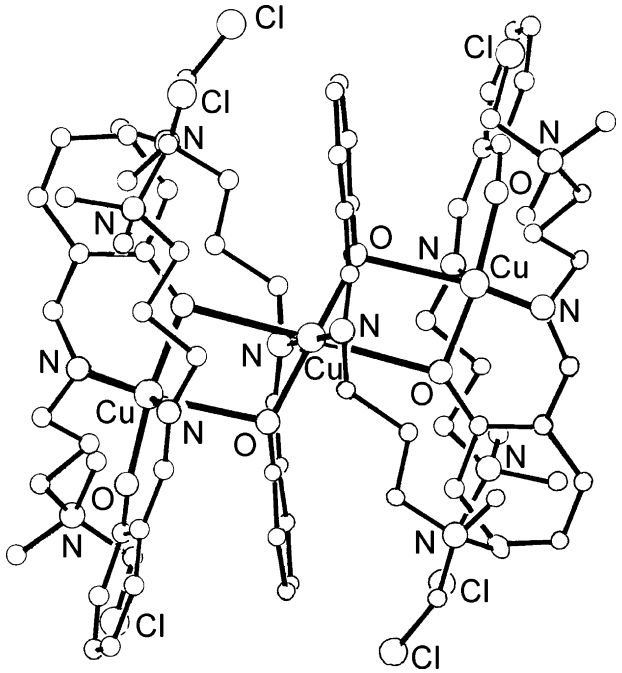

Fig. 16. Structure of $\{[Cu_3(\mathbf{15})_6]\}^{8+}$.

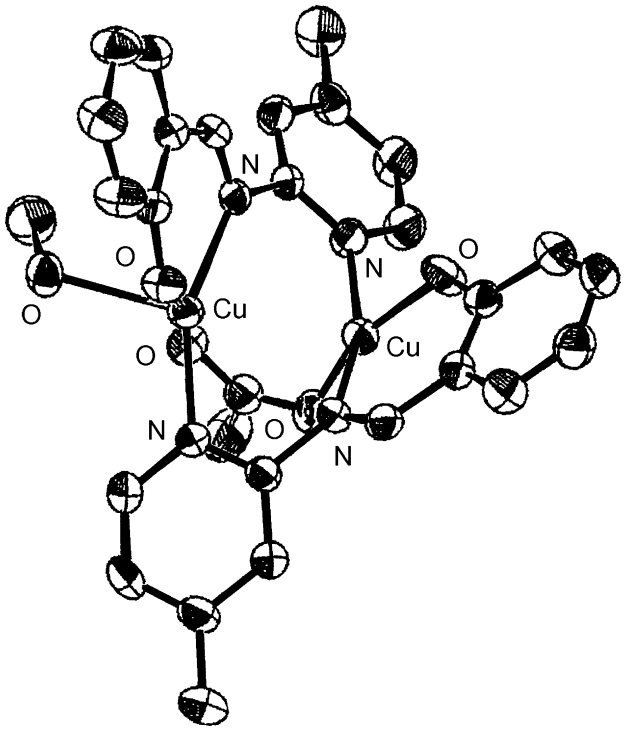

Fig. 17. Structure of $[Cu_2(\mathbf{17})_2(CH_3COO)(CH_3OH)]^+$.

$[Cu_2(\mathbf{17})_2(CH_3COO)(CH_3OH)](ClO_4)$, where the copper ions are 2.832 Å apart. Both copper(II) ions adopt a square pyramidal geometry, although with a different coordination environment (Fig. 17). Magnetic and EPR studies suggest a weak ferromagnetic interaction ($J = 17.8\ cm^{-1}$) between the two copper(II) centers. Cyclic voltammetric studies point a two-step electron transfer, indicating the reduction of the two copper(II) ions to the copper(I) ones, i.e., $Cu^{II}Cu^{II} \rightleftharpoons Cu^{II}Cu^{I} \rightleftharpoons Cu^{I}Cu^{I}$ [42].

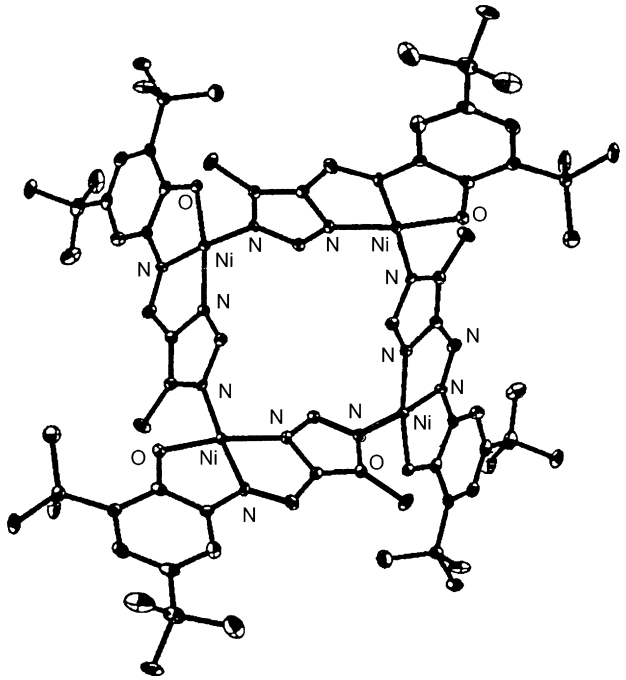

Fig. 18. Structure of $[Ni_4(\mathbf{19})_4]$.

H_2-**18**, prepared in a two-step process involving the condensation of 6-amino-2,4-di-*tert*-butylphenol with 5-methyl-3H-imidazole-4-carbaldehyde followed by reduction of the Schiff base, is susceptible to aerial oxidation in methanol containing triethylamine to a not stable radical, presumably an iminosemiquinone, as indicated by the EPR spectrum at room temperature, which oxidizes to the iminophenolate

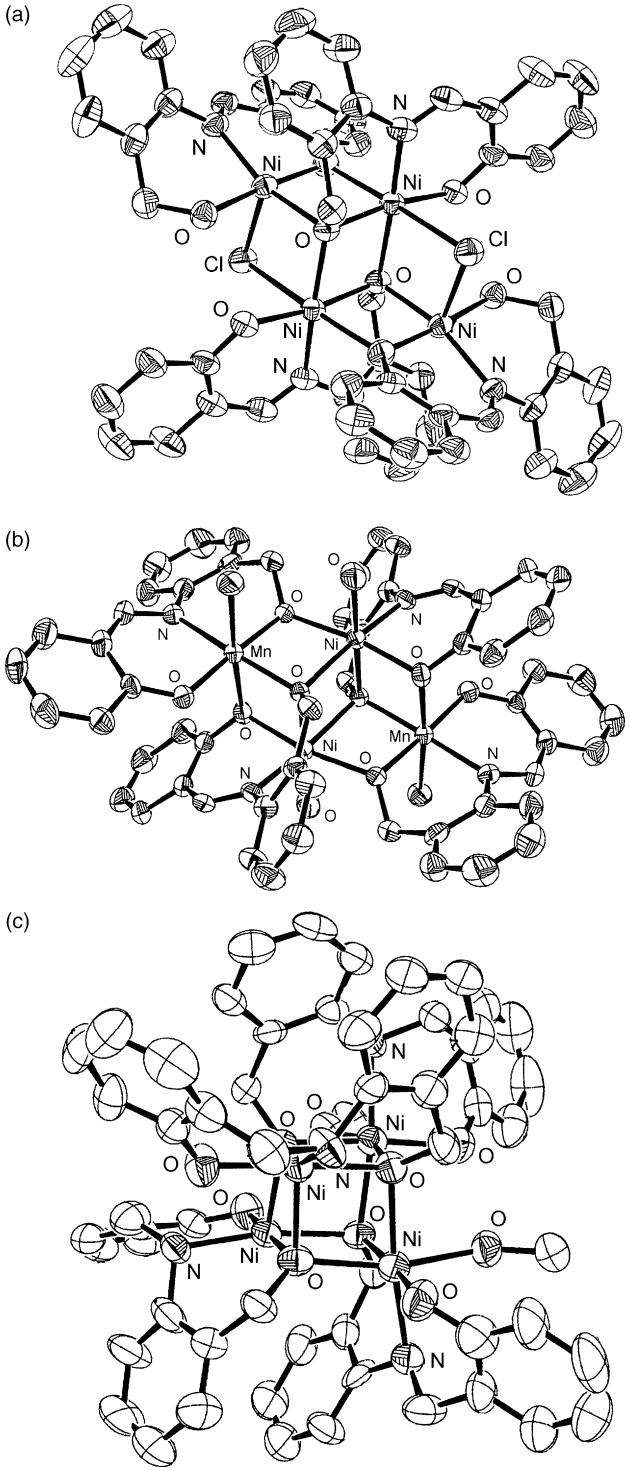

Fig. 19. Structure of $[Ni_4(\mathbf{20})_2(H\text{-}\mathbf{20})_2(\mu\text{-}Cl)_2]$ (a), $[Mn_2Ni_2(\mathbf{20})_4(Cl)_2(H_2O)_2]$ (b) and $[Ni_4(\mathbf{21})_4(CH_3OH)_2]$ (c).

form of H_2-**19** upon complexation with nickel(II) or copper(II) salts, forming $[Ni_4(\mathbf{19})_4]$ and $[Cu_4(\mathbf{19})_4]$, respectively [43].

In $[Ni_4(\mathbf{19})_4]\cdot 9CH_2Cl_2$ the distorted square planar nickel centers are 5.851 Å apart, arranged in a butterfly form and coordinated by the N_2O donor set of the deprotonated ligand and by the nitrogen atom of the imidazolate ring from the adjacent NiN_2O unit (Fig. 18) [43]. Also in $[Cu_4(\mathbf{19})_4(THF)_4]$ the distorted square pyramidal copper(II) centers form a butterfly structure. The four copper(II) centers are antiferromagnetically coupled ($J = -49\ cm^{-1}$) [43].

$[Ni_4(\mathbf{20})_2(H\text{-}\mathbf{20})_2(Cl)_2]$ has been prepared by reaction of H_2-**20** with $NiCl_2\cdot 6H_2O$; similarly, $[Mn_2^{III}Ni_2^{II}(\mathbf{20})_4(H_2O)_2(Cl)_2]$ has been obtained by reaction of $MnCl_2\cdot 6\ H_2O$ with H_2-**20** followed by the addition of $NiCl_2\cdot 6\ H_2O$. Finally, $[Ni_4(\mathbf{21})_4(CH_3OH)_2]$, derived from the reaction of the reduced ligand H_2-**21** with anhydrous $NiCl_2$ in the presence of potassium *tert*-butoxide, is unstable under open atmosphere: the coordinating ligands $[\mathbf{21}]^{2-}$ are easily oxidized to $[\mathbf{20}]^{2-}$ with the consequent formation of $[Ni_4(\mathbf{20})_4(CH_3OH)_2]$ [44].

In $[Ni_4(\mathbf{20})_2(H\text{-}\mathbf{20})_2(\mu\text{-}Cl)_2]\cdot 4CH_2Cl_2$ the four nickel(II) ions, located at the four corners of a defective double-cubane

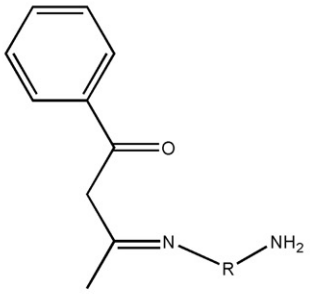

	R
H-**13a**	CH_2CH_2
H-**13b**	$CH_2CH(CH_3)$
H-**13c**	$CH_2CH_2CH_2$

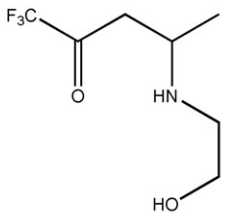

H_2-**13d**

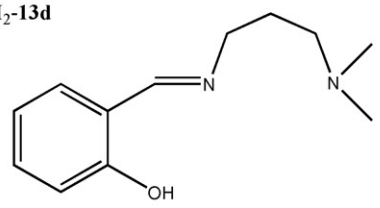

H-**14**

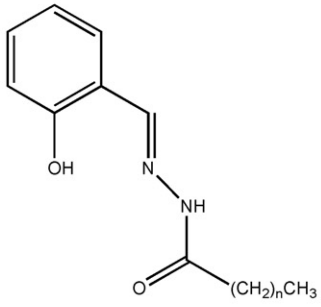

	n
H_2-**16a**	0
H_2-**16b**	4
H_2-**16c**	5
H_2-**16d**	6
H_2-**16e**	12
H_2-**16f**	16

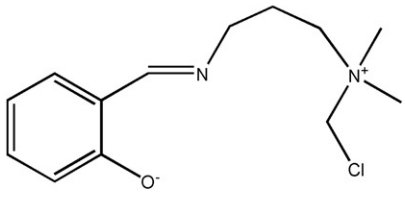

15

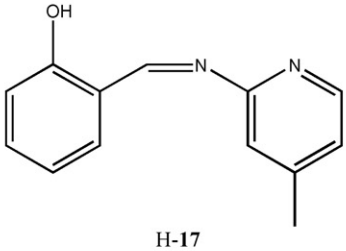

H-**17**

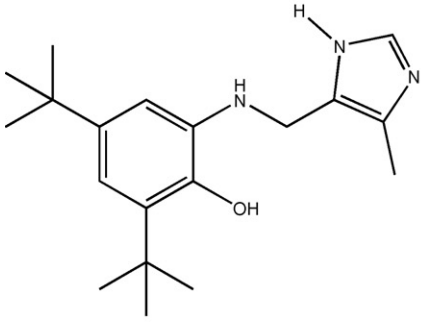

H_2-**18**

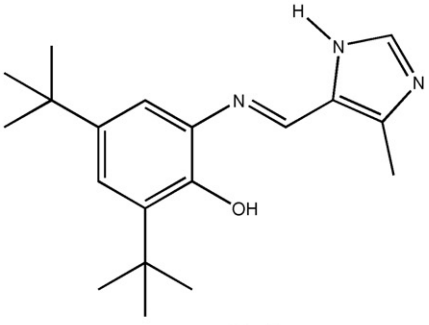

H_2-**19**

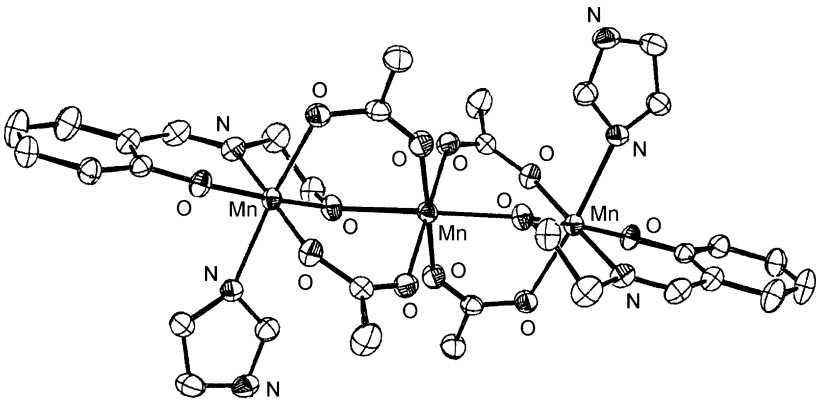

Fig. 20. Structure of $[Mn_3(\mathbf{22})_2(CH_3COO)_4(H\text{-}Im)_2]$.

core, are bridged by two μ_3-alkoxo, μ-phenoxo and μ-chloro groups. The alcoholic oxygen atoms of [H-**20**]$^-$ are protonated and coordinated to the nickel(II) ions without bridging. The shorter Ni···Ni distances are in the range 3.067–3.179 Å, while the longer one is 5.304 Å. Coordination geometries about the nickel(II) ions have been described as distorted octahedral and distorted square pyramidal, respectively (Fig. 19a) [44].

The same defective double-cubane core occurs also in $[Mn_2Ni_2(\mathbf{20})_4(Cl)_2(H_2O)_2]\cdot 2CH_2Cl_2$. Each manganese(III) ion is positioned in both edges of double-cubane and each nickel(II) ion resides in central position. Octahedral geometries about the nickel(II) and the manganese(III) ions occur. The Ni···Mn, Ni···Ni and Mn···Mn distances are 3.096 and 3.082, 3.1311 and 5.326 Å, respectively (Fig. 19b) [44].

$[Ni_4(\mathbf{21})_4(CH_3OH)_2]$ has a remarkably distorted cubane-like Ni_4 core structure, which can be regarded as a dimer-of-dimers structure composed by alkoxo-bridged dinickel units. The Ni···Ni distances for bis-μ-alkoxo units are 3.112 and 3.124 Å. Two nickel ions are octahedral owing to the additional coordination of methanol, while other two nickel(II) ions are square pyramidal (Fig. 19c) [44].

The effective magnetic moments of $[Ni_4(\mathbf{20})_2(\text{H-}\mathbf{20})_2(\mu\text{-}Cl)_2]$ and $[Ni_4(\mathbf{21})_4(CH_3OH)_2]$ correspond to common values for mononuclear octahedral nickel(II) complexes. In the $Mn_2^{III}Ni_2^{II}$ complex a ferromagnetic interaction between the metal ions was observed ($J_{NiMn} = 1.5\,cm^{-1}$; $J_{NiNi} = 20\,cm^{-1}$) while in $[Cu_4(\mathbf{20})_4]$ antiferromagnetic couplings were found [44].

$[Mn_3(\mathbf{22})_2(CH_3COO)_4(H\text{-}Im)_2]$ (H-Im = imidazole), prepared by reaction of $[Mn_3(O)(CH_3COO)_6(H\text{-}Im)_3]\cdot dmf$ [45] with salicylaldehyde and ethanolamine, contains three hexacoordinate manganese ions, arranged in a linear fashion at a Mn···Mn distance of 3.475 Å between adjacent manganese ions. The central manganese(II) ion is in a O_6 octahedral environment while each external manganese(III) ion is in a N_2O_4 octahedral coordination geometry (Fig. 20). An antiferromagnetic interaction occurs in this trimeric structure ($J = -10.2\,cm^{-1}$), stabilizing a $S_T = 3/2$ ground state [46].

A tetranuclear pseudo-cubane core was found also in $[Cu_4(\mathbf{22})_4]\cdot C_2H_5OH\cdot 2H_2O$, synthesized by reaction of H_2-**22** and $Cu(ClO_4)_2\cdot 6H_2O$ in the presence of $N(C_2H_5)_3$ (Fig. 21). The distorted square planar copper ions are 3.176···3.531 Å apart. Ferromagnetic interactions among copper(II) centers ($J = 5.15\,cm^{-1}$) within the tetranuclear core and weak intercluster antiferromagnetic interactions ($zJ' = -0.33\,cm^{-1}$) were found [47].

$Fe(CH_3COO)_2$ or $MnCl_2$ and H_2-**22** afford $[Fe_3(\mathbf{22})_3(CH_3COO)_3]$ and $[Mn_4(\mathbf{22})_4(Cl)_4]$, where an oxidation of the iron(II) or manganese(II) ions to iron(III) or manganese(III) ions by oxygen from the air occurs. The reaction of $Ni(CH_3COO)_2$ or $NiCl_2$ with $[Na_2(\mathbf{22})]$ gives rise to $[Ni_4(\mathbf{22})_4(CH_3OH)_4]$. These complexes incorporate the doubly-deprotonated ligand $[\mathbf{22}]^{2-}$ although the synthesis of $[Ni_4(\mathbf{22})_4(CH_3OH)_4]$ is the only one that specifically requires the use of a base to deprotonate the ligand [48].

$[Fe_3(\mathbf{22})_3(CH_3COO)_3]$ possesses an $[Fe_3(\mu_2\text{-}O)_3]^{3+}$ core, with three iron(III) ions connected by alkoxo bridges at the corners of a scalene triangle. Each pair of iron(III) centers is additionally bridged by a μ_2-acetate ligand (Fig. 22a) [48].

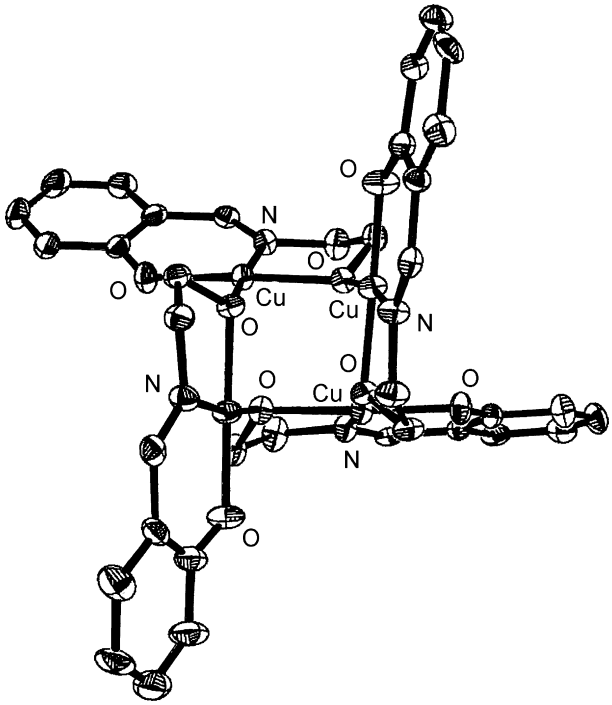

Fig. 21. Structure of $[Cu_4(\mathbf{22})_4]$.

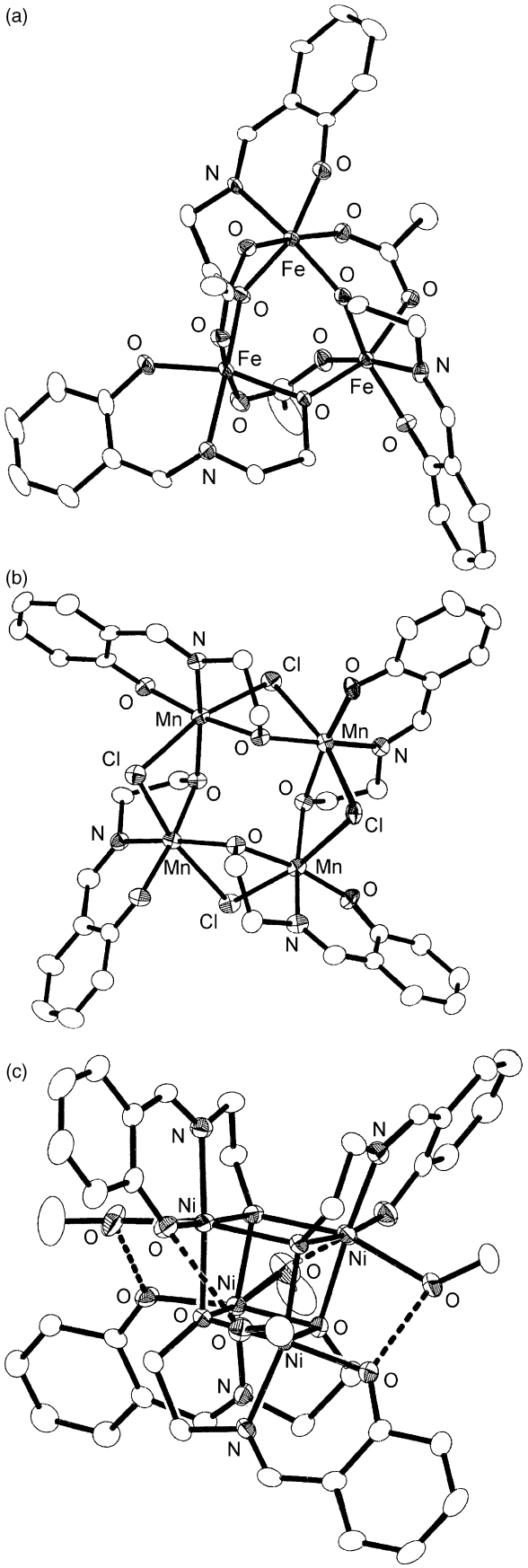

Fig. 22. Structure of $[Fe_3(\mathbf{22})_3(CH_3COO)_3]$ (a), $[Mn_4(\mathbf{22})_4(Cl)_4]$ (b) and $[Ni_4(\mathbf{22})_4(CH_3OH)_4]$ (c).

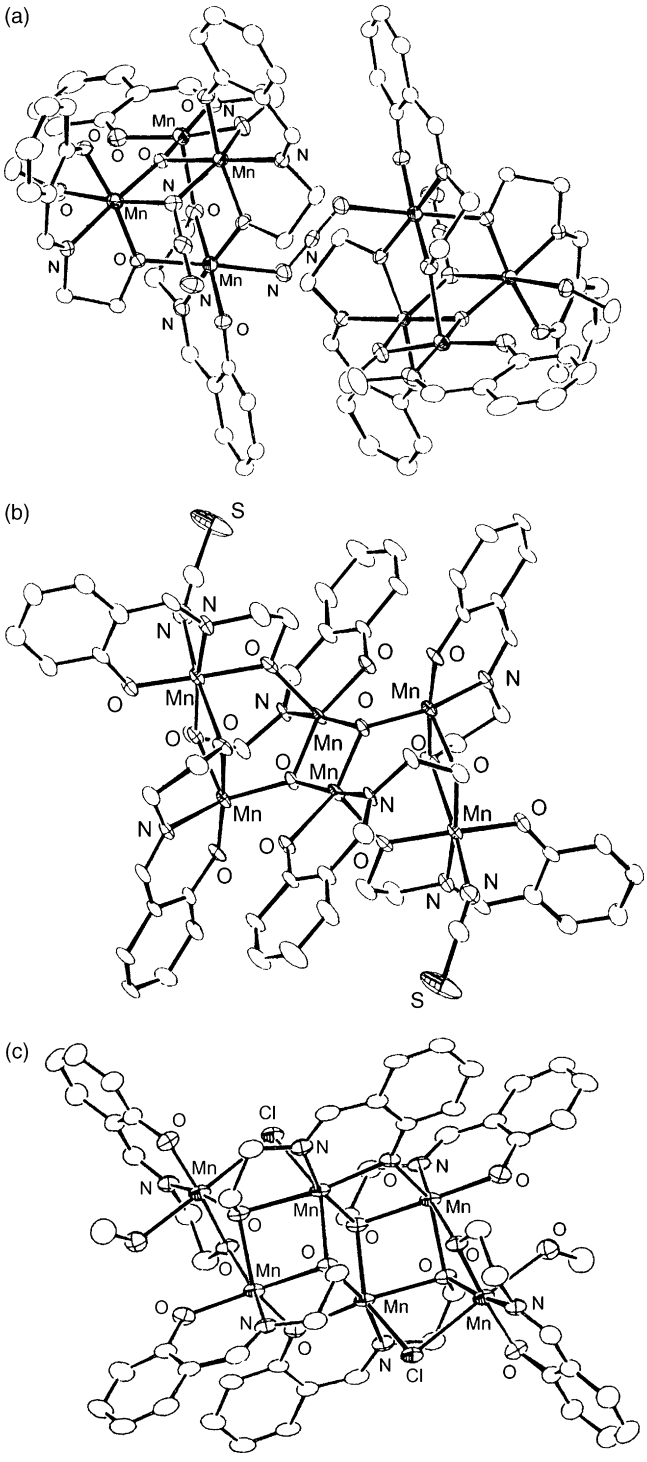

Fig. 23. Structure of $[\{Mn_4^{III}(\mathbf{22})_4(\mu_3\text{-}O)(\mu_3\text{-}N_3)(CH_3OH)\}_2(\mu_3\text{-}N_3)]^+$ (a), $[Mn_6^{III}(\mathbf{22})_6(\mu_3\text{-}O)_2(NCS)_2]$ (b) and $[Mn_4^{II}Mn_2^{III}(\mathbf{22})_6(Cl)_2(CH_3OH)_2]$ (c).

$[Mn_4(\mathbf{22})_4(Cl)_4]$ contains a $\{Mn_4(\mu_2\text{-}O)_4(\mu_2\text{-}Cl)_4\}$ core with the four manganese centers essentially coplanar in an approximately square arrangement. Each side of the square is comprised of an alkoxo and a chloro bridge connecting pairs of manganese centers, with the core oxygen and chlorine atoms lying around the square on alternating sides of the Mn_4 plane (Fig. 22b) [48].

$[Ni_4(\mathbf{22})_4(CH_3OH)_4]$ has a $[Ni_4(\mu_3\text{-}O)_4]$ cubane core similar to that observed in $[Fe_3(\mathbf{22})_3(CH_3COO)_3]$ and $[Mn_4(\mathbf{22})_4(Cl)_4]$, except that in $[Ni_4(\mathbf{22})_4(CH_3OH)_4]$ the ethoxo oxygen atoms bridge in a μ_3- rather than in a μ_2-manner, the peripheral ligation being completed by four terminal methanol ligands (Fig. 22c) [48].

For $[Fe_3(\mathbf{22})_3(CH_3COO)_3]$ an overall antiferromagnetic interaction ($J_A = -9.8\,cm^{-1}$; $J_B = -9.4\,cm^{-1}$; $J_C = 8.3\,cm^{-1}$) operates while in $[Mn_4(\mathbf{22})_4(Cl)_4]$ an overall ferromagnetic interaction occurs ($J = 1.7\,cm^{-1}$); below 20 K the rapid decrease in $\chi_M T$ at low temperature was attributed to a combination of zero-field splitting and antiferromagnetic intermolecular interactions. Ferromagnetic interactions ($J_A = 3.8\,cm^{-1}$; $J_B = 9.0\,cm^{-1}$) were found also for $[Ni_4(\mathbf{22})_4(CH_3OH)_4]$ [48].

$[\{Mn_4^{III}(\mathbf{22})_4(\mu_3\text{-}O)(\mu\text{-}N_3)(CH_3OH)\}_2(\mu\text{-}N_3)](N_3)$ and $[Mn_6^{III}(\mathbf{22})_6(\mu_3\text{-}O)_2(NCS)_2]$ were prepared by reaction of $Mn(NO_3)_2{\cdot}6H_2O$, H-**22** and $N(C_2H_5)_3$, followed by the addition of NaN_3 or NH_4SCN; with $MnCl_2{\cdot}4H_2O$ $[Mn_4^{II}Mn_2^{III}(\mathbf{22})_6(Cl)_2(CH_3OH)_2]{\cdot}2CH_3OH$ was obtained [49].

$[\{Mn_4^{III}(\mathbf{22})_4(\mu_3\text{-}O)(\mu\text{-}N_3)(CH_3OH)\}_2(\mu\text{-}N_3)](N_3){\cdot}4CH_3OH$ consists of two tetranuclear cluster units singly bridged by azido in end-to-end mode. In each tetranuclear core, two five coordinate square pyramidal and two six coordinate octahedral manganese(III) ions occur (Fig. 23a) [49].

$[Mn_6^{III}(\mathbf{22})_6(\mu_3\text{-}O)_2(NCS)_2]{\cdot}9H_2O$ contains two units with three independent manganese(III) ions. Within each unit, one octahedral manganese ion is coordinated by a O_5N donor set while the other two metal ions are distorted square pyramidal and are bridged to one manganese ion of the neighboring trimer by two μ_3-oxide atom. Two manganese ions, belonging to neighboring trimers, are doubly bridged by μ_3-oxide atoms with an interatomic Mn···Mn distance of 2.815 Å (Fig. 23b) [49].

In $[Mn_4^{II}Mn_2^{III}(\mathbf{22})_6(Cl)_2(CH_3OH)_2]{\cdot}2CH_3OH$ (Fig. 23c) the six octahedral or pseudo-octahedral manganese ions are bridged by μ_2- and μ_3-alkoxide atoms from the Schiff base ligands. Two pairs of $Mn^{II}\cdots Mn^{III}$ ions are also bridged each by a μ_2-chloride ion. Magnetic susceptibility measurements indicate the occurrence of antiferromagnetic interactions among the manganese ions [49].

$Ni(CH_3COO)_2{\cdot}4H_2O$, $NiCl_2{\cdot}6H_2O$ and H_3-**23** yield $[Ni_2(H_2\text{-}\mathbf{23})_2(CH_3COO)_2(CH_3OH)_2]$ where the two nickel(II) ions are doubly bridged by the phenoxo groups of $[H_2\text{-}\mathbf{23}]^-$ with a Ni···Ni separation of 3.093 Å (Fig. 24). The magnetic behavior indicates an antiferromagnetic interaction ($J = -6.9\,cm^{-1}$) [50].

$[Mn^{III}Cu^{II}(\mathbf{24})_2(Cl)(CH_3OH)]$, derived from the reaction of $CuCl_2{\cdot}2H_2O$ with $MnCl_2{\cdot}4H_2O$ and H_2-**24**, contains a manganese(III) and a copper(II) ion, 3.000 Å apart, in a distorted

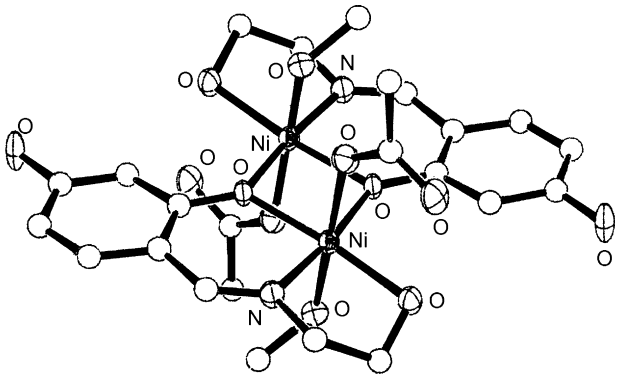

Fig. 24. Structure of $[Ni_2(H_2\text{-}\mathbf{23})_2(CH_3COO)_2(CH_3OH)_2]$.

octahedral and square planar coordination geometry, respectively (Fig. 25). In $[MnCu(\mathbf{24})_2(Cl)(CH_3OH)]$ ferromagnetic interactions occur, and fitting gives a $S = 5/2$ spin ground state with an exchange coupling constant J_{MnCu} of $78\,cm^{-1}$. The complex behaves as a single-molecule magnet [51].

Treatment of $Fe(CH_3COO)_2$ with H_2-**25** in ethanol or H_2-**26** in acetonitrile affords $[Fe_3(\mathbf{25})_3(CH_3COO)_3]$ and $[Fe_3(\mathbf{26})_3(CH_3COO)_3]$, respectively, isostructural with $[Fe_3(\mathbf{22})_3(CH_3COO)_3]$. When recrystallized from non-coordinating solvents, $[Fe_3(\mathbf{25})_3(CH_3COO)_3]$ turns into $[Fe_5(\mathbf{25})_4(O)(OH)(CH_3COO)_4]$, the additional oxo and hydroxo ligands apparently resulting from residual H_2O in the solvent. A similar treatment of $Fe(CH_3COO)_2$ in methanol or ethanol with H_2-**26** or recrystallization from the appropriate alcohol of $[Fe_3(\mathbf{26})_3(CH_3COO)_3]$ give $[Fe_4(\mathbf{26})_4(CH_3COO)_2(OR)_2]$ ($R = CH_3$, C_2H_5) [52].

Carboxylate exchange for $[Fe_3(\mathbf{22})_3(CH_3COO)_3]$ and $[Fe_3(\mathbf{26})_3(CH_3COO)_3]$ with a variety of carboxylates proved difficult to obtain pure species. Nevertheless, the reaction of $[Fe_3(\mathbf{22})_3(CH_3COO)_3]$ in acetonitrile/toluene with three equivalents of $p\text{-}NO_2C_6H_4COO_2H$ affords $[Fe_5(\mathbf{22})_4(O)(OH)(p\text{-}NO_2C_6H_4COO)_4]$. A similar treatment of $[Fe_3(\mathbf{26})_3(CH_3COO)_3]$ with six equivalents of C_6H_5COOH affords $[Fe_5(\mathbf{26})_4(O)(OH)(C_6H_5COO)_4]$. Again, the new oxo and hydroxo ligands in the pentanuclear species probably result from residual water in the solvent. Finally, the reaction of $[Fe_3(\mathbf{22})_3(CH_3COO)_3]$ with three equivalents of 2-picolinic acid (H-pic) forms $[Fe_2(\mathbf{22})_3(pic)_2]$ which contains a $\{Fe_2^{III}(\mu_2\text{-}O)_2\}^{2+}$ core, where the iron centers are bridged by the ethoxo-type oxygen atoms from the $[\mathbf{22}]^{2-}$ ligand [52].

$[Fe_4(\mathbf{26})_4(CH_3COO)_2(OCH_3)_2]$ contains a $\{Fe_4^{III}(\mu_2\text{-}O)_6\}^{2+}$ core, where four of the bridging oxygen atoms are ethoxo-type oxygen atoms from $[\mathbf{26}]^{2-}$ and the other two are from additional μ_2-OCH_3 units. The iron centers are located on the vertexes of a rectangle with two long (3.5 Å) and two short (3.1 Å) Fe···Fe separations (Fig. 26a) [52].

$[Fe_5(\mathbf{22})_4(O)(OH)(p\text{-}NO_2C_6H_4COO)_4]$, $[Fe_5(\mathbf{25})_4(O)(OH)(CH_3COO)_4]$ and $[Fe_5(\mathbf{26})_4(O)(OH)(C_6H_5COO)_4]$ are also isostructural with an incomplete $\{Fe_5(\mu_3\text{-}O)_2(\mu_2\text{-}O)_5\}^+$ cubane core structure extended at one face by an incomplete adamantane unit. The five μ_2-oxygen atoms are from the Schiff

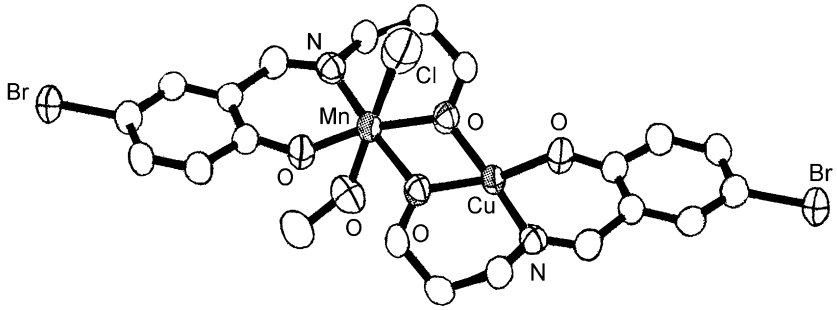

Fig. 25. Structure of [MnCu(**24**)$_2$(Cl)(CH$_3$OH)].

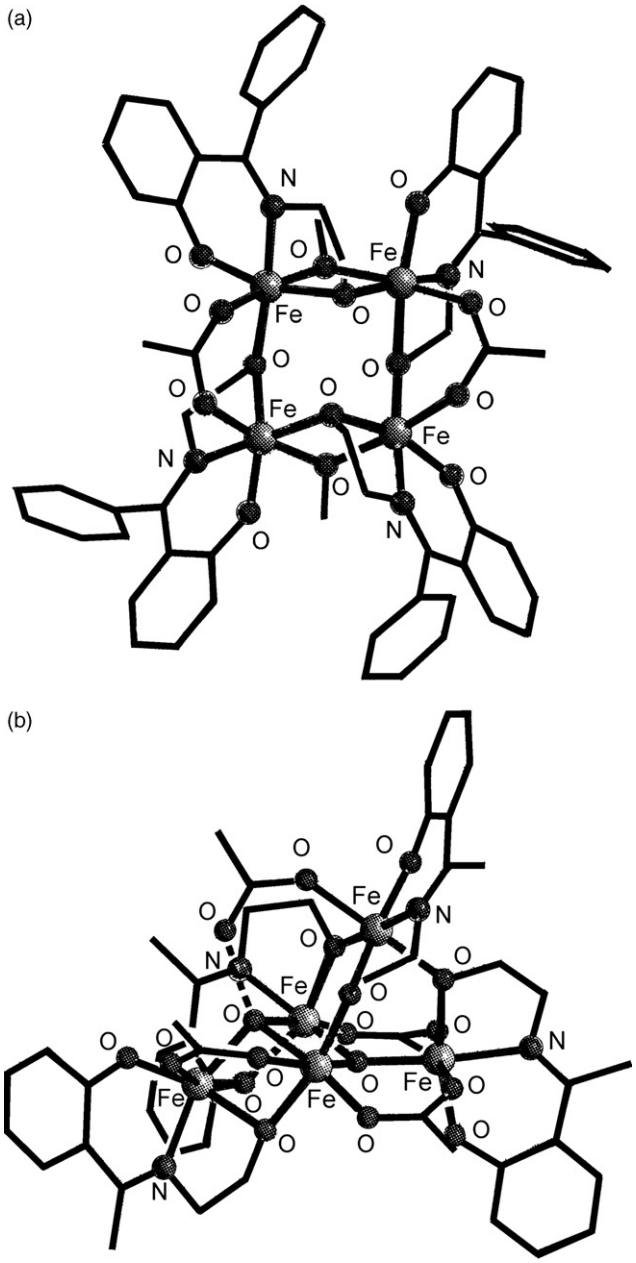

Fig. 26. Structure of [Fe$_4$(**26**)$_4$(CH$_3$COO)$_2$(OCH$_3$)$_2$] (a) and [Fe$_5$(**25**)$_4$(O)(OH)(CH$_3$COO)$_4$] (b).

base ligands and are ethoxo-type or phenoxo-type, while μ_3-bridges are oxo and hydroxo groups. The four carboxylato ligands provide additional bridges, three binding in the typical μ_2-mode, while the fourth binds in a terminal manner (Fig. 26b) [52].

Mössbauer data are consistent with five high spin iron(III) centers for each complex. Variable-temperature magnetic measurements indicate spin ground states of $S = 0$, 1/2, 0 and 5/2 for the bi-, tri, tetra- and pentanuclear complexes, respectively, and exclusively antiferromagnetic exchange interactions. In addition, an easy-axis-type magnetic anisotropy has been observed for the pentanuclear complexes. A low-temperature micro-SQUID study of one of the pentanuclear complexes reveals magnetization hysteresis at nonzero field, attributed to an anisotropy-induced energy barrier to magnetization and of molecular origin. Finally, an inelastic neutron scattering study of one of the trinuclear complexes has revealed that the magnetic behavior arises from two distinct species [52].

[Cu(H-**22**)$_2$] or [Cu(H-**27**)$_2$] and [Cu$_4$(**22**)$_4$], [Cu$_4$(**27**)$_4$], [Cu$_4$(H-**28**)$_4$] or [Cu$_4$(H$_2$-**29**)$_4$] have been synthesized from the reaction of copper(II) acetate with the related ligand ratio, respectively. In solution the mononuclear complexes can be converted in the corresponding tetranuclear ones by the addition of copper(II) acetate and, alternatively, the tetranuclear complexes to the corresponding mononuclear ones with the addition of the ligand. [Cu$_4$(**22**)$_4$] and [Cu$_4$(**27**)$_4$], but not [Cu(**22**)$_2$], exhibit ability to oxidize 3,5-di-*tert*-butylcathecol (DTBC) to the corresponding quinone (DTBQ) [53].

In [Cu$_4$(H$_2$-**29**)$_4$] a cubane like structure occurs while the structure of [Cu$_4$(**27**)$_4$] can be visualized as a pseudodouble cubane type, where both the cubes share a common face and in each cube one of the copper(II) corners is missing. Each copper center is five coordinates (Fig. 27a) [53].

When H$_2$-**27** was reduced to the corresponding amine derivative H$_2$-**30**, the tetranuclear pseudo-double cubane structure in [Cu$_4$(**27**)$_4$] was converted to a linear tetranuclear one in [Cu$_4$(H-**30**)$_2$(**30**)$_2$(CH$_3$OH)$_2$](CH$_3$COO)$_2$·4CH$_3$OH where the three interconnected Cu$_2$O$_2$ rhombi, formed through sharing two copper centers, exhibit a Cu$_4$O$_6$ chair type core structure. The resulting geometry around each copper(II) ion is distorted square pyramidal with Cu···Cu distances of 3.0–3.5 Å (Fig. 27b) [53].

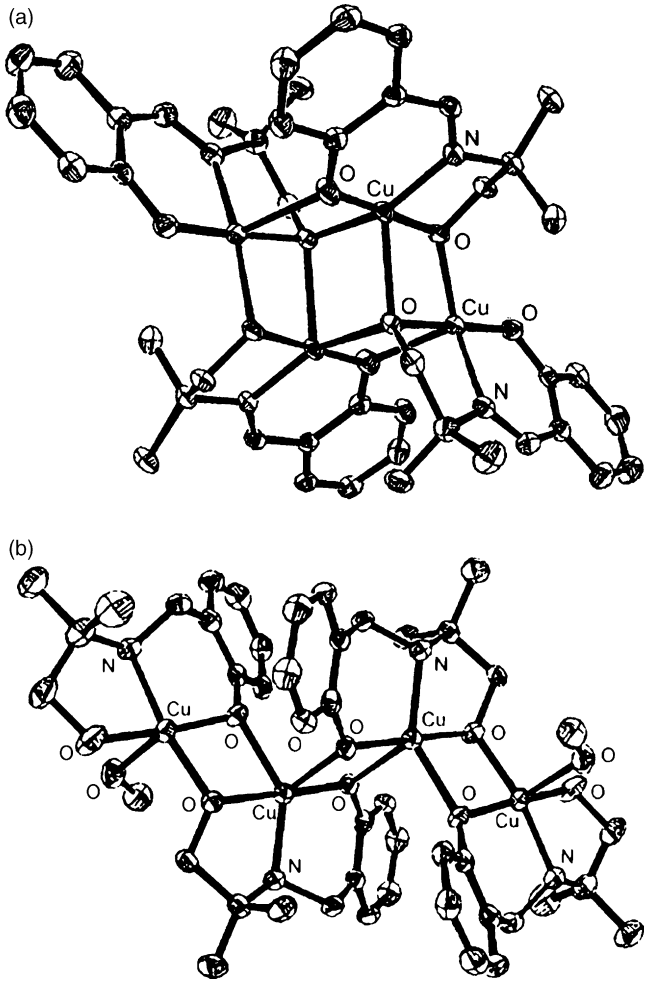

Fig. 27. Structure of $[Cu_4(\mathbf{27})_4]$ (a) and $[Cu_4(H\text{-}\mathbf{30})_2(\mathbf{30})_2(CH_3OH)_2]^{2+}$ (b).

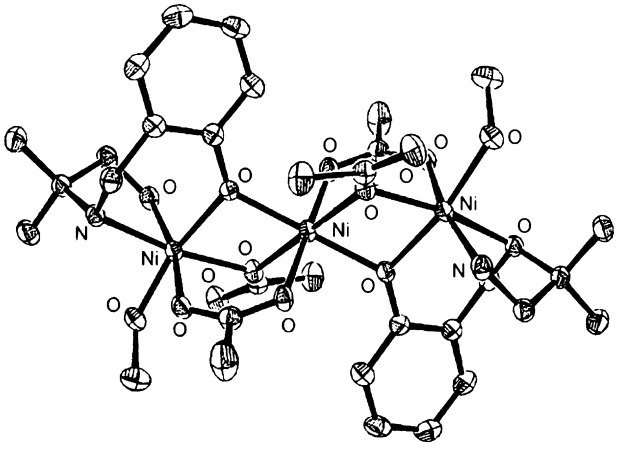

Fig. 28. Structure of $[Ni_3(H\text{-}\mathbf{30})_2(CH_3COO)_4(CH_3OH)_2]$.

Mononuclear and dinuclear nickel(II) complexes with H_2-**22**, H_2-**27**, H_3-**28** and H_4-**29** were synthesized from the reaction of 1:2 or 1:1 nickel acetate to ligand ratios. The more flexible reduced ligand H_2-**30** reacts with nickel(II) acetate in a 1:1: molar ratio to form $[Ni_3(H\text{-}\mathbf{30})_2(CH_3COO)_4(CH_3OH)_2]$. In these mono-, di-, and trinuclear complexes, each nickel(II) center is in a distorted octahedral environment. In $[Ni(H\text{-}\mathbf{22})_2]$ and $[Ni(H_2\text{-}\mathbf{28})_2]$ $[H\text{-}\mathbf{22}]^-$ and $[H_2\text{-}\mathbf{28}]^-$ act as tridentate ligands through the phenolate oxygen, the imine nitrogen atoms and alcoholic oxygen atoms [54].

In $[Ni_2(H\text{-}\mathbf{L})_2(CH_3COO)_2(H_2O)_2]$ (H_2-**L** = H_2-**22**, H_2-**27**) two phenoxo oxygen bridges the two octahedral nickel(II) centers, their coordination being completed by an imine nitrogen, an alkoxo, an acetate oxygen and a water molecule (Fig. 28a) while in $[Ni_3(H\text{-}\mathbf{30})_2(CH_3COO)_4(CH_3OH)_2]$ the two terminal nickel(II) ions are bridged through a phenoxo oxygen, a monodentate acetate and a bidentate acetate, to the central nickel(II) ion (Fig. 28b) [54].

Urea forms an adduct with these dinuclear complexes while pyridine gives rise to the corresponding mononuclear complexes, as found in $[Ni(H_2\text{-}\mathbf{28})(py)_3](CH_3COO)$ where the octahedral nickel(II) ion is bound to one ligand in tridentate fashion and to three pyridine molecules [54].

$[Cu_2(H\text{-}\mathbf{31})_2(\mu\text{-}CH_3OH)_2](ClO_4)_2$, obtained by $Cu(ClO_4)_2{\cdot}6H_2O$ and H_2-**31**, contains two distorted square pyramidal copper(II) centers which are strongly antiferromagnetically coupled [55].

H_2-**31a**$\cdot H_2O$ and H_2-**31b** react with $Cu(ClO_4)_2{\cdot}6H_2O$ and NaOH to form $[Cu_4(\mathbf{L})_4]$ with a cubane Cu_4O_4 core: four slightly distorted square pyramidal copper(II) ions and four oxygen atoms occupy the alternative vertices of the cube (Fig. 29) [56]. The same reaction in the presence of *o*-phenanthroline (phen) affords $[Cu_2(\mathbf{31b})_2(phen)_2](ClO_4)_2$, where the two highly distorted trigonal bipyramidal copper ions, separated by 3.147 Å, are doubly bridged by two phenoxides. In $[Cu_4(\mathbf{31a})_4]$, $[Cu_4(\mathbf{31b})_4]$ and $[Cu_2(\mathbf{31b})_2(phen)_2](ClO_4)_2$, the copper(II) ions are antiferromagnetic coupled [56].

In $[Cu(\mathbf{32})(L)]_2$, derived from the reaction of $[Cu(\mathbf{32})(H_2O)]$ with urea, pyridine, 2,4-dimethylpyridine, quinoline, 4-methylquinoline, isoquinoline, or 3-methylisoquinoline (L), two square pyramidal copper(II) ions, 3.109 Å apart, are bridged by two phenolate oxygen atoms which, together with the nitrogen atom of $[\mathbf{32}]^-$ and an oxygen atom of urea, form the basal plane around each copper(II) ion, while the apical site is occupied by a bridging phenolate oxygen atom from a neighboring molecule. Some of these complexes show a significant micro bacterial activity [57].

The two helical polymeric copper(II) complexes [Cu(H-**L**)(bipy)](Cl)$\cdot 2H_2O$, synthesized by reaction of $Cu_2Cl_2{\cdot}2H_2O$ with 2,2′-bipyridine and H_2-**L** (H_2-**32** or H_2-**33**), reveal similar structures with each distorted octahedral copper(II) ion is coordinated by two nitrogen atoms of 2,2′-bipyridine, one nitrogen atom and one oxygen atom of $[H\text{-}\mathbf{L}]^-$, another oxygen atom of an adjacent $[H\text{-}\mathbf{L}]^-$. Along the helical chain, the neighboring copper(II) centers, 6.06 Å or 6.26 Å apart, are linked by carboxyl groups of $[H\text{-}\mathbf{32}]^-$ in triatomic anti-anti configuration (Fig. 30). A ferromagnetic interaction between the copper(II) ions operates in [Cu(H-**32**)(bipy)](Cl)$\cdot 2H_2O$ ($J = 1.70\,cm^{-1}$) while a paramagnetic behavior was found in [Cu(H-**33**)(bipy)](Cl)$\cdot 2H_2O$ [58].

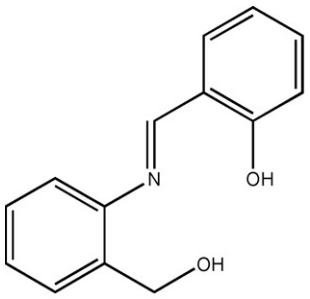

H_2-**20**

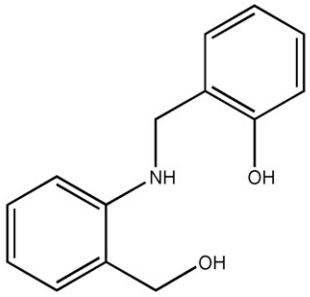

H_2-**21**

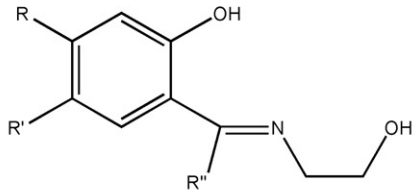

	R	R'	R"
H_2-**22**	H	H	H
H_2-**23**	OH	H	H
H_2-**24**	H	Br	H
H_2-**25**	H	H	CH_3
H_2-**26**	H	H	C_6H_5

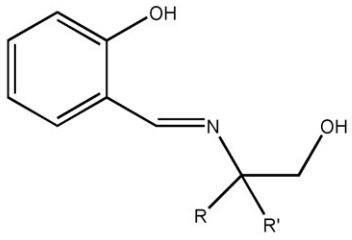

	R	R'
H_2-**27**	CH_3	CH_3
H_3-**28**	CH_3	CH_2OH
H_4-**29**	CH_2OH	CH_2OH

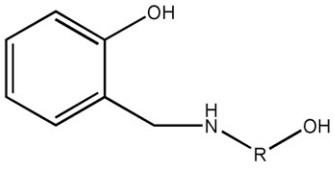

	R
H_2-**30**	$C(CH_3)_2CH_2$
H_2-**31a**	$(CH_2)_2$
H_2-**31b**	$(CH_2)_3$

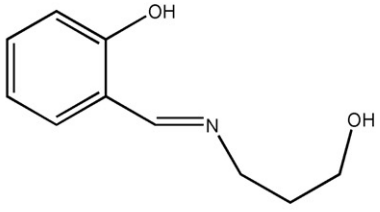

H_2-**31**

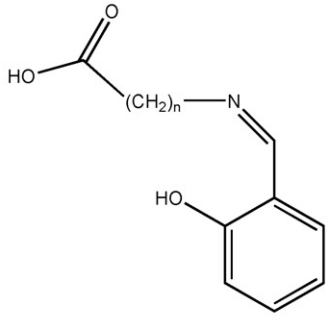

	n
H_2-**32**	1
H_2-**33**	2

H_2-**34**···H_2-**42** form $[Cu_2(\mathbf{L})_2(H_2O)_x]\cdot yH_2O$ ($x = 0$–2, $y = 0$–2), when reacted with $Cu(CH_3COO)_2\cdot 2H_2O$ in the presence of LiOH. $[Cu_2(\mathbf{35})_2(H_2O)_2]\cdot 2H_2O$ and $[Cu_2(\mathbf{35})_2(H_2O)_2]\cdot 2H_2O$ contain two square pyramidal copper(II) centers at a Cu···Cu distance of 2.974 Å and 3.004 Å, respectively. On the contrary, $[Cu_2(\mathbf{35})_2(H_2O)]_n$ and $[Cu_2(\mathbf{42})_2(H_2O)]_n$ are one dimensional polymers with the dinuclear copper fragment $\{Cu_2(\mathbf{L})_2\}$ as a building block. Both copper(II) ions are in a distorted square pyramidal geometry: a water molecule is coordinated to one copper(II) ion while the neighboring carbonyl oxygen atom is coordinated to the other copper(II) ion to form a helical polymer (Fig. 31). $[Cu_2(\mathbf{35})_2(H_2O)_2]\cdot 2H_2O$ and $[Cu_2(\mathbf{42})_2(H_2O)]\cdot 2H_2O$ show a moderately strong antiferromagnetic coupling. All the complexes with H_2-**34**···H_2-**42** show significant catalytic activity on the oxidation of 3,5-di-*tert*-butylcatechol to the corresponding quinone derivatives, which increases with increasing the length of the aliphatic chain R [59].

The condensation of glycylglycine and 2-hydroxypropiophenone in presence of $CuCl_2\cdot 2H_2O$ and

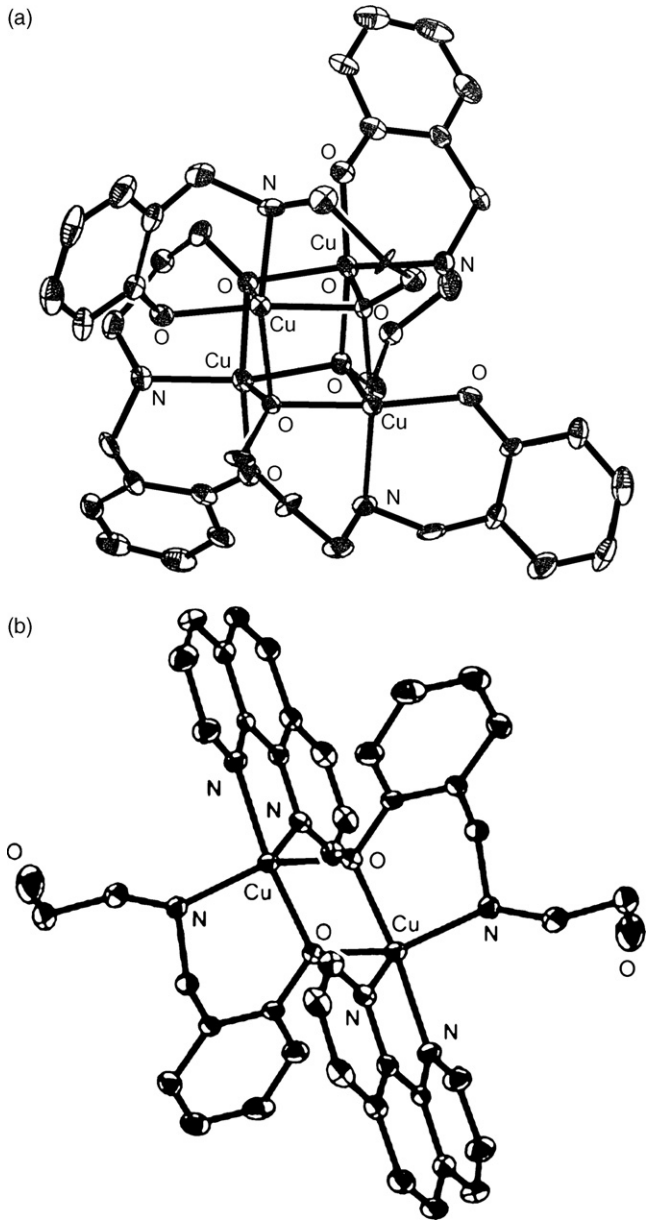

Fig. 29. Structure of $[Cu_4(\mathbf{31a})_4]$.

LiOH, followed by the addition of $BaCl_2{\cdot}2H_2O$, produces $[BaCu_2(\mathbf{43})_2(H_2O)_3]{\cdot}2H_2O$, where each copper(II) center is square planar while the barium(II) ion is eight coordinate. One $[Cu(\mathbf{43})]^-$ anion acts as a tridentate unit while the other $[Cu(\mathbf{43})]^-$ anion as a monodentate unit toward the barium ion. The Cu···Cu distance is 3.622 Å. Furthermore, the carboxylate oxygen atom of the tridentate $[Cu(\mathbf{43})]^-$ unit bridges also an adjacent barium(II) ion to form the rungs of the ladder. The nearest Ba···Ba distance is 4.307 Å (Fig. 32). The temperature dependence of magnetic susceptibility of $[BaCu_2(\mathbf{43})_2(H_2O)_3]{\cdot}2H_2O$ indicates an overall ferromagnetic coupling confirmed by the field dependence of isothermal magnetization performed at 1.8 K. At 7.3 K a weak antiferromagnetic coupling between the ferromagnetic units occurs. The ferromagnetic coupling was ascribed to the coordination bonds between $[Cu(\mathbf{43})]^-$ and the barium(II) ion and the antiferromagnetic coupling to the interchain interactions. Since the ferromagnetic coupling is much stronger than the antiferromagnetic one, the magnetic data were interpreted in terms of the ferromagnetic dimer model with a weak interdimer antiferromagnetic interaction [60].

The isostructural complexes $[Ln_2^{III}Cu_4^{II}(\mathbf{44})_4(H_2O)_{10}][Cu(\mathbf{44})]_2$ (Ln = La, Ce), prepared by condensation of glycylglycine and 5-bromo-salicyladehyde followed by the addition of $CuCl_2{\cdot}2H_2O$ and $LnCl_3{\cdot}nH_2O$, contains three types of $[Cu(\mathbf{44})]^-$ subunits where the copper(II) ion is square planar: one acts as a counter anion; another coordinates to the lanthanide(III) ions through one carboxylate oxygen and one carbonyl oxygen, and the third coordinates to the lanthanide(III) ions through two carboxylate oxygen atoms. The lanthanide ions are nine coordinate. The nearest La···La distance is 8.093 Å. Extensive hydrogen bonding forms a three-dimensional network in the solid state (Fig. 33a) [61]. In the La_2Cu_4 complex a ferromagnetic coupling between the copper(II) ions operates with a weak antiferromagnetic coupling between the hydrogen bonded ferromagnetic units, while in the Ce_2Cu_4 complex an antiferromagnetic interaction occurs [61].

H_3-**44**, derived from the condensation of 5-bromosalicylaldehyde and glycylglycine, gives rise to $[BaCu_2(\mathbf{44})_2(H_2O)_4]_n$ when reacted under basic conditions with $CuCl_2{\cdot}2H_2O$ and $BaCl_2{\cdot}2H_2O$. Each $[\mathbf{44}]^{3-}$ ligand coordinates to a square planar copper(II) ion while the barium(II) ion is ten coordinated by four water molecules and six carboxylate oxygen atoms. $[Cu(\mathbf{44})]^-$ coordinates to the barium ions as bidentate unit, forming an infinite one-dimensional chain. A two dimensional network structure arises from $[Cu(\mathbf{44})]^-$-Ba chains, via inter-chain hydrogen bonds (Fig. 33b) [62].

Glycyl-L-tyrosine and 5-bromosalicylaldehyde, in the presence of NaOH, $Cu(CH_3COO)_2{\cdot}H_2O$ and $SrCl_2{\cdot}6H_2O$, afford $\{[NaSrCu_3(\mathbf{45})_3(H_2O)_3]{\cdot}9H_2O\}_\infty$; three $[Cu(\mathbf{45})]^-$ units act as bidentate ligands toward the strontium ion through their carboxylate oxygen atoms, resulting in a tetranuclear subunit with a Sr···Cu separations of 4.373 Å. The three square planar copper(II) ions are arranged at the corners of an equilateral triangle with the Cu···Cu distance of 7.516 Å. The coordination sphere of the strontium(II) ion is completed by three aqua ligands. The six coordinate sodium ions connect two adjacent tetranuclear subunits, leading to a 1D chiral propeller-like polymeric chain self-assembly. Each chain is surrounded by six neighboring chains linked together by hydrogen bonds (Fig. 34). Magnetic measurements prove a ferromagnetic interaction between adjacent copper ions [63].

Glycylglycylglycine and salicylaldehyde, in the presence of KOH and copper(II) acetate, form K[Cu(H-**46**)]·$2H_2O$. The further addition of $MgSO_4$ or $Cu(NO_3)_2{\cdot}6H_2O$ gives rise to $[Mg(H_2O)_6][Cu(\text{H-}\mathbf{46})]_2{\cdot}3.5H_2O$ or $[Cu_2Cd(\text{H-}\mathbf{46})_2(H_2O)_4]{\cdot}3.5H_2O$, respectively. In both complexes an antiferromagnetic interaction operates [64].

$[Mg(H_2O)_6][Cu(\text{H-}\mathbf{46})]_2{\cdot}3.5H_2O$, where the two square planar copper(II) centers are 4.67 Å, apart, contains an octahedral magnesium(II) ion and two $[Cu(\text{H-}\mathbf{46})]^-$ almost parallel anions [64].

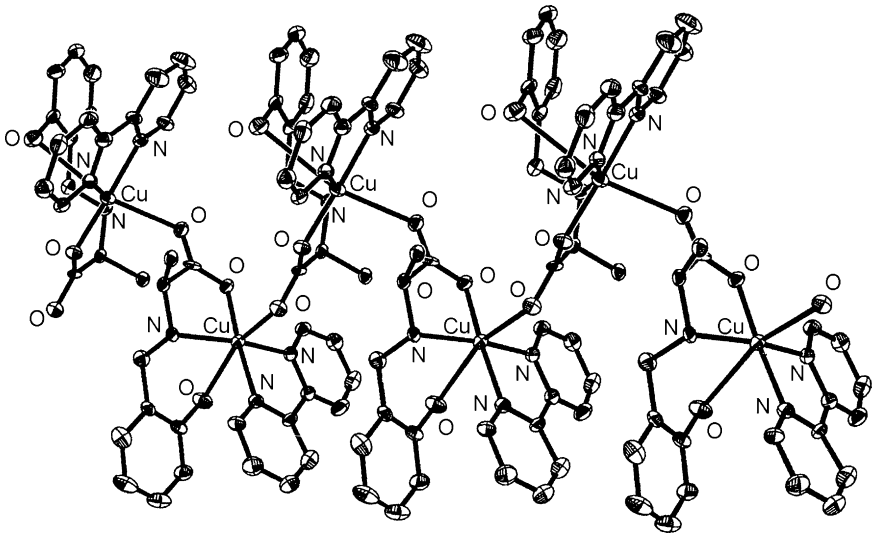

Fig. 30. Structure of $\{[Cu(H\text{-}\mathbf{33})(bipy)]^{+}\}_n$.

In $[Cu_2Cd(H\text{-}\mathbf{46})_2(H_2O)_4]\cdot 3.5H_2O$ (Fig. 35) each $[Cu(H\text{-}\mathbf{46})]^{-}$ unit coordinates to the approximately octahedral cadmium(II) ion via one carboxylate oxygen atom in a *syn*-anti-bridging mode. The interaction between copper(II) ions and imino nitrogen atom of an adjacent $[Cu(H\text{-}\mathbf{46})]^{-}$ group gives rise to a 2D hydrogen-bonded network. The distance between the two copper(II) ions is 3.422 Å [64].

H-**47**·HCl and copper(II) salts furnish $[Cu(\mathbf{47})_2]\cdot 2H_2O$ with a distorted octahedral *trans*-N_4O_2 copper(II) ion. $[Cu_6(\mathbf{47})_3(\mathbf{48})_3](ClO_4)_6\cdot 9H_2O$, isolated from the reaction of $[Cu(\mathbf{47})_2]\cdot 2H_2O$ with $Cu(ClO_4)_2\cdot 6H_2O$, contains the amino derivative $[\mathbf{47}]^{-}$ and, surprisingly the related Schiff base ligand $[\mathbf{48}]^{-}$. The copper(II) centers forms a cyclohexane-like ring, where all the $[\mathbf{47}]^{-}$ ligands are distributed on one face of the metallocyclic ring, and the ligands $[\mathbf{48}]^{-}$ are on the other face. The adjacent Cu···Cu distance in the ring is 9.424 Å (Fig. 36) [65].

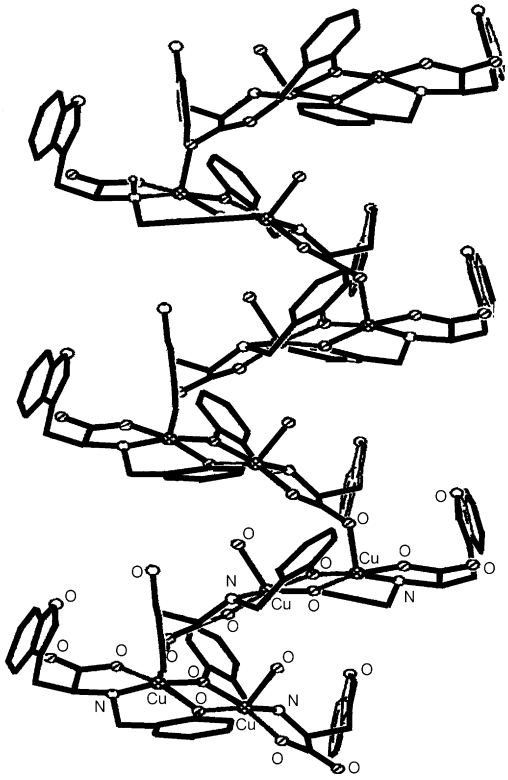

Fig. 31. Structure of $[Cu_2(\mathbf{41})_2(H_2O)]_n$.

The basic unit of $[K(ClO_4)_3\{Cu_3(\mathbf{49})_3\}](ClO_4)$, derived from $Cu(ClO_4)_2\cdot 6H_2O$, H-**49** and KOH, consists of a trimer formed by the cyclisation of $\{Cu(\mathbf{49})\}$ moieties which contain square planar copper(II) ions. The highly distorted pentagonal bipyramidal potassium(I) ion is found above the Cu_3 plane, bonded to three oxygen atoms of the $[Cu_3(\mathbf{49})_3]^{3+}$ anion and to the oxygen atoms of three perchlorate ions, which further interact with the $\{Cu_3(\mathbf{49})_3\}^{3+}$moiety (Fig. 37) [65].

When NaOH is used instead of KOH, a mixture of $[Na(ClO_4)_3\{Cu_3(\mathbf{49})_3\}](ClO_4)$ and the 1D polymeric compound $\{[Cu(\mathbf{49})(H_2O)](ClO_4)\}_n$ was isolated while LiOH and CsOH afford only $\{[Cu(\mathbf{49})(H_2O)](ClO_4)\}_n$, which also shows a meridional conformation with an aqua oxygen strongly bonded to the apex to form a distorted square pyramidal geometry at the metal center [65].

H-**50**, derived from the condensation of *o*-vanillin with *N*,*N*-dimethylethylenediamine, reacts with the appropriate nickel(II) salt to give $[Ni_2(\mathbf{50})_2(\mu_{1,1}\text{-}N_3)(N_3)(H_2O)]\cdot H_2O$, $\{[Ni_2(\mathbf{50})_2(\mu_{1,1}\text{-}NCS)(NCS)(H_2O)][Ni_2(\mathbf{50})_2(\mu\text{-}CH_3COO)(NCS)(H_2O)]\}$, $\{[Ni_2(\mathbf{50})_2(\mu_{1,1}\text{-}NCO)(NCO)(H_2O)]\cdot H_2O$. In these complexes, one of the two Schiff bases acts as a tetradentate ligand, while the other as tridentate with a nonbonded methoxy group [66].

$[Ni_2(\mathbf{50})_2(\mu_{1,1}\text{-}N_3)(N_3)(H_2O)]\cdot H_2O$ contains two octahedral nickel(II) ions, bridged by one azide anion in end-on fashion through the nitrogen atom and by μ_2-phenolate oxygen atom of the Schiff base (Fig. 38) [66]. In both the dinuclear units of $\{[Ni_2(\mathbf{50})_2(\mu_{1,1}\text{-}NCS)(NCS)(H_2O)][Ni_2(\mathbf{50})_2(\mu\text{-}CH_3COO)(NCS)(H_2O)]\}$, two pseudo-octahedral nickel(II) centers, respectively 3.328 Å

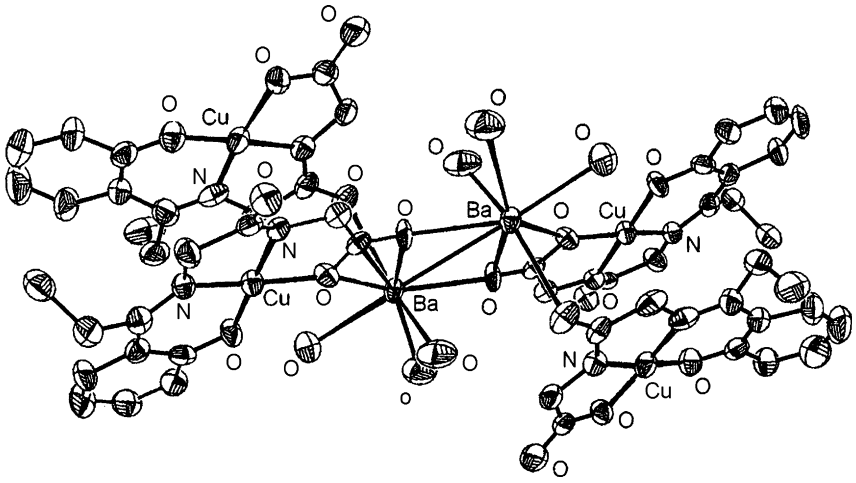

Fig. 32. Structure of $[BaCu_2(\mathbf{43})_2(H_2O)_3]_n$.

and 3.344 Å apart, one with a N_4O_2 donor set and the other with a N_3O_3 donor set, are held together by both an isothiocyanate group in a $\mu_{1,1}$-end-on fashion via a nitrogen atom and a μ_2-phenolate oxygen atom of a Schiff base ligand. $[Ni_2(\mathbf{50})_2(\mu_{1,1}\text{-NCO})(NCO)(H_2O)]\cdot H_2O$ and $[Ni_2(\mathbf{50})_2(\mu_{1,1}\text{-}N_3)(N_3)(H_2O)]\cdot H_2O$ are isostructural, the only difference being the OCN^- anion in the former instead of the N_3^- anion in the latter. The Ni···Ni distance is 3.305 Å [66]. In $[Ni_2(\mathbf{50})_2(\mu_{1,1}\text{-}N_3)(N_3)(H_2O)]\cdot H_2O$ a strong ferromagnetic coupling occurs, while $[Ni_2(\mathbf{50})_2(\mu_{1,1}\text{-NCO})(NCO)(H_2O)]\cdot H_2O$ and

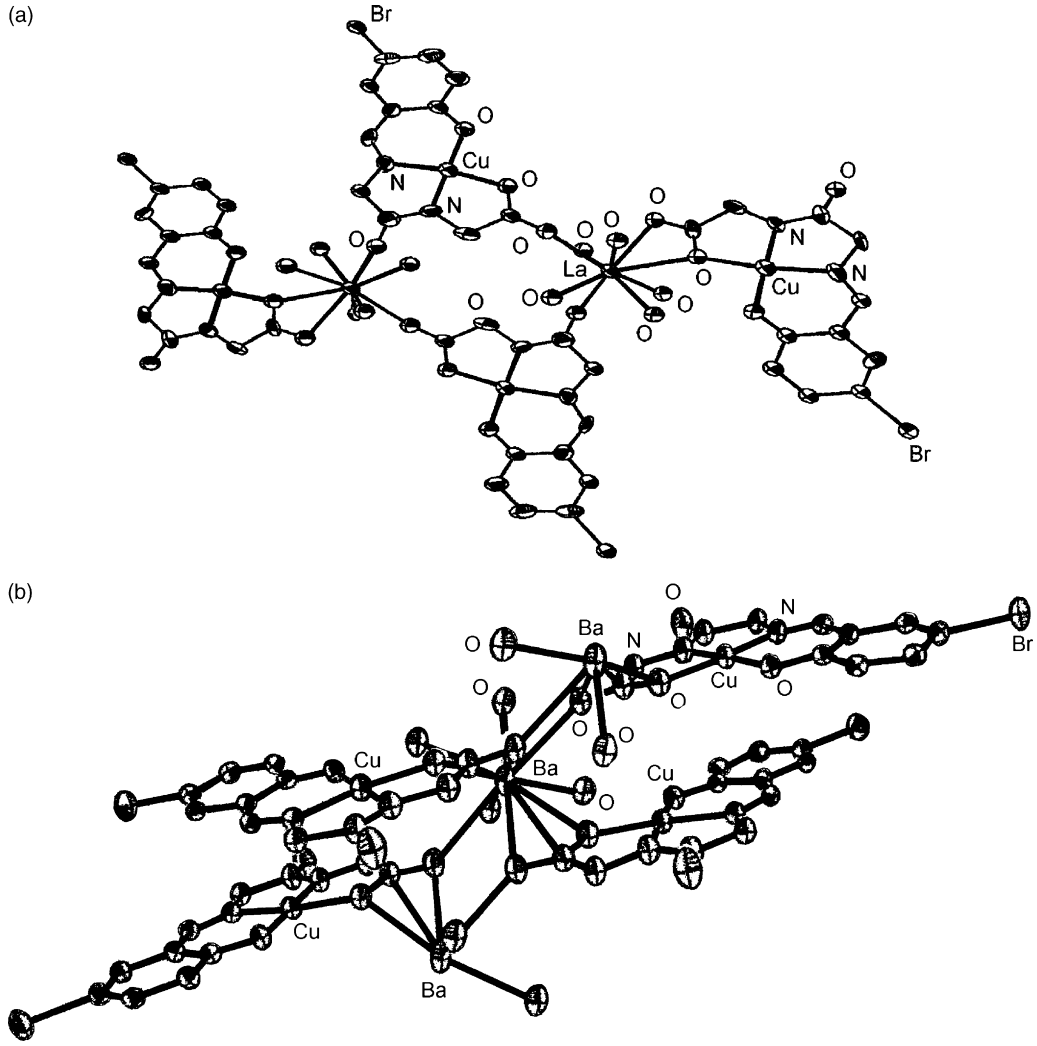

Fig. 33. Structure of $[La_2Cu_4(\mathbf{44})_4(H_2O)_{10}]^{2+}$ (a) and $[BaCu_2(\mathbf{44})_2(H_2O)_4]_n$ (b).

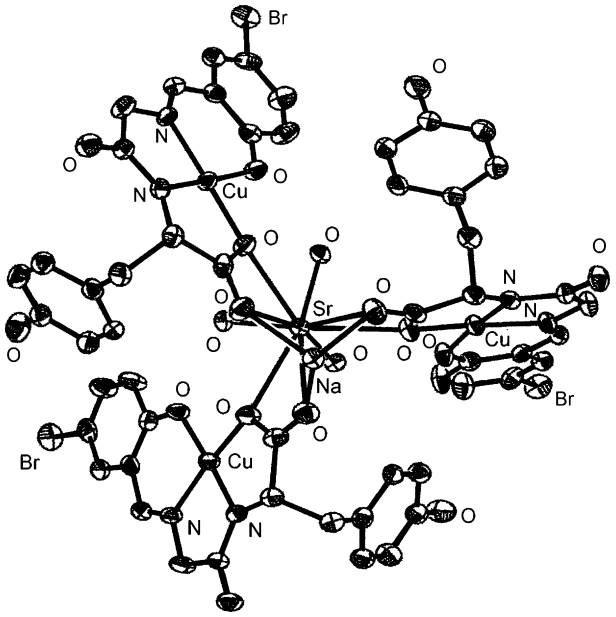

Fig. 34. Structure of $\{[NaSrCu_3(\mathbf{45})_3(H_2O)_3]\cdot 9H_2O\}_\infty$.

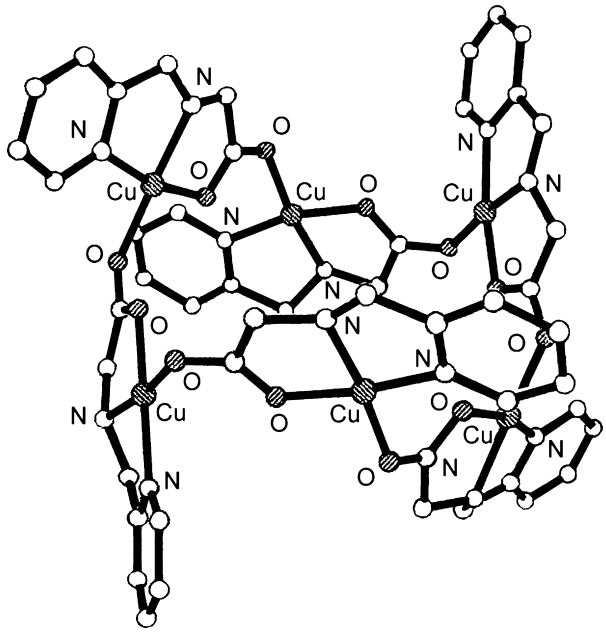

Fig. 36. Structure of $[Cu_6(\mathbf{47})_3(\mathbf{48})_3]^{6+}$.

$\{[Ni_2(\mathbf{50})_2(\mu_{1,1}\text{-NCS})(NCS)(H_2O)][Ni_2(\mathbf{50})_2(\mu\text{-}CH_3COO)(NCS)(H_2O)]\}$ show a weak ferromagnetic and a weak antiferromagnetic coupling, respectively [66].

H-**50** reacts with the appropriate salts to form $[Zn(H\text{-}\mathbf{50})_2(NCS)][Zn_2(\mathbf{50})(\mu_{1,1}\text{-}CH_3COO)(NCS)_3]$, $[Cd_2(\mathbf{50})_2(Cl)_2]$ and $[Cd_2(\mathbf{50})_2(NCS)_2]$ [67]. In $[Zn(H\text{-}\mathbf{50})_2(NCS)][Zn_2(\mathbf{50})(\mu_{1,1}\text{-}CH_3COO)(NCS)_3]$, $[Zn(H\text{-}\mathbf{50})_2(NCS)]^+$ contains a five coordinate N_3O_2 distorted trigonal bipyramidal zinc(II) while in $[Zn_2(\mathbf{50})(\mu_{1,1}\text{-}CH_3COO)(NCS)_3]^-$, one zinc(II) ion has an N_3O_2 donor set and the other zinc(II) ion an N_2O_3 donor set. The two metal centers are bridged by a $\mu_{1,3}$-acetate ligand through the oxygen atoms in *syn–syn* fashion and by the μ_2-phenolate oxygen atom of the Schiff base ligand. One zinc(II) ion exhibits a distorted square pyramidal geometry: the five coordination sites are occupied by the imino and amino nitrogen atoms, two oxygen atoms from phenoxo and acetato bridges respectively and one nitrogen from the thiocyanate ligand. The other zinc(II) ion, in a distorted trigonal bipyramidal environment, is coordinated by two nitrogen atoms from two thiocyanato ligands, one methoxy oxygen and two bridging oxygen atoms [67].

$[Cd_2(\mathbf{50})_2(Cl)_2]$ and $[Cd_2(\mathbf{50})_2(NCS)_2]$ show a very similar dinuclear structure with two equivalent cadmium(II) centers, each with a terminal chloride or thiocyanate ligand and a tridentate Schiff base $[\mathbf{50}]^-$, bonded through the imine nitrogen, the amine nitrogen and the phenoxide oxygen [67].

In $[La(H\text{-}\mathbf{50a})_3(NO_3)_3]$, derived from the condensation of 3-methoxy-2-hydroxybenzaldehyde and aniline in the presence of $La(NO_3)_3\cdot 5H_2O$ [68], the lanthanum(III) ion is 12 coordinate with six oxygen atoms from the phenoxo groups and the methoxy sidearm of the three Schiff base ligands and six oxygen atoms from three bidentate nitrato anions. The three protonated nitrogen atoms are intramolecularly hydrogen bonded with the deprotonated phenol oxygen atoms [68].

$[UO_2(\mathbf{51})_2(THF)_2]_2$, obtained by the reaction of H_2-**51** with $UO_2(NO_3)_2\cdot 6H_2O$ and KOH, contains two approximately pentagonal bipyramidal uranium(VI) ions, coordinated by six oxygen and one nitrogen and bridged by two phenoxo ligands [69].

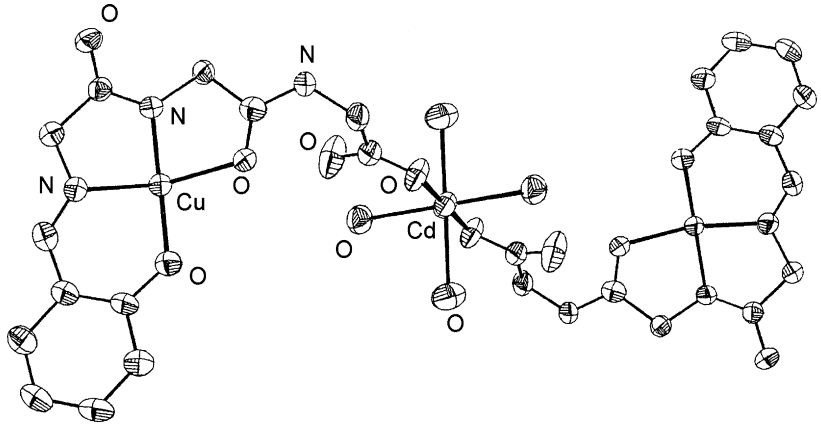

Fig. 35. Structure of $[Cu_2Cd(H\text{-}\mathbf{46})_2(H_2O)_4]$.

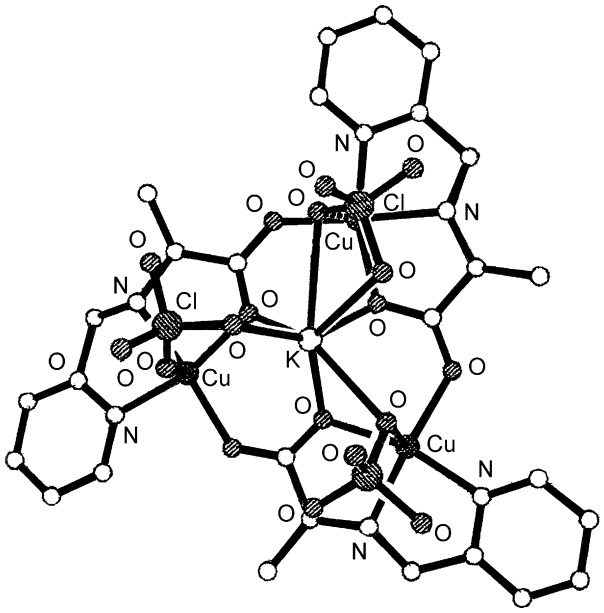

Fig. 37. Structure of $[K(ClO_4)_3\{Cu_3(\mathbf{49})_3\}]^+$.

$[Mn_3^{III}Mn^{II}Ca^{II}(\mathbf{51a})_3(\mu_4\text{-}O)(Cl)_2(CH_3COO)_{1.2}(H_2O)_{1.5}(CH_3OH)_{0.3}](Cl_{0.8})\cdot 5CH_3OH$, $[Mn_3^{III}Mn^{II}Na^{I}(\mathbf{51a})_3(\mu_3\text{-}O)(N_3)_{2.7}(CH_3COO)_{1.3}(CH_3OH)_{0.3}]\cdot 2CH_3OH\cdot 5H_2O$ and $[\{Mn_4^{III}Na^{I}(H\text{-}\mathbf{51b})_4(\mu_3\text{-}O)(N_3)_3(CH_3OH)_2](Cl)\cdot 3CH_3OH$, are readily obtained when divalent manganese salts react with the ligands H_2-**51a** or H_3-**51b** in the presence of triethylamine and either $CaCl_2$ or NaN_3. The two Schiff bases are formed by the in-situ condensation of *o*-vanillin with 2-hydroxypropylamine or 2-aminopropan-1,3-diol, respectively [70].

The central core of $Mn_3^{III}Mn^{III}Ca^{II}$ and $Mn_3^{III}Mn^{II}Na$ complexes consists of three manganese(III) centers, chelated by $[\mathbf{51a}]^{2-}$ via the deprotonated phenol and propanol oxygen atoms and the imino nitrogen. Two monodentate ligands, (μ-Cl) in the $Mn_3^{III}Mn^{II}Ca^{II}$ complex or (μ,η^1-N_3) in the $Mn_3^{III}Mn^{II}Na^{I}$ one and a bidentate acetate provide further bridges between these three Mn^{III} centers to give an isosceles Mn_3O triangle with

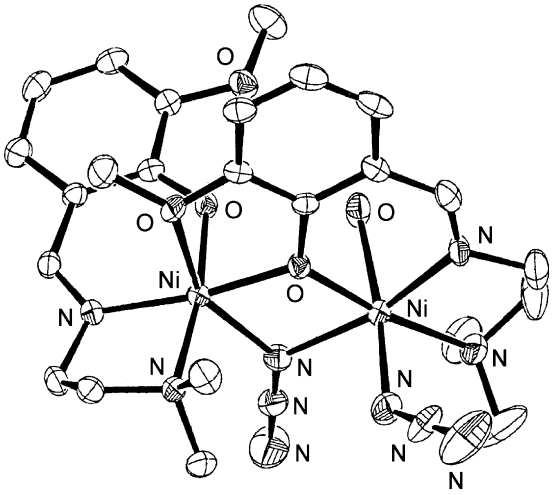

Fig. 38. Structure of $[Ni_2(\mathbf{50})_2(\mu_{1,1}\text{-}N_3)(N_3)(H_2O)]$.

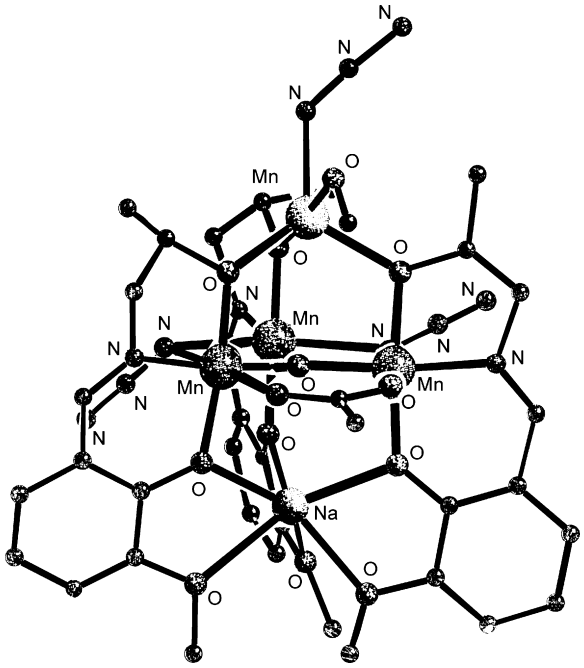

Fig. 39. Structure of $[Mn_3^{III}Mn^{IV}Na(\mathbf{51a})_3(\mu_3\text{-}O)(N_3)_{2.7}(CH_3COO)_{1.3}(CH_3OH)_{0.3}]$.

two shorter Mn···Mn distances and one longer. Two deprotonated phenol oxygen atoms and one deprotonated propanol oxygen bridge to the manganese(II) ion with a terminal chloride completing the coordination sphere. Conversely, two deprotonated propanol and one deprotonated phenol oxygen atoms bridge to the calcium(II) cation, which is further legated by the central oxo ligand, a water and a disordered mixed monodentate ligand [70]. In the $Mn_3^{III}Mn^{II}Na^{I}$ complex the three ligands are oriented mutually parallel. The three deprotonated propanol oxygen atoms each bridge between their respective manganese(III) and the manganese(II) centre, while on the other side of the Mn_3O triangle the three deprotonated phenol oxygen atoms each bridge to the sodium(I) ion with the three methoxy groups providing additional chelation of the sodium cation. The coordination sphere of the manganese(II) ion is completed by a methanol ligand and a disordered mixed anion (70% N_3/30% acetate) (Fig. 39) [70].

In the $Mn_4^{III}Na$ complex two ligands $[H\text{-}\mathbf{51b}]^-$ adopt the same structural motif as in the $Mn_3^{III}Mn^{II}Na$ one with their alkoxo oxygen atoms bridging to the apical manganese(III) ion and the deprotonated phenol and methoxy oxygen atoms legating the sodium cation. An end-on azide ligand bridges the second short edge of the Mn_3O unit, while the long edge is occupied by a hydrogen bond from a methanol ligand to the deprotonated phenol oxygen of the parallel ligand. The fourth ligand chelates the apical manganese(III) ion with its alkoxo oxygen forming the remaining bridge to the Mn_3O triangle. A ($\mu_{1,3}$-η^1,η^1-N_3) ligand bridges between two apical manganese(III) ion of neighboring molecules, forming a weak dimer (Fig. 40) [70]. Magnetic susceptibility measurements indicate the presence of dominating antiferromagnetic interaction between the manganese ions in these pentanuclear complexes [70].

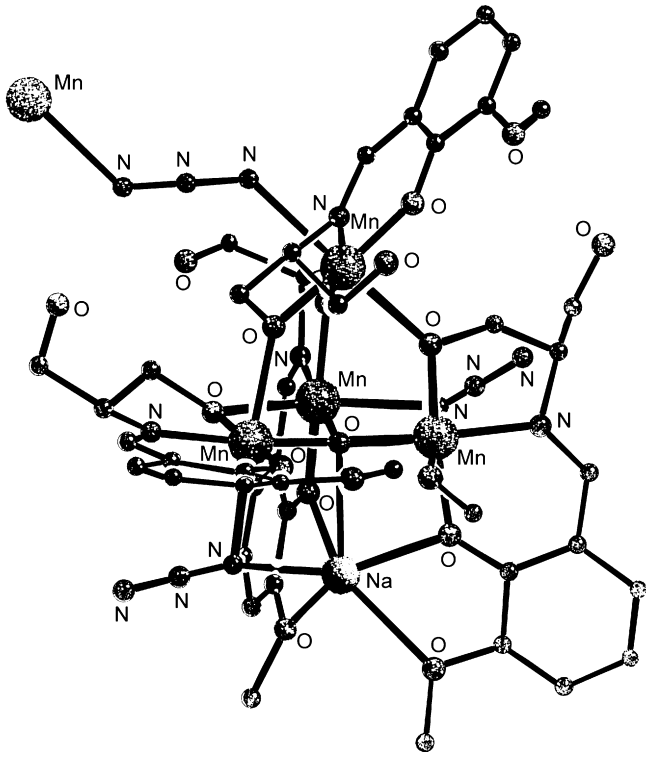

Fig. 40. Structure of $[\{Mn_4{}^{III}Na(H\text{-}\mathbf{51b})_4(\mu_3\text{-}O)(N_3)_3(CH_3OH)\}_2]^+$.

Glycylglycine, *o*-vanillin and LiOH react with $CuCl_2{\cdot}2H_2O$ and then with $AgNO_3$ to form [CuAg(**52**)]. The Schiff base ligand $[\mathbf{52}]^{3-}$ coordinates to the approximately square planar copper(II) ion, giving rise to a $[Cu(\mathbf{52})]^-$ anion. The three coordinate silver(I) ion is in a distorted T-shaped O_3 coordination environment. The $[Cu(\mathbf{52})]^-$ anions coordinate to the silver ions as a tridentate unit forming a infinite one-dimensional ribbon (Fig. 41) [71].

H_2-**53a**, oxalic acid and copper(II) perchlorate lead to $[Cu_2(\mathbf{53a})(C_2O_4)]$ where the two copper ions, 5.482 Å apart, are connected by the oxalato group in a bisbidentate bridging mode. Each distorted square pyramidal copper ion is coordinated by two oxygen atoms arising from the oxalato bridge, one phenolic oxygen and two nitrogen atoms arising from the organic ligand (one nitrogen atom from the azomethine group, and the other one from pyridyl ring). The magnetic data agree with an antiferromagnetic coupling between the two copper(II) ions ($J = -9.0\,cm^{-1}$) [72].

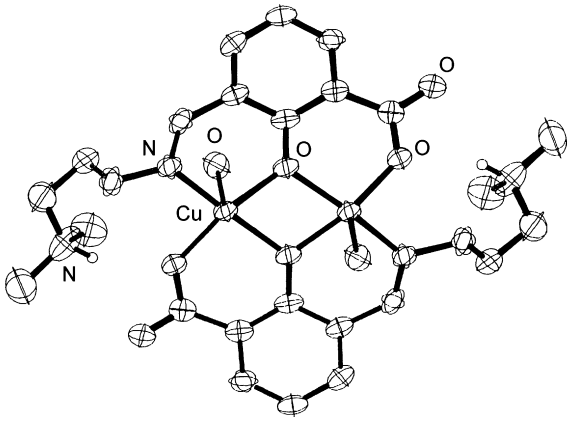

Fig. 42. Structure of $[Cu_2(\mathbf{53b})_2(H_2O)_2]^{2+}$.

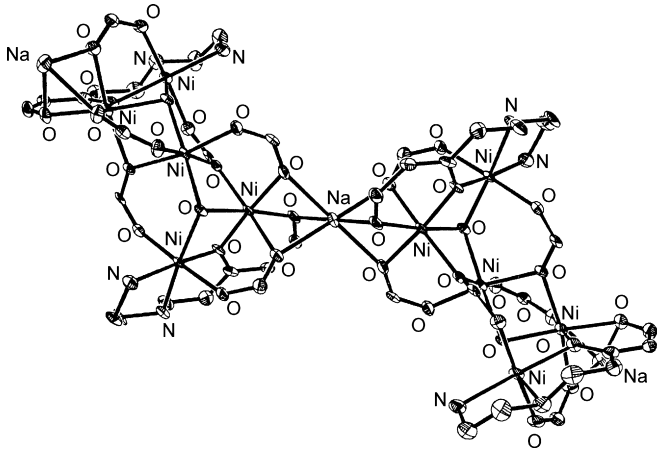

Fig. 43. Structure of $[Ni_5Na(\mathbf{55a})_2(CH_3COO)_6(OH)_2]_2{}^{2+}$.

The formation of $[Cu_4Mn(\mathbf{53a})_4](ClO_4)_2{\cdot}2H_2O$ from $[Cu_2(\mathbf{53a})_2]$ and manganese(II) perchlorate was verified by ESI-mass spectrometry, where the peaks due to $[Cu_4Mn(\mathbf{53a})_4(ClO_4)]^+$, $[Cu_4Mn(\mathbf{53a})_4(H_2O)_4]^+$ and $[Cu_4Mn(\mathbf{53a})_4]^{2+}$ have been detected. Cryomagnetic investigations reveal antiferromagnetic interactions between the copper(II) and manganese(II) ions ($J = -9.7\,cm^{-1}$) [73].

$CuCl_2{\cdot}2H_2O$ and H_2-**53b** in the presence of base produce $[Cu_2(H\text{-}\mathbf{53b})_2(H_2O)_2](ClO_4)_2$ where the uncoordinated tertiary amino groups are protonated. The square pyramidal copper ions are 3.008 Å apart (Fig. 42). A Cryomagnetic investigation reveals a strong antiferromagnetic coupling between the two copper(II) ions [74].

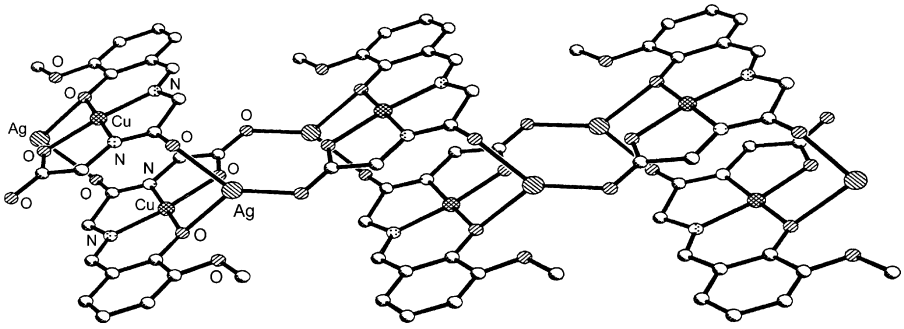

Fig. 41. Structure of [CuAg(**52**)].

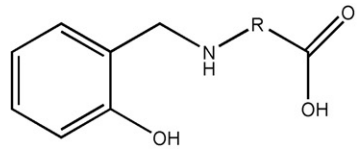

	R
H_2-**34**	CH_2
H_2-**35**	$CH(CH_3)$
H_2-**36**	$C(CH_3)_2$
H_2-**37**	$(CH_2)_2$
H_2-**38**	$(CH_2)_3$

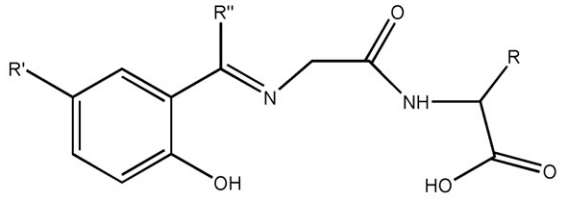

	R	R'	R"
H_3-**43**	H	H	CH_2CH_3
H_3-**44**	H	Br	H
H_3-**45**	p-C_6H_4OH	Br	H

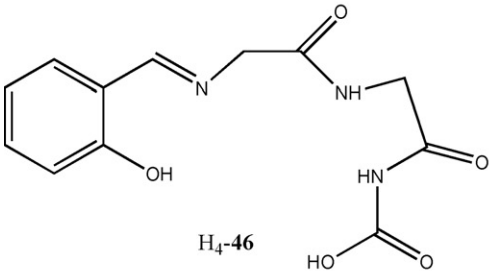

H_4-**46**

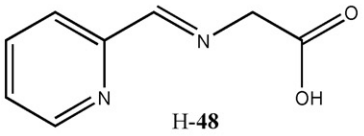

H-**48**

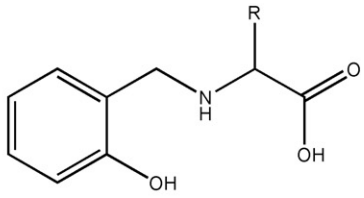

	R
H_2-**39**	$CH(CH_3)_2$
H_3-**40**	
H_3-**41**	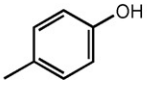
H_3-**42**	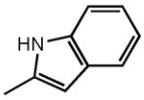

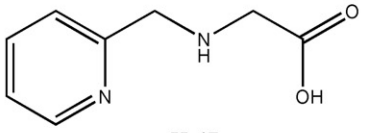

H-**47**

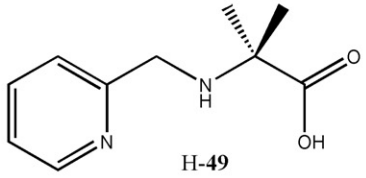

H-**49**

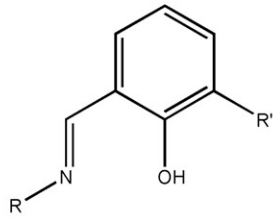

	R	R'
H-**50**	$(CH_2)_2N(CH_3)_2$	OCH_3
H-**50a**	C_6H_5	OCH_3
H_2-**51**	o-C_6H_4OH	OCH_3
H_2-**51a**	$CH_2CH(CH_3)OH$	OCH_3
H_3-**51b**	$CH(CH_2OH)_2$	OCH_3
H_3-**52**	$CH_2CONH(CH_2)_2COOH$	OCH_3
H_2-**53a**	$(CH_2)_2C_5H_4N$	COOH
H_2-**53b**	$(CH_2)_3N(CH_3)_2$	COOH

4. [1 + 1] Asymmetric end-off systems

The [1 + 1] asymmetric end-off Schiff bases derive from the condensation of equimolar amounts of 2-formyl 4-methyl (or bromo)-phenol, containing additional functionalities at the six-position, and monoamines with an aliphatic or aromatic chain bearing donor groups. [1 + 1] Asymmetric Schiff bases have also been obtained by condensation of the amino precursor $H_2NCH_2CH(OH)CH_2NRR'$ with the appropriate aldehyde, ketone or thioketone in a 1:1 molar ratio. In both the synthetic pathways, the final result is the formation of a compartmental ligand with two dissimilar adjacent chambers capable of giving rise to hetero-dinuclear or hetero-polynuclear complexation (Scheme 3).

As observed for other precursors, the formyl derivatives can serve as compartmental ligands, giving rise to mononuclear or, more frequently, polynuclear complexes. H-**54**,

prepared by reacting equimolar amount of 5,5,7,12,12,14-hexamethyl-1,4,8,11-tetraazatricyclo[9.3.1.1]hexadecane with 3-chloromethyl-5-bromosalicylaldehyde in acetonitrile followed by hydrolysis of the resulting compound with NaOH, forms [Ni(**54**)]$(ClO_4)\cdot H_2O$ (Fig. 43a) when mixed with $Ni(ClO_4)_2\cdot 6H_2O$ [74].

On the contrary, the reaction of $Ni(CH_3COO)_2\cdot 4H_2O$ and $NaBPh_4$ with the formyl precursor H-**55a**, having adjacent N_2O and O_2 donor sets, gives the pentanuclear nickel(II) cluster $\{[Ni_5Na(\mathbf{55a})_2(CH_3COO)_6(OH)_2](BPh_4)\}_n$ (Fig. 43b), bridged by a sodium(I) cation, repeating throughout the crystal structure. The polymeric chain is made up of symmetry equivalent $Ni_{2.5}Na_{0.5}$ units. The complex incorporates a variety of bridging species, μ_2-bridging phenolates, μ_3-bridging hydroxides and μ_3-bridging acetates. The six coordinate sodium cation has an O_6 donor set of two μ_2-bridging carbonyl oxygen atoms, and four μ_3-bridging acetates in a near perfect octahedral geometry. The nickel(II) ions are six coordinate in a distorted octahedral environment. The Ni···Ni and Ni···Na distances, ranging from 2.963 Å to 5.438 Å, are due to the different bridging groups [75].

H-**55b**, prepared by reaction of 3-chloromethyl-2-hydroxy-5-methylbenzaldehyde and methyl(2-pyridin-2-ylethyl)amine, affords H-**56**···H-**59** when condensed with the appropriate amine. These ligands react with the required metal salt and NaNCS to give $[Ni_3(\mathbf{56})_2(CH_3COO)_2(NCS)_2]$, $[Ni_3(\mathbf{56})_2(CH_3COO)_2(CH_3OH)_2](BPh_4)_2$, $[Co_3(\mathbf{56})_2(CH_3COO)_2(NCS)_2]$, $[Ni_3(\mathbf{57})_2(CH_3COO)_2(NCS)_2]$, $[Ni_3(\mathbf{57})_2(CH_3COO)_2(CH_3OH)_2](BPh_4)_2$, $[Co_3(\mathbf{57})_2(CH_3COO)_2(NCS)_2]$,

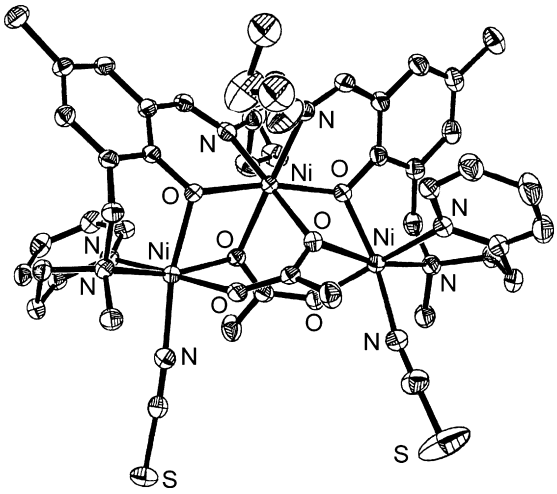

Fig. 44. Structure of $[Ni_3(\mathbf{58})_2(CH_3COO)_2(NCS)_2]$.

$[Ni_3(\mathbf{58})_2(CH_3COO)_2(NCS)_2]$, $[Ni_3(\mathbf{59})_2(CH_3COO)_2(NCS)_2]$, $[Mn_3(\mathbf{59})_2(CH_3COO)_2(NCS)_2]$, respectively. In these complexes (Fig. 44) each metal ion has a distorted octahedral geometry. The three pairs of metal ions are each doubly bridged: two pairs of metal ions are each bridged by a cresolate oxygen and by an oxygen atom from an acetate while the third pair of metal ions is bridged by the *syn*-anti-bidentate oxygen atoms from μ_3-acetato-κO:κO:κO′ groups. The oxygen atom of the pendant 2-methoxyethylimino arm in $[Ni_3(\mathbf{59})_2(CH_3COO)_2(NCS)_2]$ does not coordinate to a metal ion so paralleling the behavior of the sulfur atoms in the 2-methylsulfanylalylimino pendant arms in the trinuclear complexes derived from H-**60** and H-**61**. The metal ions

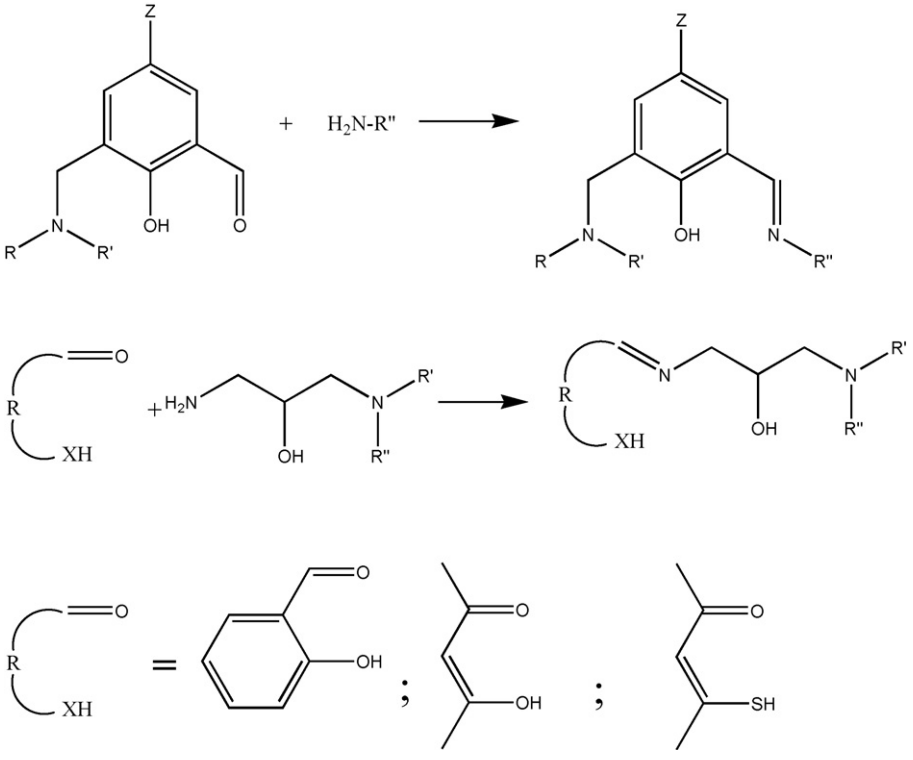

Scheme 3. Synthesis of the [1 + 1] asymmetric end-off ligands.

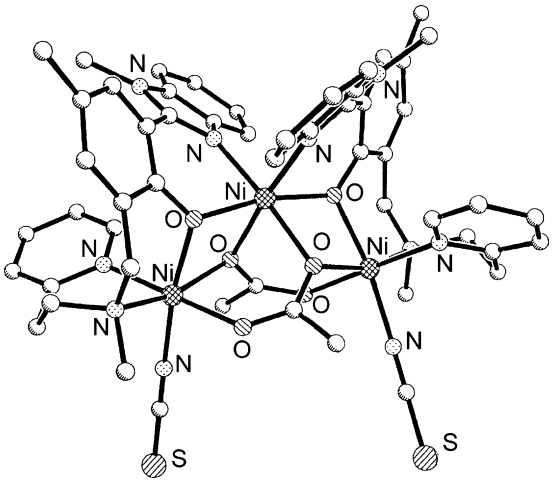

Fig. 45. Structure of $[Ni_3(\mathbf{65})_2(CH_3COO)_2(NCS)_2]$.

form an isosceles triangle with two M···M distances ≈3.2 Å and the third one ≈5 Å. Cryomagnetic studies indicate weak antiferromagnetic interactions between the adjacent metal ions with little or no magnetic interactions between the terminal metal ions [76].

In $[Zn(H_2\text{-}\mathbf{62})(H_2O)(NO_3)](NO_3)$ and $[Mg(H_2\text{-}\mathbf{62})(H_2O)_3](NO_3)_2{\cdot}H_2O$, prepared by condensation of H-**55c** with glycine in the presence of the appropriate metal salt, H_2-**62** coordinates to the metal ion through the deprotonated phenolic oxygen, the carboxylate group and the imine nitrogen. The amine nitrogen atoms are both protonated and remain uncoordinated [77].

The transmetalation of $[Zn(H_2\text{-}\mathbf{62})(H_2O)(NO_3)](NO_3)$ with magnesium(II) salts was studied in different solutions. Thanks to the strong tendency of the magnesium(II) ion to bind six water molecules in aqueous solution, no reaction of $[Zn(H_2\text{-}\mathbf{62})(H_2O)(NO_3)](NO_3)$ with magnesium salts was observed in this solvent. Accordingly, the addition of $Zn(NO_3)_2$ to a solution of $[Mg(H_2\text{-}\mathbf{62})(H_2O)(NO_3)](NO_3)$ in D_2O (pD 9.7) resulted in the conversion into $[Zn(H_2\text{-}\mathbf{62})(H_2O)(NO_3)](NO_3)$. By contrast, the zinc(II) ion is replaced by the magnesium(II) ion when $[Zn(H_2\text{-}\mathbf{62})(H_2O)(NO_3)](NO_3)$ is treated with $MgCl_2$ in DMSO. The same reaction does not occur with $Mg(NO_3)_2$, $Mg(ClO_4)_2$ or $MgSO_4$ while two equivalents of $Mg(CH_3COO)_2$ yield 38% of $[Mg(H_2\text{-}\mathbf{62})(NO_3)(H_2O)](NO_3)$. Addition of increasing concentrations of NaCl to a 1:1 mixture of $[Zn(H_2\text{-}\mathbf{62})(NO_3)(H_2O)](NO_3)$ and $Mg(ClO_4)_2$ promotes formation of $[Mg(H_2\text{-}\mathbf{62})(NO_3)(H_2O)](NO_3)$ up to ca. 40%. $Na(CH_3COO)$ is even more effective than chloride in promoting replacement of the zinc ion from $[Zn(H_2\text{-}\mathbf{62})(NO_3)(H_2O)](NO_3)$ by the magnesium one. No zinc/magnesium exchange is observed in the presence of fluoride, bromide and iodide ions. In line with the effect of the anions described so far, the magnesium(II) ion is completely substituted by the zinc(II) ion when $[Mg(H_2\text{-}\mathbf{62})(NO_3)(H_2O)](NO_3)$ is treated with one equivalent of $Zn(NO_3)_2$ in the absence of chloride or acetate, while treatment of $[Mg(H_2\text{-}\mathbf{62})(NO_3)(H_2O)](NO_3)$ with one equivalent of $Zn(CH_3CO_2)_2$ gives a mixture of 68% $[Zn(H_2\text{-}\mathbf{62})(NO_3)(H_2O)](NO_3)$ and 32% $[Mg(H_2\text{-}\mathbf{62})(NO_3)(H_2O)](NO_3)$ [77].

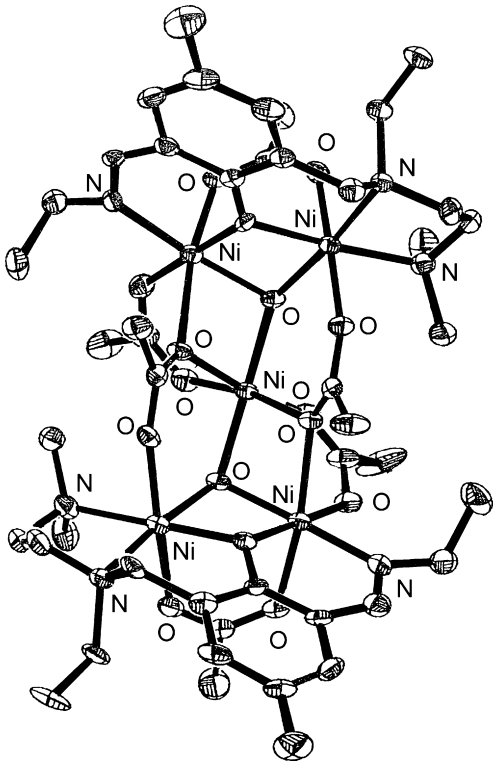

Fig. 46. Structure of $[Ni_5(\mathbf{66})_2(CH_3COO)_6(OH)_2]$.

In DMSO, $MgCl_2$ and $Mg(CH_3COO)_2$ substitute the zinc(II) ion in $[Zn(H\text{-}\mathbf{62a})(H_2O)]_2$ more easily than in $[Zn(H_2\text{-}\mathbf{62})(NO_3)(H_2O)](NO_3)$, while $Mg(NO_3)_2$, $Mg(ClO_4)_2$ and $MgSO_4$ are ineffective. Furthermore, no substitution takes place in the presence of iodide, bromide or fluoride ions [77].

The condensation of H-**55b** with *N*-methyl-benzene-1,2-diamine affords H-**63** which, owing to the presence of a

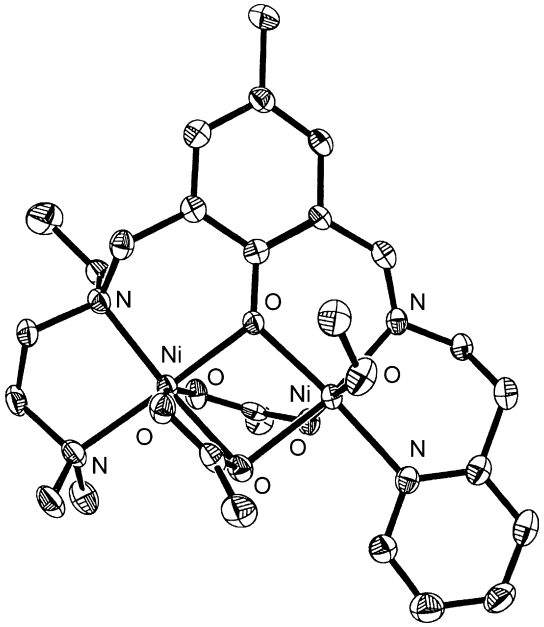

Fig. 47. Structure of $[Ni_2(\mathbf{69})(CH_3COO)_2(CH_3OH)]^+$.

secondary amine, suffers a cyclisation at the imine bond leading to H_2-**64**, whose reaction with $Ni(CH_3COO)_2{\cdot}4H_2O$ and NaNCS gives $[Ni_3(\mathbf{65})_2(CH_3COO)_2(NCS)_2]$ where the dihydrobenzoimidazole ring system of H_2-**64** has been oxidized to the benzoimidazole ring system of H-**65**. The core of the structure is an isosceles triangle of distorted octahedral nickel(II) ions (Ni···Ni distances of 3.19 Å and 4.91 Å), the apical oxygen atoms of the central nickel(II)-based octahedron serving also as apices at the other two nickel(II) ions, respectively. The terminal and the central nickel(II) ions are each bridged by a phenolate oxygen atom and by a monodentate oxygen atom from an acetate while the two terminal nickel(II) ions are bridged by the *syn*-anti-bidentate oxygen atoms from two μ_3, η^1, η^2-acetates (Fig. 45) [78].

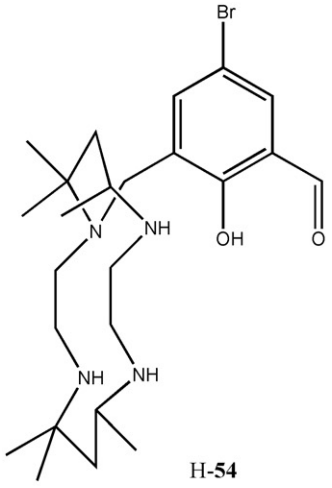

H-**54**

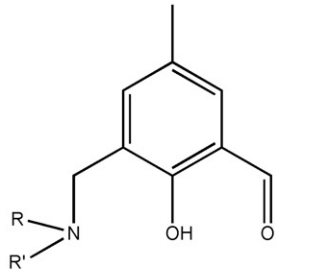

	R	R'
H-**55a**	CH_3	
H-**55b**	CH_3	
H-**55c**	C_2H_5	
H-**55d**	C_2H_5	

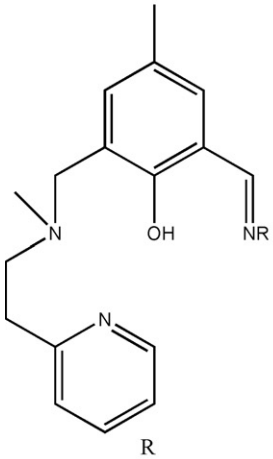

	R
H-**56**	C_2H_5
H-**57**	n-C_3H_7
H-**58**	n-C_4H_9
H-**59**	$(CH_2)_2OCH_3$
H-**60**	$(CH_2)_2SCH_3$
H-**61**	$(CH_2)_3SCH_3$

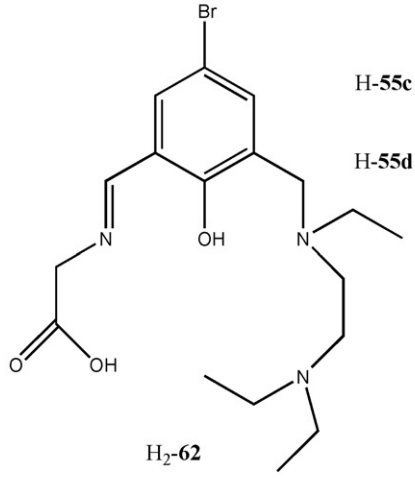

H_2-**62**

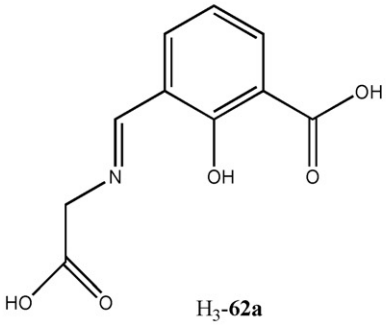

H_3-**62a**

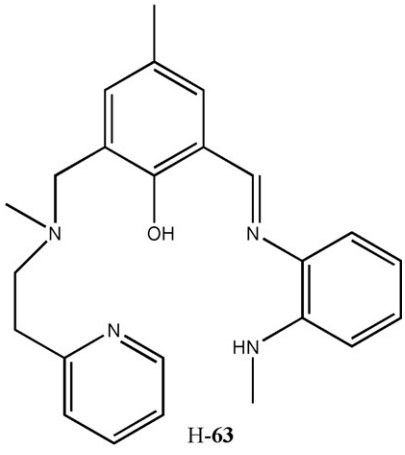

H-**63**

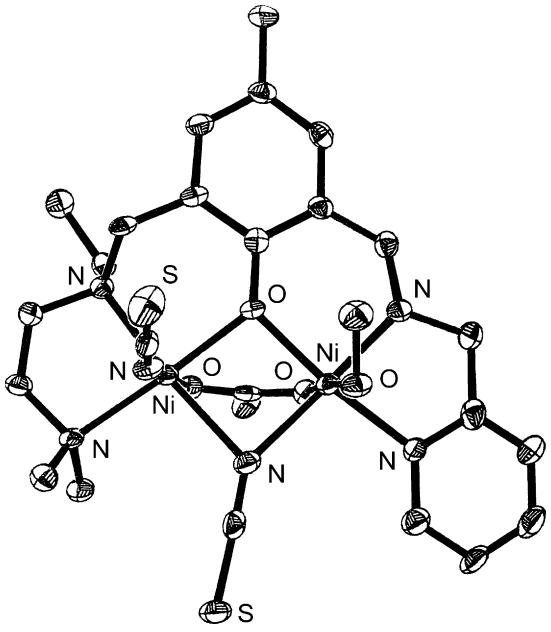

Fig. 48. Structure of [Ni_2(**69**)(CH_3COO)(NCS)(CH_3OH)].

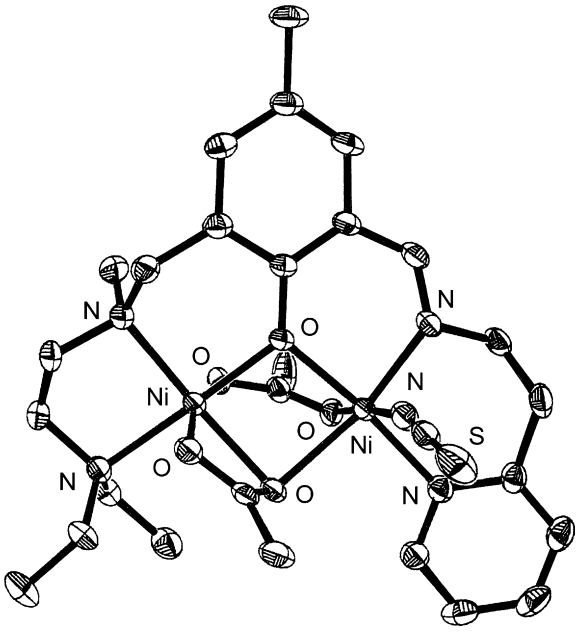

Fig. 49. Structure of [Ni_2(**76**)(CH_3COO)$_2$(NCS)].

The complexes [Ni_5(**L**)$_6$(CH_3COO)$_6$(OH)$_2$]·nCH_3OH·mH_2O (H-**L** = H-**66**, H-**67**, H-**68**), prepared by addition of Ni(CH_3COO)$_2$·4H_2O to the appropriate ligand, have a closely similar pentanuclear core (Fig. 46). The structure of [Ni_5(**67**)$_2$(CH_3COO)$_6$(OH)$_2$]·2CH_3OH·0.5H_2O and [Ni_5(**68**)$_2$(CH_3COO)$_6$(OH)$_2$]·CH_3OH·2H_2O shows the non-bonding nature of the 3-methylsulfanylpropylimino pendant arms. The pentanuclear core of the complexes comprises two dinuclear {Ni_2(**L**)} units linked to the third nickel(II) ion by bridging μ_3-hydroxo groups and by *syn–syn* bidentate bridging and monodentate bridging acetate anions such that the central nickel(II) ion is six coordinate in a distorted O_6 octahedron. The remaining nickel(II) ions are also six coordinate in a NO_5 distorted octahedron for two terminal nickel(II) ions and in a N_2O_4 donor set for the other two terminal nickel(II) ions [79].

A range of ligands, bearing one imine and one amine arm, has been prepared and used to generate dinuclear nickel(II) complexes. The nature of the terminal nitrogen donor atom in the pendant arms was varied to give combinations derived from pyridine, imidazole and tertiary amino groups; changing the spacer present in the side arm allows either five-membered or six-membered chelate rings to be generated at the metal centers and so a series of complexes having adjacent [5,5], [5,6], [6,5] and [6,6] binding compartments was constructed, providing opportunity to investigate the effect of changing the nature of the compartment on the bonding capacity of the ligand.

H-**69**, derived from the condensation of 2-(2-aminoethyl)pyridine and H-**55d**, reacts with Ni(CH_3COO)$_2$·4H_2O in the presence of $NaBF_4$ to yield [Ni_2(**69**)(CH_3COO)$_2$(CH_3OH)](BF_4), which contains a dinuclear core, derived from a bridging cresolate and a bidentate bridging acetate together with a monodentate bridging acetate [80]. Chelation of the pendant nitrogen atoms provides six-membered chelate rings from the imine arms to one nickel(II) ion and five membered chelate rings from the amine arms to the other nickel(II) ion. Both nickel(II) ions are six coordinate (Fig. 47) [80]. The structure therefore relates directly to that of [Ni_2(**68**)(CH_3COO)$_2$(NCS)], prepared by reaction of H-**68** with Ni(CH_3COO)$_2$·4H_2O and NaNCS, where the non symmetric monobridging acetate and cresolate bridges gives a Ni···Ni separation of 3.048 Å, slightly longer than that in [Ni_2(**69**)(CH_3COO)$_2$ (CH_3OH)]BF_4 (3.029 Å) [81].

The same reaction in presence of NaNCS affords [Ni_2(**69**)(CH_3COO)(NCS)$_2$(CH_3OH)], where the two closely octahedral nickel(II) ions are bridged by the phenolate oxygen atom of [**69**]$^-$, an isothiocyanato nitrogen atom and a *syn–syn* bidentate acetate. Chelation from the pendant nitrogen atoms provides five membered chelate rings from the imine and

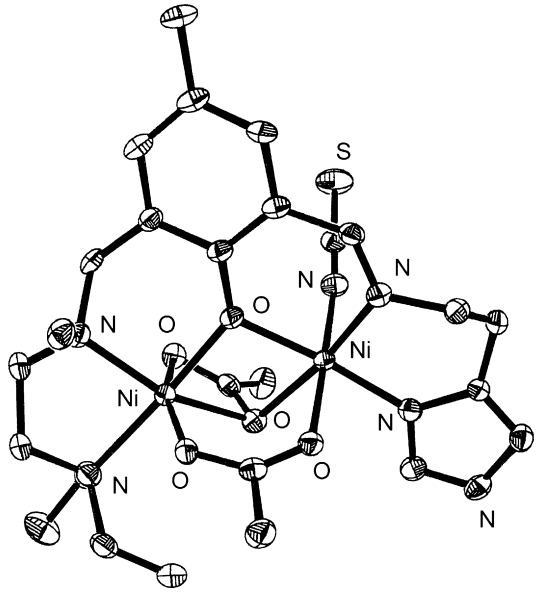

Fig. 50. Structure of [Ni_2(**79**)(CH_3COO)$_2$(NCS)].

amine arms. Again six coordination at each nickel(II) ion occurs (Fig. 48) [81].

The generality of this reaction, in which both chelate rings are five-membered giving a [5,5] coordination set, is shown by the availability of the analogous dinickel(II) complexes $[Ni_2(\mathbf{L})(CH_3COO)(NCS)_2(CH_3OH)]$ where $H_2\mathbf{L}$ = H-**67**, H-**70**, H-**71** and H-**72**.

H-**73** and H-**74**, which provide a [6,5] coordination set, give rise to $[Ni_2(\mathbf{L})(CH_3COO)(NCS)_2(CH_3OH)]$, containing bridging groups similar to those occurring in $[Ni_2(\mathbf{L})(CH_3COO)(NCS)_2(CH_3OH)]$ (H-$\mathbf{L}$ = H-**67**, H-**70**, H-**71**, H-**72**) [81].

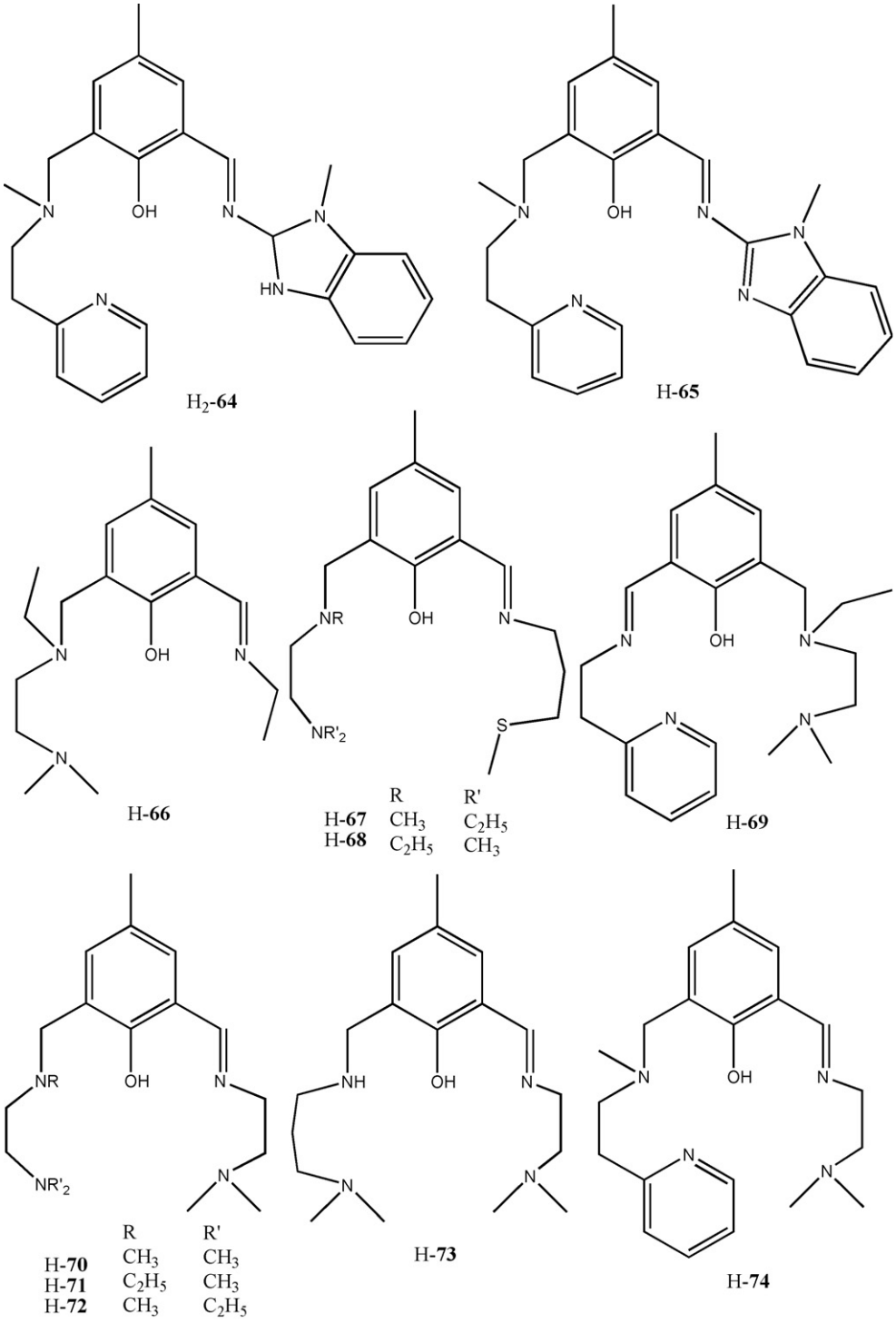

H_2-**64**

H-**65**

H-**66**

	R	R'
H-**67**	CH_3	C_2H_5
H-**68**	C_2H_5	CH_3

H-**69**

	R	R'
H-**70**	CH_3	CH_3
H-**71**	C_2H_5	CH_3
H-**72**	CH_3	C_2H_5

H-**73**

H-**74**

This structural type, having a *syn–syn* bidentate bridge and a monodentate thiocyanate bridge, seems to be promoted by the presence of a five-membered chelating ring at the iminic pendant arm. Under the same reaction conditions, H-**75** and H-**76**, providing [5,6] coordination sets, gave $[Ni_2(\mathbf{L})(CH_3COO)_2(NCS)]$. The introduction of a six-membered chelate ring, on complexation by the iminic arm provided by $[\mathbf{75}]^-$ or $[\mathbf{76}]^-$, leads to a different stoichiometry in the resulting dinuclear complexes. The overall structural features of $[Ni_2(\mathbf{75})(CH_3COO)_2(NCS)]$ and $[Ni_2(\mathbf{76})(CH_3COO)_2(NCS)]$ are comparable, revealing that whilst a basic dinuclear core derived from a bridging phenolate and a bidentate bridging acetate was retained, a monodentate bridging acetate had replaced the bridging isothiocyanate. The six coordinate nickel(II) ions, 3.094 Å apart, are again bridged by the phenolic oxygen atom of $[\mathbf{75}]^-$ and a *syn–syn* bidentate acetate but further bridging is now provided by a monodentate bridging ethanoate anion. Chelation from the pendant nitrogen atoms provides six-membered chelate rings from the iminic arms to one nickel(II) ion and five membered chelate rings from the aminic arms to the other nickel(II) ion. The isothiocyanate anion has migrated to the nickel(II) ion in the iminic compartment when compared to its position in the above $[Ni_2(\mathbf{L})(CH_3COO)_2(NCS)(CH_3OH)]$ and a methanol molecule at the same nickel(II) ion has been lost (Fig. 49) [81].

Also in $[Ni_2(\mathbf{L})(CH_3COO)_2(NCS)]$ (H-**L** = H-**77**, H-**78**, H-**79**), where the aliphatic aminic arm provides a five membered chelate ring while the iminic arm provides a six-membered chelating ring bearing a dimethylamino group (H-**77**, H-**78**) or histamine (H-**79**), a monodentate bridging ethanoate occurs and the coordination geometries at the metal ions resemble that in $[Ni_2(\mathbf{76})(CH_3COO)_2(NCS)]$ as confirmed by the structure of $[Ni_2(\mathbf{79})(CH_3COO)_2(NCS)]\cdot H_2O$ (Fig. 50), where the two six coordinate distorted octahedral nickel(II) ions are 3.080 Å apart [81].

A group of ligands, with both pendant arms, providing six-membered chelate rings at both metal ions, was then prepared together with their structurally similar $[Ni_2(\mathbf{L})(CH_3COO)_2(NCS)]$ (H-**L** = H-**80**, H-**81**, H-**82**) [81,82].

In $[Ni_2(\mathbf{80})(CH_3COO)_2(NCS)]$ the two six coordinate nickel(II) ions are again bridged by the phenolate oxygen atom or the deprotonated ligand, a *syn–syn* acetate and a monodentate bridging acetate anion. The dinuclear core is very similar to that in $[Ni_2(\mathbf{76})(CH_3COO)_2(NCS)]\cdot H_2O$ but chelation from the pendant nitrogen atoms provides a six-membered chelate ring from the iminic arm to the related nickel(II) ion and a second six-membered chelate ring from the aminic arm to the other nickel(II) ion. The nickel(II)···nickel(II) separation is 3.099 Å [81].

H-**83**, capable of providing a [5,5] coordination set, derives from the condensation of 2-(methylthio)aniline and H-**55a**. It reacts with cobalt(II) acetate and sodium thiocyanate to give $[Co_2(\mathbf{83})(CH_3COO)(NCS)_2(CH_3OH)]$ whose structural core parallels that found in the nickel(II) complexes with similar ligands providing [5,5] coordination set. The cobalt(II) ions are bridged by the cresolato oxygen atom, an isothiocyanato nitrogen atom and a *syn–syn* bidentate acetate group. Chelation from the 2-methylsulfanylphenylimino pendant arm provides a five membered chelate ring to one cobalt ion, and together with a thiocyanato nitrogen atom gives an overall N_2O_2S donor set. Chelation from the *N*,*N*-diethylamino-bearing arm provides a five membered chelate ring to the other cobalt(II) ion, and together with a methanol oxygen atom gives an overall N_4O_2 donor set (Fig. 51) [82].

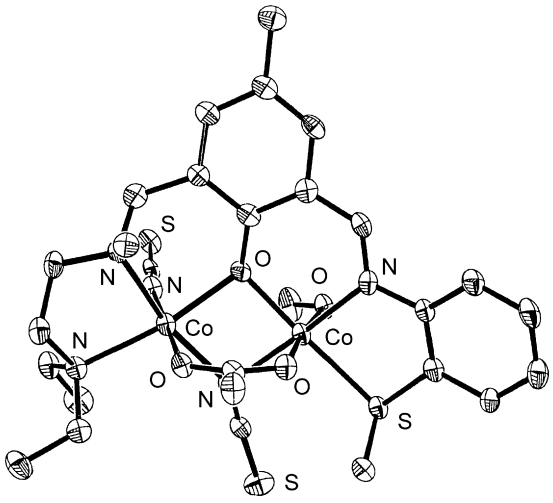

Fig. 51. Structure of $[Co_2(\mathbf{83})(CH_3COO)_2(NCS)_2(CH_3OH)]$.

In contrast to the above generation of dinuclear complexes, the reaction of the appropriate metal(II) acetate, NaNCS and H-**84** or H-**61**, where the 2-methylsulfanylphenylimino pendant arm has been replaced by 2-methylsulfanylethylimino- or by 3-methylsulfanylpropylimino-pendant arms, respectively, gives $[Ni_3(\mathbf{L})_2(CH_3COO)_2(NCS)_2]\cdot 2H_2O$ and $[Mn_3(\mathbf{61})_2(CH_3COO)_2(NCS)_2]$. The overall structures resemble each other with a triangle of metal ions. In the manganese complex the three pairs of distorted octahedral manganese(II) ions, 3.287 Å, 5.202 Å and 3.294 Å apart, are each doubly

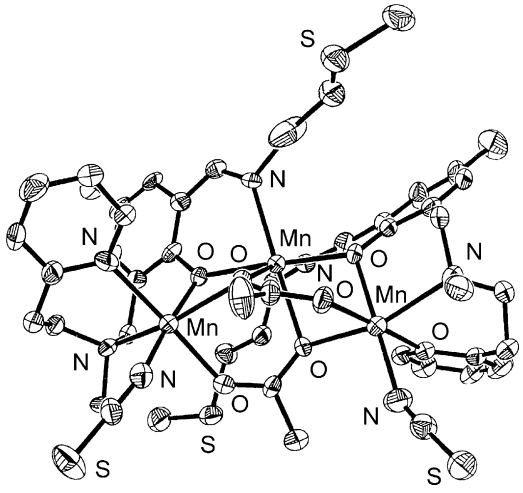

Fig. 52. Structure of $[Mn_3(\mathbf{61})_2(CH_3COO)_2(NCS)_2]$.

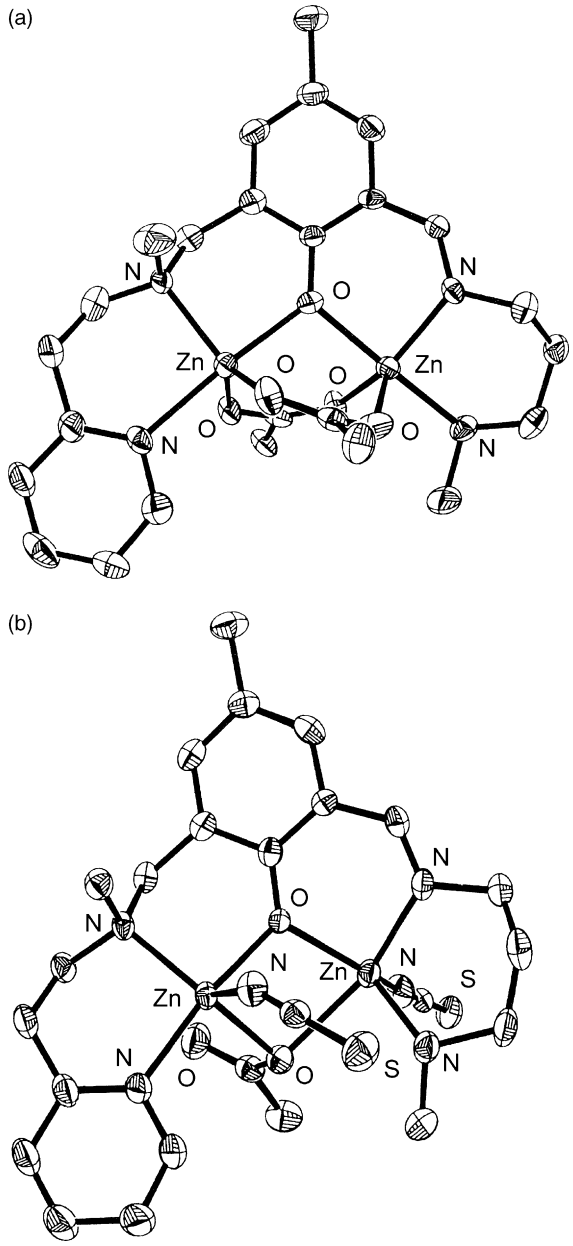

Fig. 53. Structure of $[Zn_2(\mathbf{81})(CH_3COO)_2]^+$ (a) and $[Zn_2(\mathbf{81})(CH_3COO)(NCS)_2]$ (b).

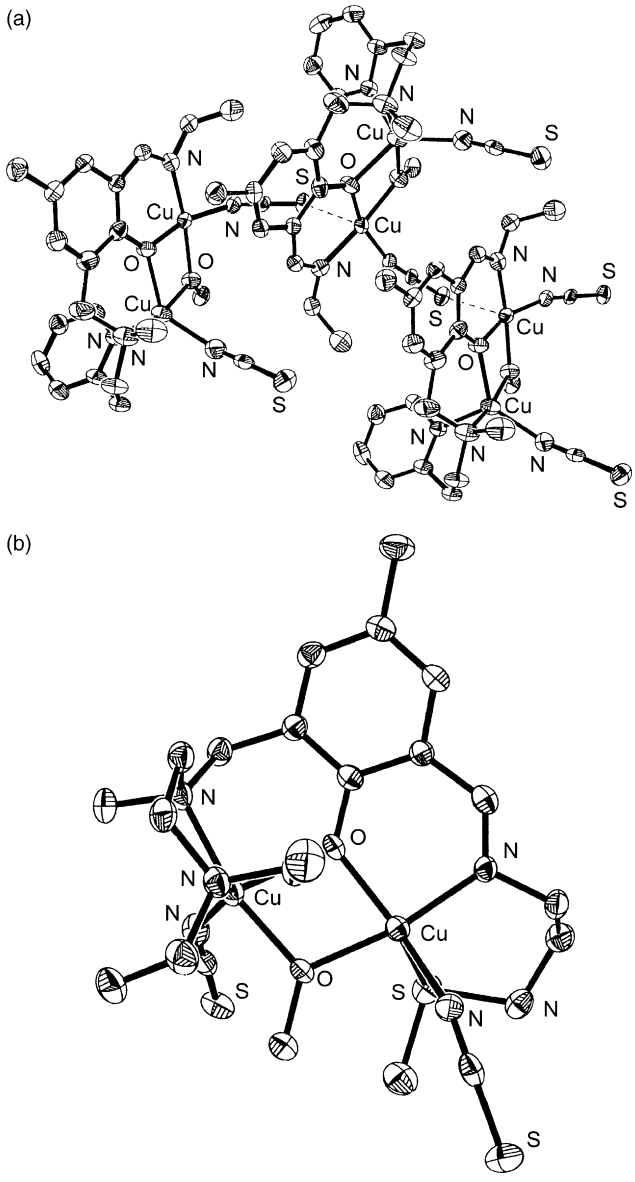

Fig. 54. Structure of $[Cu_2(\mathbf{56})(\mu\text{-}OCH_3)(NCS)_2]$ (a) and $[Cu_2(\mathbf{67})(\mu\text{-}OCH_3)(NCS)_2]$ (b).

bridged: two pairs of external . . . internal metal ions are bridged by a cresolate oxygen and by a monodentate oxygen atom from an acetate while the two external manganese ions are bridged by the *syn*-anti-bidentate oxygen atoms from two μ_3-acetato-κO:κO;κO′ groups. The sulfur atoms from the pendant arms are not coordinated. Vacant coordination sites arise at the metal ion incorporated into the iminic compartment and provide an opportunity for the generation of a complex with enhanced nuclearity via interaction with the corresponding iminic donor set from a second ligand molecule to satisfy the octahedral requirement of the incorporated metal herein the pivotal manganese ion (Fig. 52) [82].

$[Zn_2(\mathbf{81})(CH_3COO)_2]$ (BPh_4), derived from the reaction of H-**81** with $Zn(CH_3COO)_2{\cdot}2H_2O$ and $NaBPh_4$, contains a di-μ-acetato-μ-cresolato-dizinc(II) core [83]. Each acetato bridge is *syn–syn* bidentate and this contrasts with the binding mode found in $[Ni_2(\mathbf{81})(CH_3COO)_2(CH_3OH)](BPh_4)$, where a di-μ-acetato-μ-cresolato-dinickel(II) core occurs, but with one *syn–syn* bidentate acetato bridge and one monodentate bridging acetate present. This latter core has been found consistently with the introduction of a six-membered chelating ring at the iminic binding site in dinuclear nickel(II) complexes of unsymmetrical Schiff base compartmental ligands [85]. The Zn···Zn separation is 3.309 Å, which is longer than those observed in related dinickel(II) complexes derived from compartmental ligands bearing [5,6] and [6,6] coordination sets where the separation ranges from 3.080–3.099 Å

(3.096 Å in [Ni_2(**81**)($CH_3COO)_2$(CH_3OH)](BPh_4)] [84]. This longer separation is clearly capable of supporting the two three-atom *syn–syn* bidentate acetate bridges. Both zinc(II) ions are five coordinate, compared to the six coordinate nickel(II) ions in [Ni_2(**81**)($CH_3COO)_2$(CH_3OH)](BPh_4): one zinc(II) ion is in a distorted trigonal bipyramidal geometry and the other zinc(II) ion in a square pyramidal geometry (Fig. 53a) [83].

The same reaction in presence of NaNCS gives [Zn_2(**81**)(CH_3COO)($NCS)_2$] where a μ-acetato-μ-cresolato-dizinc(II) core occurs with an unusually monodentate acetato bridge. The two zinc(II) ions, 3.254 Å apart, are in a distorted square pyramidal geometry with the thiocyanate anions *trans* to each other (Fig. 53b) [84].

H-**56**, H-**57** and H-**67** form [Cu_2(**L**)(μ-OCH_3)($NCS)_2$] when treated with $Cu(CH_3COO)_2{\cdot}H_2O$ in the presence of NaNCS [85]. In these three dinuclear copper(II) complexes the presence of μ-methoxy groups occurs rather than the μ-acetato groups, regularly found in the related dinuclear nickel(II) complexes [87]. μ-Methoxides have also been found in dinuclear copper(II) complexes prepared from symmetric compartmental ligands and copper(II) acetate [86].

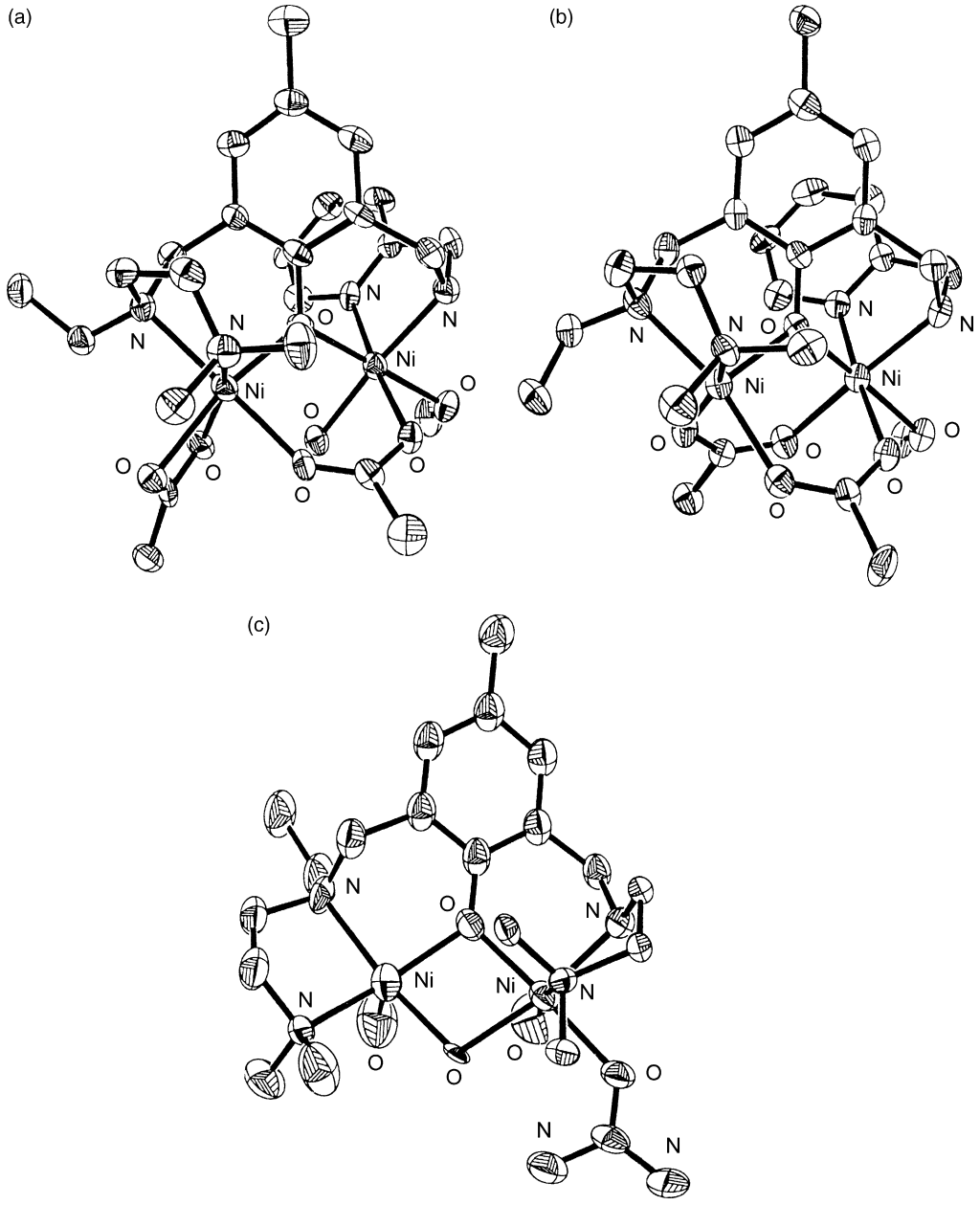

Fig. 55. Structure of [Ni_2(**85**)(μ-CH_3COO)(CH_3COO)(H_2O)(CH_3OH)]$^+$ (a), [Ni_2(**85**)(μ-$CH_3COO)_2$(CH_3OH)]$^+$ (b) and [Ni_2(**86**)(OH)($H_2O)_2$(urea)]$^{2+}$ (c).

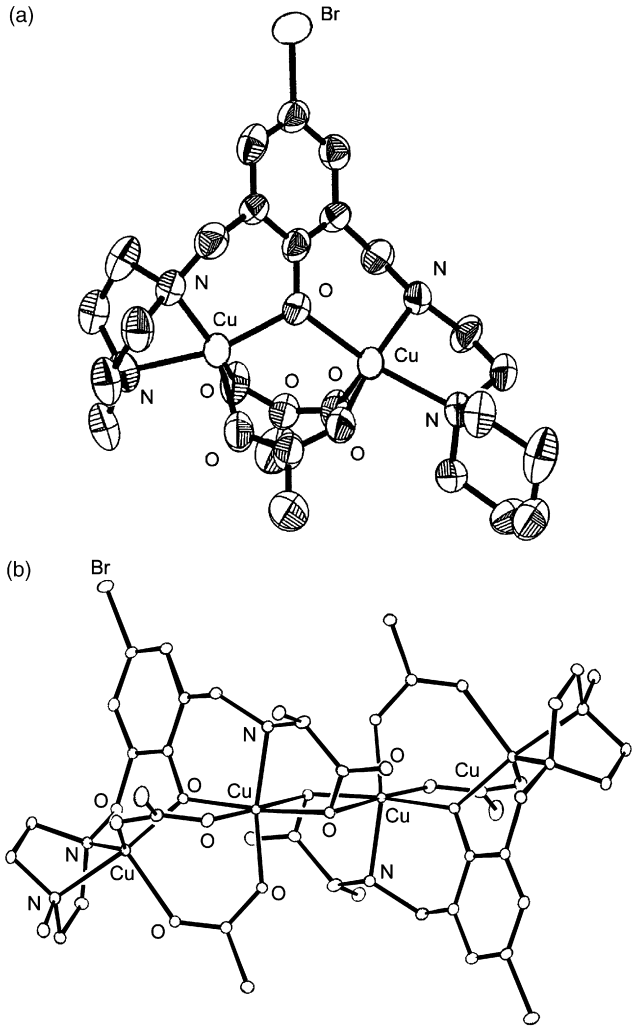

Fig. 56. Structure of $[Cu_2(\mathbf{89})(\mu\text{-}CH_3COO)_2]^+$ (a) and $[Cu_4(\mathbf{92})_2(CH_3COO)_4]$ (b).

In $[Cu_2(\mathbf{56})(\mu\text{-}OCH_3)(NCS)_2]$ the copper ions, 3.074 Å apart, are asymmetrically bridged by the cresolato oxygen and symmetrically by a methoxy oxygen atom. The copper ion in the aminic compartment is five coordinate intermediate between square pyramidal and trigonal bipyramidal while the four coordinate copper ion in the iminic compartment shows a weak fifth interaction with the sulfur atom of the NCS^- group of an adjacent complex. The overall chain structure of the resulting coordination polymer is propagated by a continuum of Cu-S intermolecular interactions (Fig. 54a) [86]. A similar crystal structure was found for $[Cu_2(\mathbf{57})(\mu\text{-}OCH_3)(NCS)_2]$.

Also in $[Cu_2(\mathbf{67})(\mu\text{-}OCH_3)(NCS)_2]$, the copper(II) ions, at a distance of 3.096 Å, are similarly bridged by the cresolato oxygen and a methoxy oxygen atom. However, a discrete species is detected in which the five coordinate copper ion in the iminic compartment is bound to the sulfur atom of the pendant arm, its coordination being completed by the bridging oxygen atoms, the iminic nitrogen atom, and an isothiocyanate nitrogen atom. This is in contrast with the behaviour of the terminal thiomethyl sulfur atom in reactions of related compartmental ligands with $Ni(CH_3COO)_2$, where use of aliphatic pendant arms (as in H-**60** and H-**61**) gave trinuclear complexes and aromatic pendant arms were required to induce dinuclear complexes. It is presumed that this difference derives from an increased thiophilicity of the copper(II) ion relative to the nickel(II) ion. The copper ion in the aminic compartment is distorted square pyramidal. The donor atoms at one copper(II) ion are N_3O_2 and those at the other copper(II) ion are N_2OS (Fig. 54b) [85].

In order to avoid the risk of hydrolytic cleavage occurring in reactions of asymmetric compartmental ligands with nickel salts in the presence of weakly or non-coordinating anions, the Schiff base ligands H-**68** and H-**70** were reduced to the corresponding amine derivatives H-**85** and H-**86**. The subsequent reaction of H-**85** with $Ni(CH_3COO)_2{\cdot}4H_2O$ and $NaPF_6$ forms $[Ni_2(\mathbf{85})(\mu\text{-}CH_3COO)\ (CH_3COO)(H_2O)(CH_3OH)](PF_6)$, where the two six coordinate N_2O_4 distorted octahedral nickel(II) ions are bridged by a cresolate oxygen atom and a *syn–syn* bidentate bridging acetate anion. Chelation from the pendant nitrogen atoms provides five membered chelate rings at each nickel(II) ion (Fig. 55a) [88]. The same reaction also gives $[Ni_2(\mathbf{85})(\mu\text{-}CH_3COO)_2(CH_3OH)](PF_6)$, cocrystallised with $[Ni_2(\mathbf{85})(\mu\text{-}CH_3COO)_2(H_2O)(CH_3OH)](PF_6)$. The crystal structure again shows the same dinuclear core containing, however, one six coordinate N_2O_4 octahedral nickel(II) ion bound to one arm of $[\mathbf{85}]^-$ via the articular N(H) and pyridinyl nitrogen atoms and to a methanol molecule and the other five coordinate N_2O_3 square pyramidal nickel(II) ion bound to the articular $N(C_2H_5)$ atom and terminal $N(CH_3)_2$ of the second arm of $[\mathbf{85}]^-$. The Ni···Ni separation is 3.334 Å (Fig. 55b). The vacant site in $[Ni_2(\mathbf{85})(\mu\text{-}CH_3COO)_2(CH_3OH)](PF_6)$ is occupied by a water molecule in $[Ni_2(\mathbf{85})(\mu\text{-}CH_3COO)_2(H_2O)(CH_3OH)](PF_6)$, where the two six coordinate distorted octahedral nickel(II) ion are 3.417 Å apart [88].

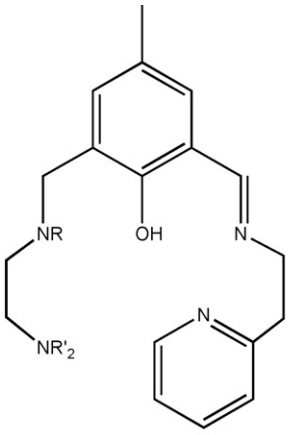

	R	R'
H-**75**	C_2H_5	CH_3
H-**76**	CH_3	C_2H_5

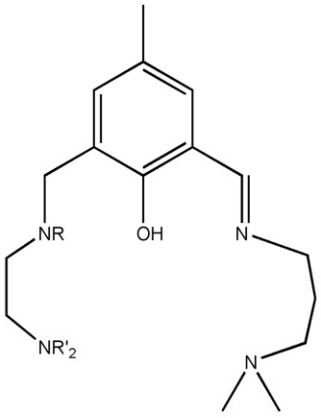

	R	R'
H-**77**	C_2H_5	CH_3
H-**78**	CH_3	C_2H_5

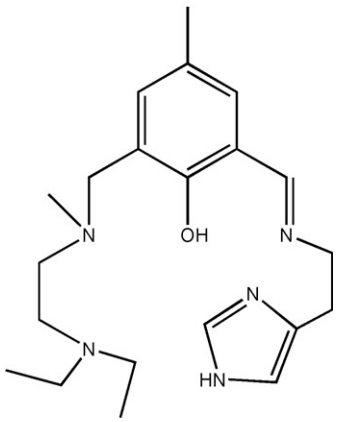

H-**79**

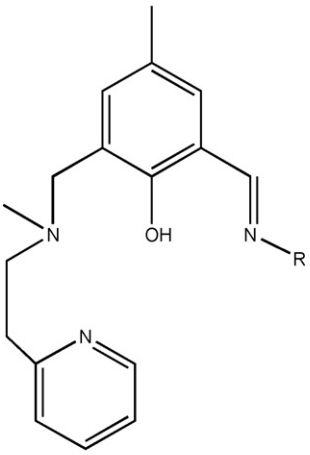

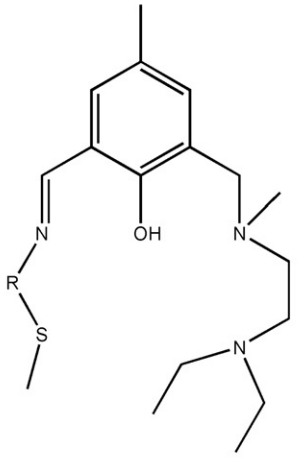

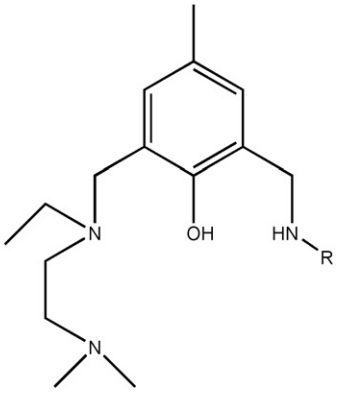

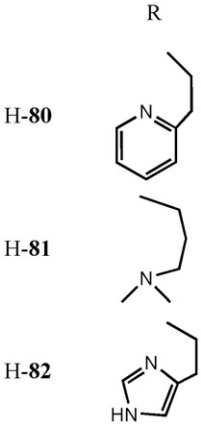

H-**80**

H-**81**

H-**82**

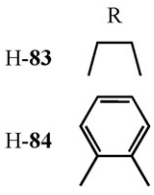

H-**83**

H-**84**

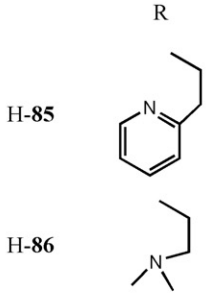

H-**85**

H-**86**

The structure of $[Ni_2(\mathbf{85})(\mu\text{-}CH_3COO)_2(CH_3OH)_2](BPh_4)$, isolated when $[BPh_4]^-$ was used instead of $[PF_6]^-$, is closely similar to that of $[Ni_2(\mathbf{85})(\mu\text{-}CH_3COO)_2(H_2O)(CH_3OH)](PF_6)$: two methanol molecules are coordinated to the nickel(II) ions where previously a water molecule and a methanol molecule were coordinated [88].

The dinuclear core of $[Ni_2(\mathbf{86})(OH)(H_2O)_2(urea)](BPh_4)_2$, derived by mixing H-**86**, $Ni(ClO_4)_2{\cdot}4H_2O$, $NaBPh_4$ and urea, contains a bridging cresolate oxygen atom and an hydroxide anion. The nickel(II) ion, bound by the $[\mathbf{86}]^-$ arm bearing an articular N(H) and a terminal $N(CH_3)_2$ group, is N_2O_4 six coordinate and the other one, bound by the $[\mathbf{86}]^-$ arm bearing an articular $N(C_2H_5)$ atom and a terminal $N(CH_3)_2$ group, is five coordinate in a distorted square pyramidal N_2O_3 coordination. The Ni···Ni separation is 3.049 Å, shorter than that found in the dinuclear nickel(II) complexes with $[\mathbf{85}]^-$, this reflecting the reduced connectivity of the bridges (Fig. 55c) [88].

Cyclic voltammetric studies of $[M(\mathbf{87a})](ClO_4){\cdot}H_2O$, $[M_2(\mathbf{87a})](ClO_4)_2{\cdot}2H_2O$, $[M(\mathbf{88b})](ClO_4){\cdot}H_2O$ and $[M_2(\mathbf{88b})](ClO_4)_2{\cdot}2H_2O$ ($M = Cu^{II}$, Ni^{II}), prepared by the condensation of 2-formyl-4-methyl-6-[(4-methylpiperazine-

1-yl)methyl]phenol with *N*-β-amino-ethylisonitrosoethyl-methylketimine or *N*-β-amino-methylethylisonitrisoethyl-methyl-ketimine in the presence of the appropriate metal perchlorate, prove one quasireversible reduction wave for all mononuclear complexes and two quasi reversible one electron reduction waves for the dinuclear complexes. An antiferromagnetic interaction occurs in the dicopper(II) complexes; in particular, $[Cu_2(\mathbf{87})](ClO_4)_2{\cdot}2H_2O$ shows a $-2J$ value of 283 cm^{-1} [89].

The formyl precursor H-**89a**, deriving from the Mannich reaction of 4-bromo-2-hydroxybenzaldehyde and *N*-methylpiperazine, affords the related Schiff bases by condensation with $H_2NCH_2CH_2NH(CH_2CH_2)_2X$ (X = CH_2,O,S). These compounds can be easily reduced to H-**89**, H-**90** and H-**91** which react with $Cu(CH_3COO)_2{\cdot}H_2O$ and $N(C_2H_5)_3$ to give $[Cu_2(\mathbf{L})(\mu\text{-}CH_3COO)_2](BF_4)$ where the two square pyramidal copper ions, at a Cu···Cu distance of 3.304, 3.263, 3.299 Å, respectively, are bridged by the μ-phenoxo-oxygen of $[\mathbf{L}]^-$ and by two acetate anions (Fig. 56a) [90].

Kinetic studies of the oxidation of 3,5-di-*tert*-butylcatechol to the corresponding quinone, in air saturated methanol solution of these complexes, show that the turnover numbers of the complexes increase in the order H-**89** < H-**90** < H-**91**. DFT calculations and ESI-MS experiments suggest that a higher affinity of the group at the 4 position of the piperidine ring of the ligand to the copper ion enhances removal of one acetate bridge. The resulting free coordination site can be used for substrate binding, thereby resulting in higher turnover numbers for the catechol oxidation [90].

The condensation of H-**89a** and l-alanine in presence of NaOH followed by in situ reduction of the resulting Schiff base, forms H_2-**92** which reacts with $Cu(CH_3COO){\cdot}H_2O$ to yield $[Cu_4(\mathbf{92})_2(CH_3COO)_4]{\cdot}2CH_3CN{\cdot}2H_2O$ (Fig. 56b), where two dinuclear units are connected by acetate bridging groups. In each dinuclear unit, the two copper centers are connected through two acetate bridges in a *syn–syn* manner and are bridged internally by the phenolate oxygen of $[\mathbf{92}]^{2-}$ which acts as a pentadentate donor. One copper(II) ion is in a distorted O_5N octahedral coordination. The second five coordinate copper center is in a distorted N_2O_3 square pyramidal arrangement. The Cu···Cu separation inside each dinuclear unit is 3.282 Å. The Cu···Cu distance between dinuclear entities is 3.449 Å [90].

H-**93**, prepared by methyl chlorination of 5-methylsalicylaldehyde at the 3-position of the phenol ring subsequently substituted by di-(2-pycolyl) amine of the phenol ring, forms H-**94** by [1 + 1] condensation with 2-(amino methyl)pyridine [91,92]. The first dinuclear complexes with H-**93**, obtained by hydrolysis of H-**94** in the presence of nickel(II) salts with non- or weakly coordinating anions, were found to have very similar crystal structures, comprising a bimetallic core with two bridging phenolato groups from two ligands. The coordination environment around each metal ion was completed by three nitrogen donor atoms from an amino arm of the ligand and an oxygen atom of the formyl group formed by hydrolysis, to give a distorted octahedron [92].

When reacted with $CuBr_2$, $CuCl_2{\cdot}2H_2O$ or $MnCl_2$, H-**93** forms the closely similar complexes $[M(\text{H-}\mathbf{93})(X)_2]$. $[Cu(\text{H-}\mathbf{93})(Cl)_2]{\cdot}H_2O$ is converted, under basic conditions, into $[Cu(\mathbf{93})(Cl)]{\cdot}H_2O$. The copper(II) ion is in a distorted N_3OCl_2 octahedral geometry in $[Cu(\text{H-}\mathbf{93})(Cl)_2]{\cdot}H_2O$ and square pyramidal in $[Cu(\mathbf{93})(Cl)]{\cdot}H_2O$ [93,94]. $[Cu(\text{H-}\mathbf{93})(Cl)_2]$ and $[Cu(\mathbf{93})(Cl)]$ are able to cleave very rapidly unactivated peptide bonds from bovine serum albumine (BSA) and the thermo stable enzyme Taq DNA polymerase at micromolar concentration, under mild pH and temperature conditions. These complexes are apparently not selective for hydrolysis of a specific peptide bond but rather for a specific region of the protein [93].

H-**93** and $Cu(NO_3)_2$ afford $[Cu_2(\mathbf{93})(\mu\text{-}NO_3)(NO_3)_2]$ [93] with the two copper ions, 3.065 Å apart, bridged by an endogenous μ-phenoxo group and by an exogenous bidentate nitrate anion: one copper(II) ion is five coordinate in an almost ideal square N_3O_2 pyramidal geometry. The other copper(II) ion is six coordinate with a much distorted O_6 octahedral geometry (Fig. 57). The magnetic susceptibility measurements indicate a ferromagnetic behavior for this dinuclear nitrate complex ($J = 3.2\ cm^{-1}$) [94]. Whereas the structure of the mononuclear complexes appears to be mostly retained upon dissolution, the dinuclear nitrate complex dissociates in methanol [94].

H-**93** and cobalt or manganese salts of weakly coordinating or no coordinating anions yield the isomorphous complexes $[Co_2(\mathbf{93})_2](ClO_4)_2{\cdot}0.7CH_3OH$, $[Co_2(\mathbf{93})_2](BF_4)_2{\cdot}CH_3OH$ (Fig. 58) and $[Mn_2(\mathbf{93})_2](BF_4)_2{\cdot}(C_2H_5)_2O$, with the metal ion coordinated by three nitrogen donor atoms of a pendant arm, two oxygen atoms from deprotonated cresolate moieties and the oxygen atom of the formyl group. The two metal ions, in a significantly distorted N_3O_3 octahedron surrounding and with a Co···Co or Mn···Mn separation of 3.203 Å and 3.401 Å, are bridged by two μ-phenoxy bridges from two deprotonated cresolates. In $[Co_2(\mathbf{93})_2](ClO_4)_2{\cdot}0.7CH_3OH$ and $[Co_2(\mathbf{93})_2](BF_4)_2{\cdot}CH_3OH$ an antiferromagnetic interaction occurs ($-J = 3.56\ cm^{-1}$ and 3.30 cm^{-1}) while for $[Mn_2(\mathbf{93})_2](BF_4)_2{\cdot}(C_2H_5)_2O$ a J value of 0.57 cm^{-1} was found [95].

$Cu(NO_3)_2{\cdot}3H_2O$ and H-**95**, H-**95a** or H-**95b**, obtained by reduction of the related Schiff bases, form $[Cu_2(\mathbf{L})(NO_3)_2(H_2O)_{1.5}](NO_3)$, where only an endogenous phenolato bridge occurs, which promotes the large Cu···Cu separation of 3.900 Å [91]. One copper(II) ion is in a much distorted N_3O_3 octahedron while the other copper ion is in a distorted N_2O_4 octahedron (Fig. 59). The complex shows weak ferromagnetic coupling between the two copper ions ($J = 4.6\ cm^{-1}$). Cyclic voltammogram of $[Cu_2(\mathbf{95})(H_2O)_{1.5}(NO_3)_2](NO_3)$ in acetonitrile, shows two successive irreversible one-electron electrochemical signals, at −0.13 V and at −0.33 V attributed to the formation of $Cu^{II}Cu^{I}$ and $Cu^{I}Cu^{I}$ species, respectively. In addition, a very broad peak at ca. −0.7 V suggests the reduction of both copper ions to Cu^0 [91].

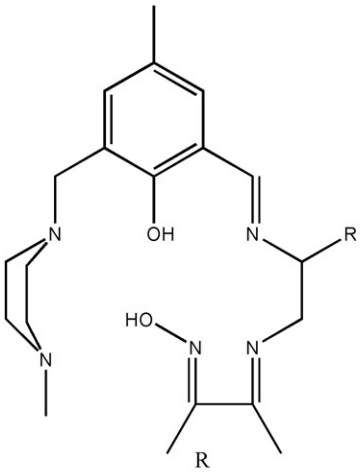

R

H_2-**87** H

H_2-**88** CH_3

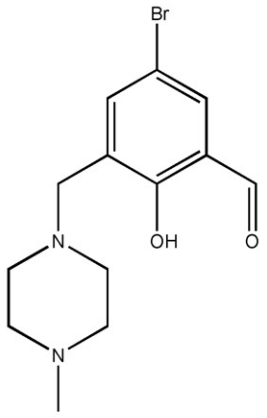

H-**89a**

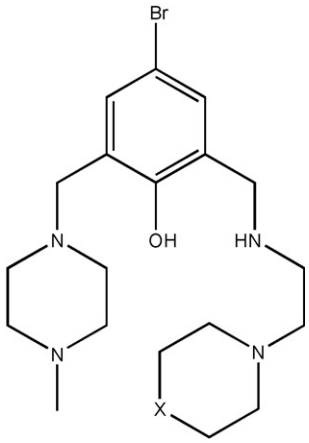

X

H-**89** CH_2

H-**90** O

H-**91** S

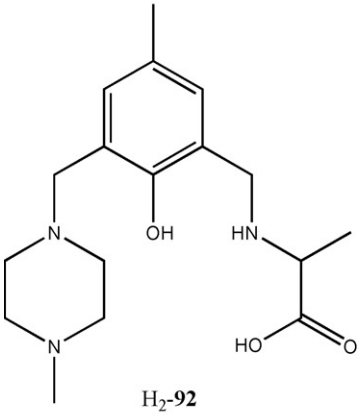

H_2-**92**

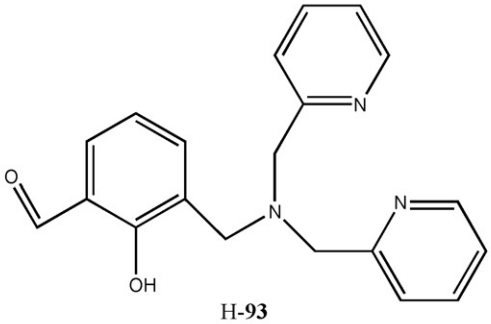

H-**93**

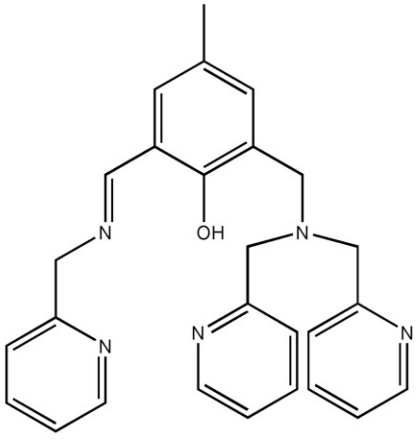

H-**94**

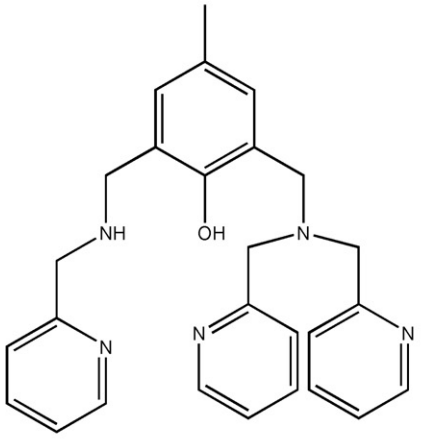

H-**95**

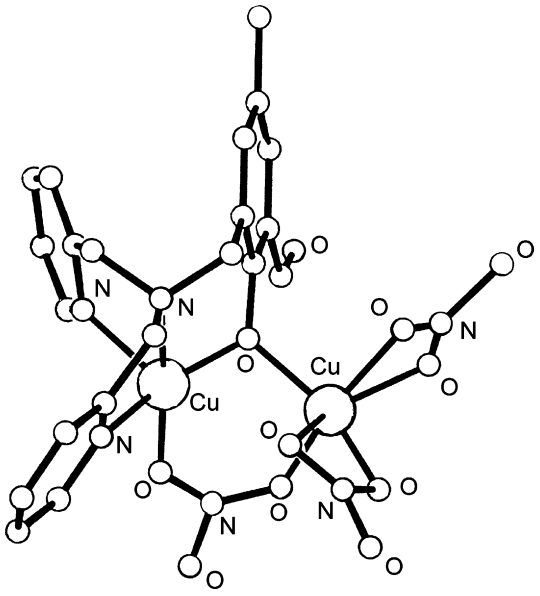

Fig. 57. Structure of $[Cu_2(\mathbf{93})(\mu\text{-}NO_3)(NO_3)_2]$.

H-**95b** and $CuCl_2$ or $Cu(ClO_4)_2$ in the presence of $NH_2OH{\cdot}HCl$ form the structurally similar $[Cu_2(H\text{-}\mathbf{95b})_2(\mu\text{-}Cl)_2](CuCl_4)_2$ and $[Cu_2(H\text{-}\mathbf{95b})_2(\mu\text{-}Cl)_2](ClO_4)_4{\cdot}6CH_3OH$, respectively, where the phenol group of H-**95b** and the secondary amine nitrogen atom are protonated. Two mononuclear units are doubly bridged by two chloride anions, which hold the two octahedrally distorted copper ions at a distance of 3.439 or 3.521 Å, respectively [95].

H-**95**, H-**95a** and H-**95b** form highly active copper-catalysts in the oxidative coupling of 2,6-dimethylphenol (DMP) with the formation of poly(1,4-phenylene ether) (PPE) together with small percentage of diphenoquinone (DPQ). The highest conversion to PPE was obtained by the copper(II) complex of H-**95b** [95].

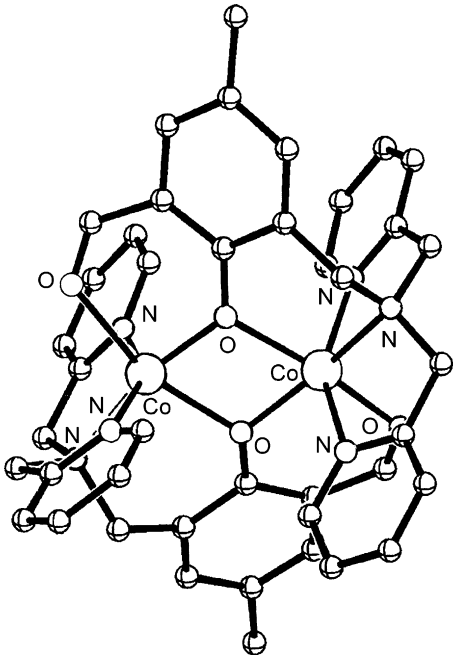

Fig. 58. Structure of $[Co_2(\mathbf{93})_2]^{2+}$.

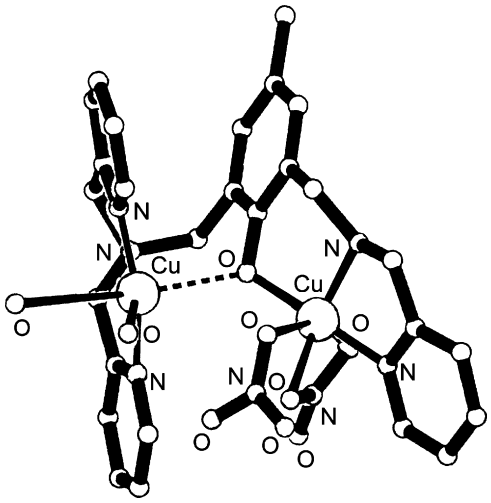

Fig. 59. Structure of $[Cu_2(\mathbf{95})(NO_3)_2(H_2O)_{1.5}]^+$.

H-**96**, derived from the condensation of H-**93** with *n*-propylamine, contains adjacent NO and N_3O donor sets. Addition of $Ni(CH_3COO)_2{\cdot}4H_2O$ together with $NaClO_4$ or $NaPF_6$ gave $[Ni_4Na(\mathbf{96})_2(CH_3COO)_6(CH_3OH)_2](ClO_4)$, and $[Ni_4Na(\mathbf{96})_2(CH_3COO)_6(CH_3OH)_2](PF_6)$. The same reaction in the presence of the potassium and ammonium salts affords $[Ni_3(\mathbf{96})_2(CH_3COO)_2(CH_3OH)(H_2O)](BF_4)_2$ and $[Ni_3(\mathbf{96})_2(CH_3COO)_2(CH_3OH)_2](PF_6)_2$, respectively [96].

In the closely similar structures of $[Ni_4Na(\mathbf{96})_2(CH_3COO)_6(CH_3OH)_2](PF_6)$ and $[Ni_4Na(\mathbf{96})_2(CH_3COO)_6(CH_3OH)_2](ClO_4)$, the pentanuclear core comprises two dinuclear $\{Ni_2(\mathbf{96})\}$ units which are each linked to the sodium ion by a monodentate bridging acetate and two bridging μ_3-acetato-κO:κO:κO′ groups. The intermetallic Ni···Ni separations are 3.388 Å while the Na···Ni ones are 3.008 Å, 3.006 Å, 4.903 Å and 4.901 Å. The sodium(I) ion is six coordinate in a distorted O_6 octahedral donor set. The nickel(II) ions are also six coordinate in distorted octahedral environments: two nickel(II) ions are in NO_5 donor compartments whilst the other two nickel(II) ions are in N_3O_3 donor compartments (Fig. 60) [96].

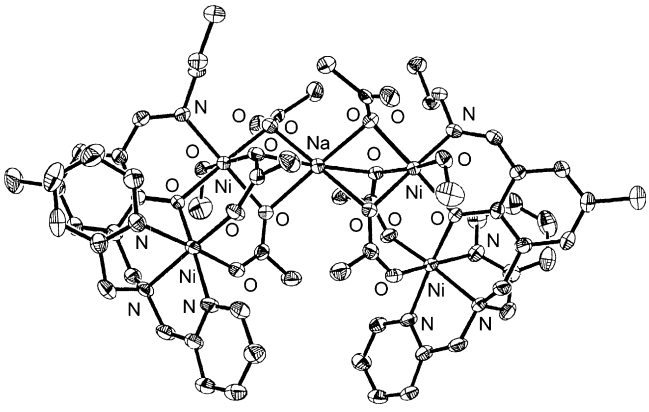

Fig. 60. Structure of $[Ni_4Na(\mathbf{96})_2(CH_3COO)_6(CH_3OH)_2]^+$.

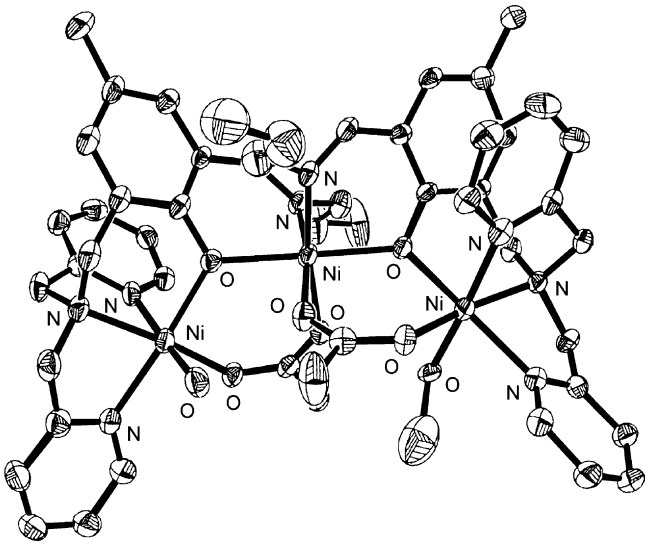

Fig. 61. Structure of $[Ni_3(\mathbf{96})_2(CH_3COO)_6(CH_3OH)(H_2O)]^{2+}$.

Also $[Ni_3(\mathbf{96})_2(CH_3COO)_2(CH_3OH)_2](PF_6)_2$ and $[Ni_3(\mathbf{96})_2(CH_3COO)_2(CH_3OH)(H_2O)](BF_4)_2$ are closely similar each other. The nickel(II) ions in $[Ni_3(\mathbf{96})_2(CH_3COO)_2(CH_3OH)(H_2O)](BF_4)_2$, form a triangle where the Ni···Ni distances are 3.644 Å, 3.639 Å and 6.627 Å, respectively. Each nickel(II) ion has a distorted octahedral geometry with the apical oxygen atoms of the one nickel(II)-based octahedron serving also as apices at the other two nickel(II) ions. Two nickel(II) ions are in N_3O_3 donor compartments whilst the third nickel(II) ion is in an N_2O_4 donor compartment provided by two bridging cresolato oxygen atoms, two acetate oxygen atoms and two imino nitrogen atoms. The oxygen atoms of the acetates occupy equatorial positions of two nickel(II) ions in the N_3O_3 compartment and both acetates form *syn–syn* bidentate bridges, between these metal ions and that in the N_2O_2 compartment (Fig. 61) [96].

In $[Fe^{III}Zn^{II}(\mathbf{97})(CH_3COO)_3](BPh_4)\cdot H_2O$, prepared by the reaction of H-**97** with $Fe(CH_3COO)_3$ and $Zn(CH_3COO)_2\cdot 2H_2O$ in the presence of sodium tetraphenylborate, the two metal ions, 3.385 Å apart, are bridged by the phenolate oxygen atom of $[\mathbf{97}]^-$ and two acetate groups in a *syn–syn* mode. The six coordinate iron(III) ion is bound to the bidentate arm while the six coordinate zinc(II) ion is bound to the tridentate arm. The site specificity of metal ions in the $Fe^{III}Zn^{II}$ complex indicates that the smaller metal ion is bound to the tridentate arm and the larger metal ion to the tridentate arm (Fig. 62a) [97].

A water/dimethylformamide solution (2:98) of the $Fe^{III}Zn^{II}$ complex (2×10^{-3} M) at 25 °C completely hydrolyses tri(*p*-nitrophenyl)phosphate (TNP) to hydrogen-di(*p*-nitrophenyl)phosphate (HDNP) in 100 min followed by hydrolysis of (DNP^-) into phenylphosphate $(MNP)^{2-}$. It was found that the {FeZn (DNP)} adduct is formed at the initial stage and the bound $(DNP)^-$ is slowly hydrolyzed into phenylphosphate $(MMP)^{2-}$. The hydrolysis of $(DNP)^-$ into $(MMP)^{2-}$ is almost completed in 700 min. Under similar conditions the analogous Zn_2 complex has no activity to hydrolyze $(DNP)^-$. The Zn complex releases the acetate bridge

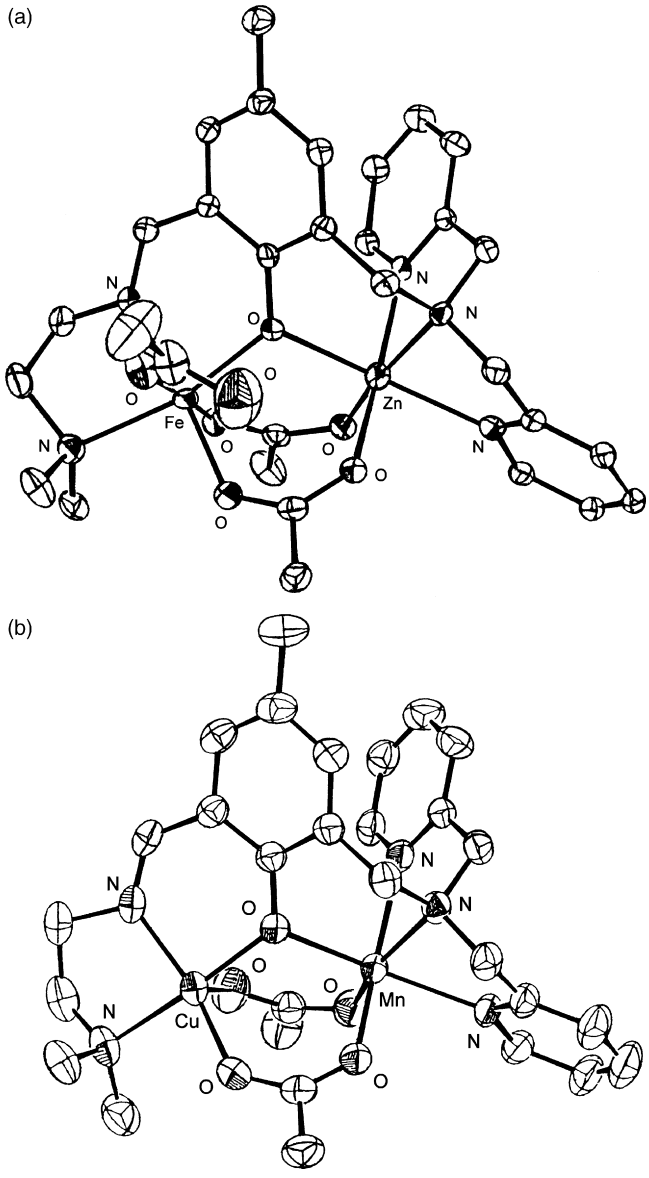

Fig. 62. Structure of $[FeZn(\mathbf{97})(CH_3COO)_3]^+$ (a) and $[CuMn(\mathbf{97})(CH_3COO)_2]^+$ (b).

more or less in a dilute solution, providing vacant sites on the two metal centers. The resulting species can accommodate $(DNP)^-$ in the chelating mode on the iron(III) center and OH^- (or H_2O) on the zinc(II) center, allowing the nucleophilic attack of the OH^- (or H_2O) to the phosphorus nucleus of $(DNP)^-$ [97].

The complexes $[M_aM_b(\mathbf{97})(CH_3COO)_2](ClO_4)$ ($M_aM_b = Cu^{II}Mn^{II}$, $Cu^{II}Fe^{II}$, $Cu^{II}Co^{II}$, $Cu^{II}Ni^{II}$, $Cu^{II}Zn^{II}$, $Zn^{II}Co^{II}$ and $Zn^{II}Ni^{II}$) were obtained by one-pot reaction of H-**97** and the desired couple of metal(II) acetates in the presence of sodium perchlorate. For $[CuNi(\mathbf{97})(CH_3COO)(NCS)_2]$ sodium thiocyanate was used instead of sodium perchlorate. FAB mass spectrometric studies demonstrate that these complexes have a discrete heterodinuclear core. For the ZnCo and for ZnNi complexes the same measurements indicate a partial disproportionation into the related homodinuclear species

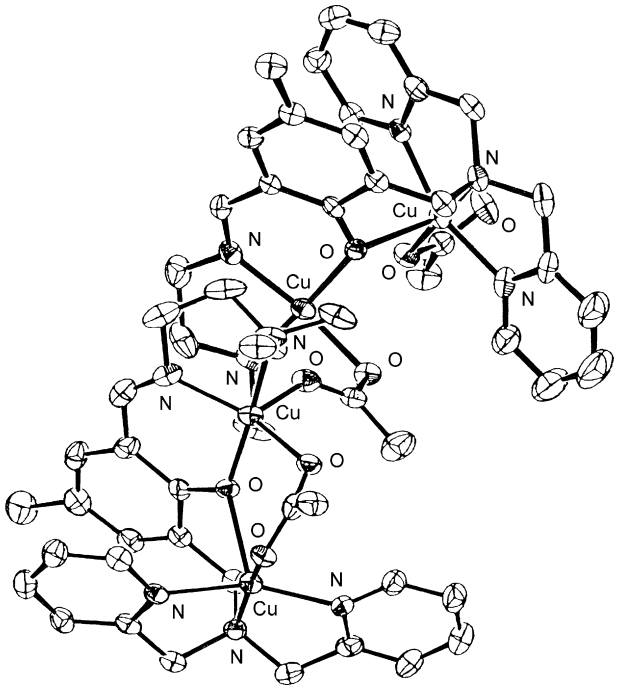

Fig. 63. Structure of $[Cu_4(\mathbf{97})_2(CH_3COO)_3]^{3+}$.

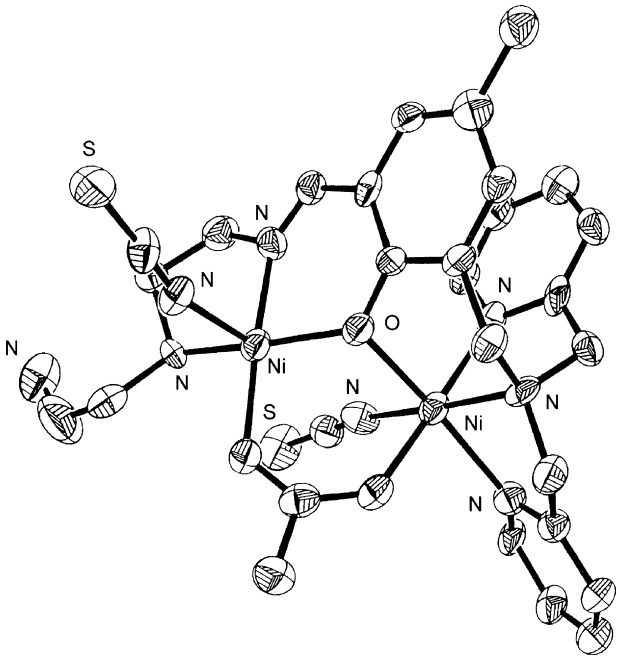

Fig. 64. Structure of $[Ni_2(\mathbf{99})(CH_3COO)(NCS)_2]$.

while for $[CuNi(\mathbf{97})(CH_3COO)(NCS)_2]$ no ion peak due to the homodinuclear species was detected [98].

$[CuM(\mathbf{97})(CH_3COO)_2](ClO_4)\cdot CH_3OH$ ($M = Mn^{II}$, Fe^{II}, Co^{II}, Ni^{II}, Zn^{II}) and $[ZnNi(\mathbf{97})(CH_3COO)_2](ClO_4)\cdot CH_3OH$ are isostructural. In the $Cu^{II}Mn^{II}$ complex the square pyramidal copper(II) ion is bound to the bidentate arm and the nearly octahedral manganese(II) ion is bound to the tridentate arm of $[\mathbf{97}]^-$. The metal ions, 3.301 Å apart, are bridged by the phenolate oxygen of $[\mathbf{97}]^-$ and two acetate groups (Fig. 62b) [98]. The site specificity of metal ions in $[ZnNi(\mathbf{97})(CH_3COO)_2](ClO_4)$, supported also by the structures of $[Zn_2(\mathbf{97})(CH_3COO)_2](ClO_4)$ and $[Ni_2(\mathbf{97})(CH_3COO)_2(CH_3OH)](PF_6)$, indicates that the zinc(II) ion is bound to the bidentate arm and the nickel(II)

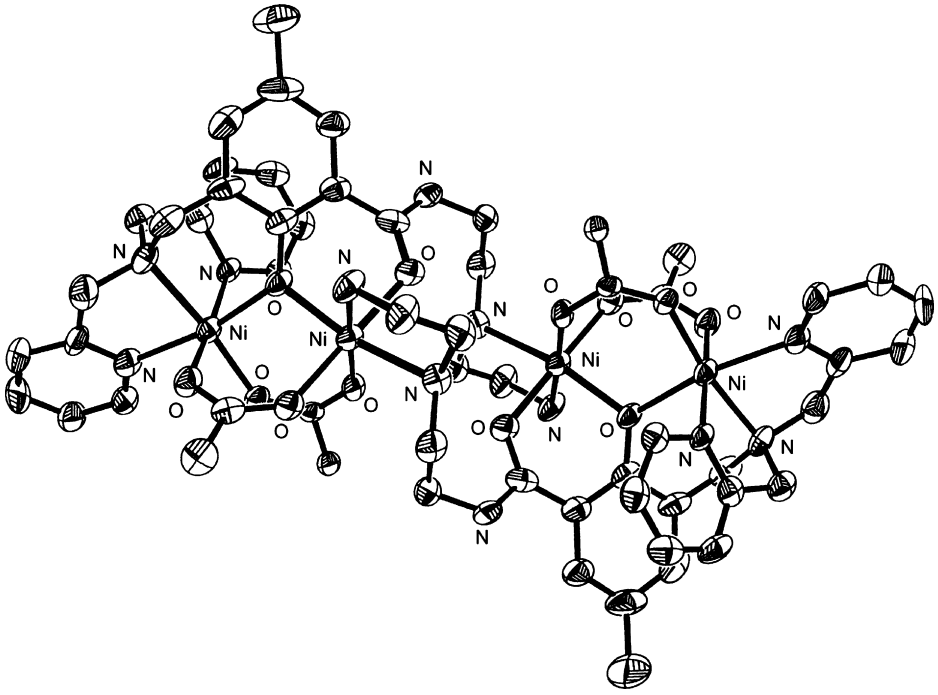

Fig. 65. Structure of $[Ni_4(\mathbf{100})_2(CH_3COO)_4]^{2+}$.

ion to the tridentate arm of [**97**]$^-$. It was supposed that [ZnCo(**97**)$(CH_3COO)_2$](ClO_4) has a zinc(II) and cobalt(II) site occupancy similar to that in [ZnNi(**97**)$(CH_3COO)_2$](ClO_4). In [CuNi(**97**)$(CH_3COO)(NCS)_2$] the square pyramidal copper(II), bound to the bidentate arm, and the six coordinate nickel(II) ion, bound to the tridentate arm of [**97**]$^-$, are 3.402 Å apart [98].

Attempts to form homodinuclear copper(II) complexes by the reaction of H-**97** and $Cu(CH_3COO)_2{\cdot}H_2O$ in the presence of sodium perchlorate, yield [Cu_4(**97**)$_2(CH_3COO)_3$]$(ClO_4)_3{\cdot}H_2O$ which shows a dimer-of-dimers structure, comprised of two dissimilar $\{Cu_2(\mathbf{97})(CH_3COO)\}^{2+}$ units (A and B) bridged by another acetate group. In the unit A, two square pyramidal copper(II) ions are doubly bridged by the phenolic oxygen atom and an acetate group. In unit B, the two copper(II) ions are singly bridged by the phenolic oxygen atom; one copper(II) ion, bound to the bidentate arm, assumes a planar geometry while the geometry around the other copper(II) ion is square pyramidal (Fig. 63) [98]. [Cu_4(**97**)$_2(CH_3COO)_3$]$(ClO_4)_3{\cdot}H_2O$ when reacted with [Zn_2(**97**)$(CH_3COO)_2$](ClO_4) (1:2) in dimethylformamide at 60 °C for 6 h almost quantitatively forms [CuZn(**97**)$(CH_3COO)_2$](ClO_4), [98].

H-**98** and H-**99**, prepared by in situ condensation of H-**93** with the requisite amine, react with nickel(II) acetate to give, after the addition of $NaBF_4$ or NaNCS, [Ni_2(**98**)$(CH_3COO)_2$](BF_4) and [Ni_2(**99**)$(CH_3COO)(SCN)_2$], whose structure has a common tilted metallocyclic core derived from a bridging phenolate, a bidentate bridging acetate and a pair of nickel(II) ions with a further acetate bridge in [Ni_2(**98**)$(CH_3COO)_2$](BF_4) and an asymmetric isothiocyanato bridge in [Ni_2(**99**)$(CH_3COO)(SCN)_2$]. In [Ni_2(**98**)$(CH_3COO)_2$](BF_4) the terminal –OH group of the aminic pendant arm binds to a nickel ion but in [Ni_2(**99**)$(CH_3COO)(SCN)_2$] an isothiocyanate anion binds in the corresponding position with the terminal $–NH_2$ group of the non-coordinated pendant group. This appears to reflect the comparative bond strengths of the putative donor groups: in [Ni_2(**98**)$(CH_3COO)_2$](BF_4) the counter ion is non-coordinating and so the pendant arm binds fully, whereas in [Ni_2(**99**)$(CH_3COO)(NCS)_2$] the isothiocyanate anion binds preferentially to the nickel ion [99]. [Ni_2(**98**)$(CH_3COO)_2$](BF_4) contains two six coordinate nickel(II) ions, one in a N_2O_4 octahedral environment and the other in a N_3O_3 distorted octahedral environment, bridged by the phenolate oxygen atom of [**98**]$^-$ and by two *syn–syn* bidentate acetate anions.. The Ni···Ni separation is 3.332 Å (Fig. 64a). In [Ni_2(**99**)$(CH_3COO)(NCS)_2$] the six coordination of the nickel(II) ion in the aminic compartment is completed by interaction with the three nitrogen atoms of the dipodal arm and the nitrogen atom of an isothiocyanate anion. The coordination geometry at the nickel(II) in the iminic compartment is square pyramidal, with an NCS^- in an axial position. [**99**]$^-$ provides a molecular cleft into which the metal ions fit. The terminal amino function is not coordinated and the Ni···Ni separation is 3.208 Å (Fig. 64b) [99].

The reaction of 2-(2-aminoethylamino)ethanol and 3-[(bispyridin-2-ylmethylamino)methyl]-2-2-hydroxy-5-methylbenzaldehyde, followed by the addition of $Ni(CH_3COO)_2{\cdot}4H_2O$ and NaNCS affords

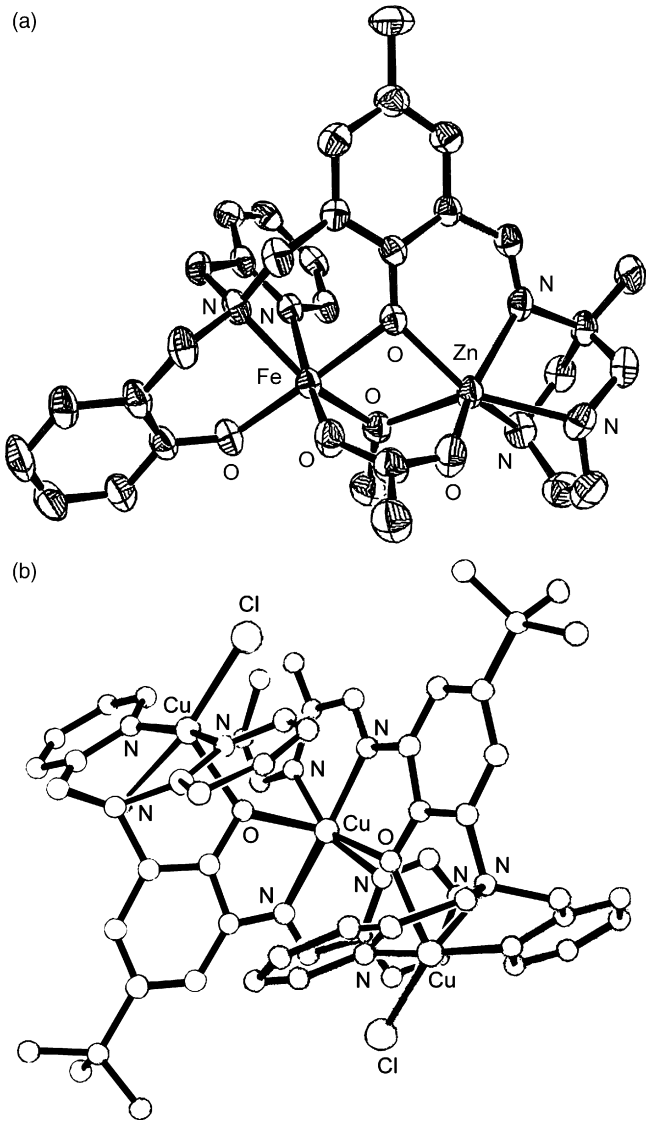

Fig. 66. Structure of [FeZn(**101**)(μ-OCH_3)(μ-CH_3COO)]$^+$ (a) and [Cu_3(**101b**)$_2(Cl)_2$]$^{2+}$ (b).

[Ni_2(**98**)$(CH_3COO)(NCS)_2$], whose structure is closely similar to that of [Ni_2(**99**)$(CH_3COO)(NCS)_2$], contains two six coordinate nickel(II) ions, 3.332 Å apart, bridged by the cresolate oxygen atom of [**98**]$^-$, and a *syn–syn* bidentate ethanoate anion.

On the contrary the reaction of the preformed or formed in situ H-**99** with $Ni(CH_3COO)_2{\cdot}4H_2O$ in the presence of either BF_4^- or PF_6^- counter anions gives [Ni_4(**100**)$_2(CH_3COO)_4$]$(X)_2$ ($X = BF_4^-$, PF_6^-), where the iminic pendant arm of [**99**]$^-$ has been converted into the amidic pendant arm of [**100**]$^-$. Each nickel ion is in a pseudo-octahedral geometry: the nickel(II) ions in the aminic compartments are coordinated by N_3O_3 donor sets and those in the amidic compartments are coordinated by N_2O_4 donor sets. The octahedral share an oxygen apex, and the pairs of nickel ions are bridged by the cresolato oxygen atoms and by two *syn–syn* acetates. The average Ni···Ni separations are 3.415 Å (Fig. 65). A possible pathway for the generation of [Ni_4(**100**)$_2(CH_3COO)_4$]$(X)_2$

was proposed, where the initially formed dinuclear complex $[Ni_2(\mathbf{99})(CH_3COO)_2]^+$ is hydrolyzed at the imine to give $[Ni_2(\mathbf{93})(CH_3COO)_2(H_2NCH_2CH_2NHCH_2CH_2NH_2)]^+$. Two molecules of this complex self assemble to produce the tetranickel(II) carbinolamine complex $[Ni_4(\mathbf{100a})_2(CH_3COO)_4]^{2+}$, which undergoes oxidation of the carbinolamine C–N bond followed by tautomerisation to produce the amidic product $[Ni_4(\mathbf{100})_2(CH_3COO)_4](X)_2$ [100].

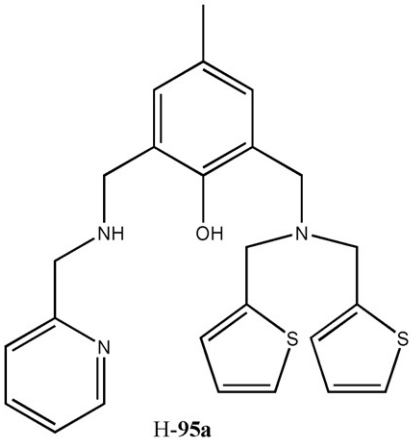

H-**95a**

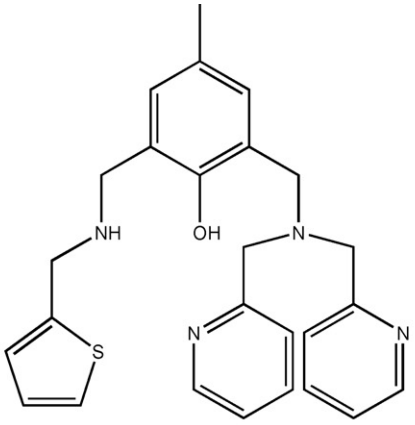

H-**95b**

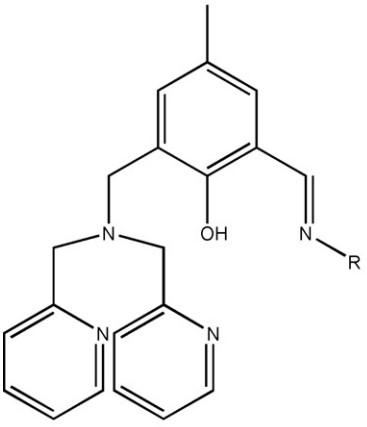

R

H-**96** C_3H_7

H-**97**

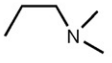

H-**98**

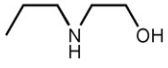

H-**99**

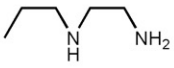

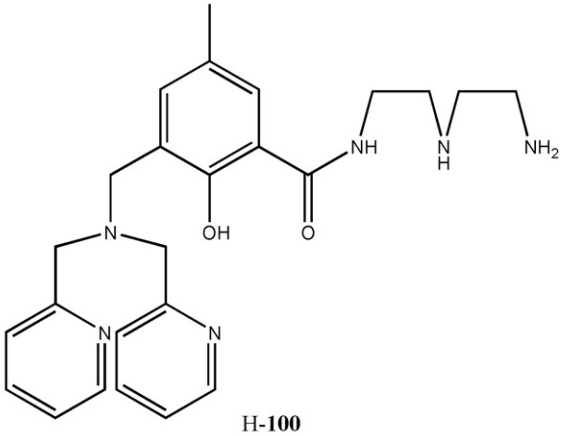

H-**100**

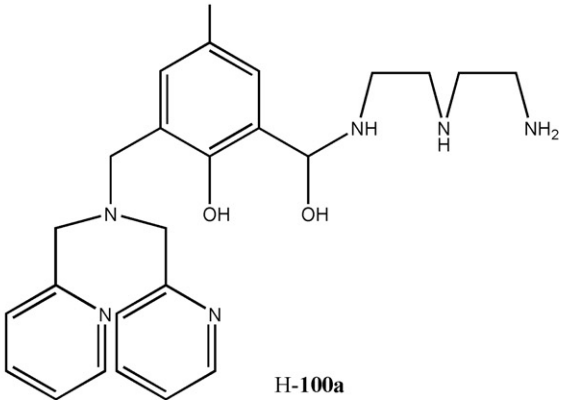

H-**100a**

The formyl precursor H-**101′**, prepared by reaction of (2-chloromethyl-4-methyl-6-formyl)phenol with *N*-(2-hydroxybenzyl)-*N*-(2-pyridylmethyl)amine [101], forms H_2-**101** by condensation with 2-amino-6-methylperhydro-1,4-diazepine [102]. The same condensation in the presence of $Zn(CH_3COO)_2{\cdot}6H_2O$, $Fe(ClO_4)_3{\cdot}9H_2O$ and $Na(CH_3COO)$ affords $[Fe^{III}Zn^{II}(\mathbf{101})(\mu\text{-}OCH_3)(\mu\text{-}CH_3COO)](ClO_4)$ [103] where the iron(III) ion in a N_2O_4 octahedral environment and the zinc(II) ions in a highly distorte N_3O_3 octahedral environment, 3.08 Å apart, are bridged by the phenolate oxygen of $[\mathbf{101}]^{2-}$ and by exogenous carboxylate and methoxy groups (Fig. 66a) [103].

$[Cu(CH_3CN)_4](ClO_4)$ and H-**101a**, derived from 2-chloropycolylchloride and 4-*tert*-butyl-2,6-diaminophenol, form $[Cu_2^{I}(\text{H-}\mathbf{101a})(CH_3CN)_2](ClO_4)_2$. The further addition of O_2 at 80 °C in nitrile solvent gives rise to $[Cu_2^{II}(\mathbf{101a})(OOH)(RCN)_2]^{2+}$ (R = CH_3, CH_3CH_2, $C_6H_5CH_2$), which thermally turns into $[Cu_3^{II}(\mathbf{101b})_2(Cl)_2](PF_6)_2$: a multiple oxidative reaction, as revealed by the X-ray structure, has transformed $[\mathbf{101a}]^-$ into the Schiff base $[\mathbf{101b}]^-$. The presence of chloride ligands indicates that CH_2Cl_2, used as solvent, has been involved in the complicated and multistep reaction. The trinuclear complex is constructed of a dimer of the modified Schiff base ligand $[\mathbf{101b}]^-$, connected by coordination to an additional central copper(II) ion. The terminal copper(II) ions are slightly distorted square pyramidal while the central copper(II) ion is six coordinate (Fig. 66b) [104].

H_2-**102**, obtained by [1 + 1] condensation of methyl-2-aminocyclopenten-1-ene-1-dithiocarboxylate with 1,3-diamino-2-hydroxypropane followed by addition of 1-hydroxomethylpyrazole to the resulting Schiff base, reacts with the appropriate nickel(II) salt in the presence of base and pyrazole (H-Pz) or 2-mercaptopyridine (H-Spy) to generate $[Ni_2(\mathbf{102})(\mu\text{-pz})(H_2O)](ClO_4){\cdot}CH_3COCH_3$ or $[Ni_2(\mathbf{102})(\mu\text{-Spy})](BPh_4)$. In both the complexes, the nickel center, bound to the bidentate NS arm of $[\mathbf{102}]^{2-}$, has approximate square planar geometry while the other nickel(II) center has a distorted octahedral geometry in $[Ni_2(\mathbf{102})(\mu\text{-pz})(H_2O)](ClO_4){\cdot}CH_3COCH_3$ and a square pyramidal geometry in $[Ni_2(\mathbf{102})(\mu\text{-Spy})](BPh_4)$ (Fig. 67) [105].

Magnetic moments of 3.23 and 3.16 μ_B at room temperature are in agreement with the presence of only one high-spin nickel(II) center in both $[Ni_2(\mathbf{102})(\mu\text{-pz})(H_2O)](ClO_4){\cdot}CH_3COCH_3$ and $[Ni_2(\mathbf{102})(\mu\text{-Spy})](BPh_4)$. Electrochemical results from $[Ni_2(\mathbf{102})(\mu\text{-pz})(H_2O)](ClO_4){\cdot}CH_3COCH_3$ and $[Ni_2(\mathbf{102})(\mu\text{-Spy})](BPh_4)$ thus indicate the possible involvements of the five binuclear nickel species $Ni^{II}Ni^{II} \rightleftharpoons Ni^{II}Ni^{III} \rightleftharpoons Ni^{III}Ni^{III}$ and $Ni^{II}Ni^{II} \rightleftharpoons Ni^{II}Ni^{I} \rightleftharpoons Ni^{I}Ni^{I}$. In $[Ni_2(\mathbf{102})(\mu\text{-pz})(H_2O)](ClO_4){\cdot}CH_3COCH_3$, process $Ni^{II}Ni^{II} \rightleftharpoons Ni^{II}Ni^{III}$ is reversible at low temperature and at higher scan speeds (>500 mV s^{-1}) and probably involves electron transfer at the octahedral site [105].

The homodinuclear complexes $[Cu_2(\mathbf{104})(\mu\text{-pz})](ClO_4)$ and $[Cu_2(\mathbf{103})(\mu\text{-pz})](ClO_4)$ or the hetero-dinuclear $[CuZn(\mathbf{104})(\mu\text{-pz})](ClO_4)$ and $[CuZn(\mathbf{103})(\mu\text{-pz})](ClO_4)$ derive from the

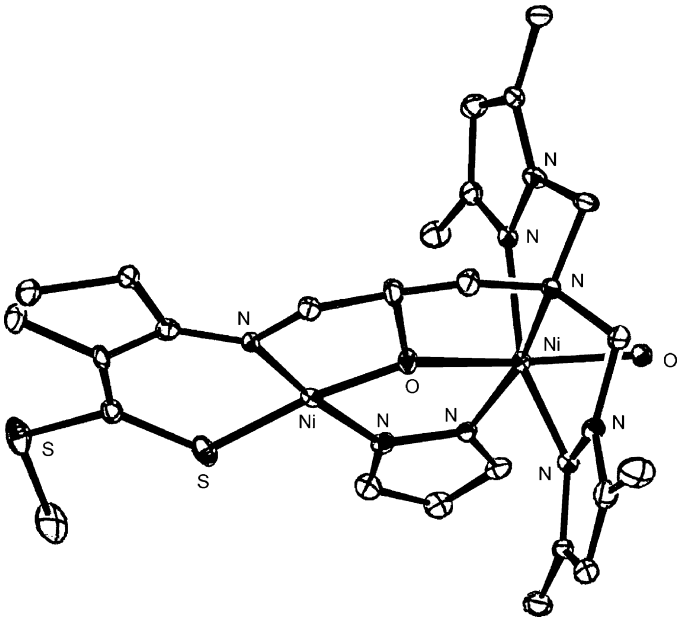

Fig. 67. Structure of $[Ni_2(\mathbf{102})(\mu\text{-pz})(H_2O)]^+$.

one-pot reaction of $[Cu(CH_3CN)_4](ClO_4)$ or $Zn(ClO_4)_2{\cdot}6H_2O$ and $[Cu(CH_3CN)_4](ClO_4)$ with H_2-**102** and H_2-**103** in the presence of base and pyrazole, followed by exposure to atmospheric oxygen. Noticeably, H_2-**103** was prepared is the same way as H_2-**102**, using 1-hydroxymethylpyrazole instead of 1-hydroxymethyl-2,5-dimethylpyrazole). During the reaction, H_2-**102** undergoes an interesting change to H_2-**104** when dimethylpyrazole from one of its pyrazolyl arms gets exchanged with an extraneous pyrazole molecule, the latter being added to bridge the metal centers as confirmed by mass spectrometry and crystal structure analysis. Reversal of the sequence of metal ion addition in the formation of hetero-dinuclear complexes does not however affect the course of this reaction. The regioselective nature of these asymmetric binucleating ligands can selectively bind copper(I) in one of the sites that involves the ONS donor set, thus offering an opportunity to isolate a heterodinuclear compound by a single step reaction [105].

$[CuZn(\mathbf{104})(\mu\text{-pz})](ClO_4)$ has the ligand $[\mathbf{102}]^{2-}$ in the modified form $[\mathbf{104}]^{2-}$. The steric constraints imposed by the dimethylpyrazolyl arms of $[\mathbf{102}]^{2-}$ could be the driving force for such exchange reaction. This explanation gains further evidence by the isolation of a compound with ligand structure of $[\mathbf{102}]^{2-}$ remaining intact when a larger cation as cadmium(II) is used to replace the zinc(II) ion in the above reaction. Use of imidazole as a bridging ligand in the above syntheses did not yield the desired products. The X-ray structures of $[Cu_2(\mathbf{104})(\mu\text{-pz})](ClO_4)$ and $[CuZn(\mathbf{104})(\mu\text{-pz})](ClO_4)$ confirm the modified structure of $[\mathbf{104}]^{2-}$ involving the replacement of dimethylpyrazolyl part by pyrazole in one of the appended arms. In $[Cu_2(\mathbf{104})(\mu\text{-pz})](ClO_4)$, one of the copper(II) centers has an approximate square planar geometry while the adjacent copper(II) center is five coordinate with a highly distorted square pyramidal geometry. The Cu···Cu separation is 3.368 Å. $[CuZn(\mathbf{103})(\mu\text{-pz})](ClO_4)$ shows an essentially similar structure

to that of [CuZn(**104**)(μ-pz)](ClO$_4$), with a Cu···Zn separation of 3.340 Å [105].

A strong antiferromagnetic coupling was observed in [Cu$_2$(**104**)(μ-pz)](ClO$_4$) ($J = -285\,cm^{-1}$) and [Cu$_2$(**103**)(μ-pz)](ClO$_4$) ($J = -296\,cm^{-1}$) in agreement with EPR silent spectra at room temperature and at 77 K both in CH_3CN/toluene and solid state. Both the complexes undergo two one-electron reductions and a single step two-electron oxidation at ca. −0.26, −1.40, and 1.0 V versus Ag/AgCl reference, respectively. The quasi reversible process at −0.26 V is due to a one-electron $Cu^{II}Cu^{II} \rightleftharpoons Cu^{II}Cu^{I}$ reduction involving the square pyramidal copper site, while the Cu^{II}-$Cu^{I} \rightleftharpoons Cu^{I}Cu^{I}$ reduction at more negative potential involves the square planar copper center. The oxidation $Cu^{II}Cu^{II} \rightleftharpoons Cu^{III}Cu^{III}$ process involves a couple of electrons, resulting in a single-step two-electron transfer [105].

5. [1 + 2] Symmetric end-off systems

The [1 + 2] symmetric end-off compartmental ligands derive from the condensation of the diformyl precursors 2,6-diformyl-pyridazine, 2,6-diformyl-4-methylphenol, 2,6-diformyl-4-methylthiophenol or 3,5-diformylpyrazole with the primary amine precursors of Scheme 4. The reaction of these Schiff bases, containing two identical adjacent coordination chambers, with d-metal ions in a 1:2 molar ratio and in the presence of base as deprotonating agent, gives rise to the corresponding homodinuclear complexes, while the use of a 1:1 molar ratio favours mononuclear complexation. The same results may be obtained by a template procedure. Analogously, the related polyamine derivatives, synthesized by reduction of the [1 + 2] Schiff base, form quite easily homodinuclear complexes when

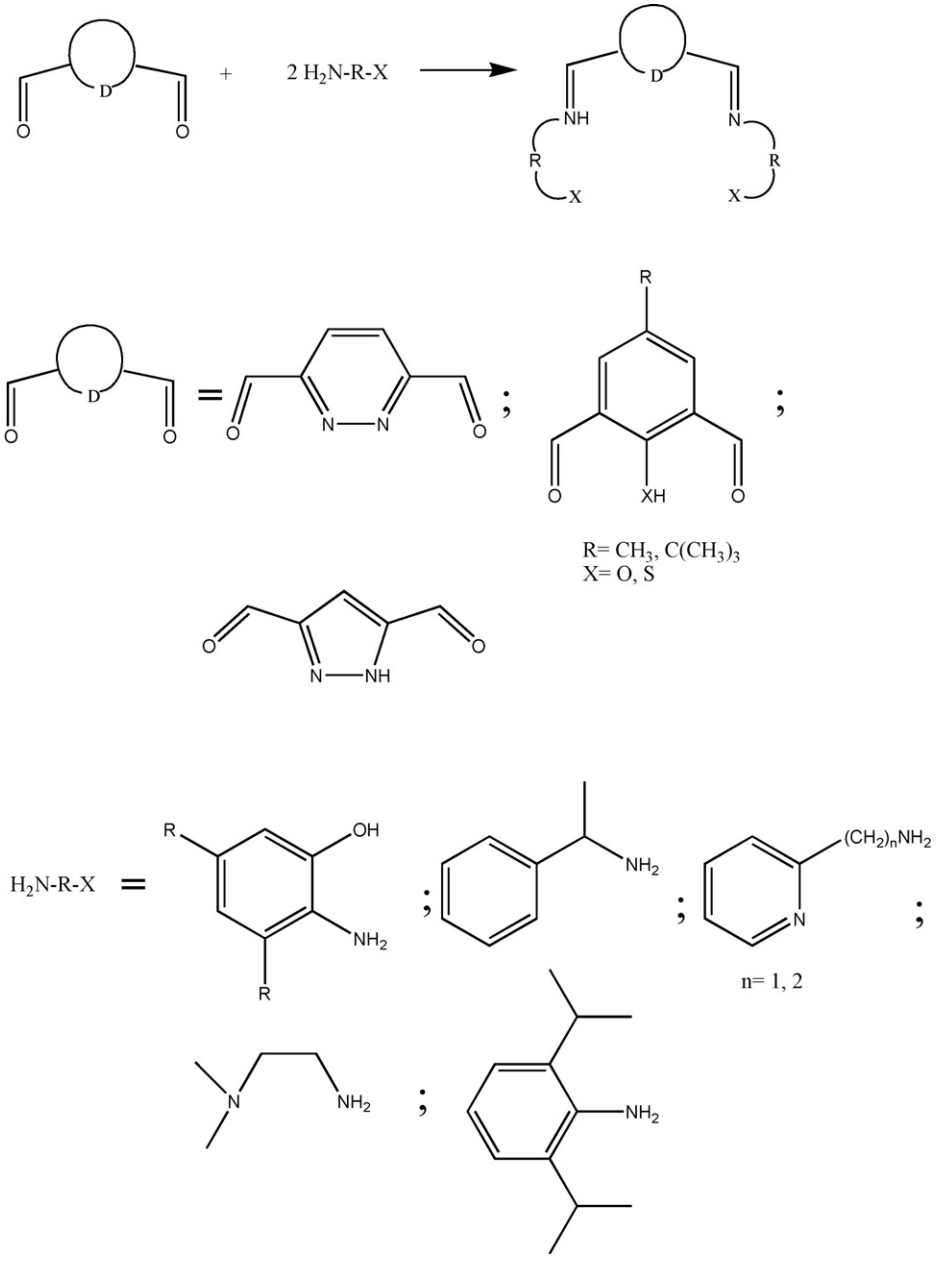

Scheme 4. Synthesis of the [1 + 2] symmetric end-off ligands.

reacted with the appropriate metal salt in the presence of base. The resulting dinuclear complexes contain an endogenous pyridazine N=N; phenolate oxygen $-O^-$ or a thiophenolate sulfur S^- and an exogenous bridging group. This last may form, under appropriate conditions, an additional intermolecular bridge, linking two dinuclear entity and giving rise to polynuclear species.

H_2-**105**, prepared by condensation of 3,6-diformylpyridazine and *o*-aminophenol, adopts an all *trans* configuration with the pyridazine ring rotated ca. 180° away from the imine nitrogen atoms and phenolic protons. The pyridazine diimine unit is fairly flat. With the appropriate metal acetate it forms $[Co_2(\mathbf{105})(CH_3COO)_2]$, $[Ni_2(\mathbf{105})(CH_3COO)_2(H_2O)]$ and $[Cu_2(\mathbf{105})(CH_3COO)_2(H_2O)_2(CH_3CN)]$; IR spectra support a 1,3-bridging bidentate coordination mode for the acetate groups in these complexes. The magnetic moments are typical for high spin octahedral nickel(II) or cobalt(II) complexes [106].

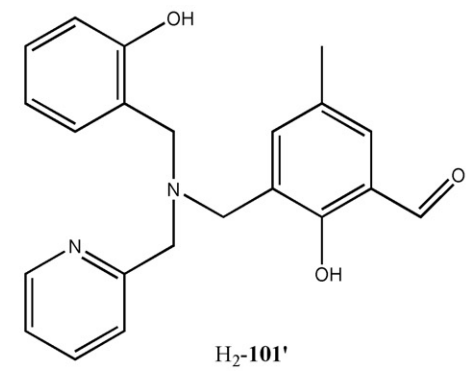

H_2-**101'**

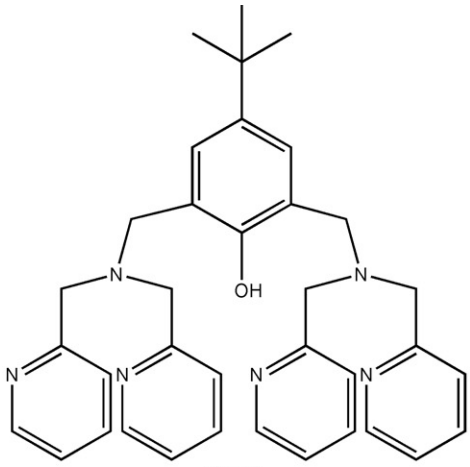

H-**101a**

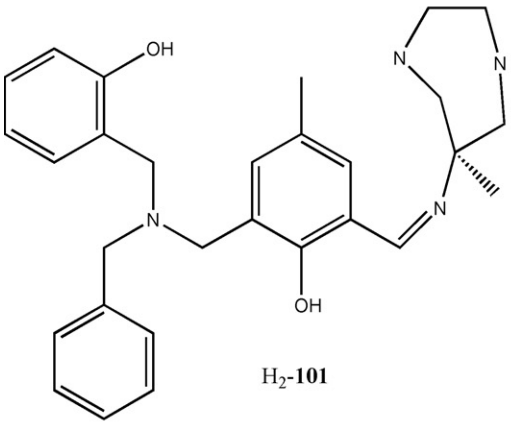

H_2-**101**

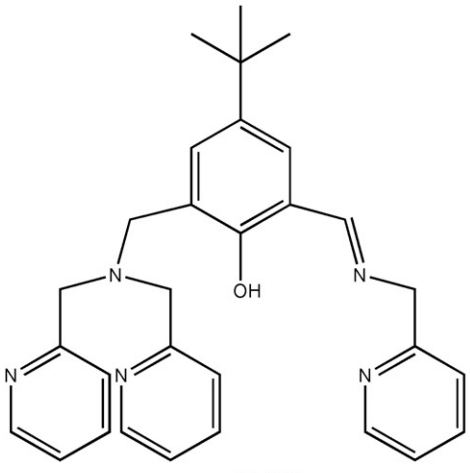

H-**101b**

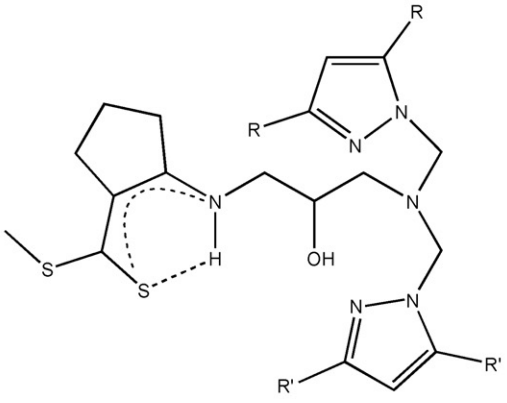

	R	R'
H_2-**102**	CH_3	CH_3
H_2-**103**	H	H
H_2-**104**	CH_3	H

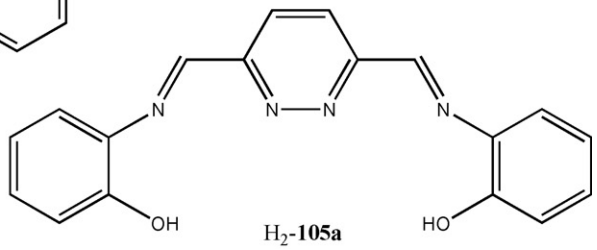

H_2-**105a**

106a, prepared by condensation of 3,6-diformylpyridazine with *p*-anisidine, forms $[Cu_4(\mathbf{106a})_4](PF_6)_4\cdot CH_3CN\cdot H_2O\cdot 0.25C_2H_5OC_2H_5$, $[Cu_4(\mathbf{106a})_4](BF_4)$, $[Zn_2(\mathbf{106a})_2(CH_3CN)_2(H_2O)_2](ClO_4)_4\cdot CH_3CN$, $[Ni_2(\mathbf{106a})_2(CH_3CN)_4](BF_4)_4\cdot 0.25C_2H_5OC_2H_5$, $[Co_2(\mathbf{106a})_2(H_2O)_2(CH_3CN)_2](ClO_4)_4\cdot 0.5CH_3CN$ and $[Mn_2(\mathbf{106a})_2(Cl)_4]\cdot 3H_2O$, when reacted with the corresponding metal salt. The tetranuclear complexes, by further reaction with thiocyanate anions, led to $[Cu_2(\mathbf{106a})_2(NCS)_2]\cdot H_2O$, also directly obtained from a mixture of **106a**, $[Cu(CH_3CN)_4](BF_4)$ and thiocyanate anions [107].

$[Cu_4(\mathbf{106a})_4](PF_6)_4\cdot CH_3CN\cdot H_2O\cdot 0.25C_2H_5OC_2H_5$ contains distorted tetrahedral copper(I) centers coordinated by two almost perpendicular and fairly flat strands of **106a** in a [2 × 2] grid arrangement. Each **106a** strand provides two bidentate N_2 donor sets to two different copper(I) ions. The pyridazine groups bridge each copper(I) centre to two neighboring copper(I) centers, forming a rhombus of bridged copper ions (Fig. 68a) [107].

In marked contrast, $[Zn_2(\mathbf{106a})_2(CH_3CN)_2(H_2O)_2](ClO_4)_4$, $[Ni_2(\mathbf{106a})_2(CH_3CN)_4](ClO_4)_4$ and $[Co_2(\mathbf{106a})_2(CH_3CN)_2(H_2O)_2](ClO_4)_4$ are similarly self-assembled as side-by-side structures, where each distorted octahedral metal(II) ion is bound by two almost coplanar N_2 bidentate moieties from two different **106a** strands, and by two axial acetonitrile and/or water molecules. The two **106a** ligand strands are significantly twisted. A comparable M···M separation occurs in these homodinuclear complexes: 4.066 Å for the Co_2, 4.050 Å for the Zn_2 and 4.056 Å for the Ni_2 complex, respectively (Fig. 68b). $[Mn_2(\mathbf{106a})_2(Cl)_4]\cdot 3H_2O$, not structurally characterized, was proposed to adopt the same side-by-side architecture. Variable temperature magnetic susceptibility studies yielded small negative J values for these side-by-side complexes: $J = -21.6\,cm^{-1}$ for $[Ni_2(\mathbf{106a})_2(H_2O)_4](BF_4)_4$; $J = -7.6\,cm^{-1}$ for $[Co_2(\mathbf{106a})_2(H_2O)_4](ClO_4)_4$; $J = -3.2\,cm^{-1}$ for $[Mn_2(\mathbf{106a})_2(Cl)_4]\cdot 3H_2O$ [107].

The product, derived from the reaction of equimolar amounts of **106a** and silver(I) tetrafluoroborate, contains two distinctly different [2 × 2] grids in a 1:4 ratio: one nearly square with exact S_4 symmetry and the other rhombically distorted, nearly planar with approximate C_2 symmetry leading to $[C_2\text{-}Ag_4(\mathbf{106a})_4]_4[S_4\text{-}Ag_4(\mathbf{106a})](BF_4)_{20}$. Each silver(I) centre is situated at the intersection of two approximately orthogonally arranged ligands, each of which provides two nitrogen donor sets, resulting in three sets of subtly different flattened tetrahedral geometries. The architecture of the $[C_2\text{-}Ag_4(\mathbf{106a})_4]^{4+}$ grid, where the four nearly coplanar silver(I) ions form a rhombus, is similar to that of the analogous copper(I) structure with **106a**. In the $[S_4\text{-}Ag_4(\mathbf{106a})_4]^{4+}$ grid there is a small tetrahedral distortion of the Ag_4 square with the silver(I) ions alternating above and below the Ag_4 mean plane. In contrast to $[C_2\text{-}Ag_4(\mathbf{106a})_4]^{4+}$, the neighboring pyridazine rings are orthogonal (Fig. 68c) [107].

The reaction of **106b** with $AgBF_4$ gives $[Ag_2(\mathbf{106b})_2](BF_4)_2$, with a dinuclear side-by-side architecture (Fig. 68d) rather than the tetranuclear [2 × 2] grid architecture formed by **106a**. The silver(I) ions, 3.800 Å apart, are in a N_4 tetrahedrally distorted square planar geometry somewhat shorter than in the silver(I) grid complexes of **106a**. [107].

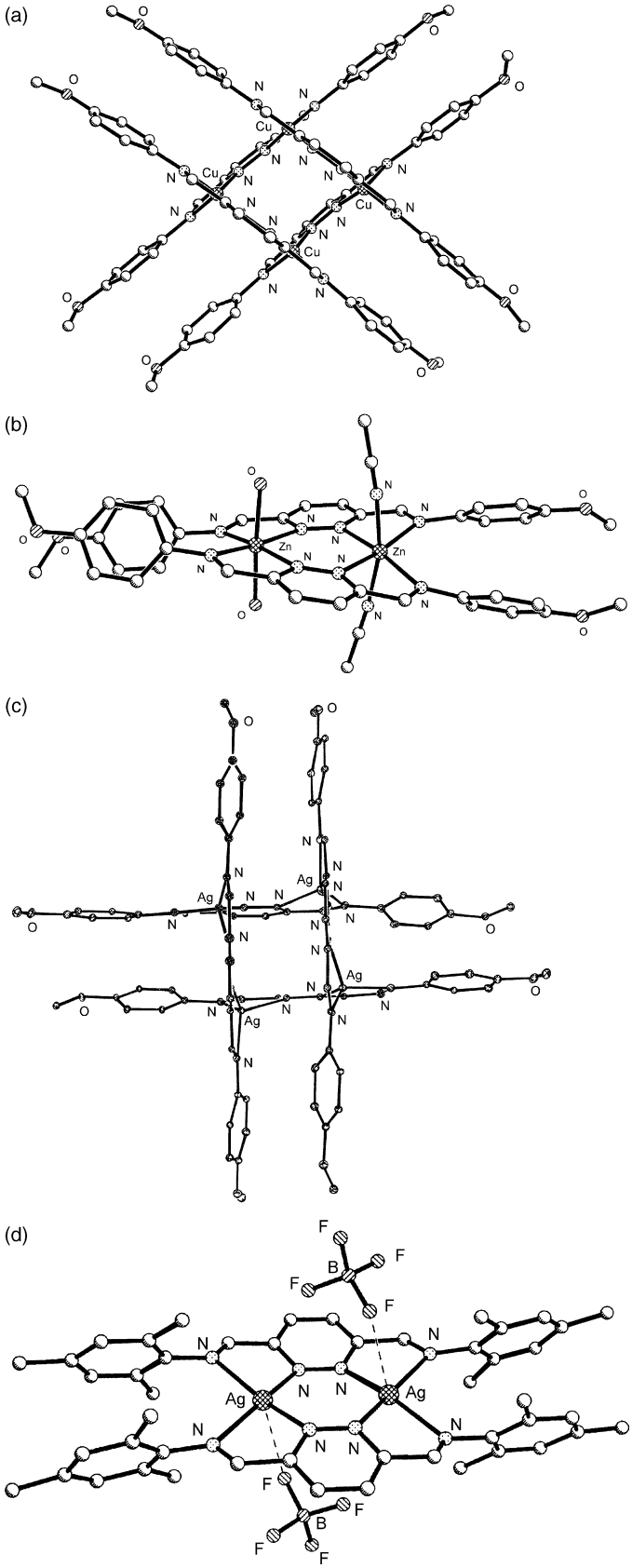

Fig. 68. Structure of $[Cu_4(\mathbf{106a})_4]^{4+}$ (a) and $[Zn_2(\mathbf{106a})_2(CH_3CN)_2(H_2O)_2]^{4+}$ (b), $[S_4\text{-}Ag_4(\mathbf{106a})]^{4+}$ (c) and $[Ag_2(\mathbf{106b})_2](BF_4)_2$ (d).

107a, deriving from the condensation of 3,6-diformylpyridazine and 2-(2-aminoethyl)pyridine, and the related reduced amine derivative **107b** [108] react with copper(II) or cobalt(II) perchlorate to afford $[Cu_2(\mathbf{107a})(\mu\text{-}OH)](ClO_4)_3$, $[Co_2(\mathbf{107a})(\mu\text{-}OH)(CH_3CN)_4](ClO_4)_3$ and $[Cu_2(\mathbf{107b})(\mu\text{-}OH)](ClO_4)_3$, respectively. The oil, formed by the analogous reaction using nickel(II) perchlorate, in the presence of either azide or thiocyanate ions, turns into $[Ni_2(\mathbf{107a})(\mu\text{-}NCS)(CH_3CN)_3(H_2O)](ClO_4)_3$ or $[Ni_2(\mathbf{107a})(\mu\text{-}N_3)(CH_3CN)_4](ClO_4)_3$ with the added anion acting as a one-atom bridge. Attempts to reproduce this architecture from $[Cu_2(\mathbf{107a})(\mu\text{-}OH)](ClO_4)_3$, by the addition of tetraethylammonium halide, resulted in the formation of $[Cu_2(\mathbf{107a})(\mu\text{-}OH)(Y)_2](ClO)$, ($Y = Cl^-$, Br^-) [108].

In $[Cu_2(\mathbf{107a})(\mu\text{-}OH)](ClO_4)_3$ both the hydroxide ion and the pyridazine moiety bridge the two square planar copper(II) ions, 3.392 Å apart and in a N_3O environment [108].

In $[Co_2(\mathbf{107a})(\mu\text{-}OH)(CH_3CN)_4](ClO_4)_3$ (Fig. 69a) five of the six donors of both the distorted octahedral cobalt(II) centers are nitrogen atoms, with the two pyridazine nitrogen atoms spanning the two metal centers while the sixth is a hydroxide oxygen donor which bridges the two metal centers. The Co···Co distance is 3.477 Å [108].

In $[Ni_2(\mathbf{107a})(\mu\text{-}NCS)(CH_3CN)_3(H_2O)](ClO_4)_3$ the two nickel(II) centers are in a N_6 or N_5O distorted octahedral environment, respectively with the pyridazine and thiocyanate nitrogen atoms bridging the two metal centers. One nickel(II) ion has a coordinated water molecule in place of an acetonitrile one. The Ni···Ni distance is 3.606 Å (Fig. 69b). Also in the similar $[Ni_2(\mathbf{107a})(\mu\text{-}N_3)(CH_3CN)_4](ClO_4)_3$ the nickel(II) centers are in N_6 distorted octahedral environments [108].

Strong antiferromagnetic exchange ($-2J = 1146\,cm^{-1}$) is exhibited by $[Cu_2(\mathbf{107a})(\mu\text{-}OH)](ClO_4)_3$, which is typical of hydroxide-bridged systems, whereas the competing antiferromagnetic pyridazine bridging pathway and ferromagnetic 1,1-bridging azide pathway resulted in the observation of weak antiferromagnetic exchange in $[Ni_2(\mathbf{107a})(\mu\text{-}N_3)(CH_3CN)_4](ClO_4)_3$ ($2J = -14\,cm^{-1}$). Cyclic voltammetry and coulometry results on $[Co_2(\mathbf{107a})(\mu\text{-}OH)(CH_3CN)_4](ClO_4)_3$, $[Ni_2(\mathbf{107b})(\mu\text{-}NCS)(CH_3CN)_3(H_2O)](ClO_4)_3$ and $[Cu_2(\mathbf{107b})(\mu\text{-}OH)](ClO_4)_3$ revealed multiple redox processes, tentatively assigned to a mixture of metal centered and ligand centered redox processes [108].

3,5-diformylpyrazole and 2,6-diisopropylphenylamine form H-**108a** which, by treatment with potassium *tert*-butoxide and $[Ni(Cl)_2(DME)]$ (DME = dimethoxyethane), affords $[Ni_6(\mathbf{108a})_3(Cl)_9]$, as indicated by FAB mass spectrometry and confirmed by the X-ray structure. Three dinuclear $\{N_2(\mathbf{108a})(Cl)_3\}$ building blocks have assembled via Cl-bridges to form a hexanuclear array with all the metal ions in distorted octahedral environment. The central $\{Ni_6(Cl)_9\}$ core consists of two roughly planar $\{Ni_3(Cl)_3\}$ ring systems, each capped by a μ_3-Cl ion. These two $\{Ni_3(Cl)_3\}$ planes are almost parallel and are held together by the three pyrazolate clips, thus forming a cage-like structure which accommodates a single chloride ion in its centre. Interstitial μ_6-Cl ion is bound to all the six nickel ions in an almost trigonal prismatic fashion

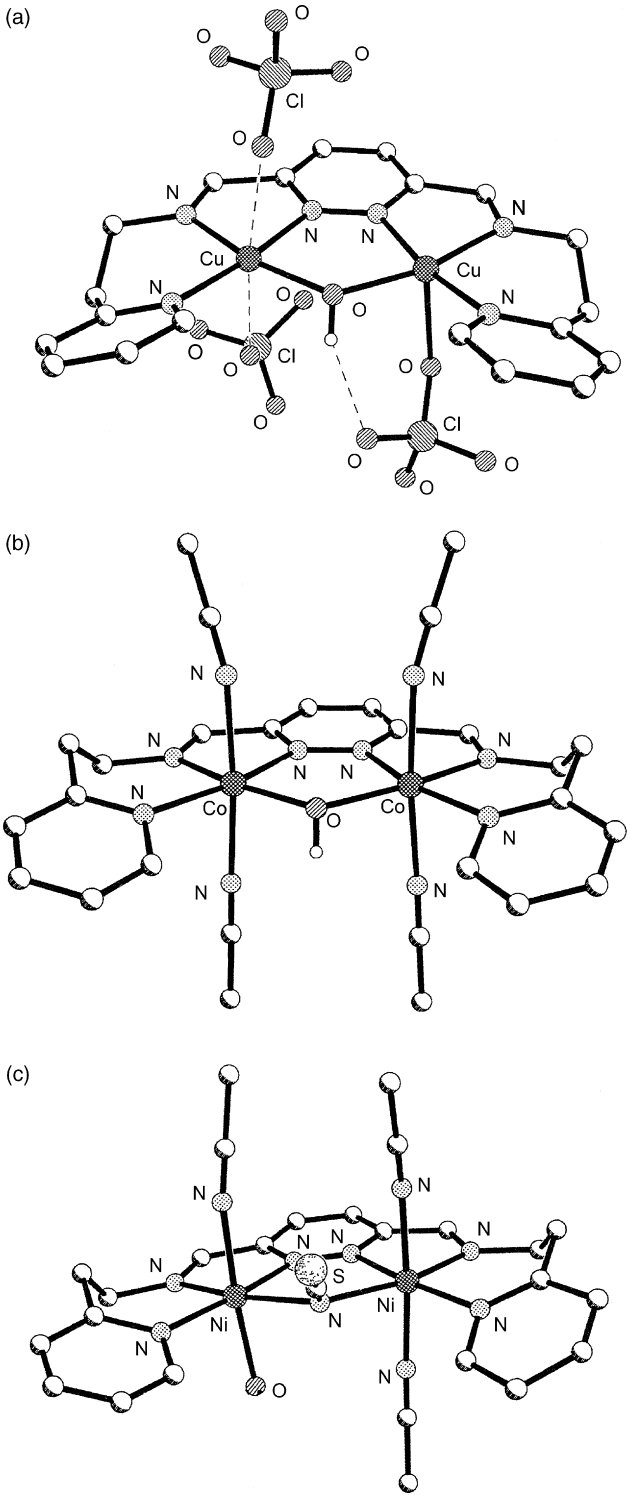

Fig. 69. Structure of $[Co_2(\mathbf{107a})(\mu\text{-}OH)(CH_3CN)_4]^{3+}$ (a) and $[Ni_2(\mathbf{107a})(\mu\text{-}NCS)(CH_3CN)_3(H_2O)]^{3+}$ (b).

(Fig. 70a). An analogous structure occurs in $[Ni_6(\mathbf{108a})_3(Br)_9]$, derived from the reaction of H-**108a** with $[Ni(Br)_2(DME)]$: the expanded $\{Ni_3(Br)_3\}$ belts give rise to an enlarged cavity suited to accommodate the larger bromide ion [108].

In the presence of ethanol, $[Ni_6(\mathbf{108a})_3(Cl)_9]$ is degraded to $[Ni_4(\mathbf{108a})_2(Cl)_6(C_2H_5OH)_4]$, where two $\{Ni_2(\mathbf{108a})Cl)_3\}$ building blocks are linked via chloride bridges to form a stair like

dimeric aggregate. The octahedral nickel(II) ions are somewhat distorted (Fig. 70b) [108].

As **108b** is an oil difficult to be purified, $[Cu_2(\mathbf{108b})(CH_3COO)_2(H_2O)_2]$ and $[Cu_2(\mathbf{108b})(NCS)_2(DMF)](BF_4)$ were formed by the template condensation of 3,5-diformylpyrazole and 2-(2-aminoethyl)pyridine in the presence of copper(II) acetate or tetrafluoroborate, the last complex in the presence of NaOH. $[Cu_2(\mathbf{108b})(CH_3COO)_3(H_2O)_2]$ features two distinct copper(II) centers bridged by the bis-tridentate pyrazolate ligand. One copper(II) ion is five coordinate in a distorted trigonal bipyramidal coordination while the other copper(II) ion is six coordinate, distorted octahedral. The Cu···Cu distance is 4.400 Å (Fig. 70c) [108]. In $[Cu_2(\mathbf{108b})(NCS)_2(DMF)](BF_4)$, $[\mathbf{108b}]^-$ coordinates as in $[Cu_2(\mathbf{108b})(CH_3COO)_3(H_2O)_2]$; both the N_4 square planar and the five coordinate N_4O square pyramidal copper(II) ions are coordinated by three nitrogen donors from $[\mathbf{108b}]^-$ and a thiocyanate nitrogen in the equatorial plane, the latter being axially coordinated by a dimethylformamide oxygen. The two copper(II) centers are 4.506 Å apart (Fig. 70d) [108].

The enantiopure ligand H-**109**, prepared by condensation of 2,6-diformyl-4-methylphenol with (*S*)-(−)-1-phenylethylamine, reacts with zinc(II) chloride but not with copper(II), cobalt(II) and nickel(II) salts to afford $[Zn(H\text{-}\mathbf{109})(Cl)_2]$, where the zinc ion is four coordinate in a distorted tetrahedral geometry. The complexation induces a proton transfer from the oxygen to the uncoordinated nitrogen [109].

A comparison of H-**109** and $[Zn(H\text{-}\mathbf{109})(Cl)_2]$ in acetonitrile reveals that the zinc ion considerably enhances (ca. 12 times) the fluorescence while the emission band of the free ligand does not shift with varying concentration. The emission band of $[Zn(H\text{-}\mathbf{109})(Cl)_2]$ is concentration-dependent: the band maxima gradually shift to lower energy with increasing concentrations. This shift could be due to the intermolecular hydrogen-bonding association of $[Zn(H\text{-}\mathbf{109})(Cl)_2]$ at relatively higher concentrations. The blue shift of the emission band at 504 nm by the zinc complex as compared to the emission band at 580 nm of free ligand was proposed to arise from an excited state, centered on H-**109**, which contains a phenolic proton, transferred to the adjacent imine nitrogen upon complexation with the zinc(II) ion as proved by the X-ray structure of $[Zn(H\text{-}\mathbf{109})(Cl)_2]$ [109].

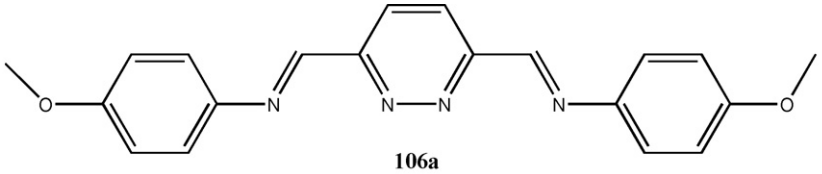

106a

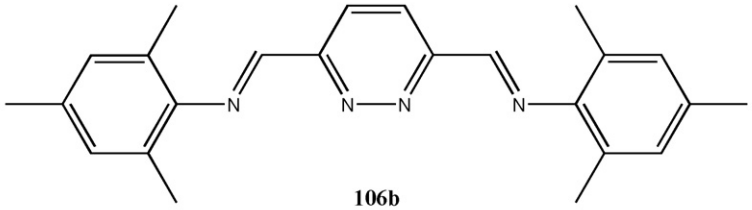

106b

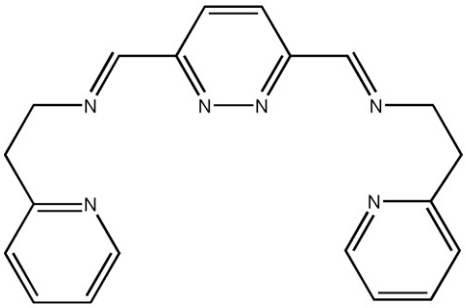

107a

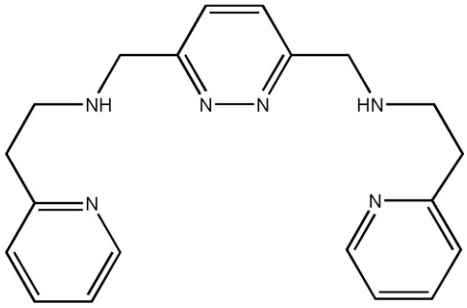

107b

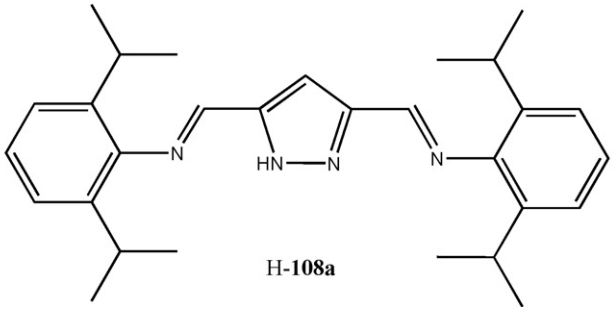

H-**108a**

The condensation of 2,6-diformyl-4-methyphenol with 6-amino-6-methylperhydro-1,4-diazepine affords H-**110a**, which forms $[Cu_2(\mathbf{110a})(OH)](ClO_4)_2{\cdot}H_2O$ in the presence of $Cu(ClO_4){\cdot}6H_2O$ and NaOH. Two five coordinate distorted square pyramidal copper(II) ions, at a distance of 2.896 Å, are bridged by the phenolate oxygen of $[\mathbf{110a}]^-$ and by an exogenous hydroxo ion [110]. $[Cu_2(\mathbf{110a})(OH)](ClO_4)_2{\cdot}H_2O$ maintains the same structure also in methanol and acetonitrile. The cyclic voltammetry, square-wave voltammetry and chronoamperometric experiments of the complex in acetonitrile indicates a quasi-reversible wave at $E_{1/2} = -0.70$ V versus NHE, assigned to the redox couple $Cu^{II}Cu^{II}/Cu^{II}Cu^{I}$. When the scan rate is increased, a second process, attributed to the formation of the $Cu^{I}Cu^{I}$ species, proved by a cathodic peak at −1.08 V versus NHE, appears. This complex can catalyze the oxidation of 3,5-di-*tert*-butylcatechol in methanol with O_2 under basic conditions. Furthermore, it promotes hydrolysis of 2,4-bis(dinitrophenyl)phosphate in water/acetonitrile at pH ≅ 6 and at 50 °C and mediate DNA phosphodiester cleavage through a hydrolytic mechanism [110].

$[M_2(\mathbf{110})(OH)(py)_2](ClO_4)_2$ (M = Zn^{II}, Ni^{II}), $[Zn_2(\mathbf{111})(\mu\text{-}OH)(py)_3](ClO_4)_2$ and $[Ni_2(\mathbf{111})(\mu\text{-}OH)(py)_4](ClO_4)_2$ were prepared by the reaction of H-**110** or H-**111** with $M(ClO_4)_2{\cdot}6H_2O$ in pyridine. The latter complex turns into $[Ni_2(\mathbf{110})(\mu\text{-}OH)(H_2O)](ClO_4)_2$ on heating [111].

The structures of $[Zn_2(\mathbf{110})(\mu\text{-}OH)(py)_2](ClO_4)_2{\cdot}(CH_3)_2CHOH$ and $[Ni_2(\mathbf{110})(\mu\text{-}OH)(py)_2](ClO_4)_2$ resemble each other: the dinuclear core, bridged by hydroxide and phenolate ions, shows a M···M interatomic separation of 3.116 Å and 3.069 Å, respectively. The metal(II) ions have a five coordinate distorted square pyramidal geometry with two pyridine molecules at the apex, *trans* with respect to the mean equatorial plane (Fig. 71) [111].

The same core, with a Zn···Zn or Ni···Ni separation of 3.139 Å and 3.156 Å, was found in $[Zn_2(\mathbf{110})(\mu\text{-}OH)(py)_3](ClO_4)_2{\cdot}0.5(CH_3)_2CHOH$ and $[Ni_2(\mathbf{111})(\mu\text{-}OH)(py)_4](ClO_4)_2$, respectively. In the former complex one zinc ion is five coordinate in a geometry intermediate between square pyramidal and trigonal bipyramidal with further coordination of one pyridine molecule, whereas the other zinc ion has a six coordinate geometry together with two pyridine molecules occupying the axial sites [111].

The zinc(II) complexes are diamagnetic while in $[Ni_2(\mathbf{111})(\mu\text{-}OH)(py)_2](ClO_4)_2$ and $[Ni_2(\mathbf{111})(\mu\text{-}OH)(py)_4](ClO_4)_2$ an antiferromagnetic interaction operates between the nickel(II) ions. The magnetic moment of $[Ni_2(\mathbf{111})(\mu\text{-}OH)(H_2O)](ClO_4)_2$ indicates the presence of a mixed-spin complex with one paramagnetic square pyramidal and one diamagnetic square planar nickel(II) ion.

While the dizinc complexes cannot hydrolyze di(*p*-nitrophenyl) phosphate into mono(*p*-nitrophenyl) phosphate, the dinickel(II) complexes facilitate this hydrolysis [111].

$[Zn_2(\mathbf{111})(\mu\text{-}CH_3COO)_2](ClO_4)$ and $[Zn_2(\mathbf{111})(\mu\text{-}CH_3CH_2COO)_2](ClO_4)$ were prepared by condensation of 2,6-diformyl-4-methylphenol with 2-(2-aminoethane)-pyridine in the presence of the appropriate zinc(II) carboxylate and $NaClO_4$. A similar condensation reaction in the presence of HCOONa and $Zn(ClO_4)_2{\cdot}6H_2O$ affords $[Zn_4(\mathbf{111})_2(\mu_{1,1}\text{-}HCOO)_2(\mu_{1,3}\text{-}HCOO)_2](ClO_4)_2$ [112].

$[Zn_2(\mathbf{111})(\mu_{1,3}\text{-}CH_3COO)_2](ClO_4)$ and $[Zn_2(\mathbf{111})(\mu_{1,3}\text{-}CH_3CH_2COO)_2](ClO_4)$ consist of two zinc ions assembled by a phenolate oxygen and a pair of *syn–syn* carboxylate bridges.

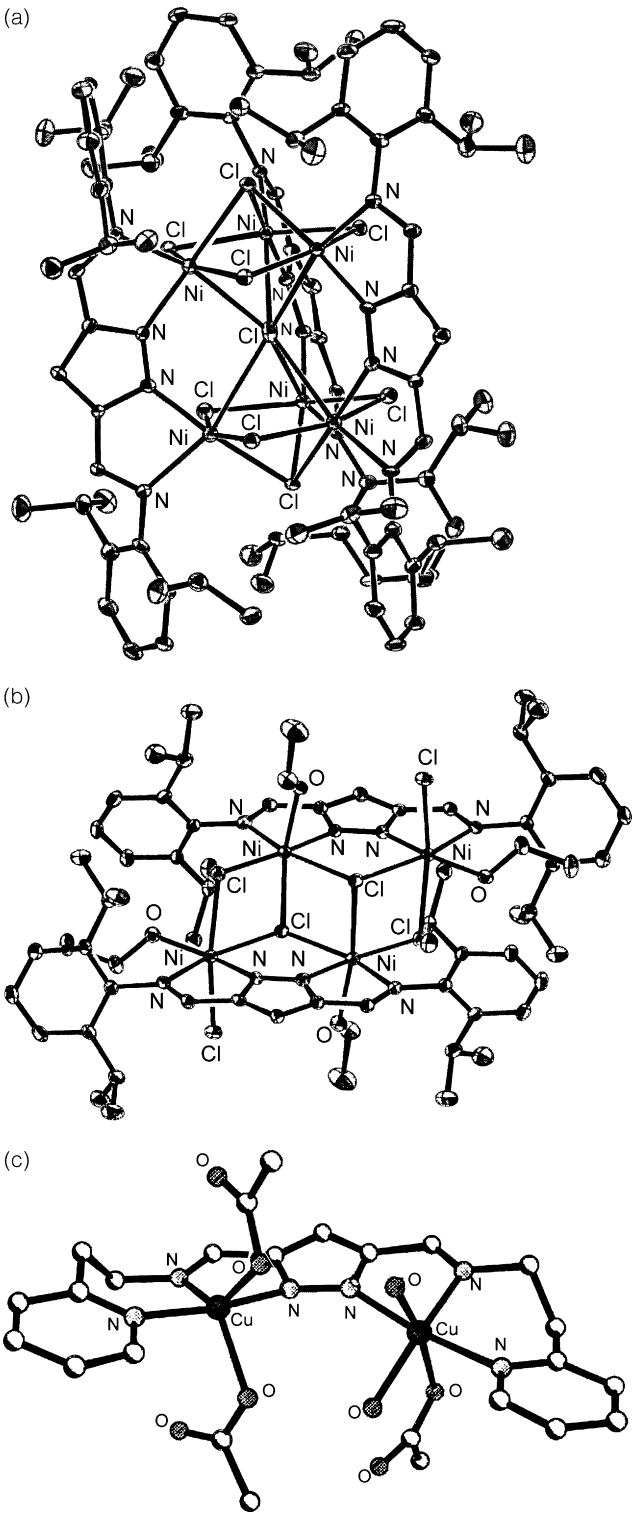

Fig. 70. Structure of $[Ni_6(\mathbf{108a})_3(Cl)_9]$ (a), $[Ni_4(\mathbf{108a})_2(Cl)_6(C_2H_5OH)_4]$ (b) and $[Cu_2(\mathbf{108b})(CH_3COO)_3(H_2O)_2]$ (c).

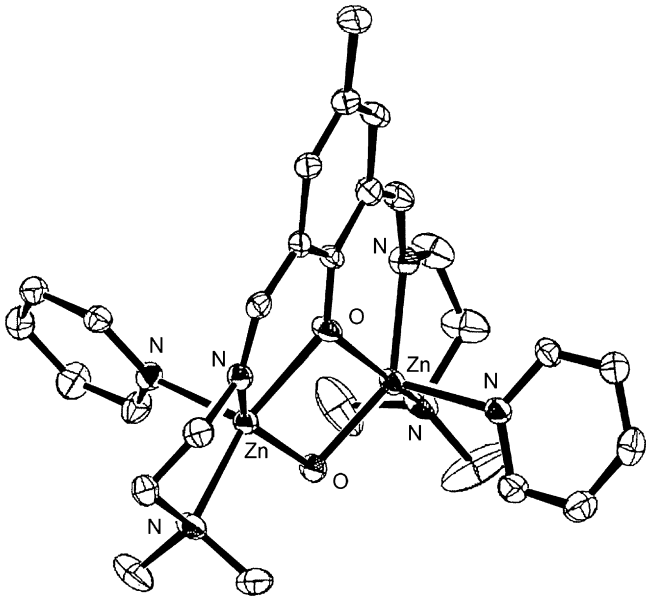

Fig. 71. Structure of $[Zn_2(\mathbf{110})(\mu\text{-OH})(py)_2]^{2+}$.

Each of the two five coordinate slightly distorted trigonal bipyramidal zinc ion is further coordinated by two nitrogen atoms form the $[\mathbf{111}]^-$ ligand, forming two ZnN_2O_3 polyhedral joined at their shared vertex by the phenoxo-bridging oxygen atom in a face-to-face fashion. The Zn···Zn separations is 3.281 Å and 3.331 Å, respectively (Fig. 72a) [112].

In $[Zn_4(\mathbf{111})_2(\mu_{1,1}\text{-HCOO})_2(\mu_{1,3}\text{-HCOO})_2](ClO_4)_2$ two identical dinuclear $[Zn_2(\mathbf{111})(\mu_{1,1}\text{-HCOO})(\mu_{1,3}\text{-HCOO})]^+$ subunits are connected each other via the coordination of the dangling oxygen from the formate to the zinc ion of the other subunit. The two zinc ions within a subunit, 3.130 Å apart, are five coordinate N_3O_2 distorted square pyramidal, while the other zinc(II) ion is six coordinate N_2O_4 distorted octahedral and bridged by a phenolate oxygen, a monodentate formate oxygen and additional *syn–syn* bidentate formates (Fig. 72b) [112].

H-**111** and $Cu(ClO_4)_2$ and in the presence of KOH afford $[Cu_2(\mathbf{111})(\mu\text{-OH})(\mu\text{-ClO}_4)](ClO_4)$; the same reaction in the further presence of 3,4-dihydroxy-methylbenzoate (H_2-cat) gives rise to $\{[Cu_2(\mathbf{111})(\mu\text{-OH})(CH_3OH)][Cu(cat)_2]_{0.5}\}(ClO_4)$. $CuCl_2$ reacts with H-**111** in the same medium but in the absence of base to form $[Cu_2(\mathbf{111})(\mu\text{-Cl})_2][Cu_2Cl_6]_{0.5}$. In these complexes, $[\mathbf{111}]^-$ acts as a pentadentate ligand bridging through the phenolate oxygen two copper(II) ions in close proximity, (2.992 Å, 3.001 and 2.970 Å, respectively). Two exogenous bridges occur, respectively an hydroxo and a perchlorate for $[Cu_2(\mathbf{111})(\mu\text{-OH})(\mu\text{-ClO}_4)](ClO_4)$ and two chlorides for $[Cu_2(\mathbf{111})(\mu\text{-Cl})_2][Cu_2Cl_6]_{0.5}$, while only one hydroxo bridge occurs in $\{[Cu_2(\mathbf{111})(\mu\text{-OH})(CH_3OH)][Cu(cat)_2]_{0.5}\}(ClO_4)$ where and oxygen atom of a coordinate methanol and a catecholate oxygen from $[Cu(cat)_2]^{2-}$ complete the coordination sphere about the two square pyramidal copper(II) ions. The copper(II) ions are square pyramidal also in $[Cu_2(\mathbf{111})(\mu\text{-OH})(\mu\text{-ClO}_4)](ClO_4)$ and intermediate between square pyramidal and trigonal bipyramidal in $[Cu_2(\mathbf{111})(\mu\text{-Cl})_2][(Cu_2Cl_6]_{0.5}$. $\{[Cu_2(\mathbf{111})(\mu\text{-OH})(CH_3OH)][Cu(cat)_2]_{0.5}\}(ClO_4)$ exhibits an uncommon

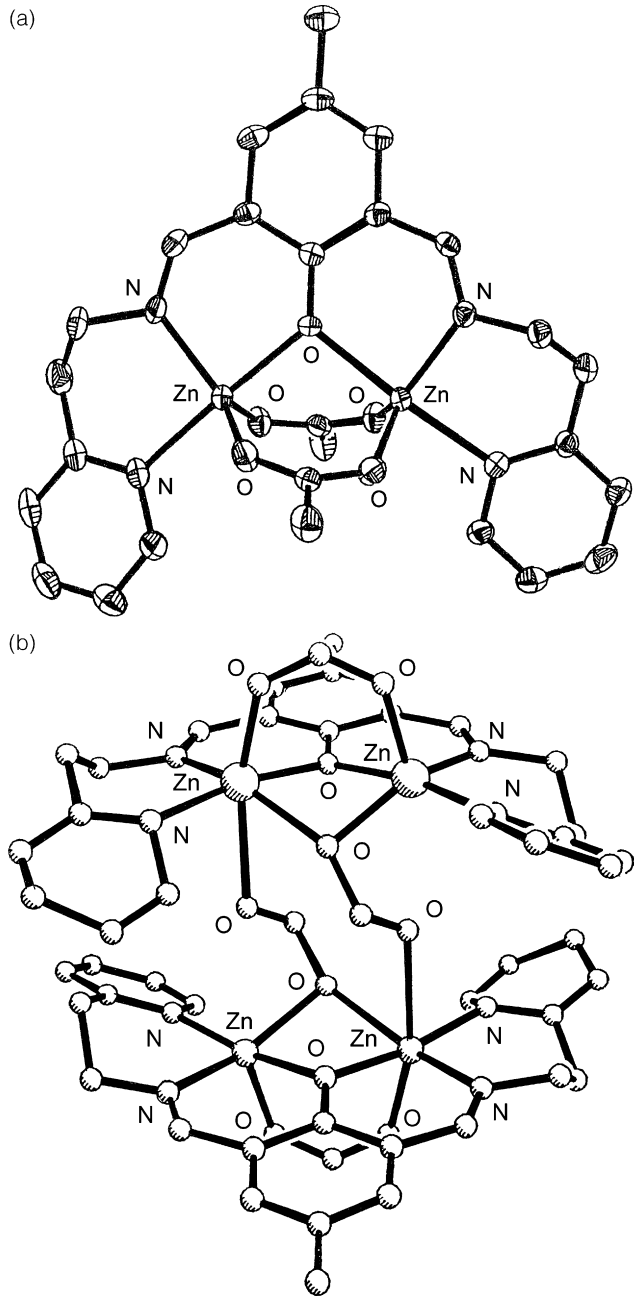

Fig. 72. Structure of $[Zn_2(\mathbf{111})(\mu_{1,3}\text{-}CH_3COO)_2]^+$ (a) and $[Zn_4(\mathbf{111})_2(\mu_{1,1}\text{-HCOO})_2(\mu_{1,3}\text{-HCOO})_2]^{2+}$ (b).

anion consisting of a bis-(catecholate) cuprate(II) moiety. $[Cu_2(\mathbf{111})(\mu\text{-OH})(\mu\text{-ClO}_4)](ClO_4)$ shows a rather low catalytic activity in the oxidation of 3,5-di-*tert*-butylcatechol under aerobic conditions, ascribed to steric limitation of the catechol to coordinate the central Cu_2O_2 core [112].

An interesting strategy for the formation of polynuclear complexes, starting from end-off compartmental dinuclear compounds was successfully experimented. The starting point is the formation of a dinuclear complex capable of turning into a polynuclear one by further coordination of suitable exo-di or -polydentate ligands [113,116]. Thus, $[Cu_2(\mathbf{111})(OH)](ClO_4)_2$, when reacted with 4-4′-bipyridine, (4-4′-bipy) or 1,2-bis(4-pyridyl)ethylene (4,4′-bpe)

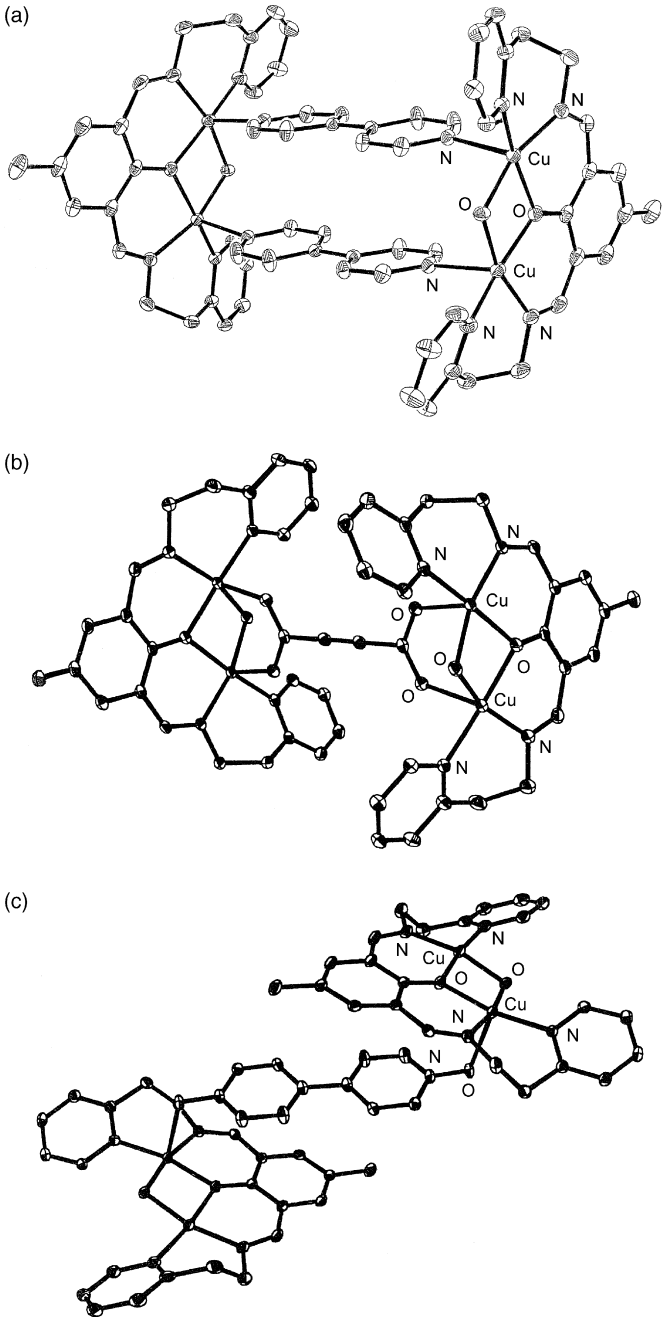

Fig. 73. Structure of $[Cu_4(\mathbf{111})_2(\mu\text{-}OH)_2(\mu\text{-}4,4'\text{-}bipy)_2]^{4+}$ (a), $[Cu_4(\mathbf{111})_2(\mu\text{-}OH)_2(\mu\text{-}acdca)]^{2+}$ (b) and $[Cu_4(\mathbf{111})_2(\mu\text{-}OH)_2(\mu\text{-}4,4'\text{-}bpno)_2]^{4+}$ (c).

forms $[Cu_4(\mathbf{111})_2(\mu\text{-}OH)_2(\mu\text{-}4,4'\text{-}bipy)_2](ClO_4)_4\cdot 3H_2O$ and $[Cu_4(\mathbf{111})_2(\mu\text{-}OH)_2(\mu\text{-}4,4'\text{-}bpe)_2](ClO_4)_4\cdot 4H_2O$. These complexes have been obtained also through a multicomponent self-assembly process, namely by mixing together the stoichiometric amounts of H-**111**, the exo-bidentate ligand and lithium hydroxide, followed by the addition of copper(II) perchlorate [113].

In these tetranuclear compounds (Fig. 73a and b) the copper(II) ions, bridged by an endogenous phenolate oxygen and by an exogenous hydroxo oxygen, exhibit a square pyramidal stereochemistry where the apical positions are occupied by the nitrogen atoms arising from the spacers. The dimensions of the rectangles, i.e. the distances between the copper ions, are: 3.069 × 11.641 Å and 3.089 × 11.725 Å for the two independent molecules in $[Cu_4(\mathbf{111})_2(\mu\text{-}OH)_2(\mu\text{-}4,4'\text{-}bipy)_2](ClO_4)_4\cdot 3H_2O$, and 3.069x13.934 Å in $[Cu_4(\mathbf{111})_2(\mu\text{-}OH)_2(\mu\text{-}4,4'\text{-}bpe)_2](ClO_4)_4\cdot 4H_2O$. An antiferromagnetic interaction ($J \cong -300\,cm^{-1}$) between the two copper ions inside the compartmental ligand has been estimated. The interaction through 4,4′-bipyridine or 4,4′-bis(4-pyridyl)ethylene was negligible with a series of dinuclear copper(II) complexes [114], the exchange coupling constant ranging between −0.05 and $-0.1\,cm^{-1}$, irrespective of the nature of the magnetic orbitals of the copper(II) ions ($d_{x^2-y^2}$ or d_{z^2}) [113].

This synthetic approach was further developed by using the exo-polydentate bridging ligands 1,2-bis(4-pyridyl)ethane (bpeta), the dianion of the acetylene-dicarboxylic acid (H_2-acdca) and 4,4′-bipyridine-*N*,*N*′-dioxide (4,4′-bpno) [115].

As in the case of the 4,4′-bipy and 4,4′-bpe linkers [113], in $[Cu_4(\mathbf{111})_2(\mu\text{-}OH)_2(\mu\text{-}bpeta)](ClO_4)_4$, obtained by reaction of $[Cu_2(\mathbf{111})(\mu\text{-}OH)](ClO_4)_2$ with bpeta, a molecular rectangle (3.090 × 13.595 Å) forms with the short edges constructed from the pre-existing μ-hydroxo and μ-phenoxo groups and the long ones constructed from anti-bpeta molecules. The copper(II) ions display a square pyramidal stereochemistry similar to the above one with the apical positions occupied by the nitrogen atoms arising from the bridging bpeta molecules [115].

Furthermore, $[Cu_2(\mathbf{111})(\mu\text{-}OH)](ClO_4)_2$ and the dianion of the acetylene–dicarboxylic acid, $[acdca]^{2-}$, afford $[Cu_4(\mathbf{111})_2(\mu\text{-}OH)_2(\mu\text{-}acdca)](ClO_4)_2$, where each carboxylato group forms a third bridge between the copper(II) ions within the dinuclear moiety (*syn–syn* bridging mode). The copper(II) ions of each dinuclear unit, 2.959 Å apart, are again five coordinate, square pyramidal with the apical positions occupied by the oxygen atoms of the carboxylato bridges (Fig. 73c) [115].

In $[Cu_4(\mathbf{111})_2(\mu\text{-}OH)_2(\mu\text{-}4,4'\text{-}bpno)](ClO_4)_4$, similarly prepared by using 4,4′-bpno as polynucleating ligand, the 4,4′-bpno molecule connects two copper(II) ions, which are disposed in *trans* position with respect to the bridge. The two dinuclear moieties are almost parallely disposed above and below the 4,4′-bpno bridge. The copper(II) ions, bridged by 4,4′-bpno, show a square pyramidal stereochemistry, with the oxygen atom arising from 4,4′-bpno in the apical position. The other two copper(II) ions, which are not bridged by 4,4′-bpno, exhibit a square planar coordination geometry. The distance between the copper ions within the binuclear moiety is 3.009 Å, while the distance between the copper ions bridged by 4,4′-bpno is 12.024 Å (Fig. 73d) [115].

The condensation of 2,6-diformyl-4-methylphenol with 2-(aminoethyl)pyridine affords H-**111**, which, by reaction with $Zn(ClO_4)_2\cdot 6H_2O$ in the presence of LiOH, gives rise to $[Zn_2(\mathbf{111})(OH)](ClO_4)_2$. The diffusion of *trans*-1,2-bis(4-pyridyl)ethylene (4,4′-bpe) into a methanol solution of $[Zn_2(\mathbf{111})(OH)](ClO_4)_2$ affords $[Zn_4(\mathbf{111})_2(\mu\text{-}OH)_2(\mu\text{-}4,4'\text{-}bpe)_2]\ (ClO_4)_4\cdot 4H_2O$ within a period of two weeks. The same synthetic pathway over a period of 2 days affords the infinite one-dimensional laden-like complex $\{[Zn_2(\mathbf{111})(\mu\text{-}OH)(\mu\text{-}4,4'\text{-}bpe)](ClO_4)_2\cdot 4H_2O\}_\infty$ [116].

The structure of the tetranuclear complex (Fig. 74a) reveals that two dinuclear $[Zn_2(\mathbf{111})(OH)]^{2+}$ units assemble with two

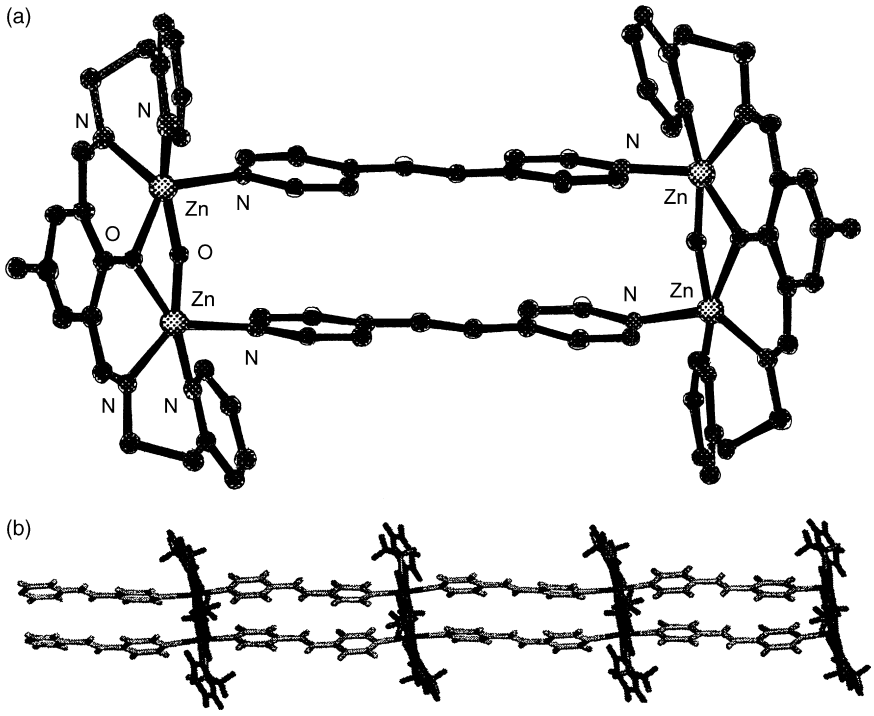

Fig. 74. Structure of $[Zn_4(\mathbf{111})_2(\mu\text{-}OH)_2(\mu\text{-}4,4'\text{-}bpe)_2]^{4+}$ (a) and $\{[Zn_2(\mathbf{111})_2(\mu\text{-}OH)_2(\mu\text{-}4,4'\text{-}bpe)_2]^{2+}\}_\infty$ (b).

molecules of 4,4′-bpe to form the tetranuclear rectangular entity $[Zn_4(\mathbf{111})_2(\mu\text{-}OH)_2(\mu\text{-}4,4'\text{-}bpe)_2]^{4+}$. The metal ions, with intradimer and interdimer Zn···Zn distances of 3.135, and 13.542 Å respectively, adopt a square pyramidal geometry where the pyridyl nitrogen atoms of 4,4′-bpe occupy the apical positions, while the remaining sites are occupied by a single oxygen, and two nitrogen atoms of $[\mathbf{111}]^-$ and a single oxygen atom of a μ_2-OH^- ion [116].

In the polymeric complex $\{[Zn_2(\mathbf{111})(\mu\text{-}OH)(\mu\text{-}4,4'\text{-}bpe)](ClO_4)_2{\cdot}2H_2O\}_\infty$ the metal ions and the organic components have assembled such that the bipyridines are in a face-to-face stacked arrangement. The two zinc ions in the dinuclear unit are separated by 3.19 Å. In contrast to the tetranuclear complex, in the polymeric one, each zinc(II) ion lies on an octahedral rather than a square pyramidal, coordination environment such that the two nitrogen atoms of two 4-pyridyl groups adopt a transoid arrangement. $[Zn_2(\mathbf{111})(\mu\text{-}OH)]$ unit and 4,4′-bpe assemble to form a 1D ladder-like coordination polymer. The Schiff base ligands are oriented anti-parallel along the polymer backbone, with the zinc ions being separated by 14.3 Å (Fig. 74b) [116].

Both the tetranuclear and the polymeric zinc(II) complexes have a suitable configuration to give rise to [2 + 2] photodimerization in the solid state. Thus, exposure of crystals of $[Zn_4(\mathbf{111})_2(\mu\text{-}OH)_2(\mu\text{-}4,4'\text{-}bpe)_2](C1O_4)_4{\cdot}4H_2O$ to UV radiation, resulted in dimerization of 4,4′-bpe to give 4,4′-tpcb, quantitatively. Optical microscopy revealed that the transparency of the single crystals remained intact during the photoreaction, which suggested that the reaction occurred via a single crystal to single crystal (SCSC) transformation. A single crystal X-ray diffraction analysis of the photoreacted sample confirms that the reaction occurred via a SCSC transformation. Overlay views of $[Zn_4(\mathbf{111})_2(\mu\text{-}OH)_2(\mu\text{-}4,4'\text{-}bpe)_2](C1O_4)_4{\cdot}'4H_2O$ and $[Zn_4(\mathbf{111})_2(\mu\text{-}OH)_2(\mu\text{-}4,4'\text{-}tpcb)_2](C1O_4)_4{\cdot}4H_2O$ reveal a olefin photodimerization to give rctt-tetrakis(4-pyridyl)cyclobutane (4,4′-tpcb). In this arrangement, 4,4′-tpcb lies within $[Zn_4(\mathbf{111})_2(\mu\text{-}OH)_2(\mu\text{-}4,4'\text{-}tpcb)_2](C1O_4)_4$ such that the pyridyl groups, which adopt an unsymmetrical boat conformation, interact with the Schiff base complex within a tetranuclear assembly, similar to $[Zn_4(\mathbf{111})_2(\mu\text{-}OH)_2(\mu\text{-}4,4'\text{-}bpe)_2](C1O_4)_4{\cdot}4H_2O$. To accommodate 4,4′-tpcb, the distances between the metal ion within and between the Schiff base ligands have slightly increased and decreased, to 3.182, 13.36 Å, respectively [116].

$[Zn_4(\mathbf{111})_2(\mu\text{-}OH)_2(\mu\text{-}4,4'\text{-}tpcb)](C1O_4)_4{\cdot}H_2O$ exhibits a remarkably different fluorescence emission than $[Zn_4(\mathbf{111})_2(\mu\text{-}OH)_2(\mu\text{-}4,4'\text{-}bpe)_2](C1O_4)_4{\cdot}4H_2O$. Specifically, excitation of $[Zn_4(\mathbf{111})_2(\mu\text{-}OH)_2(\mu\text{-}4,4'\text{-}bpe)_2](C1O_4)_4{\cdot}4H_2O$ at 290 nm gives blue emission at 464 nm, while that of $[Zn_4(\mathbf{111})_2(\mu\text{-}OH)_2(\mu\text{-}4,4'\text{-}tpcb)](C1O_4)_4{\cdot}4H_2O$ gives green emission at 520 nm. Illumination of cleaved crystals of $[Zn_4(\mathbf{111})_2(\mu\text{-}OH)_2(\mu\text{-}4,4'\text{-}bpe)_2](C1O_4)_4{\cdot}4H_2O$ and $[Zn_4(\mathbf{111})_2(\mu\text{-}OH)_2(\mu\text{-}4,4'\text{-}tpcb)_2](C1O_4)_4$ using a handheld UV lamp demonstrates that the emissions are propagated from the bulk, an observation confirmed by laser scanning confocal fluorescence microscopy, which reveals a consistent difference in fluorescence between $[Zn_4(\mathbf{111})_2(\mu\text{-}OH)_2(\mu\text{-}4,4'\text{-}bpe)_2](C1O_4)_4{\cdot}4H_2O$ and $[Zn_4(\mathbf{111})_2(\mu\text{-}OH)_2(\mu\text{-}4,4'\text{-}tpcb)_2](C1O_4)_4$ as determined by comparing ratios of the fluorescence at 480 and 510 nm at different depths in each crystalline solid. Similarly, UV-irradiation of a powdered crystalline sample of $\{[Zn_2(\mathbf{111})(\mu\text{-}OH)(\mu\text{-}4,4'\text{-}bpe)](C1O_4)_2{\cdot}2H_2O\}$ for a period of 32 h produced the similar complex with 4,4′-tpcb, as determined by ^{1}H NMR

spectroscopy. A thermogravimetric analysis revealed that the solid lost approximately two of the included water molecules during the photoreaction [116].

The [1 + 2] condensation of 2,7-diformyl-1,8-naphthalenediol with *N*,*N*′-dimethylethylenediamine forms H_2-**111a**, which reacts with two equivalents of $CuCl_2{\cdot}2H_2O$ under basic conditions to give rise to a mixture of $[Cu_3(\mathbf{111a})(Cl)_3(OCH_3)(CH_3OH)]$ and $[Cu_3(\mathbf{111a})(Cl)_4(CH_3OH)]$. When the reaction is carried out using three equivalent of $CuCl_2{\cdot}2H_2O$, only the second complex forms [117].

The similar structure of both complexes demonstrates that $[\mathbf{111a}]^{2-}$ is capable of coordinating three metal ions in a linear fashion. The two terminal copper(II) ions are coordinated by an N_2O compartment of $[\mathbf{111a}]^{2-}$ while the central copper(II) ion is coordinated by the O_2 compartment of $[\mathbf{111a}]^{2-}$. In $[Cu_3(\mathbf{111a})(Cl)_4(CH_3OH)]$, the central copper(II) ion is additionally bridged to the two terminal copper(II) ions by two external chloride ions, while in $[Cu_3(\mathbf{111a})(Cl)_3(OCH_3)(CH_3OH)]$ one chloride ion is substituted by a methanolate bridge. While the coordination environment of one external copper(II) ion is close to square

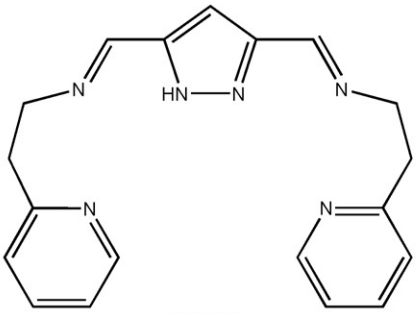

H-**108b**

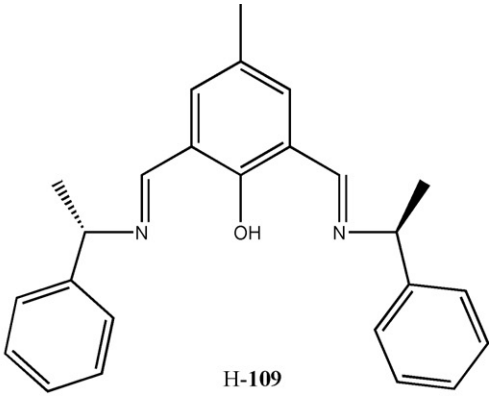

H-**109**

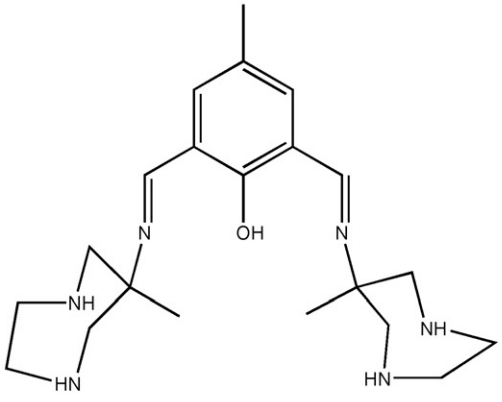

H-**110a**

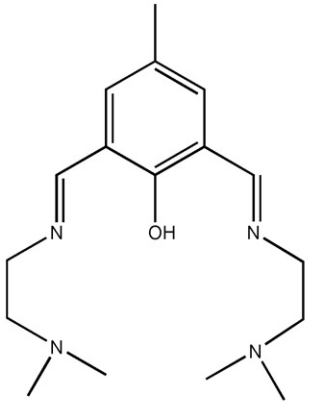

H-**110**

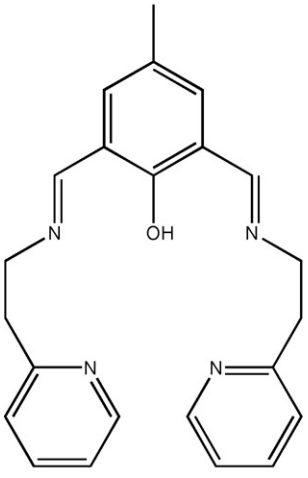

H-**111**

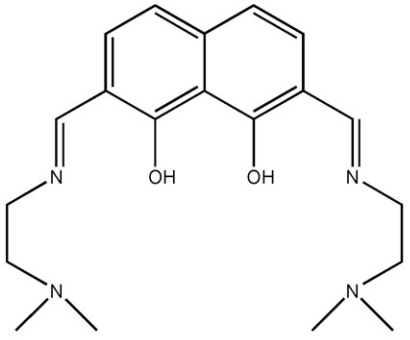

H_2-**111a**

pyramidal, the coordination environments of the other two copper(II) ions exhibit severe distortions towards trigonal bipyramidal (Fig. 75). In [Cu_3(**111a**)$(Cl)_4(CH_3OH)$] antiferromagnetic interactions between the central and the two external metal ions occur ($J_{12} = -291\ cm^{-1}$; $J_{23} = -162\ cm^{-1}$; $J_{13} = 0$) [117].

The Schiff base precursors, prepared by [1 + 1] condensation of ethylenediamine or 1,3-diaminopropane with salicylaldehyde or 3-methoxy-2-hydroxybenzaldehyde, respectively, react in situ with 2,6-diformyl-4-methyl (or-*tert*-butyl) phenol to form H_3-**112a**···H_3-**112c** [118]. The keto-enol tautomeric forms of these ligands were studied in polar and non-polar solvents: the keto-amine tautomeric form occurs in non polar solvents as toluene or hexane while the enolimine form is formed in polar solvents as methanol, ethanol or dioxane/water. These ligands, when treated with $CuCl_2{\cdot}2H_2O$ or $CdCl_2{\cdot}2H_2O$, form [M_2(**L**)](Cl): tetrahedral and square planar coordination about the metal(II) ions was proposed for the cadmium(II) and the copper(II) complexes, respectively. In [Cu_2(**L**)](Cl) an antiferromagnetic interaction between the two copper(II) centers occurs [118].

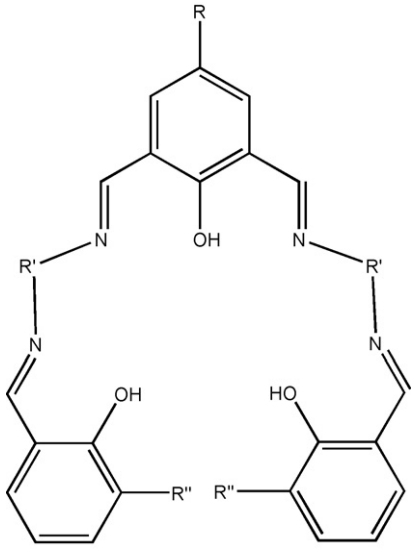

	R	R'	R''
H_3-**112a**	CH_3	$(CH_2)_2$	H
H_3-**112b**	CH_3	$(CH_2)_3$	OCH_3
H_3-**112c**	$C(CH_3)_3$	$(CH_2)_3$	OCH_3

H_3-**112d**, derived from the [1 + 2] condensation of 2,6-diformyl-4-methylphenol and 6-amino-2,4-di-*tert*-butylphenol, reacts in air with various transition metal compounds to form the related di- or polynuclear complexes. In particular, when nickel(II) acetate and H_3-**112d** are allowed to react in the presence of sodium acetate with a slight excess of urea, [Ni_2(**112d**)(μ-CH_3COO)(μ-urea) $(CH_3OH)_2$] is obtained; in the absence of urea, [Ni_4(H-**112d**)$_2$(μ$_3$-$OCH_3)_2(CH_3COO)_2(CH_3OH)_2$] forms, which can also be transformed into [Ni_2(**112d**)(μ-CH_3COO)(μ-urea)$(CH_3OH)_2$] by addition of urea. In agreement with electronic and X-ray diffractometric data, [Ni_2(**112d**)(μ-CH_3COO)(μ-urea)$(CH_3OH)_2$] contains two nickel(II) ions, 2.966 Å apart, triply bridged by the

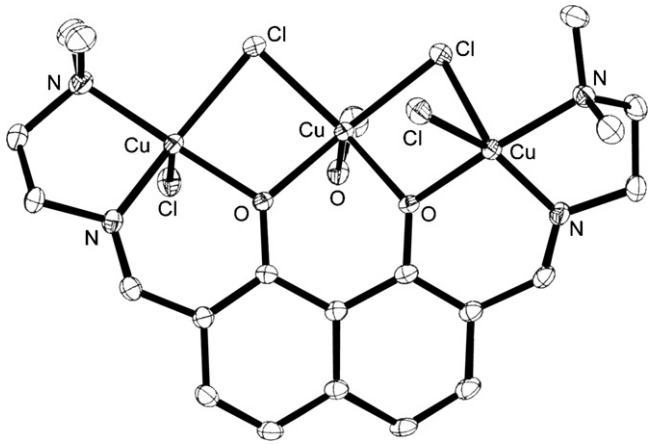

Fig. 75. Structure of [Cu_3(**111a**)$(Cl)_4(CH_3OH)$].

carbonyl oxygen of urea, the phenolate oxygen and one acetate oxygen. Each nickel ion is in a distorted octahedral NO_5 environment. The NH_2 groups of urea enter into hydrogen bonding, this making urea presumably not susceptible to alcoholysis [119].

[Ni_4(H-**112d**)$_2$(μ$_3$-$OCH_3)_2(CH_3COO)_2(CH_3OH)_2$] contains a roughly cubic Ni_4O_4 unit, consisting of two interpenetrating tetrahedra, one of four nickel ions and one of four μ$_3$-oxygen atoms originating from two cresolate and two methoxide groups. Each nickel(II) ion is in a distorted octahedral environment with an NO_5 donor set. The Ni···Ni distances on different cubic faces are also different, the shortest being 3.047 Å and the longest 3.227 Å (Fig. 76a) [119].

Copper perchlorate and H_3-**112d**, in the absence of protic solvents, afford [Cu_2(**112d**)(μ-OCH_3)$(THF)_2$] which is transformed easily into [Cu_4(**112d**)$_2$(μ$_4$-O)]; adventitious water in the solvent serves as a source of the μ$_4$-oxo ligand [119].

In [Cu_2(**112d**)(μ-OCH_3)$(THF)_2$] the distorted square pyramidal copper ions are doubly bridged by the phenoxo and the methoxide group, the five coordination being completed by two tetrahydrofuran oxygen atoms oriented *trans* to each other [119].

[Cu_4(**112d**)$_2$(μ$_4$-O)] consists of four distorted square planar copper(II) ions bridged by a central μ$_4$-oxygen atom in an approximately tetrahedral environment. The phenolate oxygen atoms of [**112d**]$^{3-}$ bridge two copper centers. The Cu···Cu distances range from 2.759 Å to 3.368 Å (Fig. 76b) [119].

The reaction of H_3-**112d** with the appropriate metal compound under basic conditions affords [Fe_2^{III}(**112d**)$_2$], [Mn_2^{III}(**112d**)$_2$], [Cr_2^{III}(**112d**)$_2$], [$(V^{IV}O)_2$(**112d**){$OCH(CH_3)_2$}] and [$(V^{V}O)_2$(**112d**)$_2$], respectively.

In [Fe_2(**112d**)$_2$]·2.5CH_3CN (Fig. 77a), two d^5-high spin, six coordinate, distorted N_2O_4 octahedral iron(III) centers, 3.32 Å apart and sharing a common edge, are bridged by two phenolate oxygen atoms. Each iron center is also coordinated to two nitrogen atoms, *trans* to each other, belonging to two different [**112d**]$^{3-}$ ligands [119].

[Mn_2^{II}(**112d**)$_2$], which is considered to possess an identical coordination sphere and atom connectivity as [Fe_2^{III}(**112d**)$_2$], yields on recrystallization from tetrahydrofuran [Mn_2^{III}(**112d**)$_2(THF)_2$], in which the phenolate bridge between two manganese centers prevailing in

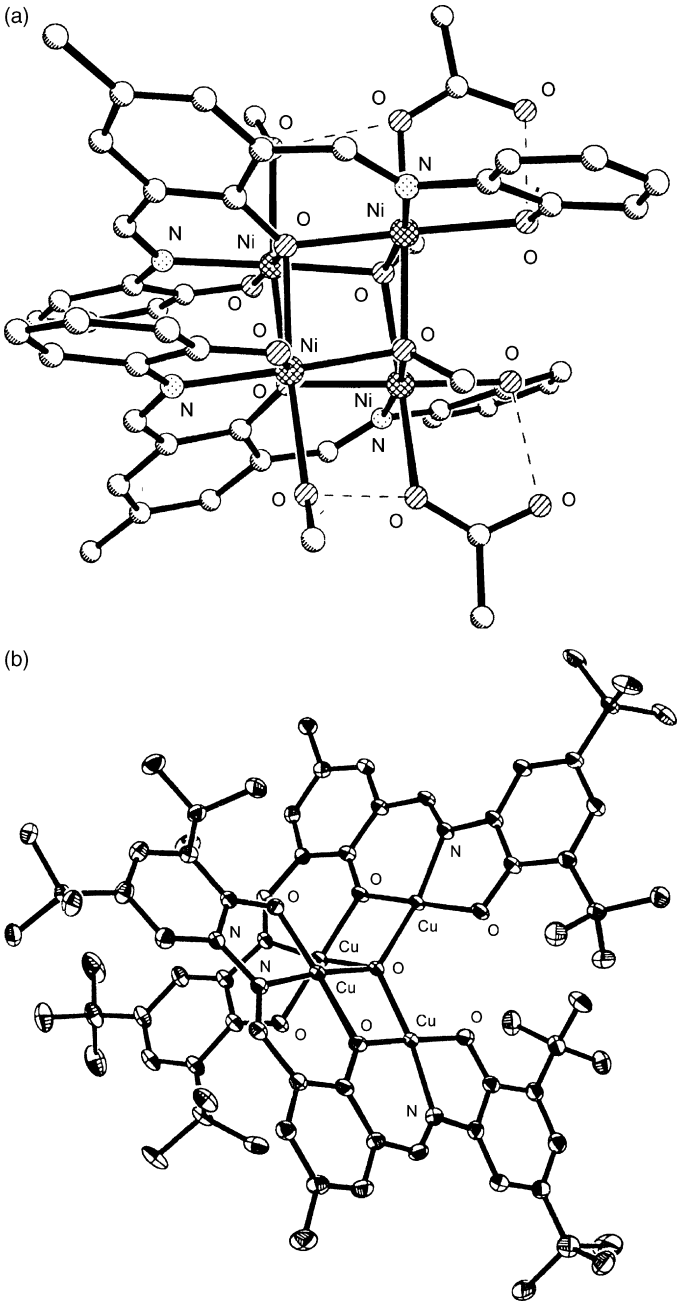

Fig. 76. Structure of $[Ni_4(H\text{-}\mathbf{112d})_2(\mu_3\text{-}OCH_3)_2(CH_3COO)_2(CH_3OH)_2]$ (a) and $[Cu_4(\mathbf{112d})_2(\mu_4\text{-}O)]$ (b).

$[Mn_2(\mathbf{112d})_2]$ does not persist any more, this resulting in a comparatively long Mn···Mn separation (6.45 Å). $[Mn_2^{III}(\mathbf{112d})_2(THF)_2]\cdot 4CH_3CN$ (Fig. 77b) is based on two MnO_4N_2 octahedra, in which two triply deprotonated ligands $[\mathbf{112d}]^{3-}$ span between the two d^4-high spin manganese centers [119].

$[(VO)_2(\mathbf{112d})\{OCH(CH_3)_2\}]$ contains a bridging isopropoxide originating from the vanadium isopropoxide starting material. The two five coordinate distorted square pyramidal vanadyl(IV) ions, 3.063 Å apart, are additionally bridged by a phenolate oxygen of $[\mathbf{112d}]^{3-}$. The V=O groups are *trans* to each other [119]. Also in $[(VO)_2(\mathbf{112d})_2]\cdot 2.5CH_3CN$ (Fig. 77c),

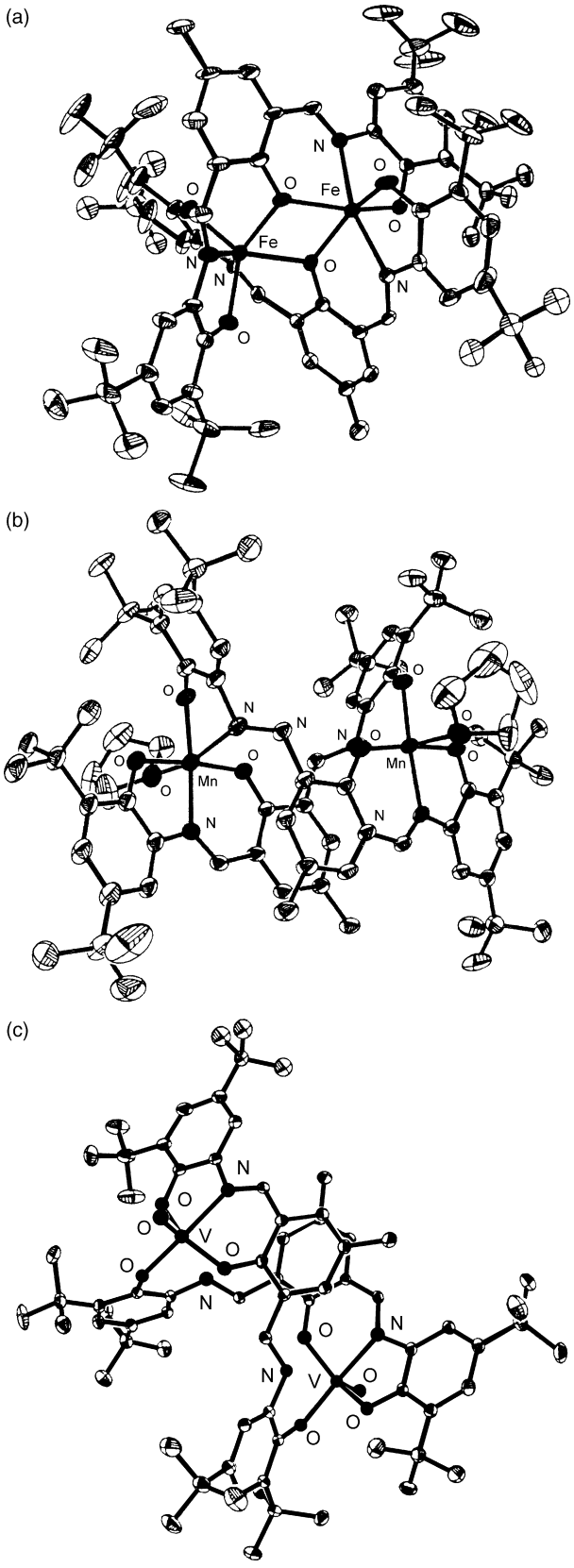

Fig. 77. Structure of $[Fe_2(\mathbf{112d})_2]$ (a), $[Mn_2(\mathbf{112d})_2(THF)_2]$ (b) and $[(VO)_2(\mathbf{112d})_2]$ (c).

the vanadium(V) ions are in a distorted O_4N square pyramidal coordination. Each $[\mathbf{112d}]^{3-}$ ligand with its five donor atoms spans between two vanadium(V) centers but one nitrogen atom does not coordinate to any of the metal centers [119].

In $[Ni_2(\mathbf{112d})(\mu\text{-}CH_3COO)(\mu\text{-urea})(CH_3OH)_2]$ an antiferromagnetic exchange coupling between the two metal centers ($J = -3.5\,cm^{-1}$) operates. The magnetic properties of $[Ni_4(H\text{-}\mathbf{112d})_2(\mu_3\text{-}OCH_3)_2(CH_3COO)_2(CH_3OH)_2]$ are dominated by a ferromagnetic exchange interaction between the nickel(II) ions as propagated by bridging phenoxides and methoxides ($J_{12} = +8.0\,cm^{-1}$, $J_{14} = J_{24} = J_{23} = J_{34} = +0.9\,cm^{-1}$ and $J_{13} = -3.95\,cm^{-1}$). In $[Cu_2(\mathbf{112d})(\mu\text{-}OCH_3)(THF)]$ a very strong intramolecular antiferromagnetic coupling occurs ($J = -192.1\,cm^{-1}$) while in $[Cu_4(\mathbf{112d})_2(\mu_4\text{-}O)]$ antiferromagnetic interactions between the four copper(II) ions dominate($J_{12} = J_{34} = -122.3\,cm^{-1}$, $J_{23} = J_{24} = J_{13} = -90.0\,cm^{-1}$ and $J_{14} = 0$). Susceptibility data indicate antiferromagnetic interactions between the metal centers: $J = -12.7\,cm^{-1}$ for $[Fe_2(\mathbf{112d})_2]$; $-2.95\,cm^{-1}$ for $[Mn_2(\mathbf{112d})_2]$; $-0.66\,cm^{-1}$ for $[Mn_2(\mathbf{112d})_2(THF)_2]$; $-7.6\,cm^{-1}$ for $[Fe_2(\mathbf{112d})_2]$ and $-128.5\,cm^{-1}$ for $[(VO)_2(\mathbf{112d})\{(\mu\text{-}OCH(CH_3)_2\}]$. The electrochemical results of these complexes suggest the generation of ligand-centered oxidation processes attributable to the phenoxyl radicals rather than the formation of unusually high oxidation states at the metal centers [119].

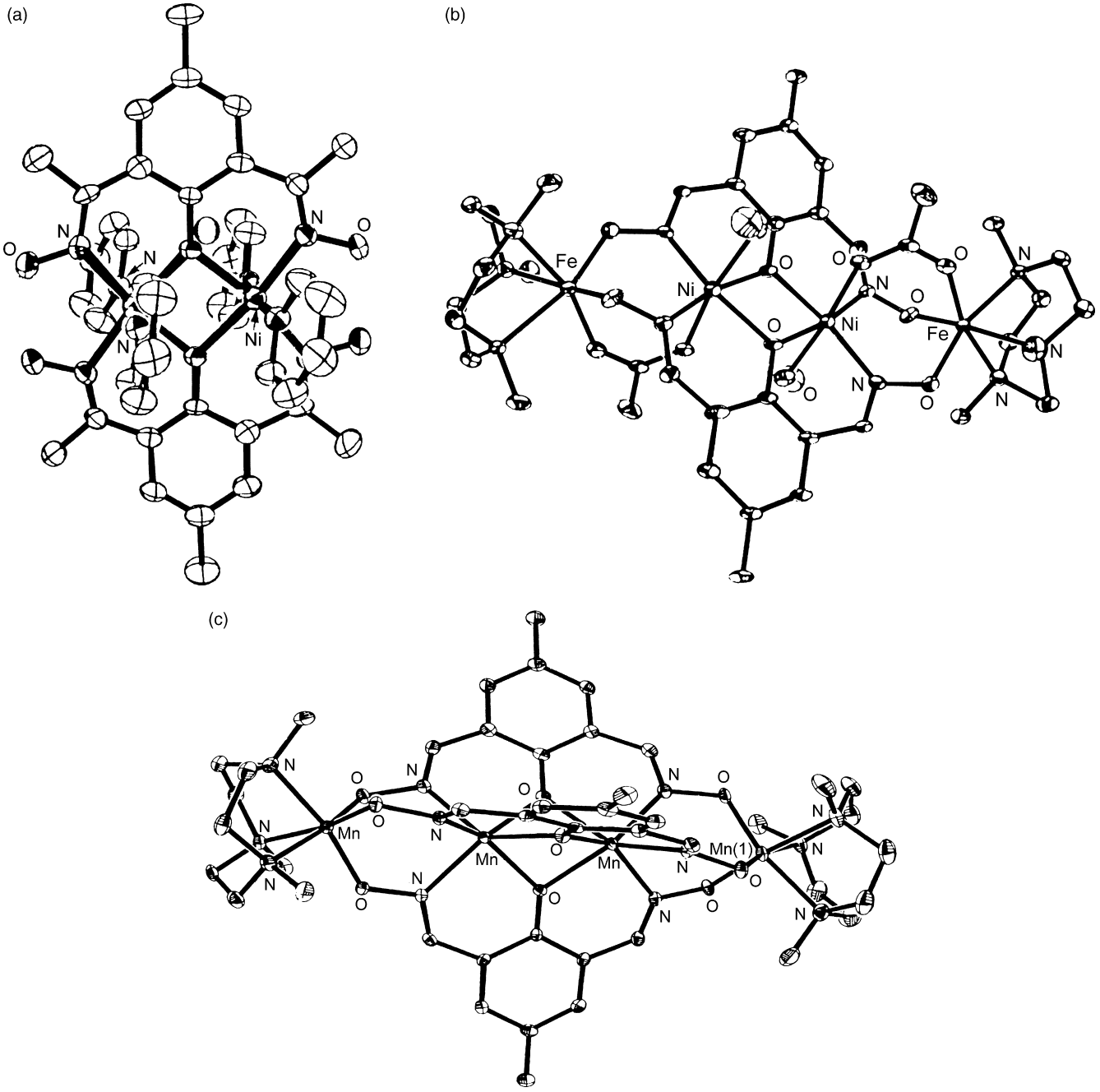

Fig. 78. Structure of $[Ni_2(H\text{-}\mathbf{113a})_2(py)_4]$ (a), $[Fe_2^{III}Ni_2^{II}(\mathbf{113c})_2(\mu\text{-}CH_3COO)_2(L)_2(CH_3OH)_2]^{2+}$ (b) and $[Mn_2^{IV}Mn_2^{II}(\mathbf{113c})_3(L)_2]^{3+}$ (c).

It is well documented that the end-off acyclic ligands H$_3$-**113a**···H$_3$-**113c**, derived from the condensation of 2,6-diacety-4-methylphenol, 2,6-diacetyl-4-*tert*-butylphenol or 2,6-diformyl-4-methylphenol with a large excess of both $NH_2OH{\cdot}HCl$ and CH_3COOK, are excellent di- or polynucleating systems. The resulting complexes show peculiar magnetic properties: their antiferromagnetic or ferromagnetic behavior, mediated by the N-O bridges, can be tuned by changing the metal ion assembly [120].

H$_3$-**113a**···H$_3$-**113c**, when mixed with the desired metal(II) acetate, afford [M$_2$(H-**113a**)$_2$] (M = Cu^{II}, Ni^{II}, Co^{II}), electrochemically reducible in two one electron steps. Pyridine solutions of $[Ni_2(H\text{-}\mathbf{113a})_2(CH_3OH)_2]{\cdot}CH_3OH$ give rise to $[Ni_2(H\text{-}\mathbf{113a})_2(py)_4]{\cdot}2py$ (Fig. 78a), where two pseudo-octahedral nickel(II) centers, separated by 3.058 Å, are bridged by two phenoxide oxygen atoms. $[Ni_2(H\text{-}\mathbf{113a})_2(py)_4]{\cdot}2py$ loses pyridine molecules in the absence of pyridine vapor and forms the square pyramidal complex $[Ni_2(H\text{-}\mathbf{113a})_2(py)_2]{\cdot}py$. In $[Co_2(H_2\text{-}\mathbf{113c})(CH_3OH)_2(H_2O)_2](Cl)_2$, $[Ni_2(H_2\text{-}\mathbf{113c})_2(H_2O)_4](ClO_4)_2$ and $[Cu_2(H_2\text{-}\mathbf{113c})_2(ClO_4)_2]$, derived from the reaction of the appropriate metal chloride or perchlorate salt and H$_2$-**113c**, the two metal ions are in an octahedral N_2O_4 environment [120].

In the isostructural tetranuclear complexes $[M_2^{III}Ni_2^{II}(\mathbf{113c})_2(\mu\text{-}CH_3COO)_2(L)_2(CH_3OH)_2](BF_4)_2$, synthesized by reaction of [M(L)(C1)$_3$] (M = Fe^{III}, Mn^{III}; L = 1,4,7-trimethyl-1,4,7-triazacyclononane), with H$_3$-**113c**, $Ni(CH_3COO)_2{\cdot}4H_2O$ and triethylamine followed by the addition of tetrabutylammonium tetrafluoroborate, each nickel(II) ion is coordinated to two azomethine nitrogen atoms and two bridging phenolate oxygen atoms from the oxime ligands. The nickel centers, 3.086 Å apart, adopt distorted octahedral environments. The coordination geometry of the terminal d^5 high-spin iron(III) or d^4 high-spin manganese(III) ions is distorted octahedral in fac-FeN$_3$O$_3$ cores. The M-Ni-Ni-M skeleton is not perfectly linear. An intramolecular separation between the terminal iron ions of 9.996 Å is found while the Fe···Ni distance is 3.505 Å (Fig. 78b) [120].

Furthermore, the complexes $[M_2^{III}Mn_2^{II}(\mathbf{113c})_3(L)_2](ClO_4)$ (M^{III} = Mn^{III}, Fe^{III}, Cr^{III}) were obtained by mixing under argon methanolic solutions of $[Mn_2^{II}(\mathbf{113c})_3]^{5-}$, derived from the reaction under basic conditions of H$_3$-**113c** and $Mn(CH_3COO)_2{\cdot}4H_2O$, with $[Mn_3(\mu\text{-}O)(CH_3COO)_6(H_2O)_3](CH_3COO)$, [Fe(L)(Cl)$_3$] or [Cr(L)(Br)$_3$] (L = 1,4,7-trimethyl-1,4,7-triazacyclononane) and $NaClO_4$ or $AgClO_4$. $[Mn_2^{IV}Mn_2^{II}(\mathbf{113c})_3(L)_2](ClO_4)_3$ was synthesized by the same procedure employed for $[Mn_2^{III}Mn_2^{II}(\mathbf{113c})_3(L)_2](ClO_4)$ but in air. The cyclic voltammetry of the Mn$_2^{III}$Mn$_2^{II}$ complex exhibits two consecutive 2e$^-$ oxidation processes in the potential range from 0.00 to 1.0 V versus Fc$^+$/Fc and one 2e$^-$ reduction at −0.75 V versus Fc$^+$/Fc. The first pair of oxidations is assigned to the oxidation of the two terminal manganese(III) centers to their manganese(IV) forms. The very similar oxidation potential for the couples indicates negligible interactions between the terminal manganese centers. The second pair of oxidations belongs to the central manganese(II) ions and the comparatively high oxidation potentials for the couple Mn^{II}/Mn^{III} reflects the highly unfavorable oxidation of central manganese(II) in aerobic conditions. Therefore, the oxidation equilibria are expressed as $Mn^{III}nMn^{II}MN^{III} \rightleftharpoons Mn^{IV}Mn^{II}Mn^{II}Mn^{IV} \rightleftharpoons Mn^{IV}Mn^{III}Mn^{III}Mn^{IV}$. The 2e$^-$ reduction step in the more negative potential (−0.75 V vs. Fc$^+$/Fc) is attributable to the equilibrium $Mn^{III}Mn^{II}Mn^{II}MN^{III} \rightleftharpoons Mn^{II}Mn^{II}Mn^{II}Mn^{II}$. The comproportionation constant, K_c, for the equilibrium $Mn^{III}Mn^{II}Mn^{II}Mn^{III} + Mn^{IV}Mn^{II}Mn^{II}Mn^{IV} \rightleftharpoons 2Mn^{IV}Mn^{II}Mn^{II}Mn^{III}$ shows that the isolation of the mixed-valence species $Mn^{IV}Mn^{II}Mn^{II}Mn^{III}$ is very unfavorable. Accordingly, all attempts to isolate the species failed [120].

The X-ray structures at 100 K of the Mn$_2^{III}$Mn$_2^{II}$, Mn$_2^{IV}$Mn$_2^{II}$ and Fe$_2^{III}$Mn$_2^{II}$ complexes (Fig. 78c) confirm that linear tetranuclear complexes have indeed been formed with a geometry in which two terminal pseudo-octahedral polyhedra are joined by three oximato N–O groups, derived from the central $[Mn_2^{II}(\mathbf{113c})_3]^{5-}$ core. As expected, the donor atoms for the metal ions of the cations in the three complexes are identical, $\{MN_3O_3\}$ for the terminal manganese(III), manganese(IV) and iron(III) and the manganese(II) ions, but not the coordination environment. For the Mn$_2^{III}$Mn$_2^{II}$ complex a Mn^{III}···Mn^{II} separation of 10.129 Å occurs while for the Fe$_2^{III}$Mn$_2^{II}$ complex a Fe^{III}···Fe^{III} distance of 10.034 Å was measured. The central dimanganese(III) face-shared dioctahedron, essentially identical with one another in these complexes, is severely distorted [120].

The copper(II) centers in $[Cu_2(H\text{-}\mathbf{113a})_2]$ are strongly antiferromagnetically coupled with a $-2J$ value of 554 cm^{-1}. The nickel(II) centers in $[Ni_2(H\text{-}\mathbf{113a})_2(CH_3OH)_2]{\cdot}CH_3OH$ and $[Ni_2(H\text{-}\mathbf{113a})_2(py)_2]{\cdot}py$ are respectively weakly ($-2J = 3.2\ cm^{-1}$) or moderately ($-2J = 19.5\ cm^{-1}$) antiferromagnetically coupled, whereas $[Ni_2(H\text{-}\mathbf{113b})_2(H_2O)_2]$ shows a moderate ferromagnetic interaction ($2J = 5.1\ cm^{-1}$). $[Co_2(H_2\text{-}\mathbf{113c})_2(CH_3OH)_2(H_2O)_2](Cl)_2$, $[Ni_2(H_2\text{-}\mathbf{113c})_2(H_2O)_4](ClO_4)_2$ and $[Cu_2(H_2\text{-}\mathbf{113c})_2(ClO_4)_2]$ show an antiferromagnetically behavior ($J = -6.9$, -16.0 and $-452\ cm^{-1}$, respectively. The magnetic interaction prevailing in $[Fe_2^{III}Ni_2^{II}(\mathbf{113c})_2(\mu\text{-}CH_3COO)_2(L)_2(CH_3OH)_2](BF_4)_2$ is antiferromagnetic in nature ($J_{12} = J_{34} = -6.8$, $J_{13} = J_{24} = -3.2$, $J_{23} = -7.7$, $J_{14} = -1.8\ cm^{-1}$). Finally, the magnetic behavior of the complexes $[M_2Mn_2^{II}(\mathbf{113c})_2(L)_2](ClO_4)_x$ (M = Mn^{III}, Fe^{III}, Cr^{III}, $x = 1$; M = Mn^{IV}, $x = 3$) indicates weak antiferromagnetic coupling between the manganese(II) centers in the central trisphenoxo-bridged dimanganese(II) core, whereas the coupling between the terminal metal ion and its neighboring manganese(II) center is weak ferromagnetic in Mn$_2^{III}$Mn$_2^{II}$ and Mn$_2^{IV}$Mn^{II} or antiferromagnetic in the Fe$_2^{III}$Mn$_2^{II}$ and Cr$_2^{III}$Mn^{II} complexes [120].

113, prepared by reduction of the condensation product of 2-(2-aminoethyl)pyridine with isophthalaldehyde, does not form pure copper(I) complexes in the solid state: $[Cu_2(\mathbf{113})(CH_3CN)_x](ClO_4)_2$ ($x = 2$ or 4), likely formed in acetonitrile by mixing under an inert atmosphere $[Cu(CH_3CN)_4](ClO_4)$ with **113**, reacts with dioxygen to give $[Cu_2(\mathbf{114})\ (OH)(ClO_4)](ClO_4)$, where intramolecular ligand hydroxylation occurs. In this complex the two five coordinate copper(II) ions, 3.006 Å apart and linked each other by a pheno-

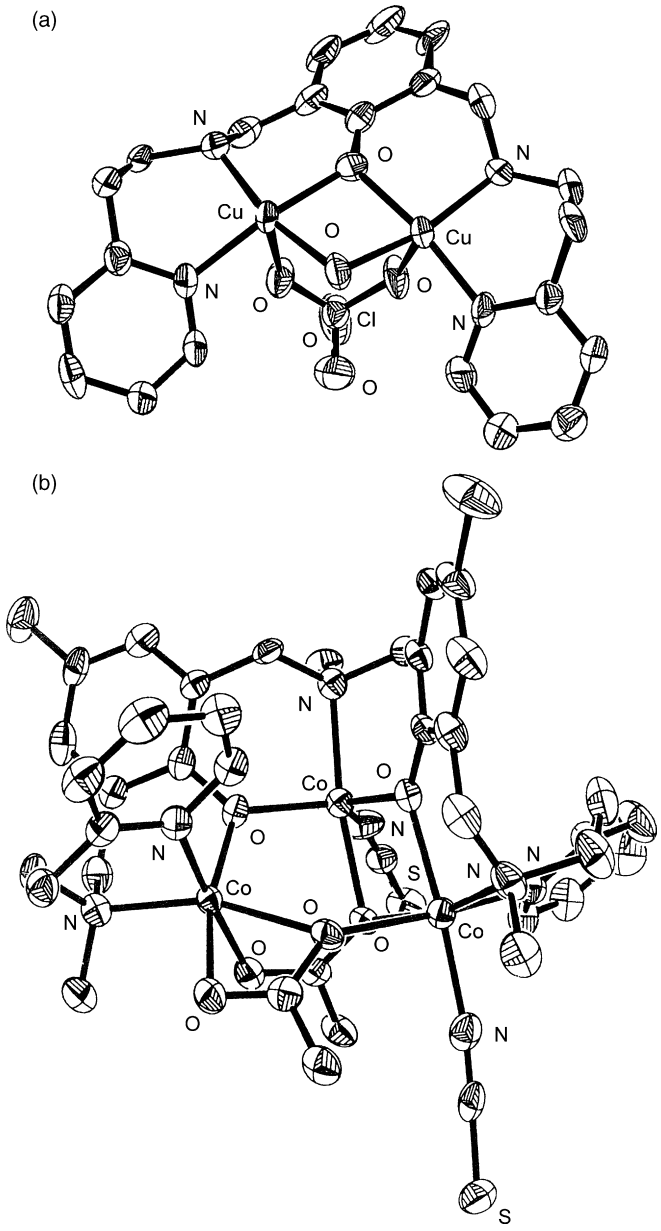

Fig. 79. Structure of $[Cu_2(\mathbf{114})_2(OH)(ClO_4)_2]^+$ (a) and $[Co_3(\mathbf{116a})(CH_3COO)_2(NCS)_2]$ (b).

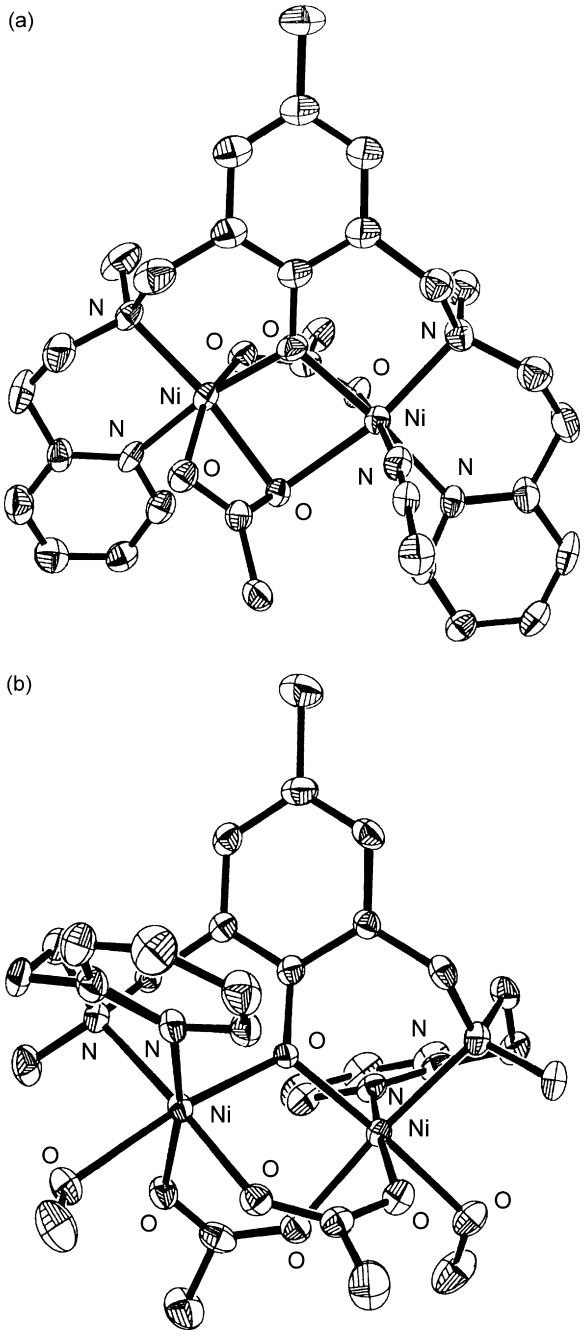

Fig. 80. Structure of $[Ni_2(\mathbf{116})(CH_3COO)_2(NCS)]$ (a) and $[Ni_2(\mathbf{116})(CH_3COO)_2(CH_3OH)_2]^+$ (b).

late oxygen of $[\mathbf{114}]^-$, one hydroxo oxygen and two perchlorate oxygen atoms, are in a square pyramidal environment (Fig. 79a) [120].

$[Cu_2(\mathbf{115a})(OH)](ClO_4)_2$, analogously prepared by oxidation of the copper(I) complexes of **115** with dioxygen, when treated with an excess of chloride ions leads to $[Cu_2(\mathbf{115a})(Cl)_3]$ which regenerates $[Cu_2(\mathbf{115a})(OH)](ClO_4)_2$ by addition of water. In $[Cu_2(\mathbf{115a})(Cl)_3]$ the two copper(II) ions, five coordinate in a distorted trigonal bipyramidal or square pyramidal geometry and 3.293 Å apart, are bridged by an endogenous phenolate and an exogenous chloride ion [120].

$[Co_3(\mathbf{116a})(CH_3COO)_2(NCS)_2]$, in which H-**116** has been modified to H_2-**116a**, derives from the reaction of H-**116** with $Co(CH_3COO)_2{\cdot}4H_2O$ and NaNCS. The trinuclear core, formed by a triangle of cobalt(II) ions, at Co···Co distances of 3.3937 Å, 3.964 Å and 3.202 Å, is supported by two tridentate acetate bridges, (one in μ_3-acetato-κO, κO; κO′-bridging mode and the other in μ_3-acetato-κO; κO′; κO-bridging mode). Two cobalt(II) ions have a distorted octahedral geometry and are donor set asymmetric with one cobalt(II) ion in an N_2O_4 environment, and the other cobalt(II) ion in an N_3O_3

environment. The third five coordinate cobalt(II) ion is in a distorted N_2O_3 trigonal bipyramidal coordination geometry. One octahedral and the trigonal bipyramidal cobalt ions are bridged by a cresolate oxygen and by an acetate oxygen. The other octahedral and the trigonal bipyramidal cobalt ions are bridged by the two acetates. Finally, the two octahedral cobalt ions are bridged by a cresolate oxygen and by the *syn*-anti-bidentate oxygen atoms from a μ_3-acetato-κO; κO; κO-bridge (Fig. 79b) [121].

a bridging cresolato oxygen atom and a bridging *syn–syn* acetate anion. This was augmented by a monodentate bridging acetate anion (μ-acetato-κO, κO′: κO) in $[Ni_2(\mathbf{116})(CH_3COO)_2(NCS)]$ and by a second bridging *syn–syn* acetate anion in $[Ni_2(\mathbf{116})(CH_3COO)_2(CH_3OH)_2](PF_6)\cdot CH_3OH$ (Fig. 80a and b). The Ni···Ni separation of the latter complex (3.4833 Å), longer than that found in the former one (3.1186 Å), reflects the addition of the longer three-atom bridge to the common core [121].

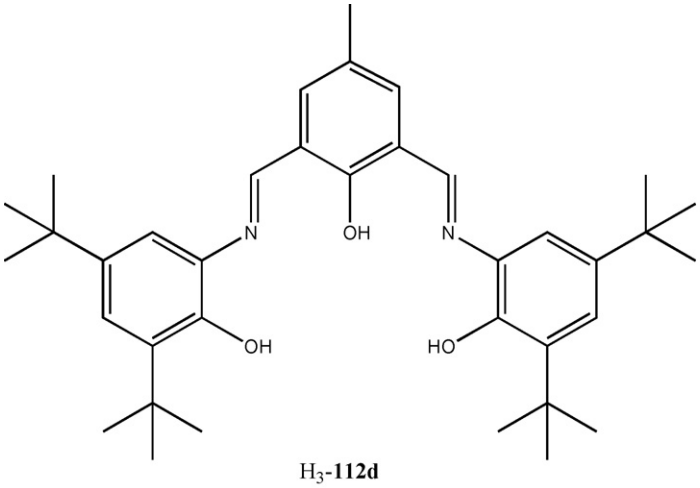

H_3-**112d**

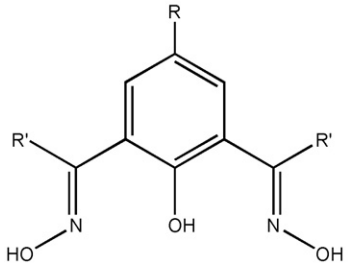

	R	R'
H_3-**113a**	CH_3	CH_3
H_3-**113b**	$C(CH_3)$	CH_3
H_3-**113c**	CH_3	H

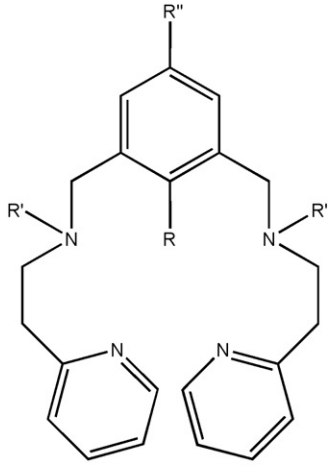

	R	R'	R"
113	H	H	H
H-**114**	OH	H	H
115	H	CH_3	H
H-**115a**	OH	CH_3	H
H-**116**	OH	CH_3	CH_3

The cobalt(II) ion appears to be a prerequisite for ligand rearrangement to occur as dinuclear copper(I) and copper(II) complexes have been reported with intact H-**116** [122,123]; furthermore, $[Ni_2(\mathbf{116})(CH_3COO)_2(NCS)]$ and $[Ni_2(\mathbf{116})(CH_3COO)_2(CH_3OH)_2](PF_6)\cdot CH_3OH$ were prepared by the reaction of H-**116** with $Ni(CH_3COO)_2\cdot 4H_2O$ and the appropriate sodium salt [121]. They contains a basic dinuclear core, derived from two six coordinate octahedral nickel(II) ions,

$[H_6\text{-}\mathbf{117a}](PO_4)$, obtained by reduction of the related Schiff base followed by treatment with phosphoric acid, reacts with $Cu(CH_3COO)_2\cdot H_2O$ and $N(C_2H_5)_3$ to give $[Cu_{18}(H\text{-}\mathbf{117})_6(PO_4)_8]C_3H_7OH\cdot 24H_2O$ [124]. Phosphate ions bridge the copper(II) ions in a μ_6-,μ_4-and μ_8-fashion, while $[H\text{-}\mathbf{117}]^{2-}$ acts as a pentadentate ligand, forming dinuclear copper(II) units $\{Cu_2(H\text{-}\mathbf{117})\}$ with the metal ions is a square pyramidal NO_4 geometry. The remaining copper(II) ions have trigonal

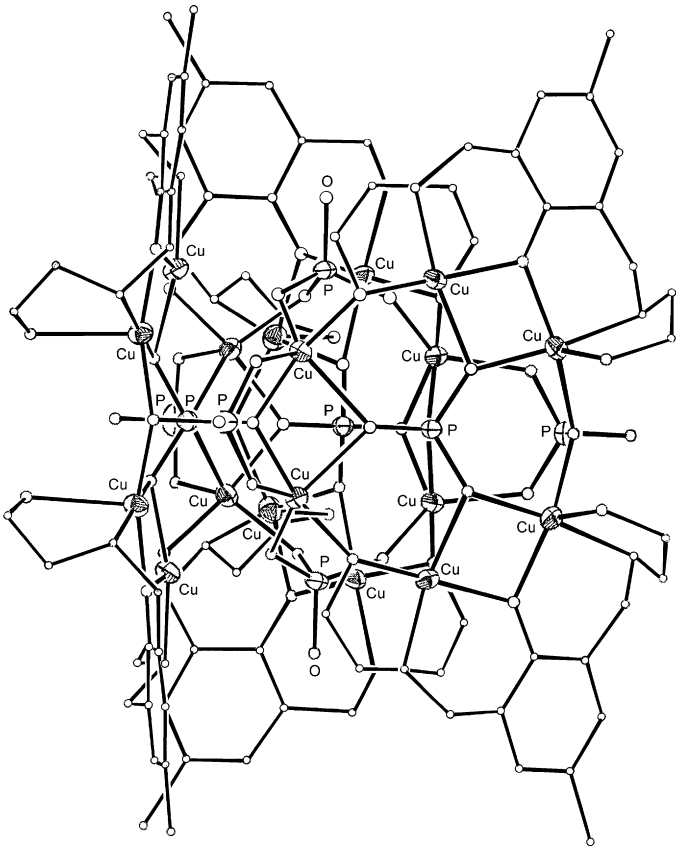

Fig. 81. Structure of $[Cu_{18}(H\text{-}\mathbf{117})_6(PO_4)_8]$.

bipyramidal O_5 environments. In the dinuclear unit, the separations between copper(II) ions are 3.014–3.021 Å, while the μ_8-, μ_6- and μ_4-phosphate bridges separate the copper(II) ions by 3.041–3.048, 3.558–3.579, and 3.542–3.590 Å, respectively (Fig. 81). According to magnetic susceptibility measurements, in $[Cu_{18}(H\text{-}\mathbf{117})_6(PO_4)_8]C_3H_7OH\ 24H_2O$ strong antiferromagnetic interactions are operative through the phenoxo bridges while weak magnetic interactions through O–P–O bridges occurs [124].

Treatment of H-**118** [125] with a mixture of $[Zn(C_2H_5)(Cl)]$ and $[Zn(C_2H_5)_2]$ afford $[Zn_2(\mathbf{118})(\mu\text{-}OC_2H_5)(Cl)_2]$ [126], structurally similar to $[Zn_2(\mathbf{118})(\mu\text{-}OCH_3)(NO_3)_2]$ reported as a β-lactamase model [127]. The reaction of $[K(\mathbf{118})]$ with MCl_2 ($M = Co^{II}$, Mg^{II}) presumably yields $[M(\mathbf{118})(Cl)_3]$ which, by metathesis with $Tl(OC_2H_5)$ affords $[M_2(\mathbf{118})(\mu\text{-}OC_2H_5)(Cl)_2]$. This method proved untenable for the dizinc(II) complex, in which case $[Zn_2(\mathbf{118})(Cl)_3]$, isolated and structurally characterized, could not be converted cleanly to $[Zn_2(\mathbf{118})(\mu\text{-}OC_2H_5)(Cl)_2]$. $[Zn_2(\mathbf{118})(\mu\text{-}OC_2H_5)(Cl)_2]$ contains one square pyramidal zinc(II) ion and one trigonal bipyramidal zinc(II) ion. The two bridging oxygen atoms are asymmetrically placed between the two zinc ions. ^1H NMR spectra showed retention of the dizinc structure in solution, although fluxionality between isomers with and without mirror symmetry (e.g., meso and RR/SS diastereomers, respectively) occurs [126].

The dicobalt(II) and dimagnesium(II) complexes contain one phenolate bridging oxygen of $[\mathbf{118}]^-$, two chloride anions in an anti disposition, and a single bridging ethoxide. In $[Co_2(\mathbf{118})(\mu\text{-}OC_2H_5)(Cl)_2]$ one metal ion is distorted trigonal bipyramidal and the other is square pyramidal. One magnesium(II) ion in $[Mg_2(\mathbf{118})(\mu\text{-}OC_2H_5)(Cl)_2]$ is six coordinate, while the other is five coordinate square pyramidal. The dimagnesium(II) complex in solution retains the dimeric structure, showing, however, a different fluxionality from the analogous dizinc complex [126].

$[M_2(\mathbf{118})(\mu\text{-}OC_2H_5)(Cl)_2]$ ($M = Zn^{II}$, Mg^{II}, Co^{II}) rapidly polymerize in tetrahydrofuran at room temperature ε-caprolactone (CL) with the formation of high molecular weight atactic polycaprolactone (PCL) with a narrow molecular weight distribution: the dimagnesium compound shows maximal activity; the CL polymerization order is: $Mg_2 > Co_2 > Zn_2$. Furthermore, these complexes catalyze the polymerization DL-lactide(LA) to atactic polylactide with a narrow weight distribution. High molecule weight polymers were only accessible with the dizinc complex. The reactivity trend for this polymerization is $Zn_2 \gg Co_2 \cong Mg_2$. The dimagnesium and the dicobalt complexes are more susceptible than the dizinc(II) one to side reactions that change the nature of the catalytically active species [126].

In the similar ligand H-**118a**, derived from the Mannich reaction between *p*-hydroxybenzaldehyde and *N*-methylpiperazine in the presence of formaldehyde, the piperazine rings are in a chair conformation. It forms $[M(\mathbf{118a})(CH_3COO)]\cdot H_2O$ ($M = Cu^{II}$, Ni^{II}), $\{Zn(\mathbf{118a})(CH_3COO)(H_2O)_2]$ or $[M_2(\mathbf{118a})(CH_3COO)_2(H_2O)_n](ClO_4)$ ($n = 1 M = Cu^{II}$, $n = 4 M = Ni^{II}$; $n = 2 M = Zn^{II}$), when reacted with the appropriate metal(II) acetate. EPR and magnetic data of the dinuclear copper(II) complexes indicate an antiferromagnetic interaction. The mononuclear nickel(II) complex is square planar and diamagnetic whereas the six coordinated dinuclear nickel(II) complex shows a magnetic moment value of 2.98 BM. Cyclic voltammetric studies in dimethylformamide (Ag/AgCl reference electrode) proved one irreversible reduction wave for all the mononuclear complexes; two irreversible one-electron reduction waves for the dinuclear complexes are obtained corresponding to the reduction processes $M^{II}M^{II} \rightleftharpoons M^{II}M^{I} \rightleftharpoons M^{I}M^{I}$. Also one irreversible oxidation wave for the mononuclear nickel(II) complex and two irreversible oxidation waves for the dinuclear nickel(II) complexes are obtained, corresponding to the processes $Ni^{II}Ni^{II} \rightleftharpoons Ni^{III}Ni^{II} \rightleftharpoons Ni^{III}Ni^{III}$. Kinetic studies on the oxidation of pyrocatechol to *o*-quinone, using these mono and dinuclear copper(II) complexes as catalysts, indicate higher activity of the dinuclear copper(II) complex than the mononuclear one. Furthermore, the hydrolysis of 4-nitrophenylphosphate using the mono and dinuclear copper(II), nickel(II) and zinc(II) complexes proves the dinuclear complexes to have higher rate constant values than those of the corresponding mononuclear complexes. The rate constant values for the complexes for the hydrolysis are in order nickel(II) > copper(II) > zinc(II) [128].

The imine-amine-thioether **119a**, prepared by condensation between **119** and *N*′,*N*′-dimethylethane-1,2-diamine, forms the tetraamine-thioether **119c** by subsequent reduction. Treatment of **119a** or **119c** with $[Pd(Cl)_2(CH_3CN)_2]$ gives, upon addition of an excess of $LiClO_4$, $[Pd_2(\mathbf{119b})(Cl)_2](ClO_4)$ or $[Pd_2(\mathbf{119d})(\mu$-

Cl)](ClO4)2, respectively. [Pd2(**119b**)(CH3COO)](ClO4)2 was prepared by a similar procedure. Thus, the thioethers **119a** and **119c** undergo a Pd-promoted S–C bond cleavage reaction to generate dinuclear palladium complexes of the binucleating thiophenolate ligand [**119b**]− and [**119d**]−, respectively [129].

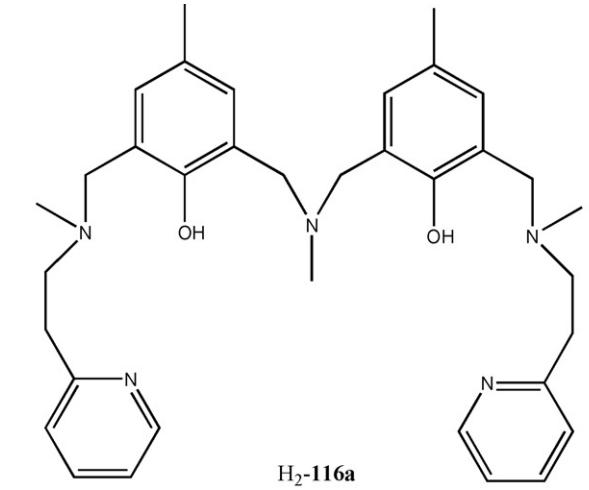

H2-**116a**

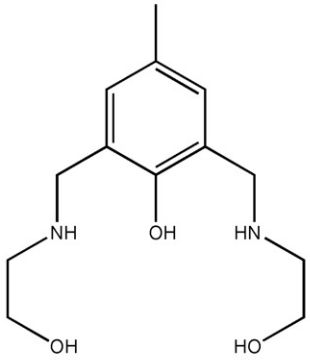

H3-**117**

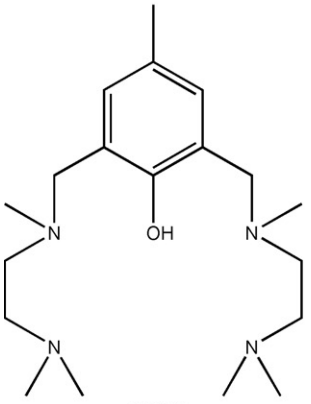

H-**118**

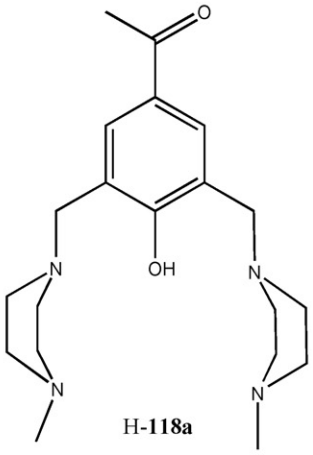

H-**118a**

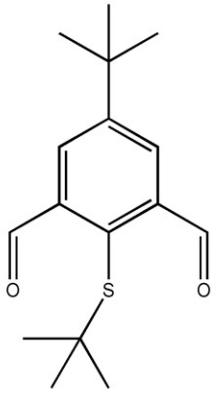

119

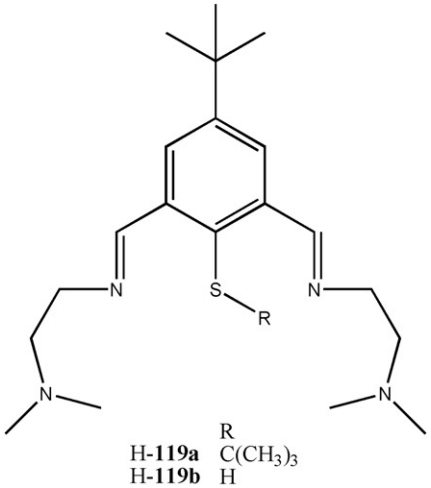

	R
H-**119a**	$C(CH_3)_3$
H-**119b**	H

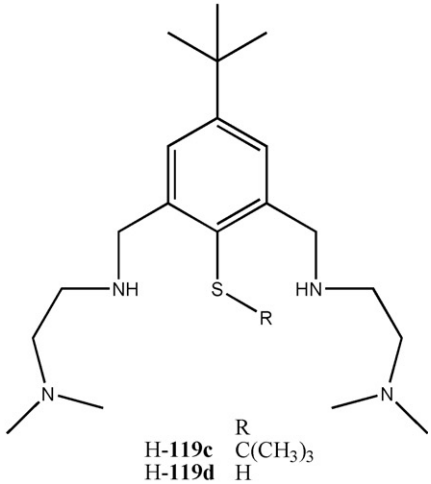

	R
H-**119c**	$C(CH_3)_3$
H-**119d**	H

The bisacetonitrile derivative [Pd2(**119b**)(CH3CN)2](ClO4)3, obtained by chloride abstraction from [Pd2(**119b**)(Cl)2](ClO4) with anhydrous Pb(ClO4)2, when treated with NaNCS or NaN3 results in the formation of [Pd2(**119b**)(SCN)2](ClO4) or [Pd2(**119b**)(N3)2](ClO4), respectively. The related tetraphenylborate derivatives were prepared by a similar procedure. The addition of Pb(ClO4)2 to [Pd2(**119b**)(Cl)2](ClO4) in propionitrile forms [Pd4(**119b**)2(μ1,2-CN)2](ClO4)4 where the cyanide ions are presumably generated via a lead(II)-mediated retro-hydrocyanation of the solvent. The reaction of [Pd2(**119b**)(CH3CN)2](ClO4)3 with water smoothly gives [Pd2(**119b**)(NHCOCH3)](ClO4)2.

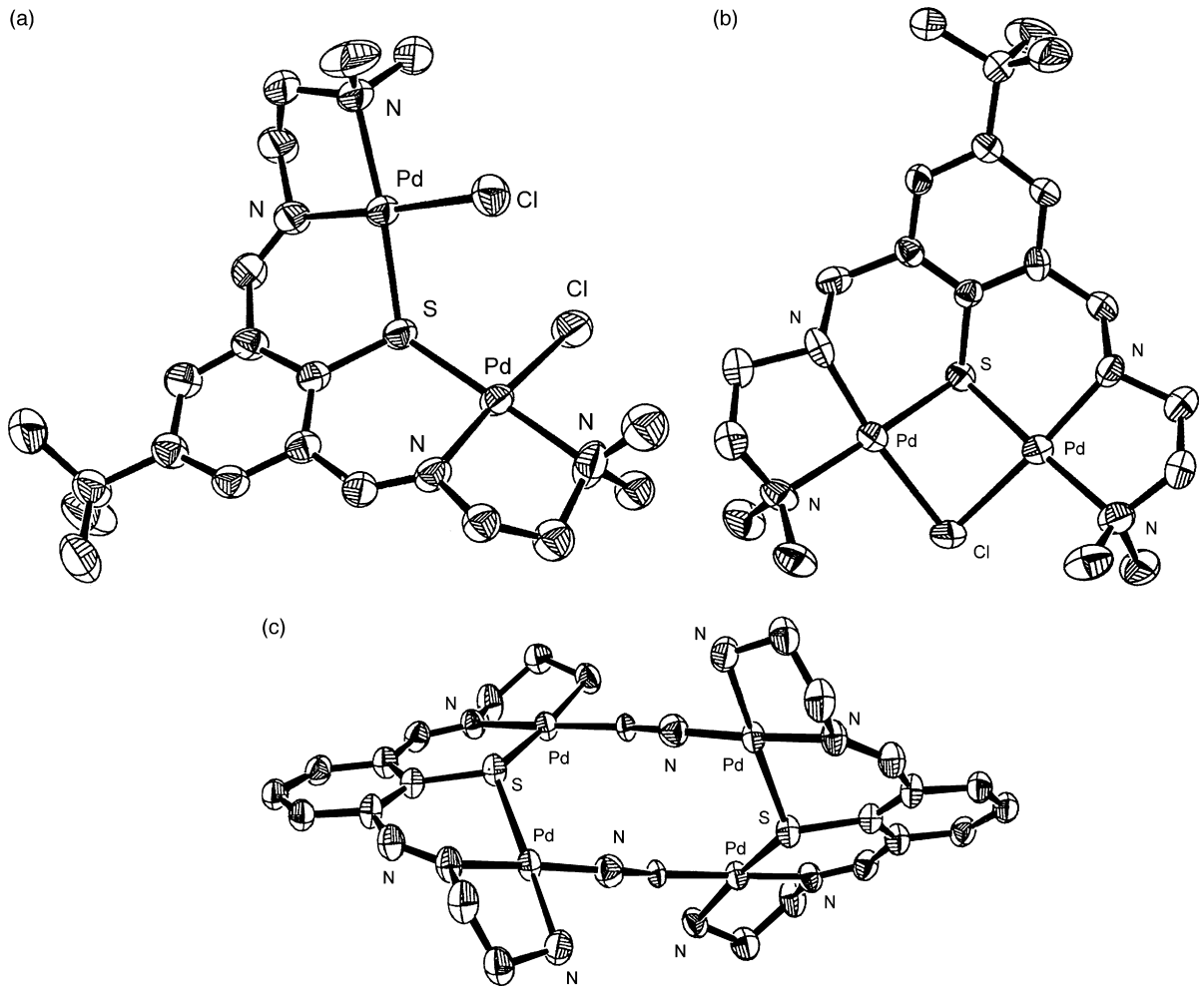

Fig. 82. Structure of $[Pd_2(\mathbf{119b})(Cl)_2]^+$ (a), $[Pd_2(\mathbf{119d})(Cl)]^{2+}$ (b), $[Pd_4(\mathbf{119b})_2(\mu\text{-}CN)_2]^{4+}$ (c).

$[Pd_2(\mathbf{119b})(NCHCH_2Cl)_2](ClO_4)_3$, prepared in situ from $[Pd_2(\mathbf{119b})(Cl)_2](ClO_4)$ and $Pb(ClO_4)_2$ in neat 2-chloroacetonitrile, is also hydrated by aqueous methanol to give $[Pd_2(\mathbf{119b})(NHOCCH_2Cl)](ClO_4)_2$; the chloro-function is not hydrolyzed under these conditions. $[Pd(\mathbf{119b})(\eta^1\text{-}Ph)_2](BPh_4)$, formed as a side product in the salt metathesis reaction between $[Pd_2(\mathbf{119b})(CH_3CN)_2](ClO_4)_3$ and $NaBPh_4$, is stable toward heat, moisture and air [129].

The structure of $[Pd_2(\mathbf{119b})(X)_2](ClO_4)$ ($X = Cl^-$, SCN^-, N_3^-) (Fig. 82a) are very similar to each other. Each distorted square planar palladium(II) ion is coordinated by one bridging thiolate sulfur atom, two nitrogen atoms and a terminal chloro ligand or a thiocyanate via its sulfur atom in a monodentate fashion or two azide ions in an end-on fashion. The Pd···Pd separation is 3.922 Å in $[Pd_2(\mathbf{119b})(Cl)_2](ClO_4)$, 3.877 Å in $[Pd_2(\mathbf{119b})(SCN)_2](ClO_4)\cdot CH_3CN$ and 3.971 Å in $[Pd_2(\mathbf{119b})(N_3)_2](ClO_4)_2$. Also in $[Pd_2(\mathbf{119d})(Cl)](ClO_4)_2\cdot CH_3OH$ each palladium ion is coordinated by one bridging thiolate sulfur atom, two nitrogen atoms and a chloro ligand, but in contrast to $[Pd_2(\mathbf{119d})(Cl)](ClO_4)_2$ the latter acts in a bridging mode. As a consequence, the Pd···Pd distance is much shorter (3.087 Å) (Fig. 82b). In $[Pd_4(\mathbf{119b})_2(\mu\text{-}CN)_2](ClO_4)_4$, the two $[Pd_2(\mathbf{119b})]^{2+}$ units are linked via two $\mu_{1,2}$-bridging cyanide ions to give a tetranuclear palladium(II) complex. The separation of the $\mu_{1,2}$-CN-bridged palladium(II) ions (5.090 Å) is much longer than the Pd···Pd distances in the $[Pd_2(\mathbf{119b})]^{2+}$ units (3.981 Å) (Fig. 82c).

In $[Pd_2(\mathbf{119b})(NHOCCH_2Cl)](ClO_4)_2$, the 2-chloroacetamidato unit bridges the two palladium ions in a $\mu_{1,3}$-bridging mode to generate a N_3S coordination environment for palladium(II) ion and a N_2OS coordination environment for the other palladium(II) ion. In $[Pd_2(\mathbf{119b})(CH_3COO)](ClO_4)_2$ each palladium ion features a planar coordination comprised of tertiary amine, imine and thiophenolate sulfur atoms from the supporting ligand $[\mathbf{119b}]^-$ and one oxygen atom of a $\mu_{1,3}$-bridging acetate ion. The Pd···Pd distance is 3.685 Å. Finally, in $[Pd(\mathbf{119b})(\eta^1\text{-}C_6H_5)_2](BPh_4)$ both phenyl groups are η^1-coordinated to the planar palladium ions, which are 3.925 Å apart [129].

119, when condensed with two equivalents of 2-(diphenylphosphino)ethyleneamine, yields **120a** as colorless oil. The subsequent reduction of the imine functions of **120a** produces the phosphanyl-substituted amine-thioether **121a**. The reaction of **120a** or **121a** with $[Pd(CH_3CN)_2(Cl)_2]$ gives, upon addition of an excess of $LiClO_4$, $[Pd_2(\mathbf{120b})(Cl)_2](ClO_4)$ or $[Pd_2(\mathbf{121b})(Cl)](ClO_4)_2$, respectively. Again the thio-

late functions of **120a** and **121b** can be selectively deprotected with $[Pd(CH_3CN)_2(Cl)_2]$ without affecting the phosphine groups. Reaction of $[Pd_2(\mathbf{120b})(Cl)_2](ClO_4)$ with $Pb(ClO_4)_2$ produces $[Pd_2(\mathbf{120b})(CH_3CN)_2](ClO_4)_3$, which reacts with various anions ($X = SCN^-$, N_3^-, I^- and CN^-) to form $[Pd_2(\mathbf{120b})(X)_2](ClO_4)$. As previously observed for $[Pd_2(\mathbf{119d})(CH_3CN)_2](ClO_4)_3$, the Pd-bound acetonitrile ligands in $[Pd_2(\mathbf{120b})(CH_3CN)_2](ClO_4)_3$ are readily transformed into acetamide in basic water, giving rise to $[Pd_2(\mathbf{120b})(NHCOCH_3)](ClO_4)_2$ [129].

In $[Pd_2(\mathbf{120b})(Cl)_2](ClO_4)\cdot C_2H_5OH$ each palladium(II) ion is surrounded by a nitrogen, a sulfur and a phosphorous atom of $[\mathbf{120b}]^-$, and a terminal chloro ligand in a distorted square planar manner. The overall conformation of $[\mathbf{120b}]^-$ in this complex is very similar to that of $[\mathbf{119b}]^-$ in $[Pd_2(\mathbf{119b})(Cl)_2](ClO_4)$. In contrast to $[Pd_2(\mathbf{119b})(Cl)_2](ClO_4)$, no strain occurs around the bridging thiophenolate sulfur atom in $[Pd_2(\mathbf{120b})(Cl)_2](ClO_4)$. The Pd···Pd distance in $[Pd_2(\mathbf{120b})(Cl)_2](ClO_4)$ (4.389 Å) is different from that in $[Pd_2(\mathbf{119b})(Cl)_2](ClO_4)$ (3.922 Å): replacement of the $-N(CH_3)_2$ groups in $[\mathbf{119b}]^-$ by the $-PPh_2$ ones in $[\mathbf{120b}]^-$ does not change the overall ligating properties of the supporting ligand but releases some strain in the ligand backbone due do a lengthening of the Pd–S bonds (Fig. 83a) [129].

In $[Pd_2(\mathbf{121b})(Cl)](ClO_4)_2$ the conformation adopted by $[\mathbf{121b}]^-$ is very similar to that of $[\mathbf{119d}]^-$ in $[Pd_2(\mathbf{119d})(\mu\text{-}Cl)](ClO_4)_2$. Thus, as was observed for $[\mathbf{120b}]^-$, the ligating properties of $[\mathbf{121b}]^-$ are not markedly affected by conversion of the $-N(CH_3)_2$ into PPh_2 groups (Fig. 83b). In $[Pd_2(\mathbf{120b})(I)_2](ClO_4)$ one palladium(II) ion is almost perfectly planar while the other palladium(II) ion is significantly distorted from square planar towards tetrahedral. In $[Pd_2(\mathbf{120b})(CN)_2](ClO_4)$ both cyanides act as monodentate ligands, generating distorted square-planar NSPC environments for both palladium ions. In $[Pd_2(\mathbf{120b})(NHCOCH_3)](ClO_4)_2\cdot CH_3CN\cdot CH_3OH$ the acetamidato unit bridges the two palladium(II) ions in a $\mu_{1,3}$-bridging mode at a Pd···Pd distance of 3.711 Å (Fig. 83c) [129].

$[Pd_2(\mathbf{120b})(Cl)_2](ClO_4)$ is active in the vinyl-addition polymerization of norbornene, when activated with methylalumoxane (MAO) or $B(C_6F_5)_3/Al(C_2H_5)_3$. Without a cocatalyst, no activity is observed and with $B(C_6F_5)_3$ alone only a very low activity can be obtained. It was suggested that the lower catalytic activity of $[Pd_2(\mathbf{120b})(Cl)_2](ClO_4)$ than that of the related (2,6-bis-(thio)semicarbazide-4-methylphenolato-N,O,O′(S))-dichloro-dipalladium(II) compounds can be due to the presence of the Ph_2P-ligating group in $[Pd_2(\mathbf{120b})(Cl)_2](ClO_4)$ which could shield the active centre with its bulkiness and because the Pd–P bond is less likely to open even in the presence of the cocatalysts to create a necessary open coordination site [129].

6. [2 + 1] Symmetric end-off systems

The [2 + 1] symmetric end-off ligands have been obtained by reaction of the appropriate formyl- or keto-derivatives with $H_2NCH_2CHOHCH_2NH_2$ or $H_2N(CH_2)_2NHCH_2CHOHCH_2NH(CH_2)_2NH_2$ in a 2:1 molar ratio, according to Scheme 5. Again the related polyamine derivatives have been synthesized by reduction of the Schiff bases with $NaBH_4$ or similar reducing agents. The homodinuclear complexes derive from the reaction of the desired preformed ligand with two equivalents of the appropriate metal salt (in the presence of an additional coordinating ligand when the anion is fairly coordinating). For the Schiff base complexes the template procedure, using comparable experimental conditions, affords the same complexes. These complexes contain an endogenous alcoholate oxygen bridge and an exogenous one formed by an additional anionic group which, when polydentate, easily forms also intermolecular linkages. Also, intermolecular interactions through the oxygen phenolate atoms of the end-off ligands can give rise to aggregates with higher nuclearity.

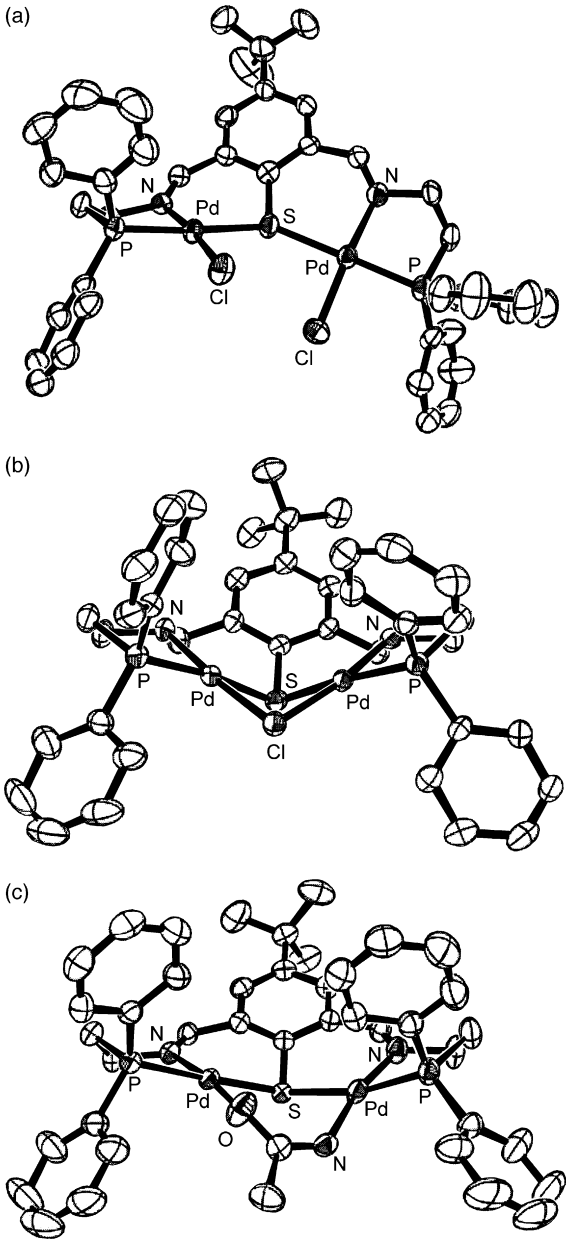

Fig. 83. $[Pd_2(\mathbf{120b})(Cl)_2]^+$ (a), $[Pd_2(\mathbf{121b})(Cl)]^{2+}$ (b) and $[Pd_2(\mathbf{120b})(NHCOCH_3)]^{2+}$ (c).

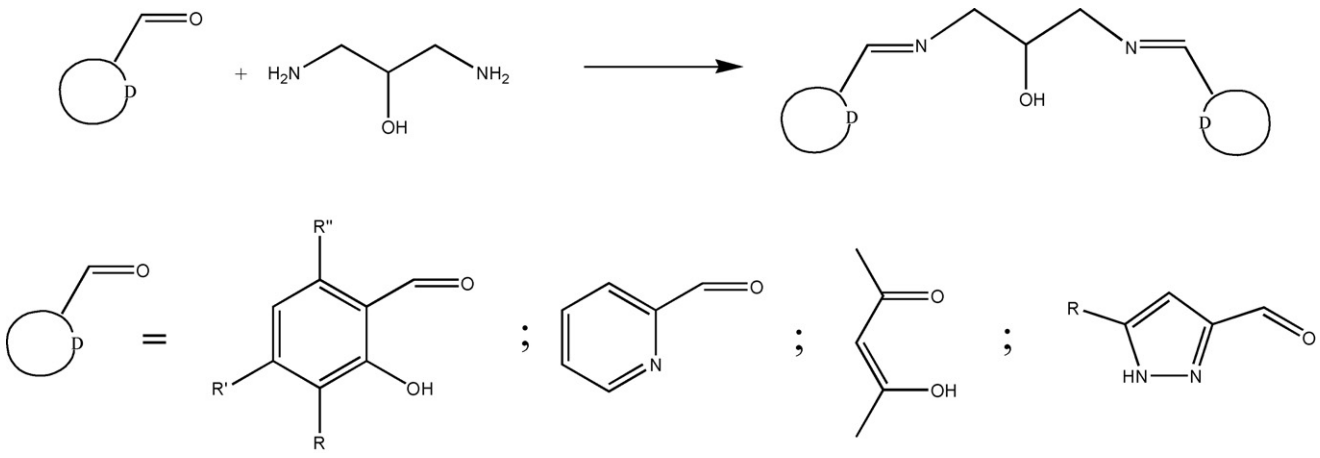

Scheme 5. Synthesis of the [2 + 1] symmetric end-off ligands.

The condensation of the appropriate aldehyde with 1,3-diamino-2-propanol in the presence of $Cu(ClO_4)_2{\cdot}6H_2O$, pyrazole (H-pz) or 7-azaindole (H-ind) and triethylamine affords the almost planar complexes $[Cu_2(\mathbf{L})(\mu\text{-pz})]$ or $[Cu_2(\mathbf{L})(\mu\text{-ind})]$ (H_3-**L** = H_3-**122a**, H_3-**122b**, H_3-**122c**), where the metal centers are doubly bridged by the alkoxo oxygen of $[\mathbf{L}]^{3-}$ and the pyrazolate or 7-azaindolate anion. In addition, each metal ion is coordinated to one imine nitrogen and one phenoxo oxygen afforded by $[\mathbf{L}]^{3-}$. The metal centers are antiferromagnetically coupled in; on the contrary, an intradimer ferromagnetic interaction occurs in $[Cu_2(\mathbf{122a})(\mu\text{-ind})]$ ($J = 26\,cm^{-1}$) and in $[Cu_2(\mathbf{122c})(\mu\text{-ind})]$ ($J = 16.7\,cm^{-1}$) [130].

Similarly, $[Cu_2(\mathbf{122c})(p\text{-}OHC_6H_4CH{=}CHCOO)]$, synthesized by the reaction of $[Cu_2(\mathbf{122c})(CH_3COO)]$ with the sodium salt of *p*-hydroxycinnamic acid (*p*-$OHC_6H_4CH{=}CHCOO{-}Na$), consists of an asymmetrically dibridged square planar NO_3 dicopper(II) unit having an alkoxo bridge of $[\mathbf{122c}]^{3-}$ and the *p*-hydroxycinnamate in a three atom bridging mode, giving a Cu···Cu distance of 3.475 Å. The complex self assembles to form a helical supramolecular structure involving the oxygen atom of the pendant –OH group of the *p*-hydroxycinnamate and one phenoxy oxygen atom of the Schiff base belonging to different symmetric units. The two metal ions antiferromagnetically interact each other ($-2J$) [131].

H_3-**123** and $Cu(CH_3COO)_2{\cdot}H_2O$ form $[Cu_2(\mathbf{123})(CH_3COO)]$, where a dicopper(II) unit is bridged by the alkoxide and acetate oxygen atoms. $[Cu_2(\mathbf{123})(CH_3COO)]$, when mixed the sodium salt of *p*-hydroxycinnamic acid, gives rise to $[Cu_2(\mathbf{123})(p\text{-}OHC_6H_4CH{=}CHCOO)(CH_3OH)]$ and $[Cu_2(\mathbf{123})(p\text{-}OHC_6H_4CH{=}CHCOO)]{\cdot}(H_2O)$ which have a (μ-alkoxo)(μ-carboxylate)-dicopper(II) core with a Cu···Cu distance of 3.504 Å and 3.501 Å, respectively. In the former complex, one copper(II) has a square planar NO_3 coordination geometry and the other copper(II) ion has a square pyramidal coordination geometry, while in the latter the copper centers have a square planar NO_3 coordination geometry. $[\mathbf{123}]^{3-}$ behaves as a pentadentate ligand with the alkoxo oxygen atom bridging the copper centers. Variable temperature magnetic studies show for all these complexes an antiferromagnetically coupled spin system: $J = -200\,cm^{-1}$ for $[Cu_2(\mathbf{122a})(\mu\text{-pz})]$ and $J = -175\,cm^{-1}$ for $[Cu_2(\mathbf{122b})(\mu\text{-pz})]$, while a singlet-triplet energy separation of 116, 160 and 132 cm^{-1} were found in $[Cu_2(\mathbf{122c})(p\text{-}OHC_6H_4CH{=}CHCOO)]$, $[Cu_2(\mathbf{123})(p\text{-}OHC_6H_4CH{=}CHCOO)(CH_3OH)]$ and $[Cu_2(\mathbf{123})(p\text{-}OHC_6H_4CH{=}CHCOO)(H_2O)]$, respectively [131,132].

In the alkoxo–phenoxo bridged tetranuclear copper(II) complexes $[Cu_4(\mathbf{122c})_2(RCOO)_2]$ (R = *p*-OHC_6H_4, *o*-OHC_6H_4), derived from $[Cu_2(\mathbf{122c})(CH_3COO)]$ and the sodium salt of *para*- or *ortho*-hydroxybenzoic acid, two $[Cu_2(\mathbf{122c})(RCOO)]$ units self assemble to the tetranuclear complex by covalent linkage through the axial ligation of the phenoxo oxygen atom of $[\mathbf{122c}]^{3-}$. Within the dimeric unit, the dicopper(II) core is bridged by the mono-atomic alkoxo oxygen of $[\mathbf{122c}]^{3-}$ and the three-atomic carboxylato oxygen atoms retaining the asymmetrically dibridged structure of $[Cu_2(\mathbf{123})(CH_3COO)]$. The Cu···Cu distance of 3.48 Å in both complexes is similar to the Cu···Cu distance in $[Cu_2(\mathbf{122c})(C_6H_5COO)]$. The other structural features also resemble with the benzoate complex except that the two copper(II) centers in the tetrameric complexes have a square pyramidal NO_4 coordination geometry (Fig. 84a) [133]. In $[Cu_4(\mathbf{122c})_2(\mu_{1,1}\text{-}N_3)_2]{\cdot}5H_2O$, obtained only by reaction of $Cu(NO_3)_2$, H_3-**122c**, and NaN_3, a distorted cubic unit $Cu_4N_2O_2$ occurs with the four copper ions bridged two by two by nitrogen atoms from two azide ions in an end-on fashion and three by three by the alkoxo oxygen atoms from two anionic ligands $[\mathbf{122c}]^{3-}$. Two copper(II) ions are five coordinate in a N_2O_3 environment while the other two copper(II) ions show a N_2O_2 planar arrangement. The Cu···Cu separation ranges from 3.156 to 3.661 Å, this depending on the involved bridging groups (Fig. 84b) [134]. $[Cu_4(\mathbf{122c})_2(p\text{-}OHC_6H_4COO)_2]$ and $[Cu_4(\mathbf{122c})_2(o\text{-}OHC_6H_4COO)_2]$ are antiferromagnetically coupled spin systems with intradimer J_1 and interdimer J_2 exchange couplings of -132 and $-72\,cm^{-1}$ for the former and -167 and $-67\,cm^{-1}$ for the latter complex, respectively [133]. Furthermore, magnetic and EPR data indicate strong antiferromagnetic interactions associated with the alkoxides and weak ferromagnetic interactions arising from the azides [134].

$[Cu_3(\mathbf{122c})(H\text{-}\mathbf{122c})(Im)](ClO_4)$ and $[Cu_3(\mathbf{122c})(H\text{-}\mathbf{122c})(CH_3\text{-}Im)](ClO_4)$, related to the trinuclear core of the

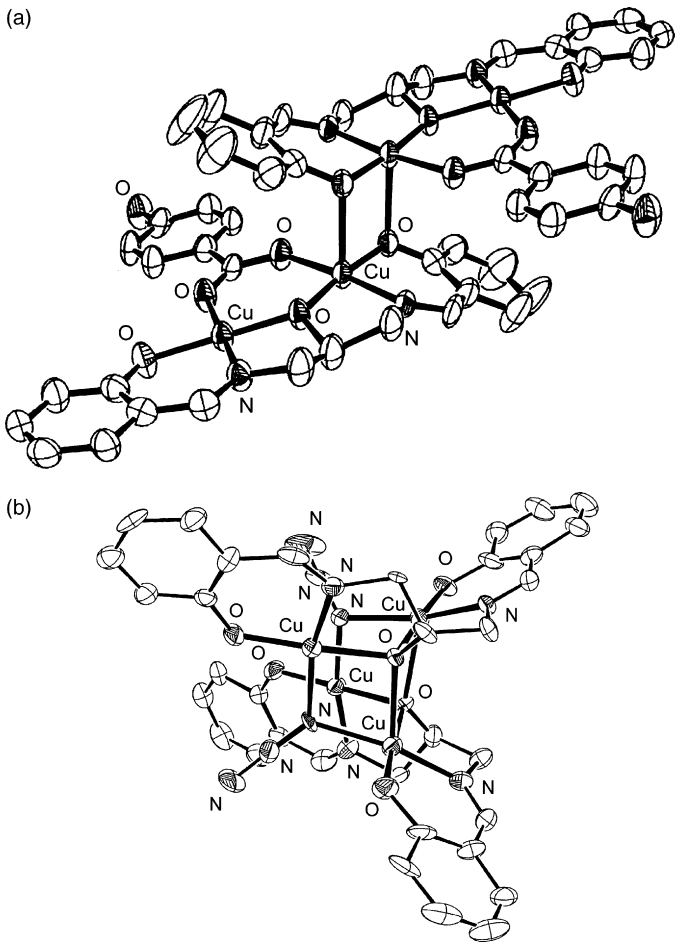

Fig. 84. Structure of $[Cu_4(\mathbf{122c})_2(p\text{-}HOC_6H_4COO)_2]$ (a) and $[Cu_4(\mathbf{122c})_2(\mu_{1,1}\text{-}N_3)_2]$ (b).

active site of ascorbate oxidase, have been prepared by mixing together $[Cu_2(\mathbf{122c})(Br)]$ and [Cu(H-**122c**)] in the presence of imidazole (H-Im) or methylimidazole (H-CH_3-Im) and $Na(ClO_4)$. Their structure consists of a trinuclear copper(II) core in which the monomeric type-2 mimic complex [Cu(H-**122c**)] forms a covalent linkage with the dinuclear type-3 mimic complex $[Cu_2(\mathbf{122c})(Br)]$ through two phenoxo oxygen atoms belonging to [Cu(H-**122c**)]. The removal of the exogenous bromide bridging ligand of $[Cu_2(\mathbf{122c})(Br)]$ results in the binding of the phenoxo oxygen atoms of [Cu(H-**122c**)] to one copper center of the $[Cu_2(\mathbf{122c})]^+$. Two copper(II) ions are four coordinate while the third copper(II) ion displays a five coordinate geometry. $[\mathbf{122c}]^{3-}$ acts as a pentadentate ligand bound to two copper(II) ions with an endogenous alkoxide bridge. The Cu···Cu distances are in the range 3.202–3.438 Å (Fig. 85a) [135].

A quite similar synthetic procedure affords also $[Cu_3(\mathbf{122c})(H\text{-}\mathbf{122c})(CH_3\text{-}Im)(H_2O)](ClO_4)$ where a monomeric unit binds to one copper center of a dinuclear unit through the phenoxo oxygen atom. The copper(II) ion of the monomeric unit is four coordinate in a N_2O_2 coordination environment. One copper(II) ion of the dinuclear unit is five coordinate in a NO_4 environment and is linked to the other two copper ions through alkoxo and

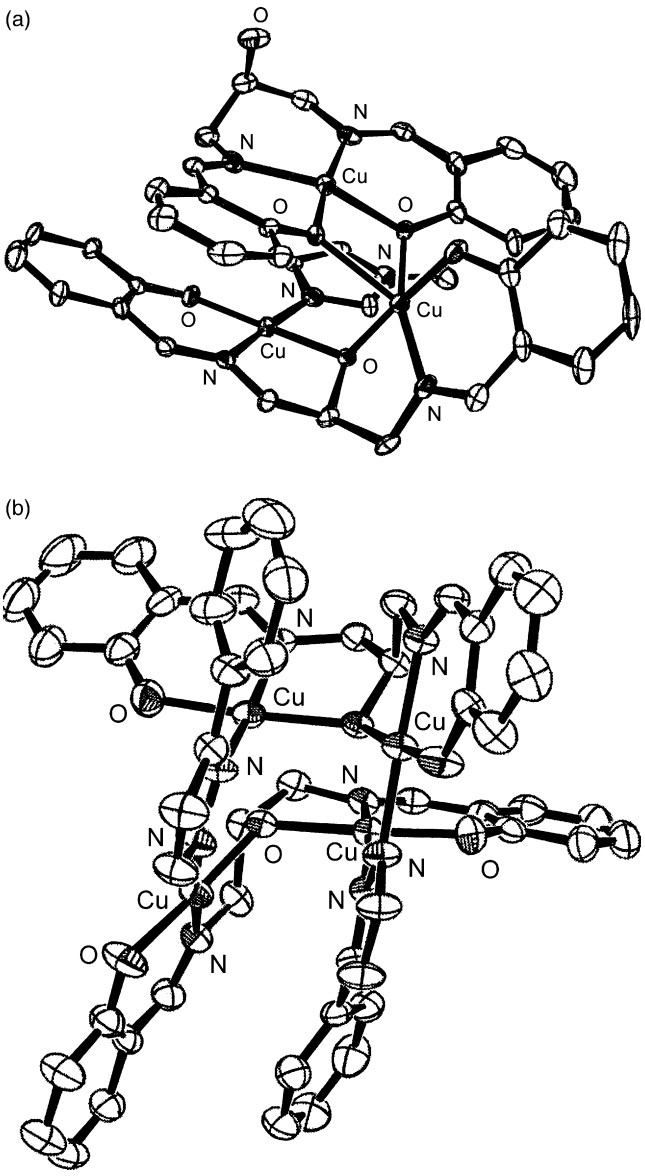

Fig. 85. Structure of $[Cu_3(\mathbf{122c})(H\text{-}\mathbf{122c})(CH_3\text{-}Im)]$ (a) and $[Cu_4(\mathbf{122c})_2(3\text{-}ppz)_2]$.

phenoxo oxygen atoms. The third copper(II) ion has a square pyramidal geometry. An antiferromagnetic behavior was observed for these trinuclear copper(II) complexes: the coupling constants J_1 and J_2 are -82.7 and $-73\,cm^{-1}$ for $[Cu_3(\mathbf{122c})(H\text{-}\mathbf{122c})(Im)](ClO_4)$ and -98.3 and $-46.1\,cm^{-1}$ for $[Cu_3(\mathbf{122c})(H\text{-}\mathbf{122c})(CH_3\text{-}Im)](ClO_4)$ [135,136].

In $[Cu_4(\mathbf{122c})_2(3\text{-}ppz)_2]$, prepared from $[Cu_2(\mathbf{122c})_2(Br)]$ and 3-phenylpyrazole (H-3-ppz), two dimeric $\{Cu_2(\mathbf{122c})\}$ units, where the pentadentate ligand $\mathbf{[122c]^{3-}}$ provides the endogenous alkoxo-bridge for the two copper(II) ions, are covalently linked by two $[3\text{-ppz}]^-$ ligands. Two copper(II) ions are five coordinate square pyramidal while the other two copper(II) ions are four coordinate square planar. The Cu···Cu distances are in the range 3.261···3.492 Å (Fig. 85b) [136].

$[Mn_4(\mathbf{122c})(O)_2(CH_3COO)_5]$ was obtained only when $[Mn_3(O)(CH_3COO)_6(py)_3]\cdot py$ and H_3-**122c** were reacted in a 2:1 molar ratio under basic conditions in the presence of a pro-

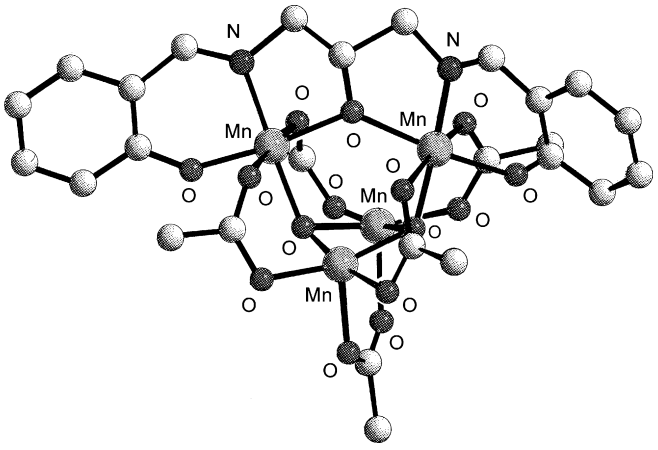

Fig. 86. Structure of $[Mn_4(\mathbf{122c})(O)_2(CH_3COO)_5]$.

tic solvent; no reaction was observed when the reaction was performed in dichloromethane. The same tetramanganese(III) complex results when $[Mn_{12}(O)_{12}(CH_3COO)_{16}(H_2O)_4]$ is treated in CH_3CN/CH_3OH with four equivalents of H_3-**122c** or when $[Mn_3(O)(CH_3COO)_6(py)_3]\cdot py$ was replaced with "manganese(III) acetate", a polymer of Mn_3 trinuclear units. The employment of $[Mn_3(O)(O_2CR)_6(py)_3]$ ($R = C_2H_5, C(CH_3)_3$) gave the corresponding complexes $[Mn_4(\mathbf{122c})(O)_2(RCOO)_5]$ [137].

$[Mn_4(\mathbf{122c})(O)_2(CH_3COO)_5]\cdot CH_3CN$ contains a $\{Mn_4O_2\}^{8+}$ core with peripheral ligation provided by five doubly-bridging acetate groups and one pentadentate ligand $[\mathbf{122c}]^{3-}$. The core has been described as derived from two triangular, oxide-bridged $\{Mn_3O\}$ units sharing an edge and thus giving a $\{Mn_4O_2\}$ butterfly-like core. Two five coordinate square pyramidal manganese(III) ions occupy the body positions of the butterfly while the other two six coordinate octahedral manganese(III) ions occupy the wingtip positions. There is a carboxylate group bridging each body-wingtip manganese pair, and a fifth carboxylate bridges the body-body manganese pair. $[\mathbf{122c}]^{3-}$ completes the peripheral ligation, chelating each wingtip manganese ion and bridging them by the central oxygen atom (Fig. 86). The structure of $[Mn_4(\mathbf{L})(O)_2(RCOO)]\cdot CH_3OH\cdot 2CH_2Cl_2\cdot C_7H_{16}$ ($R = C(CH_3)_3$) is the same except the difference in the carboxylate groups [137]. Two dominant antiferromagnetic ($J_1 = -86.3\,cm^{-1}$ and $J_2 = -47.32\,cm^{-1}$) and one minor ferromagnetic ($J_3 = 11.13\,cm^{-1}$) exchange pathways lead to a singlet magnetic ground state of $[Cu_4(\mathbf{122c})_2(3\text{-}ppz)_2]$. Also a weak antiferromagnetic intermolecular interaction operates ($J' = -0.765\,cm^{-1}$) [136]. Three intramolecular antiferromagnetic interactions between the manganese ions occurs in $[Mn_4(\mathbf{122c})(O)_2(RCOO)_5]$, the coupling constants being for $R = CH_3$ – 6.37 cm^{-1}, −5.72 cm^{-1} and −1.78 cm^{-1}; for $R = C_2H_5$ −7.64 cm^{-1}, −6.73 cm^{-1}, −2.49 cm^{-1}; and for $R = C(CH_3)_3$ −7.37 cm^{-1}, −6.57 cm^{-1} and −1.79 cm^{-1}. These complexes experience spin frustration effects observed within the Mn_4 butterfly core, giving an $S_T = 0$ ground state due to total domination of the spin alignments by the highest J value [137].

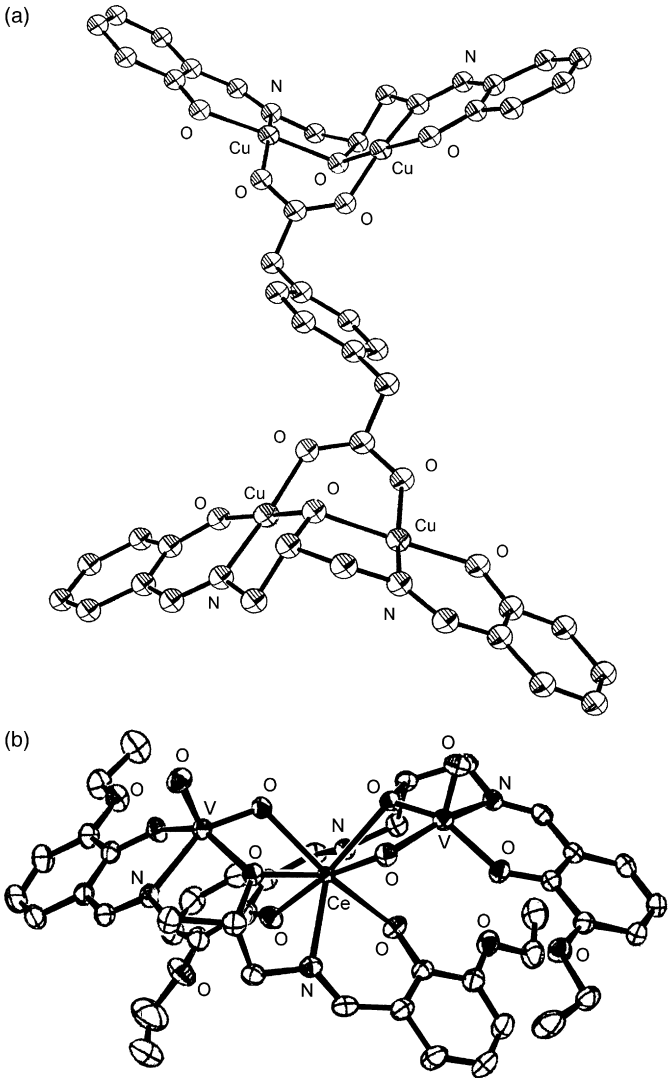

Fig. 87. Structure of $[Cu_4(\mathbf{122c})_2(\mu\text{-}OOCCH_2C_6H_4CH_2COO)]$ (a) and $[(VO_2)_2Ce(\mathbf{124c})_2]$ (b).

H_3-**124a**, H_3-**124b**, H_3-**124c**, synthesized by condensation of the appropriate substituted salicylaldehyde and 1,3-diamino-3-hydroxypropane, when mixed with $Cu(ClO_4)_2\cdot 6H_2O$ and the appropriate carboxylic or dicarboxylic acid in the presence of base, afford $[Cu_2(\mathbf{L})(\mu\text{-}HCOO)]$ or $[Cu_4(\mathbf{L})_2\{\mu\text{-}OOCCRCOO\}(DMF)_2]$ ($R = CH_2CH_2$, $C(CH_3)_2$, $CH_2C_6H_4CH_2$). $[Cu_2(\mathbf{124a})(\mu\text{-}HCOO)]$ and $[Cu_2(\mathbf{124b})(\mu\text{-}HCOO)]$ are essentially distorted square planar copper(II) dinuclear complexes, formed by one μ-alkoxo oxygen, one-μ-formate oxygen, one imine nitrogen and one phenoxo oxygen with Cu···Cu distances of 3.511 Å and 3.517 Å, respectively [138]. $[Cu_4(\mathbf{124a})_2\{\mu\text{-}OOC(CH_2)_2COO\}(DMF)_2]$ and $[Cu_4(\mathbf{124b})_2(\mu\text{-}OOC(CH_2)_2COO)(DMF)_2]$ contain two square pyramidal dinuclear metal centers, doubly bridged by the alkoxo oxygen of $[\mathbf{124a}]^{3-}$ or $[\mathbf{124b}]^{3-}$ and the dicarboxylato oxygen atoms ions of the fumarate anion [139,140].

$[Cu_4(\mathbf{122c})_2\{\mu\text{-}OOCRCOO\}]$ ($R = C(CH_3)_2$, $CH_2C_6H_4CH_2$) have been described as the stretching of the two μ-alkoxo square planar dinuclear units by the second

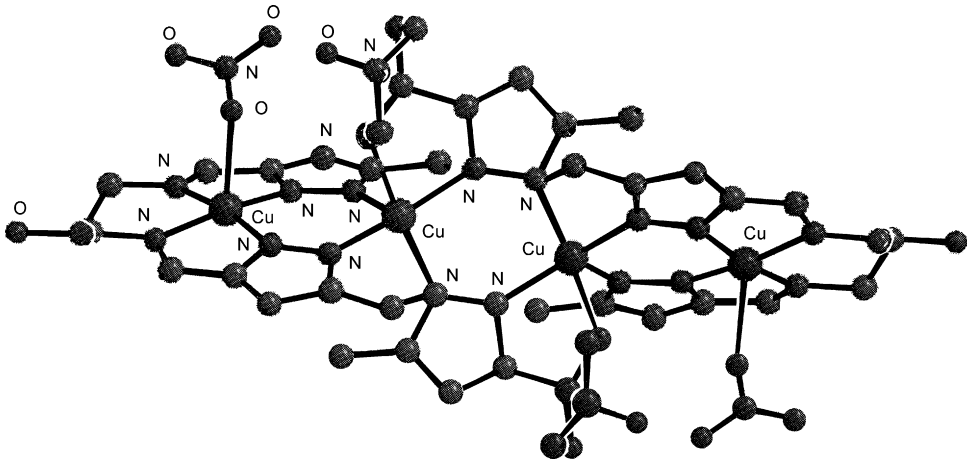

Fig. 88. Structure of $[Cu_4(H\text{-}\mathbf{125a})_2(H\text{-}\mathbf{125b})_2(NO_3)_2]$.

bridging dimethylmalonato or 1,4-phenylene-dicarboxylato ligands, respectively (Fig. 87a) [138].

The dinuclear copper(II) complexes are strong antiferromagnetically coupled ($-2J = 156$ and $152\,cm^{-1}$) while the tetranuclear copper(II) complexes, which can be considered composed of two dimers, show a strong intramolecular ferromagnetic interaction ($2J$ ranging from 54 to $155.2\,cm^{-1}$) and a weak interdimer interaction ($2J'$ ranging form -0.53 to $0.13\,cm^{-1}$, respectively) [138].

The oxidation reaction rate of 3,4-di-*tert*-butylcatechol to the corresponding quinone, catalyzed by these dinuclear and tetranuclear copper(II) complexes, follows the trend $[Cu_4(\mathbf{122c})_2(\mu\text{-}OOCCH_2C_6H_4CH_2COO)] > [Cu_4(\mathbf{122c})_2\{\mu\text{-}OOCC(CH_3)_2COO\}] > [Cu_2(\mathbf{124a})(\mu\text{-}HCOO)] > [Cu_2(\mathbf{124b})(\mu\text{-}HCOO)]$, which correlates to the averaged Cu(Cu distances in the complexes, respectively 3.081 Å for $[Cu_2(\mathbf{124a})(\mu\text{-}HCOO)] < 3.159$ Å for $[Cu_2(\mathbf{124b})(\mu\text{-}HCOO)] > 3.511$ Å for $[Cu_4(\mathbf{122c})_2\{\mu\text{-}OOCC(CH_3)_2COO)]$ and 3.517 Å for $[Cu_4(\mathbf{122c})_2(\mu\text{-}OOCCH_2C_6H_4CH_2COO)]$ [138].

$[(VO_2)_2Ce(\mathbf{124c})_2]$ and $[(VO_2)_2Ce(\mathbf{124d})_2]$ were prepared by the reaction of $[V^{IV}O(acac)_2]$ and $[Ce^{III}(acac)_3]\cdot 3H_2O$ with H_3-**124c** or H_3-**124d**, followed by oxidation of the product in air. $[(VO_2)_2Ce(\mathbf{124c})_2]$ was also obtained by the reaction in air of $[V^{IV}O(H\text{-}\mathbf{124c})]$ or $[V^{V}O_2(\mathbf{124c})]$ with $[Ce^{III}(acac)_3]\cdot 3H_2O$. $[VO(H\text{-}\mathbf{124c})]\cdot H_2O$ derives from the reaction of H_3-**124c** with $[V^{IV}O(acac)_2]$ under argon while the same reaction in air yields $[VO(\mathbf{124c})]\cdot CH_3CN$ where a distorted octahedral vanadium(V) ion occurs [138].

$[(VO_2)_2Ce(\mathbf{124c})_2]$ has a V^{V}–Ce^{IV}–V^{V} trinuclear structure with two dioxovanadium(V) moieties on each side of the cerium(IV) moiety. Two ligands $[\mathbf{124c}]^{3-}$ are bonded to the eight coordinate, square antiprismatic cerium ion. Basal oxo atoms of the five coordinate square pyramidal dioxovanadium moieties are linked to the cerium ion (Fig. 87b). The endo-structure is maintained in dimethylsulfoxide; on the contrary, a dimethylsulfoxide solution of $[(VO_2)_2Ce(\mathbf{124d})_2]$ complex contains a ≈1:1 mixture of the endo (C_2 symmetry) and exo (C_1 symmetry) isomers, with a structure different from that of $[(VO_2)_2Ce(\mathbf{124c})_2]$. Steric repulsions between the *tert*-butyl groups in $[\mathbf{124d}]^{3-}$ may cause the structural difference between the trinuclear complexes with $[\mathbf{124c}]^{3-}$ and $[\mathbf{124d}]^{3-}$ [138].

The voltammogram of $[(VO)_2Ce(\mathbf{124c})_2]$ in acetonitrile shows a quasi-reversible redox couple with $E_{1/2} = -0.60$ V versus Fc/Fc^+ while $[V^{V}O(\mathbf{124c})]$ shows a quasi-reversible V^{V}/V^{IV} redox couple with $E_{1/2} = -0.83$ V. The current peak values for the redox couple of $[(VO_2)_2Ce(\mathbf{124c})_2]$, about two times larger than those for the redox couple of $[V^{V}O(\mathbf{124c})]$, indicate, a two-electron redox reaction for $[(VO_2)_2Ce(\mathbf{124d})_2]$. The cyclic voltammogram of $[(VO_2)_2Ce(\mathbf{124c})_2]$ shows an irreversible redox couple with a reduction wave at -0.99 V and an oxidation wave at -0.41 V. Chemically reduced products of the trinuclear complexes with $[\mathbf{124c}]^{3-}$ and $[\mathbf{124d}]^{3}$ were prepared by the reaction of the complexes with equimolar amounts of ascorbic acid in methanol. Moreover the reduced complexes gradually oxidized to reform the starting complexes, respectively even in the solid state. IR spectrum suggests that the reduced species of $[(VO_2)_2Ce(\mathbf{124c})_2]$ is a hydroxo-bridged (V–OH–Ce) trinuclear complex with a V^{IV}–Ce^{IV}–V^{IV} trinuclear structure [138].

In $[Mn_2(\mathbf{124e})(\mu\text{-}OCH_3)(\mu\text{-}CH_3COO)(Br)(H_2O)]$ and $[Mn_2(\mathbf{124f})(\mu\text{-}OCH_3)(\mu\text{-}CH_3COO)(CH_3OH)_2]$ (Br), prepared by the reaction of H_3-**124e** or H_3-**124f** with

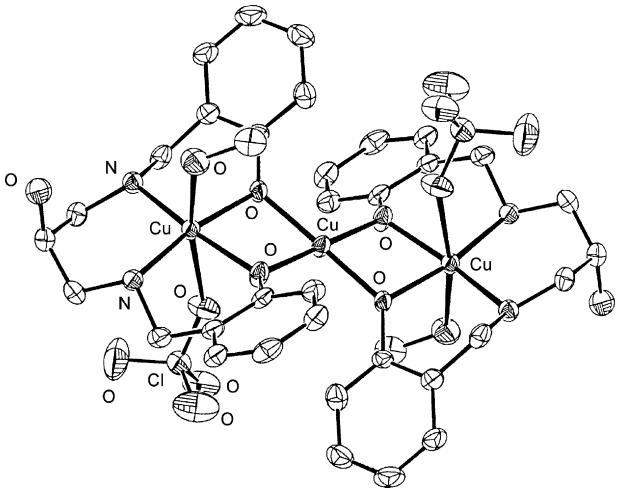

Fig. 89. Structure of $[Cu_3(H\text{-}\mathbf{126})_2(CH_3OH)_2(ClO_4)_2]$.

$Mn(CH_3COO)\cdot 2H_2O$ in the presence of an excess of NaBr, two six coordinate manganese(III) ions, 2.943 Å and 2.928 Å apart, are triply bridged by the central alcoholato oxygen of $[\mathbf{124e}]^{3-}$ and by exogenous *syn*,*syn*-acetato and methanolato ligands [140].

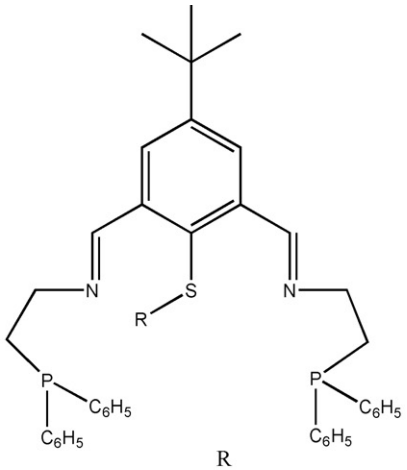

	R
120a	$C(CH_3)_3$
H-120b	H

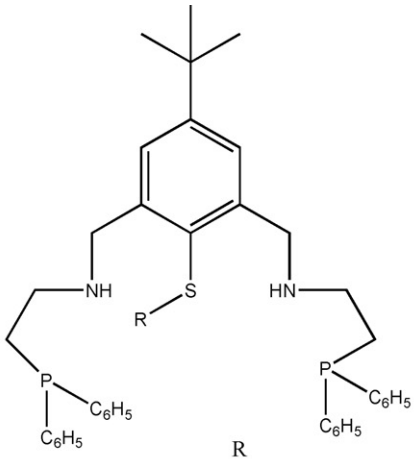

	R
121a	$C(CH_3)_3$
H-**121b**	H

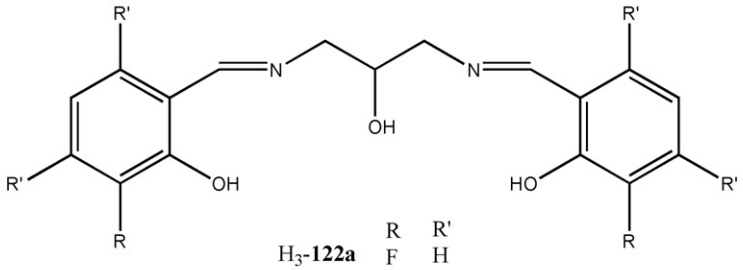

	R	R'
H_3-**122a**	F	H
H_3-**122b**	H	OCH_3
H_3-**122c**	H	H

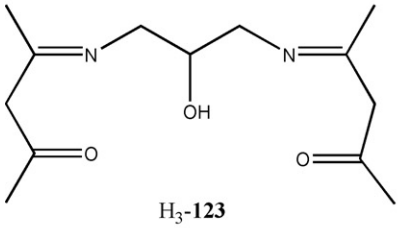

H_3-**123**

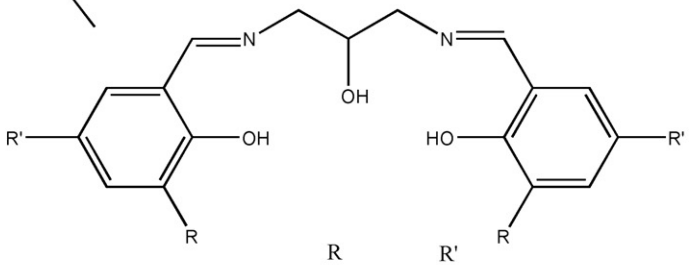

	R	R'
H_3-**124a**	H	Br
H_3-**124b**	H	Cl
H_3-**124c**	OC_2H_5	H
H_3-**124d**	$C(CH_3)_3$	$C(CH_3)_3$
H_3-**124e**	H	CH_3
H_3-**124f**	CH_3	H

The two metal ions are antiferromagnetic coupled ($J = -13.7\,cm^{-1}$ for $[Mn_2(\mathbf{124e})(\mu\text{-}OCH_3)(\mu\text{-}CH_3COO)(Br)(H_2O)]$ and $-15.1\,cm^{-1}$ for $[Mn_2(\mathbf{124f})(\mu\text{-}OCH_3)(\mu\text{-}CH_3COO)(CH_3OH)_2](Br)$. These complexes, which retain the solid structure upon dissolution as indicated by ESI-mass spectra, show catalytic activity toward disproportionation of H_2O_2, with first-order dependence on the catalyst, and saturation kinetics on $[H_2O_2]$, in methanol and dimethylformamide. In dimethylformamide, the two complexes are able to disproportionate at least 1500 eq. of H_2O_2 without significant decomposition, while in methanol they rapidly lose activity with formation of a non-coupled manganese(II) species. ESI mass spectrometry, EPR and UV/vis spectroscopy

suggest that the major active form of the catalyst occurs in the Mn_2^{II} oxidation state during cycling. In these complexes and in the analogous ones with other [**124**]$^{2-}$ derivatives the oxidation of the catalyst was assumed to be the rate-limiting step in the catalytic cycle. Formation of the catalyst-peroxide adduct is more sensitive to steric effects in dimethylformamide than in methanol. Overall, kinetics and spectroscopic studies of H_2O_2 dismutation by these complexes converge at a catalytic cycle that involves the Mn_2^{III} and Mn_2^{IV} oxidation states [140].

When two equivalents of 5-methyl-3-formylpyrazole and 1,3-diamino-2-propanol are condensed in the presence of one equivalent of $Cu(NO_3)_2$, [Cu_4(H-**125a**)$_2$(H-**125b**)$_2(NO_3)_2$] is isolated as the sole reaction product. The same reaction in the presence of a variety of copper(II) or nickel(II) salts affords [Cu(H_3-**125a**)(X)](X)·H_2O (X = Cl^-, Br^-), [Ni(H_3-**125a**)$(H_2O)_2$](X)$_2$ (X = ClO_4^-, NO_3^-, BF_4^- and [Ni(H_3-**125a**)(X)$_2$] (X = Cl^-, Br^-) [141]. H_3-**125a** acts as a tetradentate neutral donor in the mononuclear copper(II) and nickel(II) complexes, whereas in [Cu_4(H-**125a**)$_2$(H-**125b**)$_2(NO_3)_2$], [H-**125a**]^2 and [H-**125b**]$^-$ act as dinegative and uninegative, respectively. The square pyramidal copper(II) ions are 3.858(3.890 Å, apart (Fig. 88). Variable temperature magnetic susceptibility measurements for [Cu_4(H-**125a**)$_2$(H-**125b**)$_2(NO_3)_2$] are consistent with strong antiferromagnetic interactions between the copper(II) centers [141].

In [Cu_3(H-**126**)$_2(CH_3OH)_2(ClO_4)_2$], obtained by reaction of copper(II) perchlorate with H_3-**126**, i.e. the reduced amine of the Schiff base H_3-**122c**, the three copper(II) ions are in a linear array with a Cu(Cu distance of 2.986 Å. The two terminal copper(II) ions are axially elongated distorted octahedral while the central copper(II) ion is square planar (Fig. 89) [142]. H_3-**126** and copper(I) iodide in air form [Cu_3(H-**126**)$_2$(I)$_2(CH_3CN)_2$]·$2CH_3CN$. The two distorted octahedral terminal copper(II) ions are linked by two amine nitrogen atoms and two oxygen atoms of two [H-**126**]$^{2-}$ ligands in the equatorial plane and by a iodide and an acetonitrile in the axial sites. Each phenolate unit further bridges the central square planar copper(II) ion which is coordinate by four phenolate oxygen atoms. The Cu–Cu–Cu array is linear with a Cu···Cu distance of 2.974 Å [143]. A strong antiferromagnetic coupling, dominated by the interaction between adjacent copper(II) ions ($J = -511$ and $-473\ cm^{-1}$), was found in these complexes; the coupling constant between terminal copper(II) ion is negligible while the intermolecular coupling J' constant is $0.475\ cm^{-1}$ in the former complex [142,143].

Epichlorohydrin reacts with ethylenediamine in the presence of NaOH to form $H_2N(CH_2)_2NHCH_2CH(OH)CH_2NH(CH_2)_2NH_2$. This amine precursor by condensation with salicylaldehyde yields the related Schiff base, easily reduced to the potentially heptadentate polyamine H_3-**127** which reacts with nickel(II) salts to afford the structurally similar [Ni(H_2-**127**)(H_2O)](X)·nH_2O (X = ClO_4^-, $n = 3$; X = Cl^-, $n = 1$) where the slightly distorted octahedral nickel(II) ion is coordinated by an aqua oxygen atom and a [H_2-**127**]$^-$ ligand through four amine nitrogen atoms and one phenoxy oxygen atom [144]. Similarly, H_3-**127**·HCl reacts with $Co(CH_3COO)_2·4H_2O$ in the presence NaOH and $NaClO_4·H_2O$ or $Cu(ClO_4)_2·6H_2O$ and

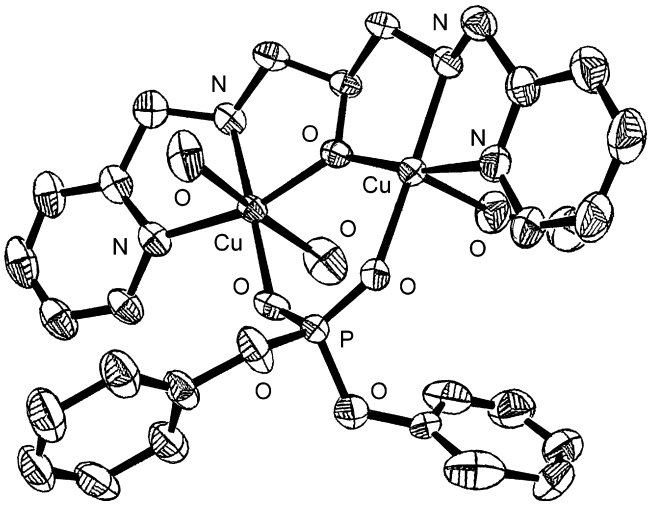

Fig. 90. Structure of [Cu_2(**128**)(dpph)$(CH_3OH)(ClO_4)_2$] (only the coordinate oxygen atoms, of the ClO_4^- groups are reported for clarity).

NaOH to form invariantly [Co(H-**127**)](ClO_4) or [Cu(H_3-**127**)(Cl)](ClO_4)·$CH_3OH·H_2O$. The cobalt(III) ion is in a distorted octahedral geometry, while the copper(II) center is coordinated by four nitrogen atoms in the equatorial plane and an axial protonated phenolic oxygen atom from a neutral H_3-**127** ligand [145].

$Cu(ClO_4)_2·6H_2O$ and [H_5-**128**]$(Cl)_4$, previously neutralized with NaOH, react in a 1:1 molar ratio to yield [Cu(H-**128**)$(ClO_4)_2$] with the copper(II) ion in an N_4O_2 coordination environment [146]. When the same reaction was carried out in a 2:1 molar ratio and in the presence of diphenylphosphate [dpph]$^-$, [Cu_2(**128**)(dpph)$(CH_3OH)(ClO_4)$](ClO_4) was obtained [146]. The two copper(II) centers, bridged by the endogenous μ-alkoxo oxygen atom and by the exogenous, μ-1,3-bridged phosphate group, have distinct geometries: one copper(II) ion has a distorted octahedral N_2O_4 coordination sphere while the other copper(II) ion is in a distorted square pyramidal N_2O_3 environment. The Cu···Cu distance is 3.499 Å (Fig. 90) [146].

Potentiometric studies in aqueous solution (I = 0.1$NaNO_3$, 298 K), show that for [Cu^{II}] ≤ [H-**128**], the mononuclear complex [Cu(H-**128**)]$^{2+}$ is the only species between pH 3 and 11. Between pH 6 and 8 in the presence of a twofold metal excess, leading to the formation of a dinuclear [Cu_2(**128**)]$^{3+}$ forms, which around pH 11 turns into [Cu_2(**128**)(OH)]$^{2+}$. The high stability and the spectroscopic parameters determined for the complex [Cu(H-**128**)]$^{2+}$ strongly suggest a N_4 coordination in the equatorial plane of the copper(II) ion, similar to that found in the X-ray structure of [Cu(H-**128**)]($ClO_4)_2$. In the presence of a metal excess, the formation of the dinuclear species causes a gradual decrease of the EPR signal intensity, due to the antiferromagnetically coupled copper(II) centers [145].

The binding of D-ribose, D-mannose, D-glucose, and D-maltose to structurally related mono- and dinuclear copper(II) complexes with H-**128** and [Cu(H-**129**)$(OH)_2$], deriving from the structurally closely related but sterically less demanding ligand H-**129**, was investigated in alkaline solution in order to

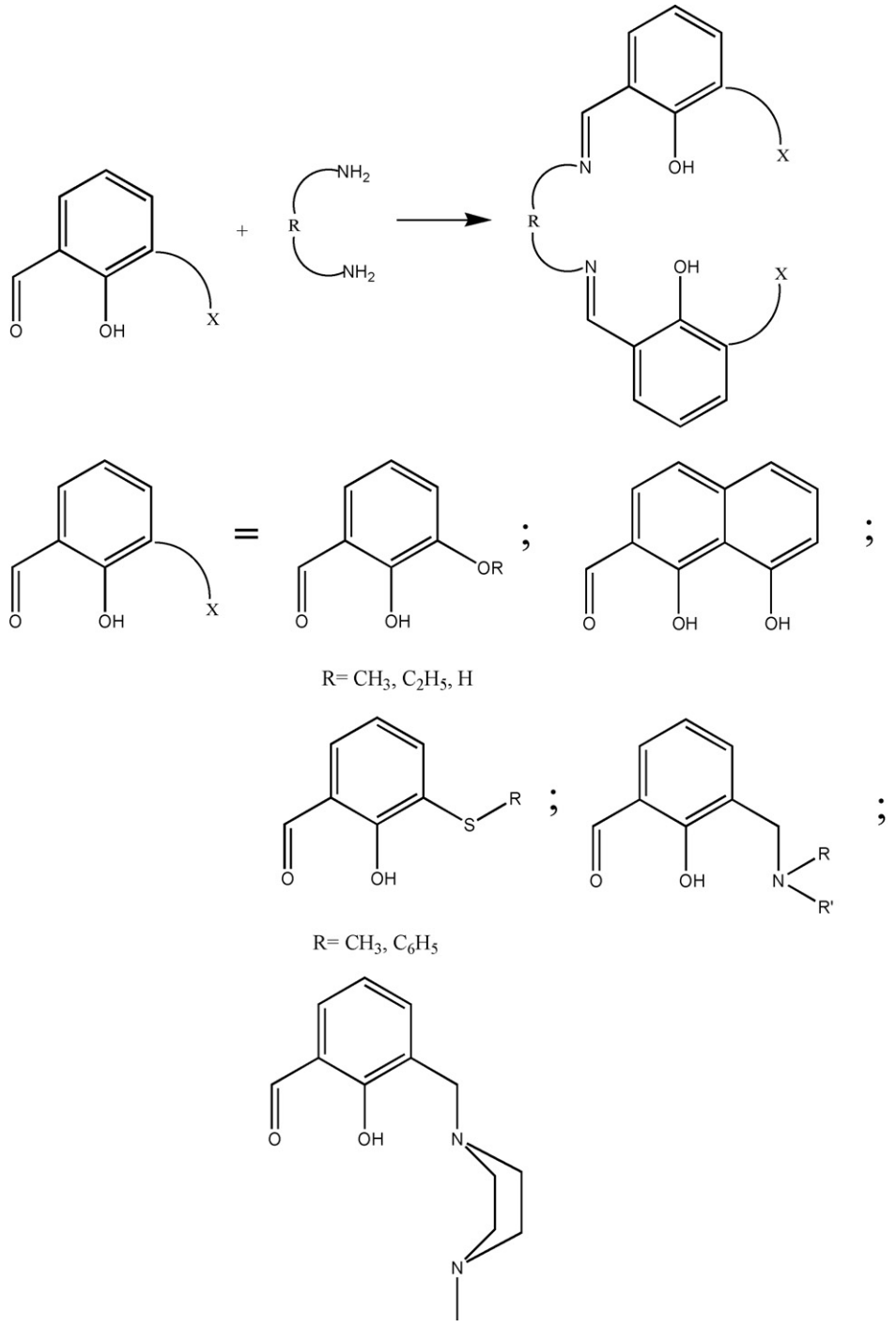

Scheme 6. Syntehsis of the [2 + 1] side-off ligands.

understand the role of the number of metal ions at the sugar binding site for carbohydrate-coordinating copper(II) complexes [146,147].

$[Cu_2(\mathbf{128})(OH)_2(H_2O)_2]^+$ is formed above pH 9 when a 2:1 molar ratio of copper(II) ions and H_2-**128** is provided, while the mononuclear complex $[Cu(H\text{-}\mathbf{128})(OH)_2]$ is formed in the presence of equimolar amounts of copper(II) ions and H-**128**. The structures proposed for the corresponding mono- and dinuclear copper(II) complexes at pH 12.40, which is used for carbohydrate coordination, are different in number of hydroxyl groups coordinated to the metal centers. A 1:1 complex occurs for all sugars investigated, independently from the metal complex used and the nature or amount of sugar applied. D-Ribose or D-mannose chelate $[Cu_2(\mathbf{128})(OH)_2(H_2O)_2]^+$ up to 1 order of magnitude stronger than $[Cu(H\text{-}\mathbf{128})(OH)_2]$ and $[Cu(H\text{-}\mathbf{129})(OH)_2]$. Both copper(II) centers in $[Cu_2(\mathbf{128})$(D-ribose)$]^+$ or $[Cu_2(\mathbf{128})$(D-mannose)$]^+$ will therefore participate in the sugar complexation. The opposite is true for coordination of D-glucose or glucose-derived disaccharide D-maltose. Here, the complex formation with the mononuclear complexes [Cu(H-

128)$(OH)_2$] or [Cu(H-**129**)$(OH)_2$] is up to 1 order of magnitude stronger than coordination to $[Cu_2(\mathbf{128})(OH)_2(H_2O)_2]^+$. The use of multinuclear instead of mononuclear copper(II) complexes is therefore not generally superior for coordination of any biologically interesting carbohydrate. Multipoint interactions are only favorable for carbohydrates that enable coordination by a *cis*,*cis*-triol, such as D-ribose or D-mannose while carbohydrates that chelate the metal complex with a *cis*-diol, such as D-mannose, enable strong coordination to mononuclear copper(II) complexes [Cu(H-**128**)$(OH)_2$] or [Cu(H-**129**)$(OH)_2$] only [147].

7. [2 + 1] Side-off systems

The [2 + 1] side-off ligands, which derive from the condensation of two equivalent of the designed formyl precursor with one equivalent of a primary diamine of the type H_2NRNH_2, generally contain an inner N_2O_2 and one adjacent outer O_2O_2, O_2S_2 or O_2N_4 coordination chamber, although more sophisticated chambers have been designed and the most relevant examples are reported in this section (Scheme 6). When reacted with d-transition metal ions, these ligands can form the related mononuclear complexes, where the metal ion generally resides into the inner N_2O_2 chamber, although, under appropriate conditions (i.e. solvent, temperature, etc.), a site migration was described especially with the copper(II) ion. These complexes easily coordinate a second equal or different metal ion in the outer chamber giving rise to the related homo- or heterodinuclear complexes [10,13,14,18].

The formyl precursors of Scheme 6, by reaction with metal salts may give rise to polynuclear complexes. For instance, H-**130** reacts with $Gd(NO_3)_3{\cdot}5H_2O$, in the presence of CsOH to form $[Gd_3(\mathbf{130})_3(OH)_2(NO_3)_2(H_2O)_4](NO_3)_2\ 4H_2O$, where the three gadolinium(III) ions are held together by a multiple bridging network supported by five oxygen atoms. Each of the two hydroxo ions simultaneously links to the three gadolinium ions which, otherwise, are linked two by two by monoatomic and tetratomic bridges afforded by the ligands $[\mathbf{130}]^-$. Two lanthanide ions achieve a nine coordination environment while the third metal ion is eight coordinate resorts. The intramolecular Gd···Gd distances are 3.559···3.573 Å while the intermolecular Gd···Gd distances vary from 8.188 to 9.734 Å (Fig. 91a). The gadolinium(III) ions are antiferromagnetically coupled [148].

Similarly, $[Dy_3(\mathbf{130})_3(\mu_3\text{-}OH)_2(Cl)_2(H_2O)_4][Dy_3(\mathbf{130})_3(\mu_3\text{-}OH)_2(Cl)(H_2O)_5](Cl)_5{\cdot}19H_2O$ and $[Dy_3(\mathbf{130})_3(\mu_3\text{-}OH)_2(Cl)(H_2O)_5](Cl)_3{\cdot}4H_2O{\cdot}2CH_3OH{\cdot}0.7CH_3CN$ have been prepared. The structure of the former complex consists of a triangle of dysprosium centers capped by two μ_3-hydroxo centers. Along each side of the triangle a $[\mathbf{130}]^-$ ligand bridges by its phenoxo groups. Aldehyde and methoxy groups also coordinate to the eight coordinate dysprosium centers (Fig. 91b). A hydrogen bonding network induces a chain formation with the concomitant π–π interactions [149].

$[Dy_3(\mathbf{130})_3(\mu_3\text{-}OH)_2(Cl)(H_2O)_5](Cl)_3{\cdot}4H_2O{\cdot}2CH_3OH{\cdot}0.7CH_3CN$ crystallizes to give solely the monochloride form of the dysprosium triangles observed in $[Dy_3(\mathbf{130})_3(\mu_3\text{-}OH)_2(Cl)_2(H_2O)_4][Dy_3(\mathbf{130})_3(\mu_3\text{-}OH)_2(Cl)(H_2O)_5](Cl)_5{\cdot}19H_2O$ [149].

These complexes show a very unusual vanishing susceptibility at low temperature, which is unprecedented in systems comprising an odd number of unpaired electrons. In spite of the almost non-magnetic ground state, features typical of single magnet molecular behavior are observed for the thermally populated excited state, suggesting that a resonant under-barrier relaxation process is also active. This observation is strongly relevant to molecular nanomagnetism because the presence of a large spin ground state appears not to be a necessary condition to observe slow relaxation of the magnetization [149].

$LnCl_3{\cdot}6H_2O$ (Ln = Tb, Er) and H-**131a** form the isostructural trinuclear complexes $[Ln_3(\mathbf{131a})_3(\mu_3\text{-}OH)_2(Cl)_3(CH_3OH)_3](Cl){\cdot}3CH_3OH$. In the terbium complex the three ligands $[\mathbf{131a}]^-$ all exhibit the same coordination mode and the average Tb···Tb distance is 3.501 Å (Fig. 91c). The central cores of these complexes are similar to the Gd_3 nitrate or chloride complexes above reported [150].

H-**131a**, $TbCl_3{\cdot}6H_2O$ and $Zn(CH_3COO)_2{\cdot}2H_2O$, afford $[Tb_{10}(\mathbf{131a})_6(\mathbf{131b})_2(\mu_3\text{-}OH)_8(\mu_2\text{-}CH_3COO)_4(\mu_3\text{-}CH_3COO)_2(Cl)_4(CH_3OH)_2(H_2O)_2](Cl)_2{\cdot}2CH_3OH$ where $[\mathbf{131}]^-$ turns partially into the hemiacetal $[\mathbf{131b}]^{2-}$. The two halves of the slipped sandwiched structure comprise a roughly planar set of four terbium(III) ions, with an average Tb···Tb distance of 3.818 Å, with a fifth terbium(III) ion at the center considerably displaced from the Tb_4 plane. The two crystallographically equivalent halves of the molecule are connected in an offset manner by two μ_3-OH groups as well as two oxygen atoms of the hemiacetal ligands $[\mathbf{131b}]^{2-}$ ligands. The other methoxide oxygen atoms of the hemiacetal are simply bound in a terminal η^1 manner. $[\mathbf{131a}]^-$ exhibits two different coordination modes (μ_2 or μ_3) with the aldehyde oxygen atom binding in either a η^1 or η^2 fashion. The coordination environments of the terbium(III) ions are completed by four μ_2-CH_3COO^-, two μ_3-CH_3COO^-, eight μ_3-OH^-, four Cl^-, two H_2O and two methanol units. Six terbium(III) ions are eight coordinate and the remaining four are nine coordinate (Fig. 92a) [150].

On the contrary, H-**131a**, $Eu(NO_3)_3{\cdot}6H_2O$ and $Zn(CH_3COO)_2{\cdot}2H_2O$ give $[Zn_4Eu_2(\mathbf{131a})_4(CH_3COO)_6(NO_3)_2(OH)_2]{\cdot}(C_2H_5)_2O$ where two equivalent Zn_2Eu moieties are linked by four bidentate acetate groups. Each Zn_2Eu unit bears two $[\mathbf{131a}]^-$ groups which bridge each Eu–Zn edge. The two zinc ions are bridged by a single acetate group and are separated by 3.364 Å. Each Zn_2Eu unit is capped by a μ_3-OH group. The two unique five coordinate zinc ions have a different geometry: one has a distorted square based pyramidal geometry while the other is distorted trigonal bipyramidal (Fig. 92b). The supramolecular framework of this complex generates extended channels filled by guest molecules (as diethyl ether) which can be removed under vacuum. This reversible encapsulation was successfully studied using a quartz crystal microbalance (QCM). The Zn_4Eu_2 complex is stable in acetonitrile solution where it maintains the same structure found in the solid state. Photophysical investigations indicate

that energy transfer from the deprotonated salicylaldehyde ligands to the europium(III) ions takes place [150].

The condensation of 2-formyl-1,8-naphtalenediol with $H_2N(CH_2)_3NH_2$ forms H_4-**132**, which is in a zwitterionic form with two hydrogen atoms close to the imine nitrogen atoms and two to the external phenolic oxygen atoms both in the solid state and in solution [150]. The reaction of H_4-**132** with one or more equivalents of $Cu(CH_3COO)_2{\cdot}2H_2O$ gives rise to [Cu(H_2-**132**)] or [Cu_2(**132**)], respectively. In the mononuclear complex, the copper(II) ion lies on the N_2O_2 compartment. In dichloromethane this complex exhibits an electrochemically quasi-reversible one-electron transfer wave corresponding to reduction process $Cu^{II} \rightarrow Cu^{I}$. In [$Cu_2$(**132**)], one square planar copper(II) ion lies in the inner N_2O_2 compartment, as in the related mononuclear complex, while the other copper(II) ion occupies the outer O_2O_2. The two metal ions are bridged by two aryloxide functions. Two [Cu_2(**132**)] complexes dimerize by weak apical copper aryloxide interactions to a tetranuclear entity, this resulting in an overall square pyramidal coordination environment for each copper center (Fig. 93a) [150,151].

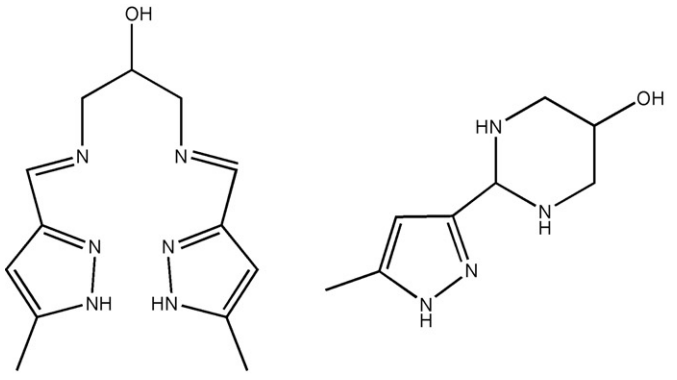

H_3-**125a**

H_2-**125b**

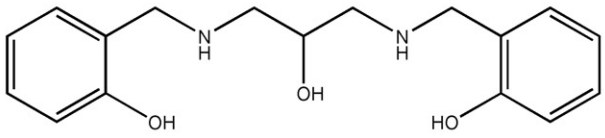

H_3-**126**

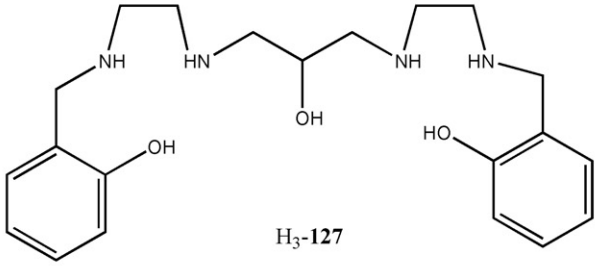

H_3-**127**

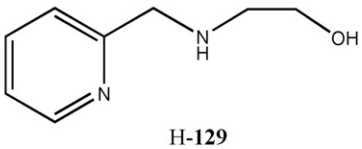

H-**129**

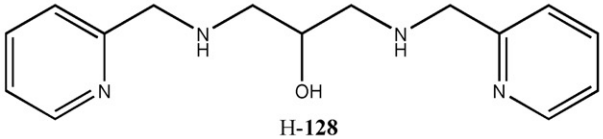

H-**128**

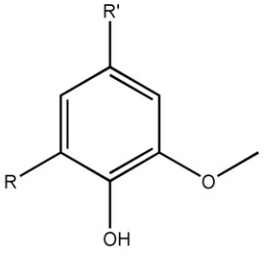

	R	R'
H-**130**	CHO	H
H-**131a**	CHO	Br
H_2-**131b**	$CH(OH)OCH_3$	Br

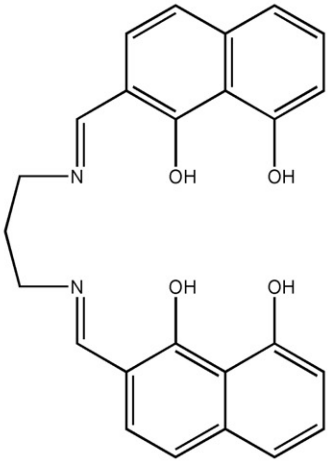

H_4-**132**

[Cu(H_2-**132**)] reacts with [VO(acac)$_2$] to form [CuVO(**132**)], where the N_2O_2 compartment is occupied by the copper(II) ion and the O_2O_2 compartment hosts the vanadyl(IV) ion. Again, two dinuclear complexes dimerize by weak apical copper-aryl oxide interactions to a tetranuclear entity. The vanadyl(IV) oxygen atoms are not involved in this dimerization. The Cu···V distance is 3.089 Å (Fig. 93b) [152].

Temperature dependent magnetic susceptibility measurements established a strong intradimer exchange coupling ($J = -371\ cm^{-1}$) for [Cu_2(**132**)] [150,151] and a ferromagnetic interaction in [CuVO(**132**)] [150,151]. The interdimer interaction is ferromagnetic in both complexes: $J = +45.6\ cm^{-1}$ for the Cu_2 complex and $J = 0.55\ cm^{-1}$ for the CuVO one [152].

Under specific experimental conditions, the above [2 + 1] condensation reaction does not give the expected side-off ligand but follows an unexpected pathway. The reaction of H-**131a** with 1,2-diaminobenzene or 1,2-diamino-4,5-dimethoxybenzene in a 2:1 molar ratio and in ethanol at room temperature gives the designed bright red Schiff bases H_2-**133** and H_2-**134**, respectively. However, when this reaction is carried out under reflux, the colorless benzoimidazole derivatives H_2-**135** and H_2-**136** are produced, as confirmed by the X-ray structure of H_2-**135** [153].

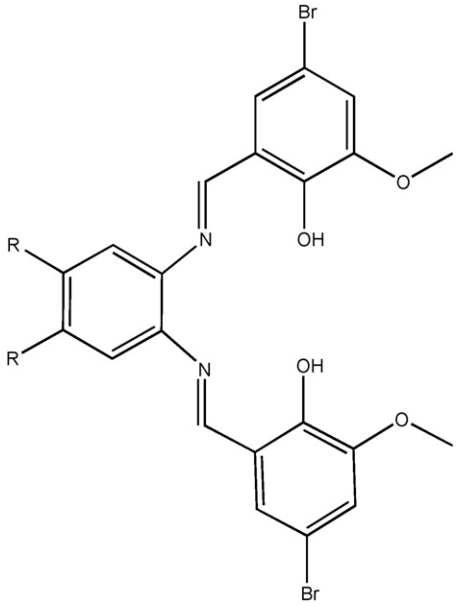

	R
H_2-**133**	H
H_2-**134**	OCH_3

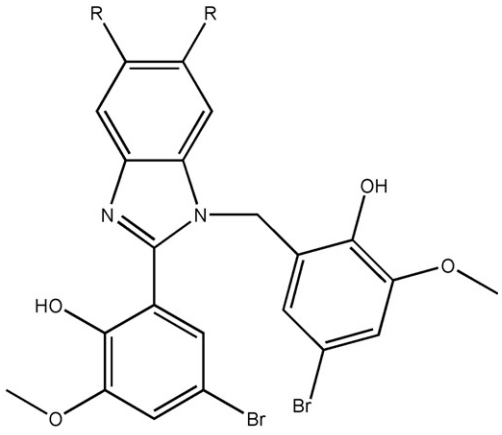

	R
H_2-**135**	H
H_2-**136**	OCH_3

A mixing of H_2-**135** or H_2-**136** with $Cu(CH_3COO)_2$ and $Ln(NO_3)_3{\cdot}6H_2O$ produces the isomorphous complexes [CuLn(H-**135**)$_2$$(NO_3)_3(CH_3CN)_2]{\cdot}2(C_2H_5)_2O$ (Ln = Eu, Tb, Er, Yb) or [CuNd(H-**136**)$_2$$(NO_3)_3(CH_3CN)_2]{\cdot}(C_2H_5)_2O$. The CuEu complex (Fig. 94) features a N_4O_2 pseudo-octahedral copper(II) and a O_{10} ten coordinate europium(III)) ions, linked by two [H-**135**]$^-$ ligands, whose deprotonated phenolic groups bridge both metal ions. The coordination about the copper(II) and the europium(III) ions is completed by two, axially weakly bonded acetonitrile molecules and by six oxygen atoms from the three bidentate nitrates, respectively (Fig. 94) [153].

As mentioned above, the complexation reactions of the [2 + 1] side-off ligands are generally carried out using a 1:1 (or 1:2) ligand:metal salt ratio; the employment of larger amounts of metal salts can originate polynuclear complexes. H_2-**137**, H_2-**138** and H_2-**139** react with a threefold excess of cadmium(II) acetate, to give the overall neutral cage-like tetranuclear structure [Cd_4(**L**)$_2$$(CH_3COO)_4$], where the cadmium(II) ions are seven coordinate. The two phenolate oxygen atoms of [**L**]$^{2-}$ behave as a μ_3-bridging ligand toward three cadmium(II) ions. Two cadmium ions are further linked to the third cadmium ion by two bridging acetate ligands. The Cd···Cd distances are in the range of 3.555–5.907 Å (Fig. 95) [154].

These complexes behave as electrolytes in methanol owing to the dissociation of one or more of the coordinated acetate ligands and as non-electrolytes in chloroform. Time-resolved spectra and lifetime measurements showed that both ligand-centered singlet (^{1}LC) and triplet (^{3}LC) emissions coexist only at 77 K, with the shoulder being the ^{1}LC fluorescence ($\tau = 3.4$–6.0 ns) and the main peak in the lower energy regime being the ^{3}LC phosphorescence ($\tau = 10.9$–44.2 ms). Comparing the relative intensity of the ^{1}LC with ^{3}LC emission at 77 K, the intersystem crossing efficiency follows the order [Cd_4(**139**)$_2$$(CH_3COO)_4$]>[$Cd_4$(**138**)$_2$$(CH_3COO)_4$]>[$Cd_4$(**137**)$_2$$(CH_3COO)_4$]. On the other hand, the ^{1}LC emission quantum efficiency is in the order [Cd_4(**137**)$_2$$(CH_3COO)_4$] > [$Cd_4$(**138**)$_2$$(CH_3COO)_4$] > [$Cd_4$(**139**)$_2$$(CH_3COO)_4$], which shows that an increase in conjugation or the presence of a heavy bromine substituent can enhance the ISC efficiency, and thus effectively suppress the ^{1}LC emission [154].

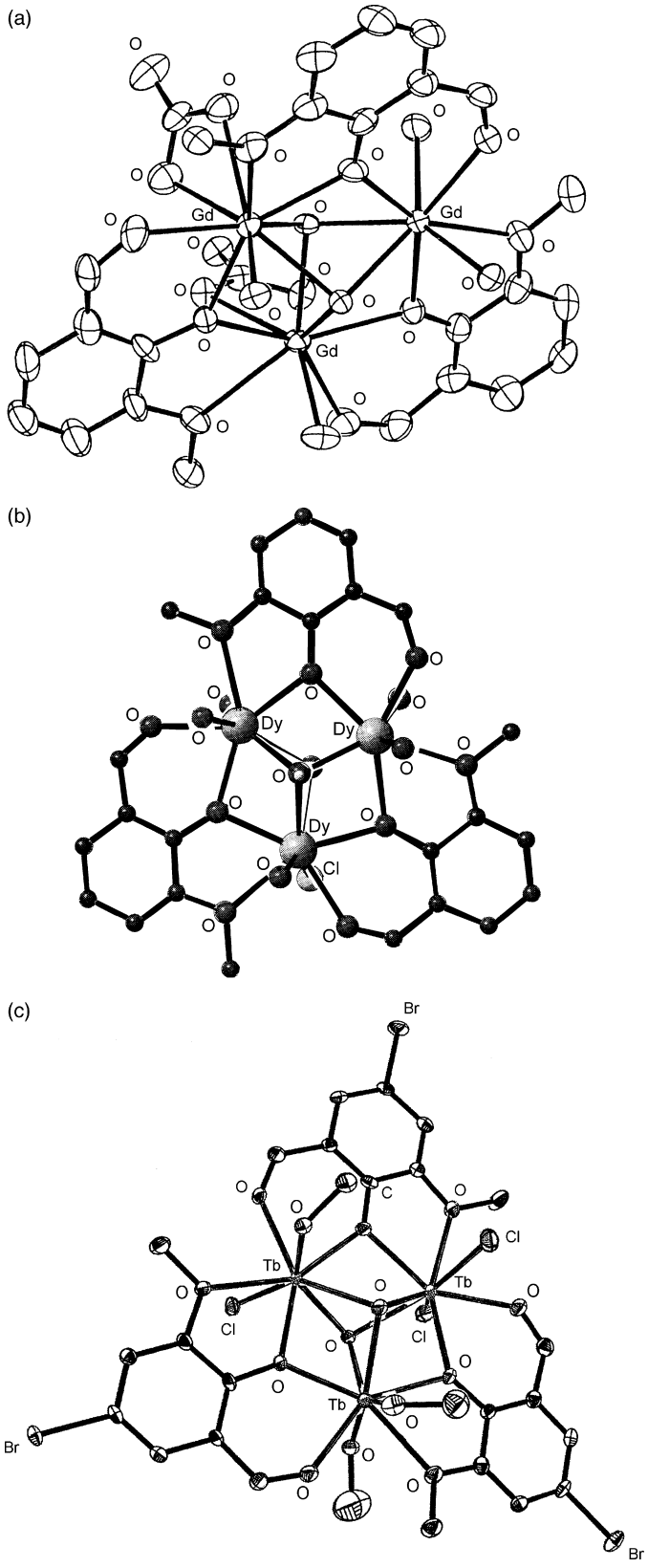

Fig. 91. Structure of $[Gd_3(\mathbf{130})_3(OH)_2(NO_3)_2(H_2O)_4]^{2+}$ (a), $[Dy_3(\mathbf{130})_3(\mu_3\text{-}OH)_2(Cl)(H_2O)_5]^{3+}$ (b) and $[Tb_3(\mathbf{131a})_3(\mu\text{-}OH)_2(Cl)_3(CH_3OH)_3]^{+}$ (c).

Reaction of H_2-**138a** with $Zn(NO_3)_2{\cdot}6H_2O$ afforded $[Zn_3(\mathbf{138a})_2(NO_3)_2]{\cdot}CH_3OH$. Two distorted square pyramidal zinc ions are located in the inner N_2O_2 cavities of the two significantly curved Schiff base ligands. The third central zinc ion is pseudo-octahedral. The adjacent Zn···Zn distances are 3.170 Å and 3.200 Å, respectively (Fig. 96) [155].

Larger metal ions as lanthanide(III) ions cannot be accommodated inside the coordination chambers of these ligands, i.e. of H_2-**137** or H_2-**140**. In the resulting complexes the metal ion is pushed out of the coordination plane of the ligand, giving rise to sandwiched or polymeric species. A mixture of equimolar amounts of $Ln(NO_3)_3{\cdot}6H_2O$ (Ln = La, Pr) and H_2-**137** yields $[Ln(H_2\text{-}\mathbf{137})(NO_3)_3(H_2O)]$, where the lanthanide ion is nine coordinate. The Schiff base is in a neutral zwitterionic form. Addition of triethylamine turns $[Pr(H_2\text{-}\mathbf{137})(NO_3)_3(H_2O)]$ into $[Pr(\mathbf{137})(NO_3)(H_2O)(CH_3OH)]$ where the eight coordinate praseodymium(III) ion binds the four N_2O_2 donors of the Schiff base ligand. Two molecules of H_2-**137** and one of $Ln(NO_3)_3$ in the presence of CsOH leads to the sandwich-like complexes $Cs[Ln(\mathbf{137})_2]$ with the lanthanide(III) ion linked to two deprotonated ligands. Addition of $Pr(NO_3)_3$ to $Cs[Pr(\mathbf{137})_2]$ afford $[Pr(\mathbf{137})(NO_3)(H_2O)(CH_3OH)]$ [156].

In the trimetallic tetra-decker complex $[Tb_3(\mathbf{140})_4(H_2O)_2](Cl)$, derived from the reaction of H_2-**140** with $TbCl_3{\cdot}6H_2O$, the two outer nine coordinate terbium(III) ions have similar environments comprising the N_2O_2 donor set of the outer $[\mathbf{140}]^{2-}$ group, the O_2O_2 set of one inner $[\mathbf{140}]^{2-}$ group and one water oxygen. The central eight coordinate terbium(III) ion has a square antiprismatic geometry, formed by the two N_2O_2 donor sets of the internal $[\mathbf{140}]^{2-}$ ligands. The phenolic oxygen atoms of the interior $[\mathbf{140}]^{2-}$ group are bridging, while those of the outer $[\mathbf{140}]^{2-}$ group are monodentate. The Tb··Tb separations are 3.884 and 3.872 Å [157].

When the reaction of $TbCl_3{\cdot}6H_2O$ with H_2-**140** is carried out in the presence of $Zn(CH_3COO)_2{\cdot}2H_2O$, the triple-decker complex $[Tb_3(\mathbf{140})_3(CH_3COO)_2(Cl)]$ is produced, where two acetate groups are able to coordinate effectively to one terbium(III) ion, preventing coordination of the fourth $[\mathbf{140}]^{2-}$ ligand (Fig. 97) [157].

Molar conductivity and NMR studies indicate that in acetonitrile $[Tb_3(\mathbf{140})_4(H_2O)_2](Cl)$ and $[Tb_3(\mathbf{140})_3(CH_3COO)_2(Cl)]$ are stable and 1:1 electrolyte and neutral, respectively, in agreement with the solid-state structures. A slow decomposition takes place in CD_3OD. Both $[Tb_3(\mathbf{140})_4(H_2O)_2](Cl)$ and $[Tb_3(\mathbf{140})_3(CH_3COO)_2(Cl)]$ exhibit green luminescence in the solid state. In solution the strong absorption bands of the free ligand H_2-**140** are all red-shifted on metal ion coordination. Excitation of the ligand-centered absorption bands of both $[Tb_3(\mathbf{140})_4(H_2O)_2](Cl)$ and $[Tb_3(\mathbf{140})_3(CH_3COO)_2(Cl)]$ produces the typical emission bands of the terbium(III) ion ($^5D_4 \rightarrow {}^7F_n$ transitions), while the ligand-centered π–π* emission was not detected. The fluorescence quantum yields (Φ_{em}) of $[Tb_3(\mathbf{140})_4(H_2O)_2](Cl)$, slightly lower than that of $[Tb_3(\mathbf{140})_3(CH_3COO)_2(Cl)]$ in CH_3CN, 0.153 and 0.181, respectively, is probably due to the coordination of two water molecules which can quench lanthanide luminescence.

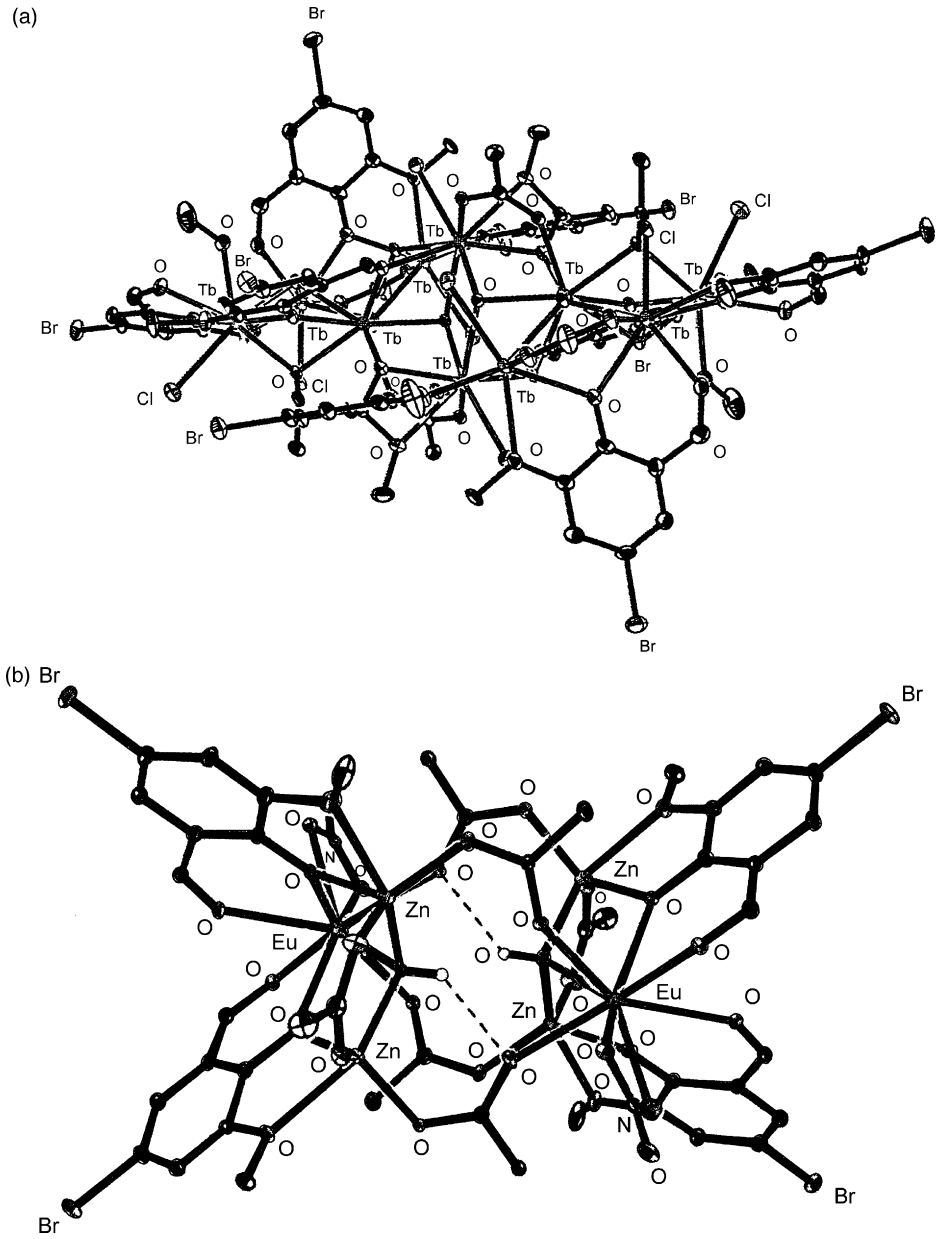

Fig. 92. Structure of $[Tb_{10}(\mathbf{131a})_6(\mathbf{131b})_2(OH)_8(CH_3COO)_6(Cl)_4(CH_3OH)_2(H_2O)_2]^{2+}$ (a) and $[Zn_4Eu_2(\mathbf{131a})_4(CH_3COO)_6(NO_3)_2(OH)_2]$ (b).

The emission intensities of both $[Tb_3(\mathbf{140})_4(H_2O)_2](Cl)$ and $[Tb_3(\mathbf{140})_3(CH_3COO)_2(Cl)]$ in CH_3CN are much higher than those in CH_3OH, where some decomposition occurs (as proved by the NMR data). The absence of typical terbium(III) ion excitation bands in the excitation spectra and the ligand-centered luminescence in the emission spectra of the $[Tb_3(\mathbf{140})_4(H_2O)_2]Cl$ and $[Tb_3(\mathbf{140})_3(CH_3COO)_2(Cl)]$ indicates that the ligand-to-metal energy transfer takes place efficiently [157].

Transmetalation reaction of a d-metal(II) ion by the larger uranium(IV) ion was also observed; $[Zn(H_2\text{-}\mathbf{141})]$, synthesized by the reaction of H_4-**141** with $Zn(acac)_2$ [157], reacts with UCl_4 in pyridine in the presence of traces of O_2 and/or H_2O to form $(PyH)_2[U_8(\mathbf{141})_4(Cl)_{10}(O)_4]$ where $[U_8(\mathbf{141})_4(Cl)_{10}(O)_4]^{2-}$ is built up of four $\{U_2(\mathbf{141})(Cl)_2(O)\}$ subunits, held together by eight μ_2-phenoxo bridges, four μ_4-oxo bridges and two additional μ_2-chloro bridges (Fig. 98) [158].

This transmetalation reaction does not take place when the appropriate lead(II) salt reacts with [M(**137**)] (M=Cu^{II} or Ni^{II}); on the contrary, $[Cu_2Pb(\mathbf{137})_2(H\text{-sal})_2]$, $[Cu_2Pb(\mathbf{137})_2(NO_3)](NO_3)$, $[CuPb(\mathbf{137})(CH_3COO)_2]$ and $[Ni_2Pb(\mathbf{137})_2(CH_3COO)](CH_3COO)$ occur. In $[Cu_2Pb(\mathbf{137})_2(H\text{-sal})_2]$, the six coordinate lead ion adopts a distorted octahedral geometry in which four of these sites are occupied by the two {Cu(**137**)} ligands and two by the salicylate $[sal]^-$ ligands, *trans* to one another, which also bridge the two five coordinate copper(II) ions. In $[Cu_2Pb(\mathbf{137})_2(NO_3)](NO_3)$ and $[Ni_2Pb(\mathbf{137})_2(CH_3COO)](CH_3COO)$ one monodentate nitrate and one bidentate acetate group, respectively, coordinates to the lead(II) ion which is distorted square pyramidal

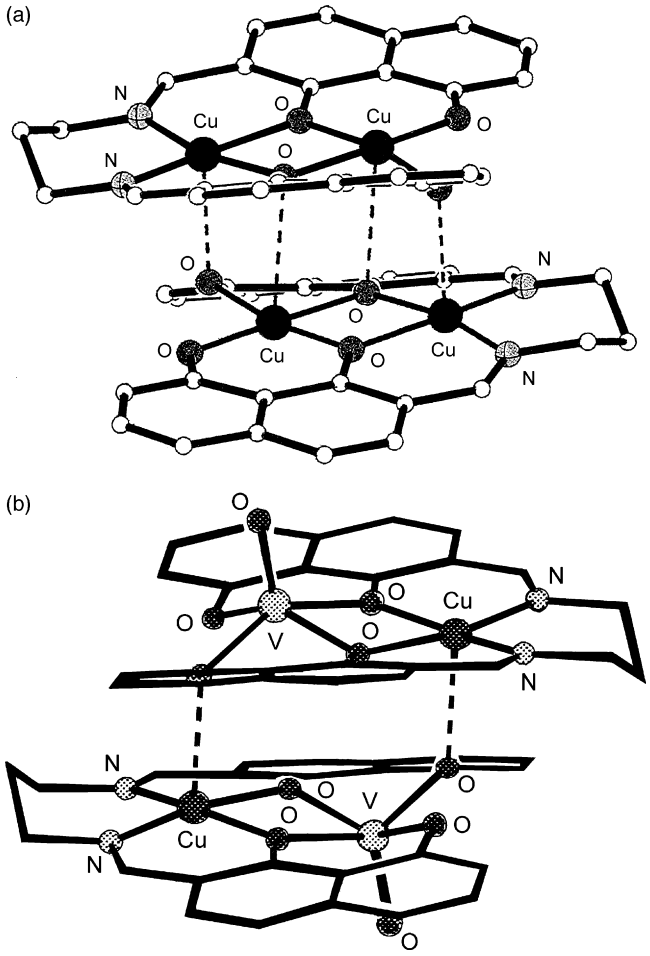

Fig. 93. Structure of $[Cu_2(\mathbf{132})]_2$ (a) and $[CuVO(\mathbf{132})]_2$ (b).

in the former complex and distorted trigonal pyramidal in the latter one. The copper centers in $[Cu_2Pb(\mathbf{137})_2(NO_3)](NO_3)$ adopt strictly four coordinate, square planar geometries. In $[Ni_2Pb(\mathbf{137})_2(CH_3COO)](CH_3COO)$ short intermolecular Ni···Ni distances occur (3.497 Å) (Fig. 99a and b) [159]. In $[CuPb(\mathbf{137})(CH_3COO)_2]$ the $\{Cu(\mathbf{137})\}$ unit acts as a monodentate ligand towards the lead(II) ion giving rise to a

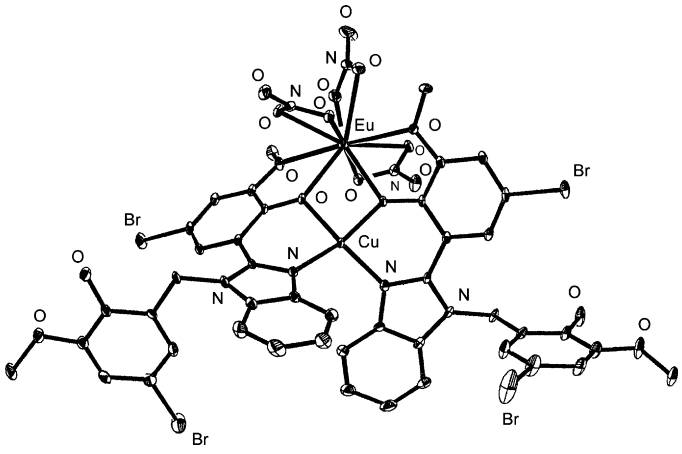

Fig. 94. Structure of $[CuEu(H\text{-}\mathbf{135})_2(NO_3)_3]$ (the two weakly bonded acetonitrile molecules are omitted for clarity).

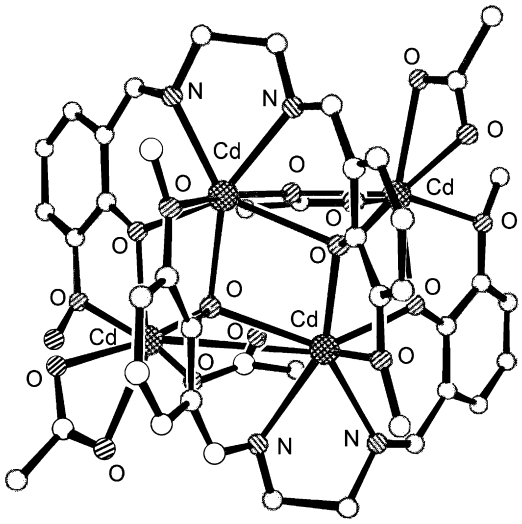

Fig. 95. Structure of $[Cd_4(\mathbf{137})_2(CH_3COO)_4]$.

lead coordination environment intermediate between a distorted tetrahedron and a distorted trigonal bipyramid (Fig. 99c) [159].

$[CuLn(\mathbf{L})(NO_3)_3(CH_3COCH_3)]$ (Ln=Ce, Nd, Gd, Dy; H_2-**L** = H_2-**137**, H_2-**142**, H_2-**143**) show closely related structures [160]. In a typical system $[CuDy(\mathbf{137})(NO_3)_3(CH_3COCH_3)]$ was prepared by a step-by-step procedure: condensation of H-**130** with ethylenediamine in the presence of $Cu(CH_3COO)_2{\cdot}H_2O$ gives $[Cu(\mathbf{137})]$ which, by further reaction with $Dy(NO_3)_3{\cdot}6H_2O$ in acetone affords $[CuDy(\mathbf{137})(NO_3)_3(CH_3COCH_3)]$, where the slightly distorted square pyramidal copper(II) and dysprosium(III) ions, 3.461 Å apart, are bridged by the phenolate oxygen atoms. The shortest interunit contacts, Dy···Cu = 8.06 Å, Dy···Dy = 9.88 Å, Cu···Cu = 10.63 Å, preclude any significant intermolecular magnetic interaction (Fig. 100) [160]. A similar structure was obtained also for $[CuGd(\mathbf{142})(NO_3)_3(H_2O)]$, where one water molecule, instead of acetone, fills the fifth axial coordination of the copper(II) ion [161].

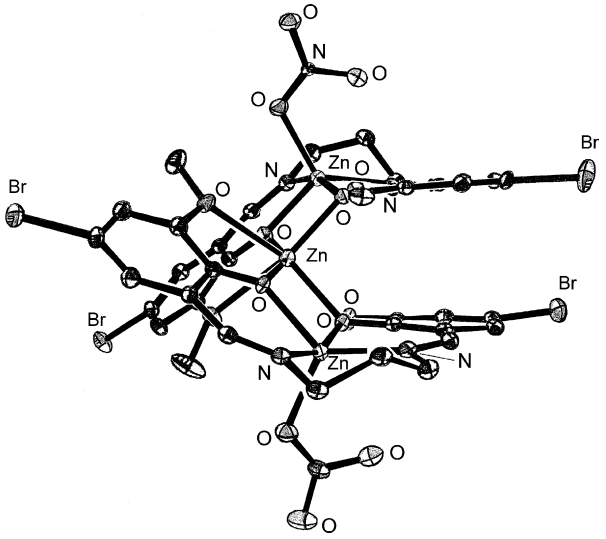

Fig. 96. Structure of $[Zn_3(\mathbf{138a})_2(NO_3)_2]$.

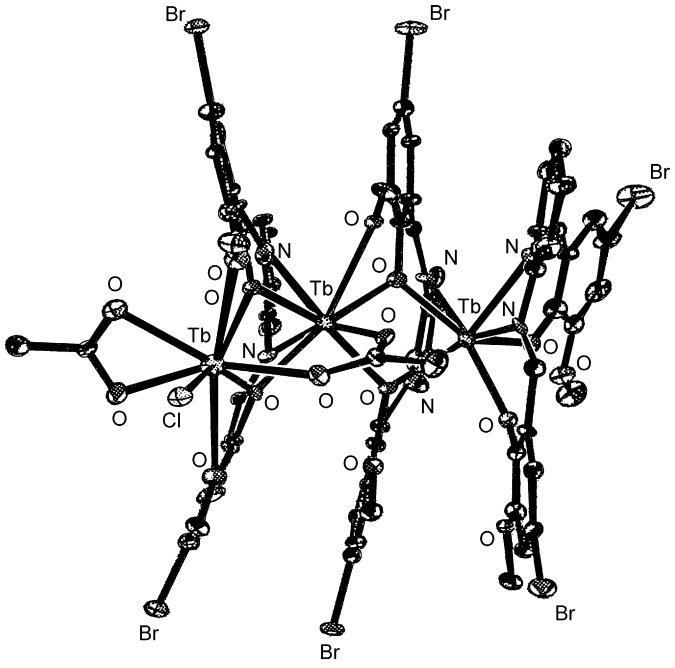

Fig. 97. Structure of $[Tb_3(\mathbf{140})_3(CH_3COO)_2(Cl)]$.

The reaction of H-**131a** with 4-methylphenylboronic acid affords the formyl precursor 5-(4′-methylphenyl)-3-methoxysalicylaldehyde, which condenses with ethylenediamine to yield H_2-**139**. [Zn(**139**)], derived from H_2-**139** and $Zn(CH_3COO)_2{\cdot}2H_2O$, gives $[ZnLn(\mathbf{139})(NO_3)_3(H_2O)_n]$ (Ln = La, Nd, Gd, Er or Yb; n = 1 or 2) by addition of $Ln(NO_3)_3$ [162]. The five coordinate zinc(II) ion, located in the inner N_2O_2 cavity, adopts a distorted square pyramidal geometry with an

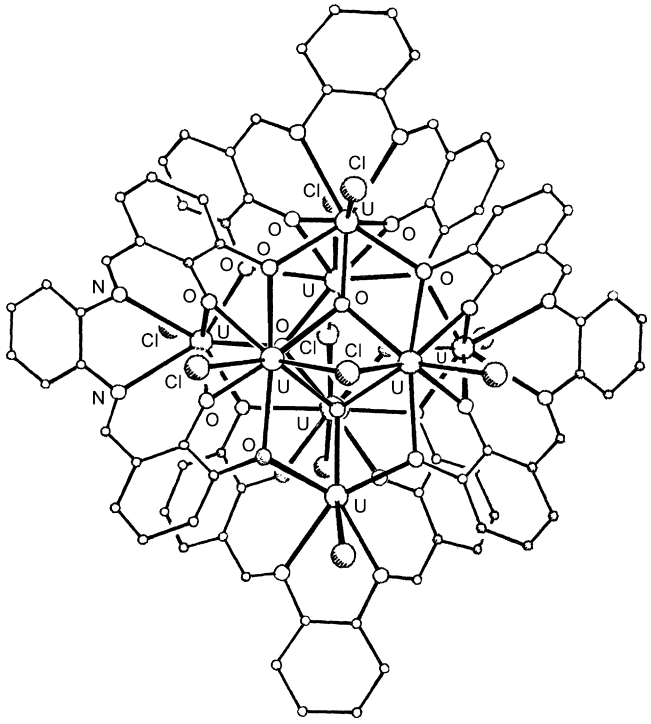

Fig. 98. Structure of $[U_8(\mathbf{141})_4(Cl)_{10}(O)_4]^{2-}$.

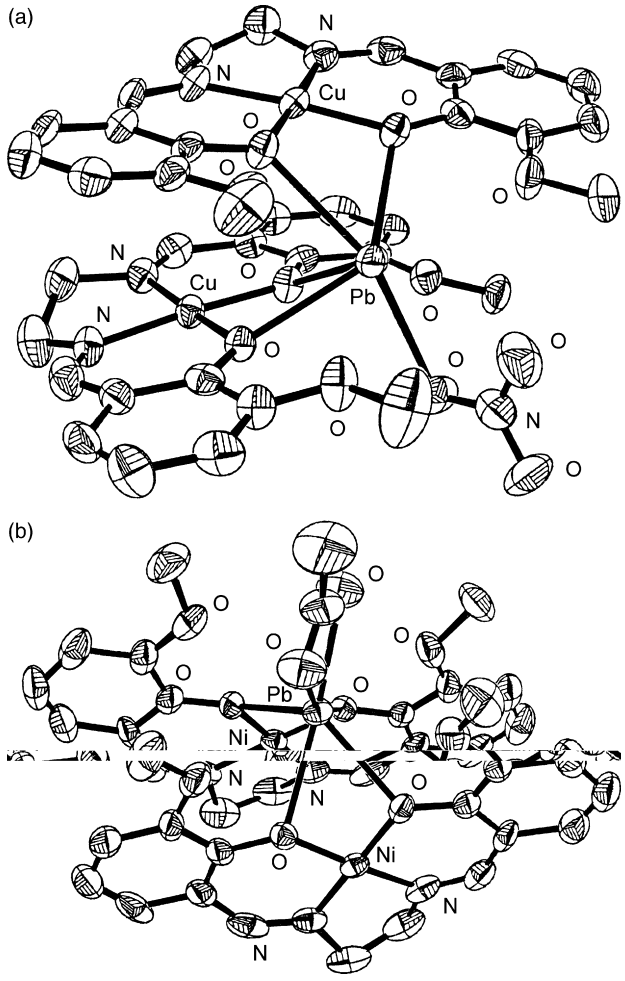

Fig. 99. Structure of $[Cu_2Pb(\mathbf{137})_2(NO_3)]^+$ (a) and $[Ni_2Pb(\mathbf{137})_2(CH_3COO)]^+$ (b).

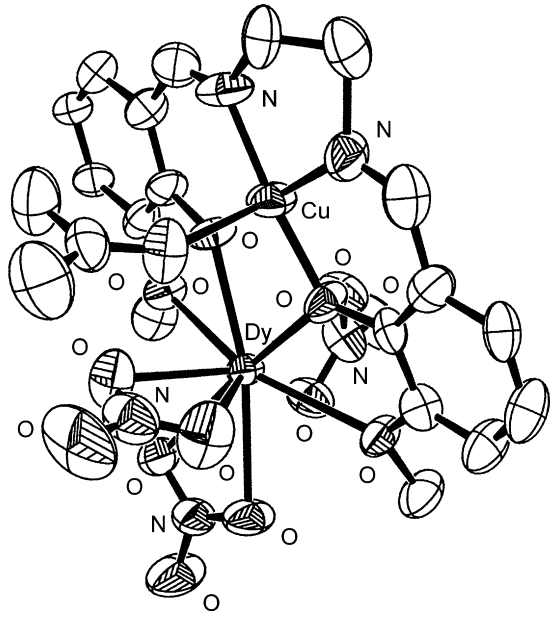

Fig. 100. Structure of $[CuDy(\mathbf{137})(NO_3)_3(CH_3COCH_3)]$.

aqua oxygen atom (Ln = La, Nd) or a monodentate nitrato oxygen atom (Ln = Er, Yb) in the axial position. Depending on the size of the lanthanide(III) ions, their coordination number varies from nine (Ln = Er, Yb) to ten (Ln = Nd) or eleven (Ln = La). The lanthanide(III) ions, located in the outer O_2O_2 cavity, complete the remaining coordination sites with the oxygen atoms from aqua and nitrato ligands. For the ZnLa complex, the remaining coordination sites are occupied by seven oxygen atoms, six from three bidentate nitrato ligands and one from the aqua oxygen; for the ZnNd complex, by six oxygen atoms, four from two bidentate nitrato ligands, one from monodentate nitrato ligand and one from the aqua oxygen; and for the ZnEr complex and the ZnTb complex, by five oxygen atoms, four from two bidentate nitrato ligands and one from the aqua oxygen. As the ionic size decreases, the lanthanide ion lowers its coordination number to relieve the congestion by converting one of its bidentate nitrato ligand to a less steric demanding monodentate nitrato ligand. Eventually, the coordination environment of the lanthanide ion is so congested that it has to transfer the nitrato ligand to the zinc(II) ion. The Zn(Ln distances are in the range 3.429···3.583 Å [163].

^{1}H NMR and ESI-mass spectra show that the complexes exist as a mixture of mononuclear, heterodinuclear and heterotrinuclear species in methanol, as verified by the X-ray of $[Zn_2Nd(\mathbf{143})_2(NO_3)_2(H_2O)_2](NO_3)$, isolated from a methanol solution of $[ZnNd(\mathbf{143})(NO_3)_3(C_2H_5OH)]$. The related complex $[Zn_2Pr(\mathbf{139})_2NO_3)_3(H_2O)]$ dissociate into a mixture containing at least $[ZnPr(\mathbf{139})(NO_3)_3(H_2O)]$ and $[Zn(\mathbf{139})]$, when dissolved in dimethylsulfoxide and remains undissociated in acetone. On the contrary, ^{1}H NMR spectra in acetonitrile indicate the occurrence of only one species with a structure similar to the solid-state one. The conductivity measurements revealed that all the ZnLn complexes are non-conductors in CH_3CN [163].

The photophysical properties of these Schiff base complexes can be tuned by changing the electronic properties of the substituents: by extending the conjugation, both the absorption and emission of the complexes are red shifted. The triplet state emission of the ZnGd complex was identified at 77 K with a lifetime of 6.10 ms. Energy transfer was observed from the triplet state of the ZnLn complex to the excited state of lanthanide metal, (Ln = Nd, Er, Yb) which emitted in the NIR region [162].

$[Zn(\mathbf{143})]$, when treated with $Nd(NO_3)_3{\cdot}6H_2O$ or $NdCl_3{\cdot}6H_2O$, affords the ZnNd heterodinuclear, the Zn_2Nd heterotrinuclear or the Zn_2Nd_2 heterotetranuclear complexes, whose structure is dependent on the Zn:Nd ratio and counter anions present. A 2:1 Zn:Nd molar ratio produces $[Zn_2Nd(\mathbf{143})_2(X)_2(H_2O)_2](X){\cdot}C_2H_5OH{\cdot}nH_2O$ ($X = NO_3^-$, $n = 1$; $X = Cl^-$, $n = 5$) irrespective of the salt used. When a 1:1 Zn:Nd molar ratio is employed, $NdCl_3{\cdot}6H_2O$ gives $[Zn_2Nd_2(\mathbf{143})_2(Cl)_6(CH_3OH)_2]{\cdot}CH_3OH$, whereas $Nd(NO_3){\cdot}6H_2O$ affords $[ZnNd(\mathbf{143})(NO_3)_3(CH_3CN)]CH_3CN$ [163].

In $[Zn_2Nd(\mathbf{143})_2(NO_3)_2(H_2O)_2](NO_3){\cdot}C_2H_5OH{\cdot}H_2O$, the two distorted square pyramidal zinc(II) ions are bound to the inner N_2O_2 cores of the two Schiff base ligands. For one zinc ion, the axial site is occupied by the oxygen atom of a nitrate group, whereas the other zinc ion bears a water molecule in this

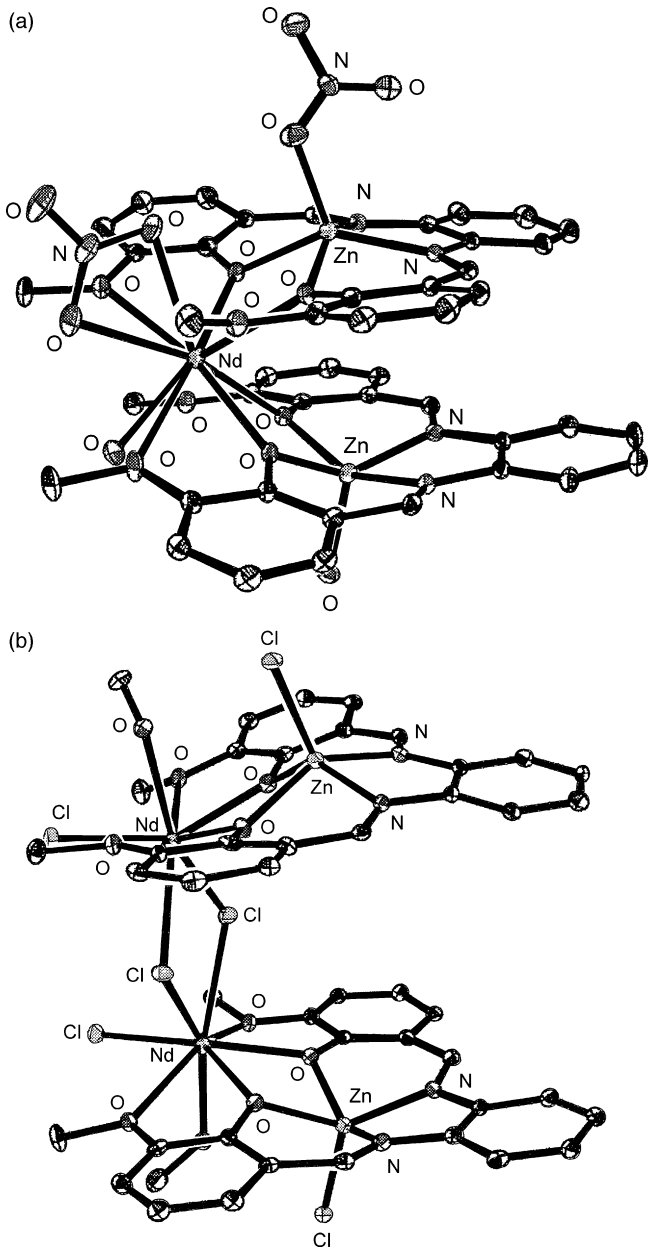

Fig. 101. Structure of $[Zn_2Nd(\mathbf{143})_2(NO_3)_2(H_2O)]^+$ (a) and $[Zn_2Nd_2(\mathbf{143})_2(Cl)_6(CH_3OH)_2]$ (b).

position. The nine coordinate neodymium(III) ion, sandwiched between the two parallel $\{Zn(\mathbf{143})\}$ units, is surrounded by four phenolate and two methoxy oxygen atoms, two oxygen atoms of a bidentate nitrate, and one water oxygen (Fig. 101a). In the similar structure of $[Zn_2Nd(\mathbf{143})_2(Cl)_2(H_2O)_3](Cl){\cdot}2CH_3OH$, each zinc ion bears a chloride ligand in an axial position while the neodymium(III) ion is surrounded by six oxygen atoms from two $[\mathbf{143}]^{2-}$ ligands and three aqua oxygen atoms. The Zn···Nd distances are 3.530 Å and 3.455 Å. $[Zn_2Nd_2(\mathbf{143})_2(Cl)_6(CH_3OH)_2]{\cdot}CH_3OH$, comprises two $\{ZnNd(\mathbf{143})\}$ units linked together by two bridging chloride ions bound to both neodymium(III) ions. The square pyramidal zinc(II) and the eight coordinate neodymium(III) ions are located in the N_2O_2 inner and O_2O_2 outer cavities of each Schiff-

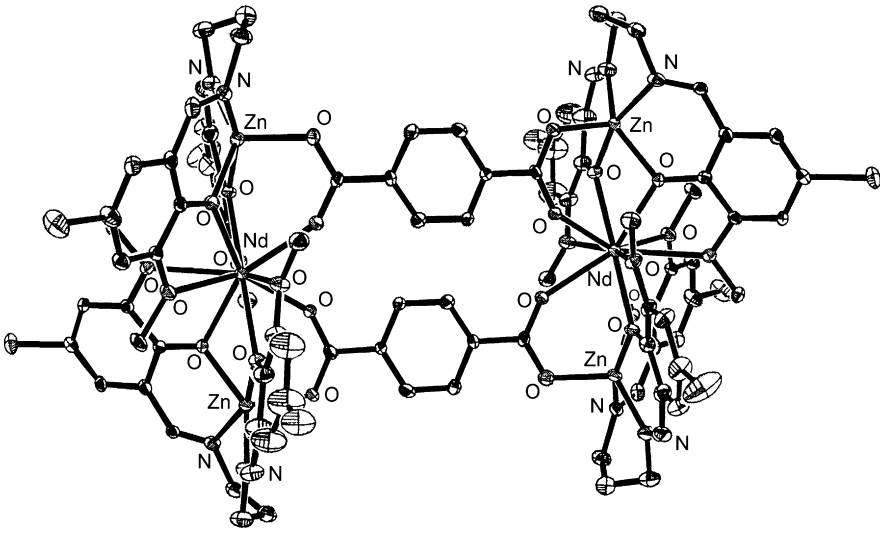

Fig. 102. Structure of $[Zn_4Nd_2(\mathbf{138a})(1,4\text{-}OOCC_6H_4COO)_2]^{2+}$.

base ligand. The Zn···Nd distances are 3.479 Å and 3.504 Å while the Nd···Nd separation is 4.477 Å (Fig. 101b) [163].

$[ZnNd(\mathbf{143})(NO_3)_3(CH_3CN)]\cdot CH_3CN$ is similar to the above reported d,f-heterodinuclear complexes with an acetonitrile molecule coordinated in an axial position of the zinc(II) ion and the neodymium(III) ion surrounded by four $[\mathbf{143a}]^{2-}$ oxygen atoms and six oxygen atoms from three bidentate nitrate groups. Furthermore, [Zn(**143a**)], prepared by reaction of H_2-**143a** with $Zn(CH_3COO)_2$, when treated with the appropriate lanthanide(III) nitrate hexahydrate gives rise to $[ZuLn(\mathbf{143a})(NO_3)_3(H_2O)_n]$ (Ln = La, Nd, Gd, Er, Yb; $n = 1,2$) [163], whose structures parallel the similar ones of the corresponding complexes with H_2-**143**, H_2-**137** and H_2-**139** [163].

The photophysical properties of [Zn(**143**)], [Zn(**143a**)], [Zn(**137**)] and [Zn(**139**)], revealed that, at 77 K, both ligand-centered triplet (^{3}LC) and singlet (^{1}LC) states existed for the ethylene-bridged complexes, whereas only the ^{1}LC state was detected for the phenylene-bridged complexes. NIR sensitization studies of $[ZnNd(\mathbf{L})(NO_3)_3(H_2O)_n]$ (H_2-**L** = H_2-**137**, H_2-**139**. H_2-**143**, H_2-**143a**) further showed that the neodymium(III) sensitization took place via the ^{3}LC and ^{1}LC states when the spacer between the imine groups of the Schiff base ligand was an ethylene and a phenylene unit, respectively. *Ab initio* calculations show that the observed differences can be attributed to the difference in the molecular vibrational properties and electron densities of the electronic states between the ethylene- and phenylene-bridged complexes [163].

According to NMR data, $[Zn_2Nd(\mathbf{143})_2(NO_3)_2(H_2O)_2](NO_3)$ is stable also in methanol, where it shows a better luminescence than $[ZnNd(\mathbf{143})(NO_3)_3(CH_3CN)]\cdot CH_3CN$, despite the fact that it has a coordinated water molecule. This may be due to the presence of two chromophores in $[Zn_2Nd(\mathbf{143})_2(NO_3)_2(H_2O)_2](NO_3)$ vs one in $[ZnNd(\mathbf{143})(NO_3)_3(CH_3CN)]\cdot CH_3CN$, which could increase the rate of energy-transfer processes. The relative emission intensity of $[Zn_2Nd(\mathbf{143})_2(NO_3)_2(H_2O)_2](NO_3)$ is similar in CH_3OH and CH_3OD, whereas for $[ZnNd(\mathbf{143})(NO_3)_3(CH_3CN)]\cdot CH_3CN$, the relative emission intensity is much higher in CH_3OD vs CH_3OH. Thus, in CH_3OD, the relative emission intensities of $[Zn_2Nd(\mathbf{143})_2(NO_3)_2(H_2O)_2](NO_3)$ and $[ZnNd(\mathbf{143})(NO_3)_3(CH_3CN)]\cdot CH_3CN$ are reversed. Conductivity studies show that $[ZnNd(\mathbf{143})(NO_3)_3(CH_3CN)]\cdot CH_3CN$ is a 1:1 electrolyte in CH_3OH, suggesting the loss of a nitrate anion from the neodymium(III) ion and the probable coordination of methanol in $[ZnNd(\mathbf{143})(NO_3)_3(CH_3CN)]\cdot CH_3CN$ with a luminescence decrease. These data suggest that interactions with solvent (methanol) are not as important in the photochemical processes in $[Zn_2Nd(\mathbf{143})_2(NO_3)_2(H_2O)_2](NO_3)$ as they are in $[ZnNd(\mathbf{143})(NO_3)_3(CH_3CN)]\cdot CH_3CN$ [163].

H_2-**138a**, $Zn(CH_3COO)_2\cdot 2H_2O$, $Nd(NO_3)_3\cdot 6H_2O$ and 1,4-benzenedicarboxylate afford $\{[Zn_4Nd_2(\mathbf{138a})_4(1,4\text{-}OOCC_6H_4COO)_2]\cdot[Nd(NO_3)_5(H_2O)]\}\cdot 2C_2H_5OH\cdot 3H_2O$, where the dicarboxylate ligands stabilize two trimetallic $\{Zn_2Nd(\mathbf{138a})_2\}$ fragments, with the zinc(II) ions in the O_2N_2 cavities of each $[\mathbf{138a}]^{2-}$ group and the neodymium(III) ion in the outer O_2O_2 sets of both $[\mathbf{138a}]^{2-}$ groups. Two benzenedicarboxylate groups bridge the Zn_2Nd moieties such that each carboxylate group spans a ZnNd set where each neodymium(III) ion is ten coordinate. The resulting complex cation has an interesting internal elongated prism-like cavity (Fig. 102) [164].

[Fe(**L**)] (H-**L** = H_2-**144**, H_2-**145**) or [Cu(**L**)(H_2O)] (H_2-**L** = H_2-**146**, H_2-**147**, H_2-**149**, H_2-**150**) when reacted with $Gd(NO_3)_3\cdot 6H_2O$ affords $[FeGd(\mathbf{L})(NO_3)_3(S)]$ or $[(CuGd(\mathbf{L})(NO_3)_3(S)]$. In agreement with previous results, the d-transition metal(II) ion enters into the inner N_2O_2 coordination site of the ligand while the gadolinium(III) ion occupies the O_2O_2 outer site. The precise structure of the final product depends on the solvent used during the preparation and/or recrystallization. Thus, the structure of $[FeGd(\mathbf{144})(NO_3)_3(CH_3OH)]$, $[FeGd(\mathbf{144})(NO_3)_3(CH_3COCH_3)]$, $[FeGd(\mathbf{145})(NO_3)_3(CH_3COCH_3)]$, $[CuGd(\mathbf{147})(NO_3)_3(CH_3COCH_3)]$, $[CuGd(\mathbf{149})(NO_3)_3(H_2O)]$ and

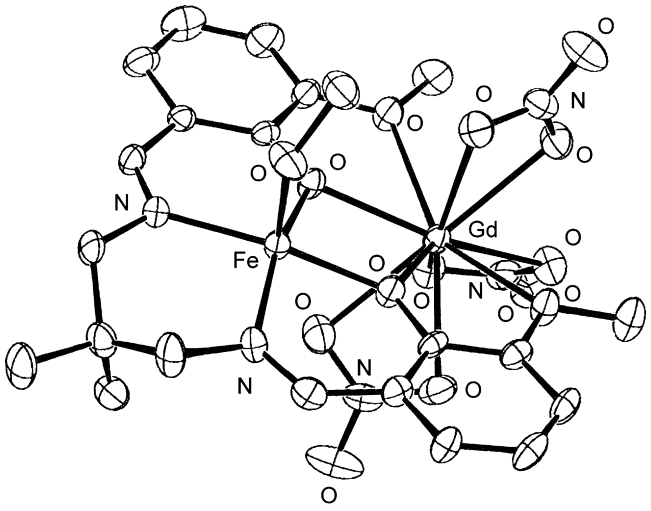

Fig. 103. Structure of [FeGd(**145**)$(NO_3)_3(CH_3OH)$].

[CuGd(**150**)$(NO_3)_3(H_2O)$] are very similar with a ten coordinate gadolinium(III) ion and a square pyramidal or planar transition metal(II) ion, the solvent molecule occupying the apex. The intermolecular Fe(Gd distances (7.610–9.416 Å) are much larger than the intramolecular ones (3.415–3.516 Å) (Fig. 103) [165,166]. The Cu(Gd distance is 3.454 Å. In particular, in [CuGd(**149**)$(NO_3)_3(H_2O)$] the cyclohexane moiety, differently from the amine precursor 1,2-diamino cyclohexane which is in an equimolar mixture of *cis* and *trans*, exists in a diequatorial *trans* configuration indicating that the condensation takes place with the diequatorial *trans* form of the diamine. The intermolecular Cu···Gd distances of 3.401 and 3.449 Å: the shortest intermolecular distances are Cu···Gd 7.657 Å and 7.192 Å, Cu···Cu 6.469 Å and 6.695 Å and Gd···Gd 8.871 Å and 9.221 Å, respectively. The experimental magnetic susceptibility and magnetization data indicate the occurrence of weak Fe^{II}–Gd^{III} ferromagnetic interactions ($J = 0.50\ cm^{-1}$ for [FeGd(**144**)$(NO_3)_3(CH_3OH)$]; $J = 0.41\ cm^{-1}$ for [FeGd(**144**)$(NO_3)_3(CH_3COCH_3)$]; $J = 0.08\ cm^{-1}$ for [FeGd(**145**)$(NO_3)_3(CH_3COCH_3)$]. The similar ferromagnetic interaction between copper(II) and gadolinium(III) ions occurs inside each dinuclear unit and antiferromagnetic interactions between neighboring dinuclear units ($zJ' = -0.027\ cm^{-1}$). Variable-temperature and variable-field magnetic measurements reveal that the metal centers in [CuGd(**149**)$(NO_3)_3(H_2O)$] and in [CuGd(**150**)$(NO_3)_3(H_2O)$] are ferromagnetically coupled ($J = 6.3\ cm^{-1}$ and $5.4\ cm^{-1}$, respectively) [165–167,169].

The reaction of $Gd(CF_3COO)_3$ with [Cu(**148**)], derived from the condensation of 3-ethoxysalicylaldehyde and 1,2-diamino-1-methylpropane in the presence of $Cu(CH_3COO)_2{\cdot}H_2O$, gives [CuGd(**148**)$(CF_3COO)_3(C_2H_5OH)_2$], where the nine coordinate gadolinium(III) ion in the outer O_2O_2 chamber of $[\mathbf{148}]^{2-}$ and the five coordinate square pyramidal copper(II) ion in the inner N_2O_2 chamber are 3.391 Å apart, triply bridged by two phenoxo oxygen atoms belonging to the hexadentate ligand $[\mathbf{148}]^{2-}$ and one bidentate-bridged carboxylate group coordinated in *syn–syn* (μ_2-η^1, η^1) fashion (Fig. 104). The complex shows a ferromagnetic interaction ($J = 4.42\ cm^{-1}$) [168].

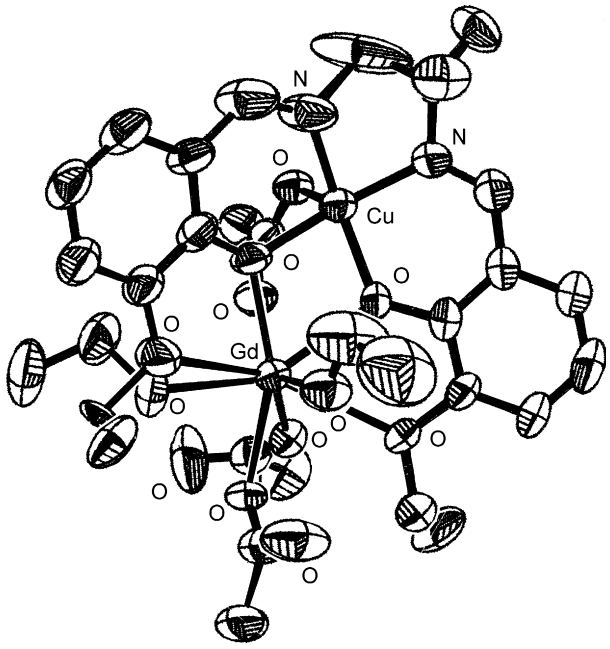

Fig. 104. Structure of [CuGd(**148**)$(CF_3COO)_3(C_2H_5OH)_2$] (the fluorine atoms are omitted for clarity).

The above reported $[Zn_3(\mathbf{138a})_2(NO_3)_2]{\cdot}CH_3CN$ and $YbCl_3{\cdot}6H_2O$ under basic conditions afford $[Zn_2Yb_2(\mathbf{138a})_2(OH)_2(Cl)_4]{\cdot}2CH_3CN$ where the central zinc ion of the Zn_3 complex is replaced by two seven coordinate ytterbium(III) ions, which are bridged by two hydroxide ions with a Yb···Yb separation of 3.588 Å. The nitrate groups are also displaced by chlorides. Each zinc(II) ion is five coordinate and sits slightly above the N_2O_2 plane of each ligand. The unique Zn···Yb distance is 3.481 Å (Fig. 105) [155].

Molar conductivity and ^1H NMR studies indicate that H_2-**138a**, $[Zn_3(\mathbf{138a})_2(NO_3)_2]{\cdot}CH_3CN$ and $[Zn_2Yb_2(\mathbf{138a})_2(\mu\text{-}OH)_2(Cl)_4]{\cdot}2CH_3CN$ are stable in CH_3CN. The UV–vis absorption bands of the free ligand H_2-**138a** become red-shifted

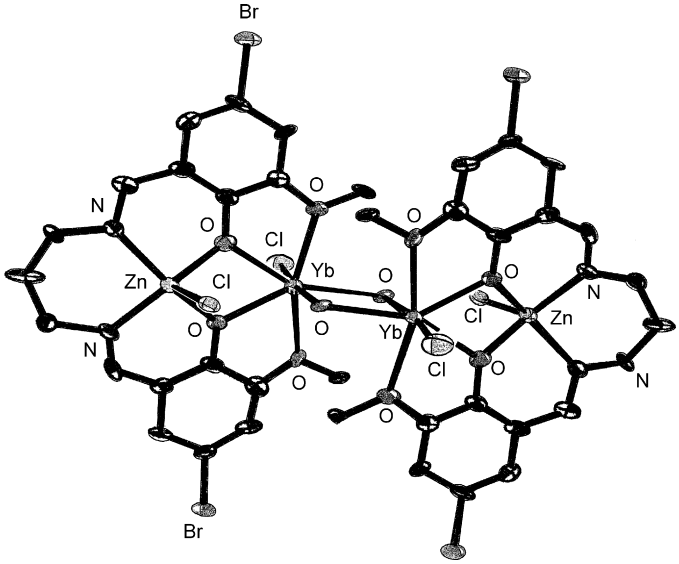

Fig. 105. Structure of $[Zn_2Yb_2(\mathbf{138a})_2(OH)_2(Cl)_4]$.

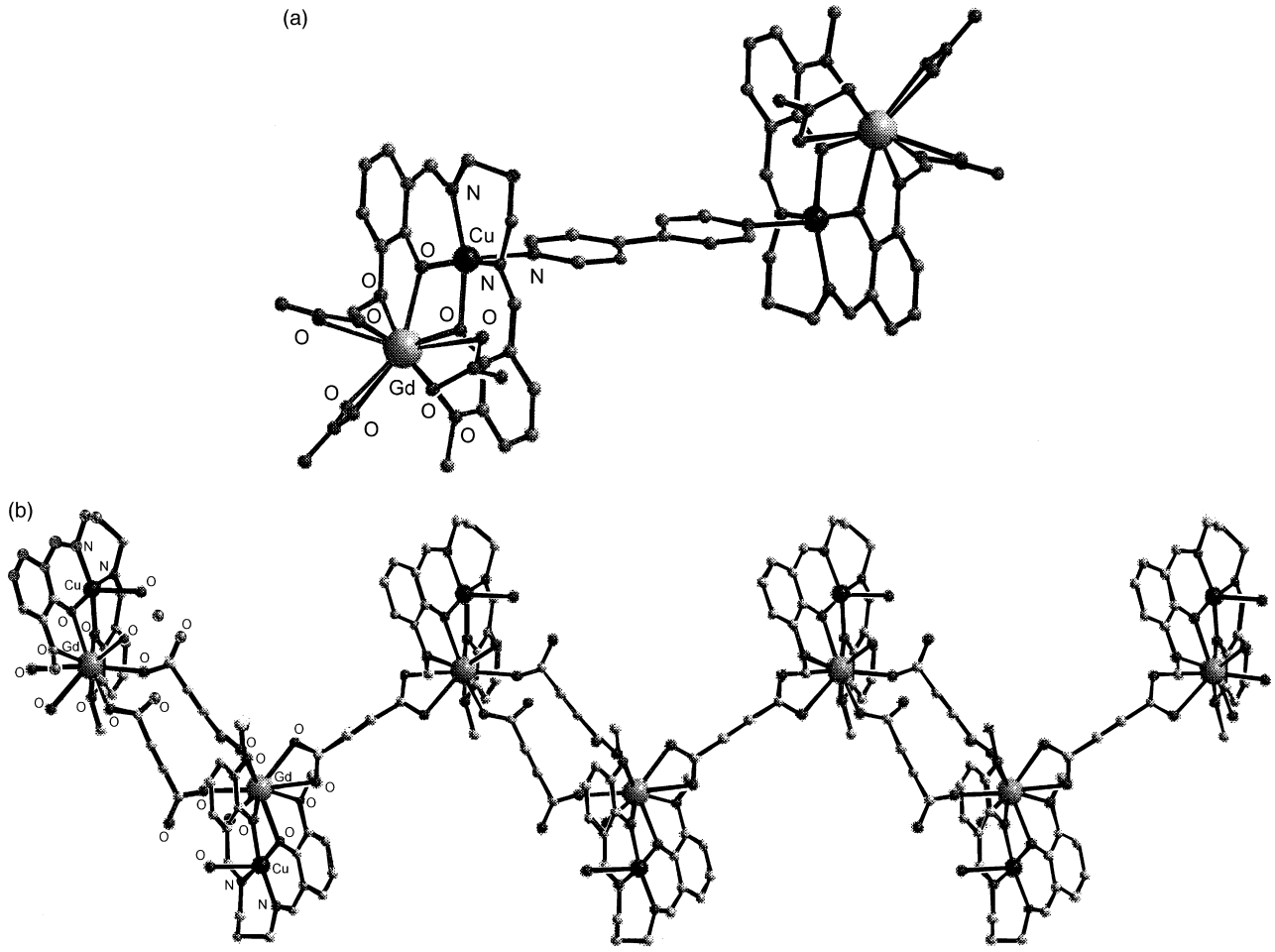

Fig. 106. Structure of $[Cu_2Gd_2(\mathbf{142})_2(NO_3)_6(\mu\text{-}4,4'\text{-bipy})]$ (a) and $[CuGd(\mathbf{142})(acdca)_{1.5}(H_2O)_2]_\infty$ (b).

upon coordination to the metal ions in $[Zn_3(\mathbf{138a})_2(NO_3)_2]$ and $[Zn_2Yb_2(\mathbf{138a})_2(\mu\text{-}OH)_2(Cl)_4]$. For $[Zn_2Yb_2(\mathbf{138a})_2(\mu\text{-}OH)_2(Cl)_4]$ the typical emission band of ytterbium(III) ion, assigned to the $^2F_{5/2} \rightarrow {}^2F_{7/2}$ transition is observed at 977 nm upon excitation of the ligand centered absorption band either at 275 or 350 nm. The free ligand H_2-**138a** and $[Zn_3(\mathbf{138a})_2(NO_3)_2]$ do not exhibit NIR luminescence in CH_3CN under similar conditions. The similar NIR luminescence, observed for $[Zn_2Yb_2(\mathbf{138a})_2(\mu\text{-}OH)_2(Cl)_4]$ in the solid state, clearly indicate that the tetra metallic Zn_2Yb_2 structure found in the solid state is maintained in acetonitrile. The relative emission intensities of $[Zn_2Yb_2(\mathbf{138a})_2(\mu\text{-}OH)_2(Cl)_4]$ and $[ZnYb(\mathbf{138a})(CH_3COO)(NO_3)_2]$ are higher in CH_3CN but significantly lower in CH_3OH, probably owing to an ability of the complexes to coordinate methanol which can quench lanthanide luminescence [155].

Polynuclear systems have been obtained from the reaction of $[CuLn(\mathbf{142})(NO_3)_3]$ (Ln = Gd, Sm, Er, Pr) with appropriate di- or polynucleating linkers. Thus 4,4′-bipyridine (4,4′-bipy) turns $[CuGd(\mathbf{142})(NO_3)_3]$ into $[Cu_2Gd_2(\mathbf{142})_2(NO_3)_6(\mu\text{-}4,4'\text{-bipy})]$, where 4,4′-bipy interacts only with the copper(II) ions, linking two $\{GdCu(\mathbf{142})\}$ units. Each copper(II) ion is five coordinate with a square pyramidal geometry while the gadolinium(III) ions preserve their coordination sphere from the binuclear precursors. The short Cu···Gd distance is 3.523 Å. The distance between the copper(II) ions bridged by 4,4′-bipy is 11.745 Å (Fig. 106a) [170].

Furthermore, $\{[CuGd(\mathbf{142})(acdca)_{1.5}(H_2O)_2]\cdot 13\,H_2O\}_\infty$, obtained by reacting $[CuGd(\mathbf{142})(NO_3)_3]$ and the monopotassium salt of acetylenedicarboxylic acid (KH-acdca) under basic conditions, contains four similar $\{CuGd(\mathbf{142})\}$ entities connected through dicarboxylato ligands, resulting in infinite zigzag chains with Cu···Gd distances ranging from 3.487 to 3.500 Å. The $\{CuGd(\mathbf{142})\}$ entities are alternatively bridged by one and two dicarboxylato ligands having different connectivity modes. With the single bridge, the acetylenedicarboxylato ligand is bis-chelating towards two gadolinium ions, whereas with the double bridge each carboxylato group acts as a unidentate ligand. Two similar, crystallographically non-equivalent chains, interconnected through hydrogen bonds, are formed: one is constructed from two $\{CuGd(\mathbf{142})\}$ units, and the other one from the other two$\{CuGd(\mathbf{142})\}$ units. The gadolinium ions are nine coordinate while the copper ions are five coordinate, with a square pyramidal geometry. The Gd···Gd distances vary from 8.827 to 9.867 Å (Fig. 106b) [170].

$\{[CuLn(\mathbf{142})(fum)_{1.5}(H_2O)_2]\cdot 4H_2O\cdot C_2H_5OH\}_\infty$ originates from the reaction of fumaric acid (H_2-fum) in ethanol with $[CuLn(\mathbf{142})(NO_3)_3]$ (Ln = Gd, Sm) and LiOH; with-

out the addition of LiOH, [CuSm(**142**)$(NO_3)_3$] affords [CuSm(**142**)(H_2O)(H-fum)(fum)]$_\infty$ [170].

[CuGd(**142**)$(fum)_{1.5}(H_2O)_2]\cdot 4H_2O\cdot C_2H_5OH$ (and the isostructural CuSm analogue) is a two-dimensional coordination polymer with a brick-wall architecture. Each {CuGd(**142**)} entity is connected through fumarato bridges to three other heterodinuclear units. Two fumarato linkers connect the gadolinium ions from three {CuGd(**142**)} units, with each carboxylato group acting as a chelator. The distances between the gadolinium ions are 9.439 and 9.463 Å. For the third fumarato linker, each carboxylato group bridges the copper(II) and gadolinium(III) ions within the {CuGd} building block (*syn–syn* bridging mode). The intranode Cu···Gd distance is 3.449 Å. The copper ions exhibit a square pyramidal stereochemistry, with the carboxylato oxygen atom in the apical position, while the nine coordination of the gadolinium ion is reached by the N_2O_2 donor set of the organic ligand, four oxygen atoms from the carboxylato groups, and one aqua oxygen [170].

In [CuSm(**142**)(H_2O)(H-fum)(fum)]$_\infty$ the $[fum]^{2-}$ and $[H\text{-}fum]^-$ anions are coordinated only to the samarium ions; $[fum]^{2-}$ acts as a bridge, while $[H\text{-}fum]^-$ is a terminal ligand, with the chelating carboxylato group coordinated to samarium. $[fum]^{2-}$ links three samarium ions from three different {CuSm} units simultaneously: one carboxylato group bridges two samarium ions in an anti-anti fashion, while the second is coordinated through one oxygen atom to the third samarium ion. This results in a double chain. $[H\text{-}fum]^-$ acts as a terminal ligand, being coordinated to a samarium ion (chelating mode). Again the copper(II) ions are five coordinate in a square pyramidal geometry, with an aqua ligand in the apical position.. The coordination number of the samarium ions is nine. The intranode Cu···Sm distance is 3.548 Å [170].

[CuEr(**142**)$(NO_3)_3$] and fumaric acid in the presence LiOH leads to {[CuEr(**142**)$(H_2O)_2$(fum)]$(NO_3)\cdot 3\,H_2O\}_\infty$ where two nitrato ligands were replaced by one fumarato dianion, resulting in a one-dimensional coordination polymer with the {CuEr(**142**)} nodes connected by $[fum]^{2-}$ bridges. The carboxylato groups are coordinated in a chelating way only to the nine coordinate erbium(III) ions. The alternate distances between the erbium ions bridged by fumarato groups are 9.262 Å and 9.308 Å. The copper(II) ions are five coordinate in a square pyramidal geometry [170].

[Cu(**142**)], $Sm(NO_3)_3\cdot 6\ H_2O$, fumaric acid and LiOH form $[\{Cu_2^{II}Sm^{III}(\mathbf{142})_2\}_2(fum)_2](OH)_2$, containing two $\{Cu_2Sm(\mathbf{142})_2\}$ moieties linked through two $[fum]^{2-}$ ions. Each carboxylato group acts as a bridge between the copper and samarium ions in the classical *syn–syn* bridging mode. Within each Cu_2Sm triad the distances between the metallic centers range from 3.473 Å to 3.511 Å. As in the above complexes, the copper(II) ions display a square pyramidal geometry. The coordination number of the samarium ions is ten [170].

The self assembly reaction between [CuGd(**142**)$(NO_3)_3$] and sodium trimesate (H_3-trim) gives rise to $\{[Cu^{II}Gd^{III}(\mathbf{142})(trim)(H_2O)_2]\cdot H_2O\}_\infty$. Each trimesate anion connects three {CuGd} nodes, resulting in a double chain. The three carboxylato groups belonging to the trimesate anion exhibit different coordination modes: bidentate chelating toward gadolinium, monodentate also to gadolinium, and *syn–syn* bidentate bridging as a third bridge between copper(II) and gadolinium(III), within a node. The six coordinate copper ions are in an elongated octahedral geometry, where the apical positions are occupied by an aqua ligand and a carboxylato oxygen atom from the trimesate linker. The nine coordination number of the gadolinium ions derives from four oxygen atoms from $[\mathbf{142}]^{2-}$, four oxygen atoms from the carboxylato groups, and one aqua ligand [170].

The structure of polymeric complex $\{Cu_2Pr(\mathbf{142})_2(C_2O_4)_{0.5}(NC\text{–}N\text{–}CN)](NC\text{–}N\text{–}CN)\cdot 2H_2O\}_\infty$, obtained by [Cu(**142**)], praseodymium nitrate, Na(NC–N–CN) and K[Cr(2,2′-bipy)$(C_2O_4)_2$], is built up of almost linear trinuclear $\{Cu_2Pr(\mathbf{142})_2\}$ units connected by dicyanamido and oxalato ligands. The praseodymium ions from two trinuclear units are bridged by an oxalato ligand, resulting in hexanuclear moieties. These are further interconnected through 1,3-dicyanamido linkers, which coordinate to the copper ions. Each ten coordinate praseodymium ion is bound to eight oxygen atoms from two organic ligands, and two oxygen atoms from the oxalato bridge. The apical positions of the five coordinate square pyramidal copper ions are occupied by nitrogen atoms from the $[NC\text{–}N\text{–}CN]^-$ bridge [170].

[CuPr(**142**)$(NO_3)_3$] and lithium isonicotinate (Li-isonicot) form [CuPr(**142**)$(NO_3)_2$(isonicot)], where the binuclear {CuPr(**142**)} units are connected by the isonicotinate ligand, which is coordinated through the carboxylato group to two praseodymium(III) ions and with the nitrogen atom to the copper(II) ion. Two praseodymium(III) ions, arising from two {CuPr(**142**)} units, are bridged by two carboxylato groups from two isonicotinato bridges in a *syn–syn* bridging mode. Each praseodymium(III) ion exhibits an O_{10} coordination: four oxygen arise from the two chelating nitrato ligands, four others from the compartmental ligand, and two oxygen atoms from the bridging carboxylato groups. The distance between two praseodymium ions bridged by the carboxylato groups is 5.525 Å. The copper(II) ion is five coordinate in a square pyramidal geometry with the apical position occupied by the nitrogen atoms arising from the pyridyl group of the isonicotinato ligand. The Pr···Cu distance within the {PrCu(**142**)} building block is 3.611 Å [171].

[CuGd(**142**)$(C_2O_4)(H_2O)_3$][Cr(2,2′-bipy)$(C_2O_4)_2]\cdot 9H_2O$, resulting from the reaction between [CuGd(**142**)$(NO_3)_3$] and K[Cr(2,2′-bipy) $(C_2O_4)_2$], is not a genuine heteropolynuclear complex: the $[Cr(2,2'\text{-bipy})(C_2O_4)_2]^-$ species are not coordinated to either copper(II) or gadolinium(III) ions. The binuclear {CuGd(**142**)} entities are connected by bis-bidentate oxalato ions, which result from the partial decomposition of the $[Cr(2,2'\text{-bipy})(C_2O_4)_2]^-$ ions. Cationic zigzag chains are thus formed. The coordination number of the gadolinium ions is nine: four oxygen atoms from the organic ligand, four from the oxalato bridges, and one aqua ligand. The alternate distances between the oxalato-bridged gadolinium ions are 6.270 Å and 6.331 Å. The six coordinate copper ions are in an elongated octahedral geometry with two aqua ligands in the

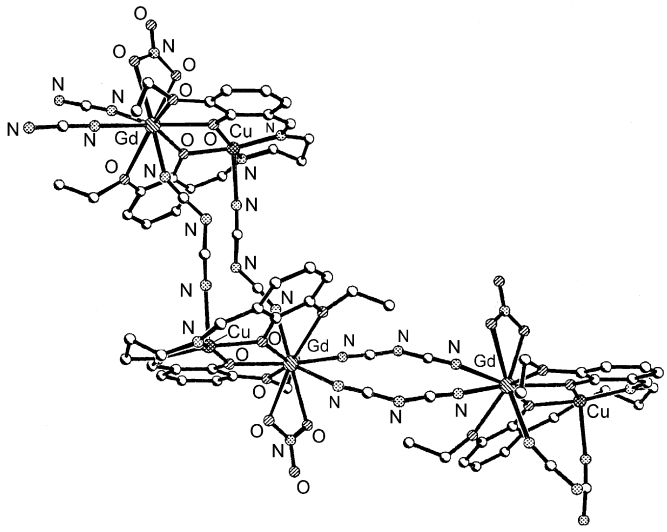

Fig. 107. Structure of $[CuGd(\mathbf{147})(NO_3)(NC–N–CN)_2]_\infty$.

apical positions. The intranode Cu···Gd distance is 3.534 Å [170].

The synthesis of the isostructural complexes $[CuGd(\mathbf{142})(H_2O)_4\{M(CN)_6\}]\cdot 3H_2O$ ($M=Fe^{III}$, Co^{III}), bearing three different spin carriers was successfully achieved by reacting $[CuGd(\mathbf{142})(NO_3)_3]$ with $K_3[M(CN)_6]$. In $[CuGd(\mathbf{142})(H_2O)_4\{Cr(CN)_6\}]\cdot 3H_2O$ the $\{CuGd(\mathbf{142})\}$ moiety preserves the structural features of the whole $Cu^{II}Ln^{III}$ family of complexes with compartmental Schiff base ligands derived from 3-methoxysalicyladimine. The $[Cr(CN)_6]^{3-}$ ion connects three metal ions, through three cyano groups. Two *cis* cyano ligands bridge the chromium(III) and copper(II) ions. The nine coordination number of the gadolinium(III) is reached by four oxygen atoms arising from the organic ligands, three aqua ligands and two nitrogen atoms from the bridging cyano groups. The copper(II) is octahedral with cyano nitrogen atom and a water molecule in axial positions. The two Cr···Gd distances are 5.635 and 5.723 Å, and the Gd···Cu distance is 3.499 Å [170].

In $[Cu_2Gd_2(\mathbf{142})_2(NO_3)_6(\mu\text{-}4,4'\text{-bipy})]$, $\{[CuGd(\mathbf{142})(acdca)_{1.5}(H_2O)_2]\cdot 13H_2O\}_\infty$, $\{[CuGd(\mathbf{142})(fum)_{1.5}(H_2O)_2]\cdot 4H_2O\cdot C_2H_5OH\}_\infty$, $\{[CuGd(\mathbf{142})(trim)(H_2O)_2]\cdot H_2O\}_\infty$, $[CuGd(\mathbf{142})(ox)(H_2O)_3][Cr(2,2'\text{-bipy})(C_2O_4)_2]\cdot 9H_2O$ the Cu^{II}–Gd^{III} exchange interaction was ferromagnetic, with J values in the range of 3.53–8.96 cm^{-1}. In $[CuSm(\mathbf{142})(H_2O)(H\text{-}fum)(fum)]_\infty$ and $[\{Cu_2^{II}Sm^{III}(\mathbf{142})_2\}_2(fum)_2](OH)_2$ most probably an antiferromagnetic interaction between copper(II) and the samarium(III) ions occurs. In $[CuGd(\mathbf{142})(H_2O)_4\{Cr(CN)_6\}]\cdot 3H_2O$ the intranode Cu^{II}–Gd^{III} ferromagnetic interaction is overwhelmed by the antiferromagnetic interaction occurring between the cyanobridged Gd^{III} and Cr^{III} ions [170].

Similarly, $[Cu(\mathbf{L})(H_2O)]$ ($H_2L = H_2$-**137**,H_2-**147**) reacts with $Gd(NO_3)_3\cdot 6H_2O$ and Na(NC–N–CN) to form the polymeric compound $[CuGd(\mathbf{L})(NO_3)(NC–N–CN)_2]\cdot CH_3COCH_3$ along with $[CuGd(\mathbf{L})(NO_3)_3]$. Also, $[Cu(\mathbf{L})(H_2O)]$ reacts with Na(NC–N–CN) to give $[Cu_2Na_2(\mathbf{L})_2(NC–N–CN)_2(H_2O)_2]$, where the $\{CuNa(\mathbf{137})(H_2O)\}$ and $\{CuNa(\mathbf{137})(NC–N–CN)\}$ entities are linked through an additional bridging dicyanamide acting in the $\mu_{1,1}$ end-on fashion. The Na···Na separation is 3.733 Å. This dicyanamide bridge yields tetranuclear Cu–Na–Na–Cu entities in which the planes defined by the equatorial N_2O_2 donor atoms afforded by the ligands $[\mathbf{137}]^{2-}$ to each square planar copper ion are roughly parallel. The structure of each dinuclear moiety is quite similar except for the coordination of the sodium ions. Both of them are coordinated to four oxygen atoms from the compartmental ligand $[\mathbf{137}]^{2-}$ and to the nitrogen atom of the bridging dicyanamide anion. The sixth position of the coordination octahedron is occupied by a water molecule for one sodium ion and by a nitrogen atom of $[NC–N–CN]^-$ for the other sodium ion. Strong intermolecular interactions between tetranuclear units lead to the formation of one-dimensional arrangement [167].

In $[CuGd(\mathbf{147})(NO_3)(NC–N–CN)_2]\cdot CH_3COCH_3$ the five coordinate copper ion sits in the N_2O_2 donor set of $[\mathbf{147}]^{2-}$ with the nitrogen atom of a $[NC–N–CN]^-$ ligand axially bonded. The slightly distorted monocapped antiprismatic polyhedron of the nine coordinate gadolinium(III) cation is formed by four oxygen atoms of $[\mathbf{147}]^{2-}$, two oxygen atoms from a chelating nitrate anion and three nitrogen atoms from dicyanamide ligands. All dicyanamide anions act as $\mu_{1,5}$-end-to-end bidentate-bridging ligands either between two gadolinium ions or between a copper and a gadolinium ion. These bridges are alternately arranged between the $\{CuGd(\mathbf{147})\}$ entities, two Cu···Gd bridges following two Gd···Gd bridges, thus generating an extended zigzag coordination polymer formulated as $\{[CuGd(\mathbf{147})(NO_3)(NC–N–CN)_2]\cdot CH_3COCH_3\}_n$. The $\{CuGd(\mathbf{147})\}$ entities are separated by Gd···Gd (8.197 Å) and Cu···Cu (8.974 Å) distances much longer than the Cu···Gd intramolecular one (3.481 Å) (Fig. 107) [167].

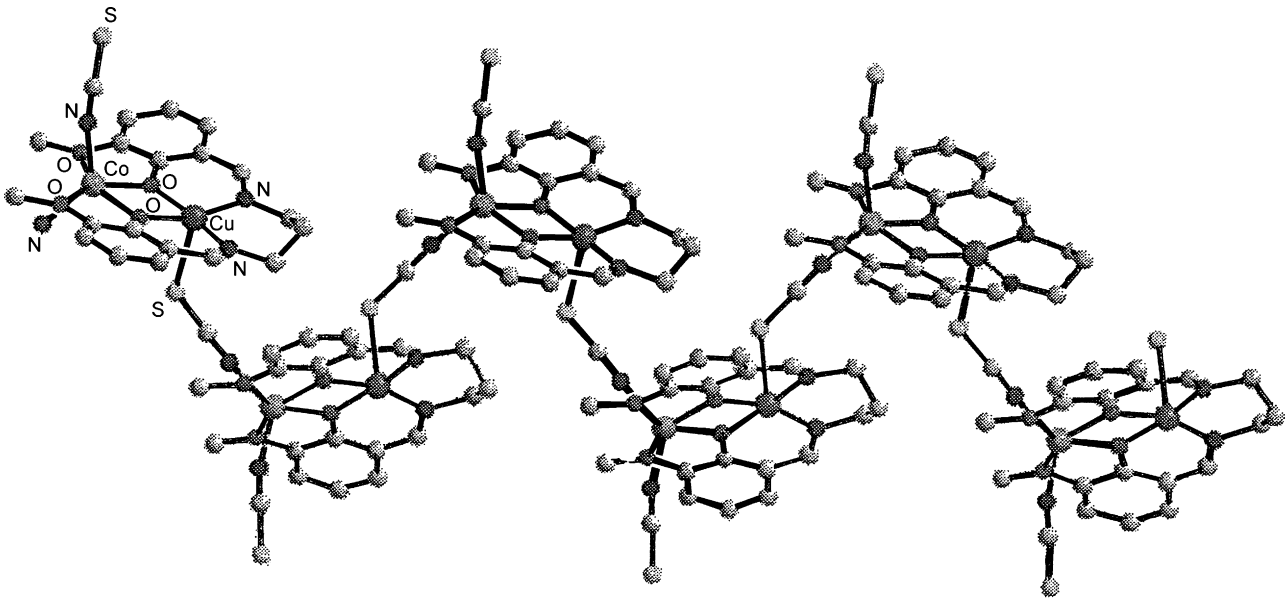

Fig. 108. Structure of $[CuCo(\mathbf{142})(NCS)_2]_\infty$.

For $[CuGd(\mathbf{147})(NO_3)(NC–N–CN)_2]$ and $[CuGd(\mathbf{137})(NO_3)_3]$ ferromagnetic interaction between copper(III) and gadolinium(III) ions occurs ($J = 8.50$ and $8.63\,cm^{-1}$, respectively), while the magnetic interaction, transmitted along the chain through the $[NC–N–CN)_2]^-$ ligands, is negligible. The experimental magnetization values confirm the ferromagnetic nature of the Cu^{II}–Gd^{III} interactions and the absence of intermolecular magnetic interactions between the dinuclear units of $[CuGd(\mathbf{147})(NO_3)(NC–N–CN)_2]$. In $[Cu_2Na_2(\mathbf{137})(NC–N–CN)_2\ (H_2O)]$, a very weak antiferromagnetic interaction between the two copper(II) ion occurs ($J = -0.6\,cm^{-1}$) [167].

A transmetalation reaction occurs when $[CuGd(\mathbf{142})(NO_3)_3]$ is reacted with $[N(Et)_4]_2\ [Co(NCS)_4]$ with the formation of $[CuCo(\mathbf{142})(NCS)_2]$, identical to that obtained by the usual route involving the reaction of $[Cu(\mathbf{142})]$ with $Co(CH_3COO)_2$ in the presence of KNCS, where "alternating" and "zig-zag" chains of dinuclear $\{CuCo(\mathbf{142})\}$ units are linked by thiocyanate bridges. Within each dinuclear $\{CuCo(\mathbf{142})\}$ unit, the distorted square pyramidal copper(II) and the tetrahedral cobalt(II) ions are bridged by two phenoxo oxygen atoms of $[\mathbf{142}]^{2-}$, with a Cu···Co separation of 3.149 Å. The bridging thiocyanate group axially coordinates to the copper(II) ion of one $\{CuCo(\mathbf{142})\}$ unit and is linked by its nitrogen atom to the cobalt ion of a neighboring $\{CuCo(\mathbf{142})\}$ unit. The cobalt(II) ion becomes six coordinate in a strongly distorted octahedral geometry, if the two longer Co–O (methoxy) distortion are considered (Fig. 108). The magnetic properties have been explained by a strong antiferromagnetic Cu^{II}–Co^{II} exchange interaction ($J = -101\,cm^{-1}$) through the phenoxo bridges and a weak ferromagnetic Cu^{II}–Co^{II} interaction ($J = 2.8\,cm^{-1}$) through the thiocyanato bridges [172].

$\{[Cu(\mathbf{146})](H_2O)\}$, an inclusion compound where a water molecule is not coordinated to the planar copper(II) ion but hydrogen bonded to the phenolate and to the ethoxy oxygen atoms, reacts with $M(ClO_4)\cdot 6H_2O$ ($M = Cu^{II}$, Co^{II}, Mn^{II}) to form $[Cu_3M(\mathbf{146})_3(H_2O)_3\}](ClO_4)_2$ which contains the $[CuM(\mathbf{146})(H_2O)_3]^{2+}$ cation and two $[Cu(\mathbf{146})]$ moieties. In the dinuclear core, one copper(II) ion occupies the inner N_2O_2 cavity, while the second compartment of $[\mathbf{146}]^{2-}$ is occupied by the other metal ion that is coordinated also to three water molecules. The two metal ions are double bridged by the two phenolate oxygen atoms. The ethoxy oxygen atoms of the ligand remain uncoordinated. The inner copper(II) ion in the dinuclear cation and the two copper(II) ions in the two mononuclear complexes are square planar while the second metal(II) ion is five coordinate with a O_5 square pyramidal environment in the Cu_2 complex cation and intermediate between square pyramidal and trigonal bipyramidal in the CuCo and CuMn complex cations. Two of the three coordinated water molecules interact with two mononuclear $[Cu(\mathbf{146})]$ moieties, resulting in the formation of the tetranuclear $[\{Cu(\mathbf{146})\}_2\{Cu(\mathbf{146})M(H_2O)_3\}]^{2+}$ system (Fig. 109). The metal ions are coupled by a weak antiferromagnetic interaction ($J = -17.4\,cm^{-1}$, $-8\,cm^{-1}$, and $-14\,cm^{-1}$ for Cu_2^{II}, $Cu^{II}Mn^{II}$ and $Cu^{II}Co^{II}$ complexes, respectively) [173].The reaction of 3-methoxysalicylaldehyde or 3-ethoxysalicylaldehyde with S-methylisothiosemicarbazide hydroiodide, followed by treatment with $AgNO_3$, removal of AgI and addition of $Cu(CH_3COO)_2\cdot H_2O$, affords $[Cu(\mathbf{151})(H_2O)]$ or $[Cu(\mathbf{152})(H_2O)]$ which give rise to $[CuLn(\mathbf{151})(NO_3)_3(H_2O)]$ and $[CuLn(\mathbf{152})(NO_3)_3(H_2O)]$ when mixed with the appropriate lanthanide(III) nitrate. In $\{[CuCe(\mathbf{151})(NO_3)_3(H_2O)]\cdot CH_3COCH_3\}$ the square pyramidal copper(II) ion and the eleven coordinate cerium(III) ion, bridged by two phenoxo oxygen atoms with a Cu···Ce distance of 3.457 Å, reside in the inner N_2O_2 and outer O_2O_2 chamber of $[\mathbf{151}]^{2-}$, respectively. A significant intermolecular interaction between the coordinated water molecule and the nitrato oxygen of the neighboring molecule occurs, forming tetranuclear $\{[CuCe(\mathbf{151})(NO_3)_3(H_2O)]\cdot CH_3COCH_3\}_2$

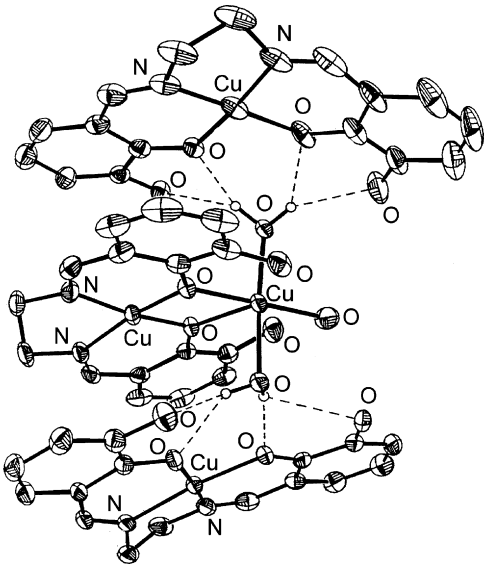

Fig. 109. Structure of $[\{Cu(\mathbf{146})\}_2\{Cu_2(\mathbf{146})(H_2O)_3\}]^{2+}$.

units, which, linked through π–π interactions, give rise to two-dimensional layers with distances between the mean planes of neighboring overlapping aromatic rings in the range of 3.45–3.52 Å. The ferromagnetic coupling between the copper(II) and the gadolinium(III) ions occurring in $[CuGd(\mathbf{151})(NO_3)_3(H_2O)]$ and $[CuGd(\mathbf{152})(NO_3)_3(H_2O)]$ ($J = 5.2$ and $5.5\,cm^{-1}$, respectively) is further supported by the magnetization values for $[CuGd(\mathbf{151})(NO_3)_3(H_2O)]$ at 2.0 K. Magnetic susceptibility and EPR data suggested that the Cu–Ce interaction is antiferromagnetic in the related complexes [174].$[M(\mathbf{L})]$ ($M = Co^{II}, Ni^{II}, Cu^{II}$; H_2-**L** = H_2-**137**, H_2-**142**, H_2-**145**, H_2-**153**, H_4-**154**) and UCl_4 afford $[U(\mathbf{L})(Cl)_2(S)_2]$ or $[U(H_2\text{-}\mathbf{L})(Cl)_2(S)_2]$ (S = solvent), identical to those obtained directly by treatment of UCl_4 with H_2-**L**. This transmetalation reaction was assumed to proceed by the initial formation of heterodinuclear complexes, the subsequent migration of Cl^- from the uranium(IV) to the transition metal(II) ion and the final transformation into $[M(\mathbf{L})(Cl)_2]$ or $[M(H_2\text{-}\mathbf{L})(Cl)_2]$ with elimination of MCl_2. In $[U(\mathbf{137})(Cl_2)(py)_2]$ or $[U(H_2\text{-}\mathbf{154})(Cl_2)(py)_2]$, obtained by substitution of the solvent ligands in the related complexes with pyridine, the uranium(IV) ion is in a dodecahedral environment [175].The reaction of $[M(H_2\text{-}\mathbf{L})]$ ($M = Co^{II}$, Ni^{II}, Cu^{II}, Zn^{II}; H_4-**L** = H_4-**154**, H_4-**155**, H_4-**156**) with $[M'(acac)_4]$ ($M' = U^{IV}$, Th^{IV}, Zr^{IV}) in a 2:1 molar ratio and in pyridine at 110 °C affords $[M_2M'(\mathbf{L})_2]\cdot npy$. By lowering the temperature to 20 °C and to 60 °C, $[CuU(\mathbf{155})(acac)_2(py)]$ together with $[Cu_2U(\mathbf{155})_2(py)]$ and $[MU(\mathbf{156})(acac)_2(py)]$ were formed, respectively, this last identical to that synthesized from $[M(acac)_2]$ and $[U(H_2\text{-}\mathbf{156})(acac)_2]$. Noticeably, a similar treatment of $[Cu(acac)_2]$ with $[U(H_2\text{-}\mathbf{L})(acac)_2]$ (H_4-**L** = H_4-**154**, H_4-**155**) gave mixtures of the CuU and Cu_2U complexes [176].The $[M_2U(\mathbf{154})_2(py)_2]$ (M = Co, Ni, Zn) compounds are isostructural, as well as the $[Cu_2An(\mathbf{154})_2(py)]\cdot 2py$ (An = U, Th) ones. They are built up by two $\{M(\mathbf{154})\}$ units, which are linked to the central actinide ion through the phenoxide oxygen atoms at the three-position of $[\mathbf{154}]^{4-}$ and the oxygen atoms

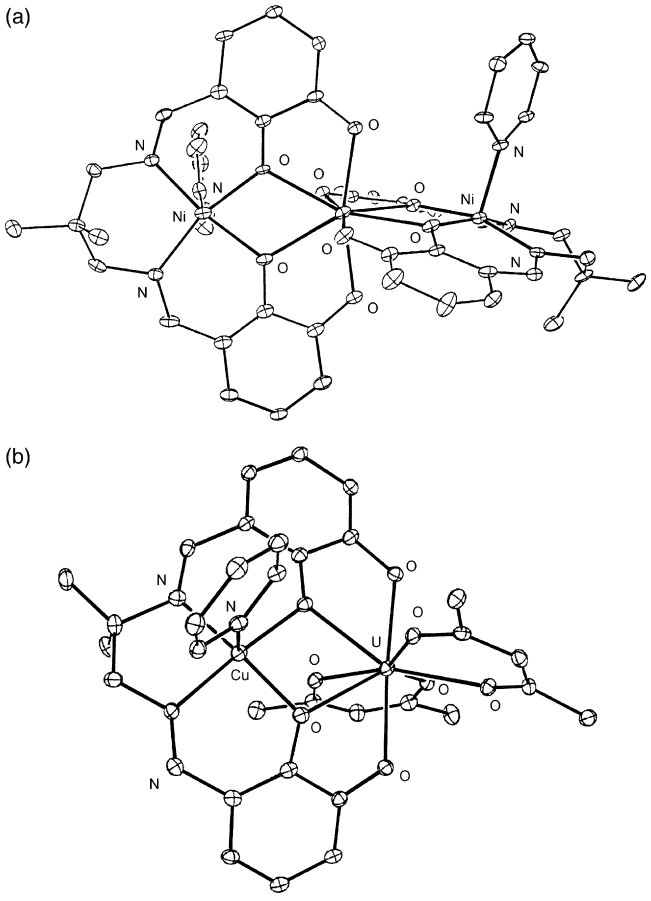

Fig. 110. Structure of $[Ni_2U(\mathbf{154})_2(py)_2]$ (a) and $[CuU(\mathbf{156})(acac)_2(py)]$ (b).

of the salicylidene fragment, which are in bridging positions between the 3d and the 5f-metal ions. The actinide(IV) ion is in a dodecahedral arrangement. The 3d ion lies in all the complexes inside the N_2O_2 cavity; in the Co_2U, Ni_2U, and Zn_2U complexes a pyridine molecule is attached to each 3d ion, which adopts a square pyramidal coordination mode. Only one copper(II) ion coordinates a pyridine molecule in the Cu_2An compounds; the other metal ion is in a square planar configuration. In all the complexes, the three metal centers are almost linear (Fig. 110a) [175]. Similar structures were found also for $[Cu_2U(\mathbf{155})_2(py)]$ and $[Zn_2U(\mathbf{156})_2(py)]$ [176].

The two copper(II) ions are not coupled in the Cu_2Zr and Cu_2Th compounds. A weak antiferromagnetic coupling was observed between the nickel(II) and the uranium(IV) ions, while a ferromagnetic interaction was revealed between the copper(II) and the uranium (IV) ions. At low temperature, when the uranium(IV) ion becomes diamagnetic, the two copper(II) ions are magnetically isolated, as demonstrated by the magnetization curve of the Cu_2U compound at 2 K. For the Co_2U complex no conclusive proposal about the absence or presence of coupling between the cobalt(II) and the uranium(IV) ions was suggested [175].In $[MU(\mathbf{156})(acac)_2(py)]$ ($M = Cu^{II}$, Zn^{II}) the 3d- and the uranium(IV) ions in the N_2O_2 and O_2O_2 cavity of $[\mathbf{156}]^{4-}$, respectively, are bridged by the two oxygen atoms of the salicylidene fragments. Four oxygen atoms from $[\mathbf{156}]^{4-}$ and four from $[acac]^-$ complete the dodecahedron around the uranium(IV)

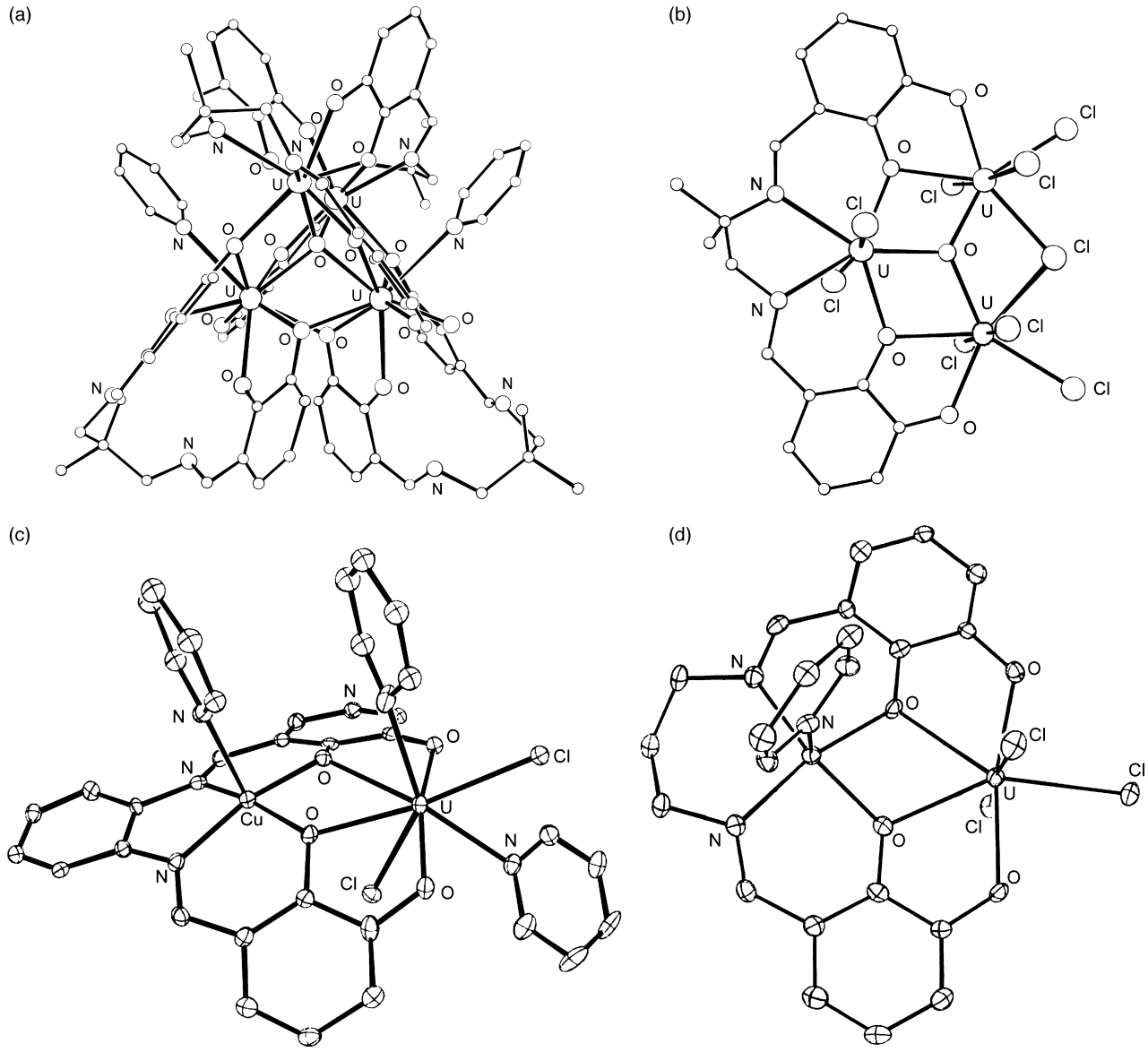

Fig. 111. Structure of $[U_4(\mathbf{154})_2(H_2\text{-}\mathbf{154})_2(O)(py)_2]^{2+}$ (a), $[U_3(\mathbf{156})(Cl)_9(O)]^{3-}$ (b), $[CuU(\mathbf{141})(Cl)_2(py)_3]$ (c) and $[CuU(\mathbf{155})(Cl)_3(py)]^{-}$ (d).

ion (Fig. 110b). The Cu···U distance in $[CuU(\mathbf{156})(acac)_2(py)]$ is 3.574 Å and the intermetallic Cu···Cu distances between two distinct molecules is 8.783 Å. In $[Cu_2U(\mathbf{L})_2]$ the Cu(Cu distances are 6.446 Å for $[\mathbf{154}]^{4-}$, 6.007 Å for $[\mathbf{155}]^{4-}$ and 5.922 Å for $[\mathbf{156}]^{4-}$. The copper(II) ion coordinating geometry and the Cu(U distance are different on going from $[\mathbf{154}]^{4-}$ or $[\mathbf{155}]^{4-}$ and $[\mathbf{156}]^{4-}$, due to the different diimino chain; these geometrical parameters seem to influence the magnetic behavior of the complexes since the copper(II)–uranium(IV) coupling in $[Cu_2U(\mathbf{L})(py)]$ (H_4-**L** = H_4-**154**, H_4-**155**) is ferromagnetic while it is antiferromagnetic in $[Cu_2U(\mathbf{156})(py)]$ and $[CuU(\mathbf{156})(acac)_2(py)]$ [176].$U(CF_3SO_3)_4$ transmetalates $[Cu(H_2\text{-}\mathbf{154})]$ in pyridine forming $[U_4(\mathbf{154})_2(H_2\text{-}\mathbf{154})_2(O)(py)_2](CF_3SO_3)_2$, while H_4-**156** and UCl_4 in pyridine give $[Hpy]_3$ $[U_3(\mathbf{156})(Cl)_9(O)]$ HpyCl·2py; in both complexes adventitious traces of oxygen and/or water probably entered the reaction flask during prolonged heating at 80 °C and 110 °C, respectively [178].In $[U_4(\mathbf{154})_2(H_2\text{-}\mathbf{154})_2(O)(py)_2](CF_3SO_3)_2$, two uranium(IV) ions are bound to the N_2O_2 donor set of the two inner Schiff base sites $[\mathbf{154}]^{4-}$, whereas the other two uranium(IV) ions are bound to the O_2O_2 donor set defining the outer site of the other two Schiff bases $[H_2\text{-}\mathbf{154}]^{2-}$. The four uranium ions are linked by the μ_4-oxo atom. Three uranium(IV) ions adopt a dodecahedral configuration; the fourth, nine coordinate uranium ion is square antiprismatic because of the coordination of an extra pyridine molecule. The U···U distances are in the range 3.646–3.937 Å (Fig. 111a) [177].In $[Hpy]_3[U_3(\mathbf{156})(Cl)_9(O)]$·Hpy·2py the seven coordinate uranium ions are in a pentagonal bipyramidal environment. One uranium(IV) ion is bound to the N_2O_2 donor set of the inner site of $[\mathbf{156}]^{2-}$ where two chlorine ions and the μ_3-oxo atom complete its coordination. The other two uranium(IV) ions are linked to two oxygen atoms of the outer site of the Schiff base. Three terminal chlorine atoms, the μ_2-chloro atom and the μ_3-oxo atom complete their coordination spheres (Fig. 111b) [177].Treatment of $[U(acac)_4]$ with H_2-**143**, H_2-**144**, H_2-**145**,

H_2-**157** gives $[U(\mathbf{L})_2]$ while $[U(\mathbf{L})(acac)_2]$ could not be isolated because of their ready disproportionation into $[U(\mathbf{L})_2]$ and $[U(acac)_4]$. The structures of $[U(\mathbf{143})_2]\cdot THF$, $[U(\mathbf{145})_2]\cdot THF$ and $[U(\mathbf{157})_2]$ present many common features, the main difference being related to the higher rigidity of $[\mathbf{143}]^{2-}$ with respect to $[\mathbf{145}]^{2-}$ or $[\mathbf{157}]^{2-}$. In all cases the metal ion is bound to the O_2O_2 donor set of the inner site of each Schiff base. The uranium ion is distorted dodecahedral in $[U(\mathbf{143})_2]$ while its coordination geometry in $[U(\mathbf{145})_2]$ and $[U(\mathbf{157})_2]$ is distorted away from the dodecahedron towards the square antiprism [178]. $[U(\mathbf{143})_2]$ and $[U(\mathbf{145})_2]$ adopt a meridional configuration in the solid state and in solution, while $[U(\mathbf{157})_2]$ exists in solution as the two equilibrating meridional and sandwich isomers and crystallizes in the meridional isomeric form [178].While $[U(acac)_4]$ and H_4-**156** afford the expected compound $[U(H_2\text{-}\mathbf{156})(acac)_2]$, H_4-**141** or H_4-**158** and $[U(acac)_4]$ are reproducibility transformed into $[U_3(\mathbf{141})(H\text{-}\mathbf{141})_2(acac)_2]$ or $[U_4(H\text{-}\mathbf{158})_4(H_2\text{-}\mathbf{158})_2]$, respectively [178]. In $[U(H_2\text{-}\mathbf{156})(acac)_2]$ the slightly distorted dodecahedral uranium(IV) ion is located in the N_2O_2 plane of $[H_2\text{-}\mathbf{156}]^{2-}$ and further bound to the four oxygen atoms of the $[acac]^-$ groups. $[H_2\text{-}\mathbf{156}]^{2-}$ adopts an umbrella configuration [177].In $[U_3(\mathbf{141})(H\text{-}\mathbf{141})_2(acac)_2]\cdot 3THF$, one distorted square antiprismatic uranium(IV) ion is bound to the inner N_2O_2 site of one Schiff base, to the terminal oxygen atom of another Schiff base and to two acetylacetonate ligands; a second distorted square antiprismatic uranium(IV) ion is bound to the inner N_2O_2 sites of the other two Schiff bases and the third distorted dodecahedral uranium(IV) ion, which bridges these two subunits, is bound to the outer O_4 site of one Schiff base and to the oxygen atoms of the other Schiff bases [178].$[U_4(H\text{-}\mathbf{158})_4(H_2\text{-}\mathbf{158})_2]$ can be viewed as two $\{U_2(H\text{-}\mathbf{158})_2\}$ moieties bridged by two distorted and elongated $[H_2\text{-}\mathbf{158}]^{2-}$ ligands. In contrast to $[U_3(\mathbf{141})(H\text{-}\mathbf{141})_2(acac)_2]$, the four uranium ions in $[U_4(H\text{-}\mathbf{158})_4(H_2\text{-}\mathbf{158})_2]$ are in rather similar dodecahedral environments, each of them being bound to the N_2O_2 donor atoms of the inner site of a Schiff base $[H\text{-}\mathbf{158}]^{3-}$, to the two oxygen atoms of the other Schiff base in the subunit, and to two oxygen atoms from the remaining bridging Schiff bases $[H_2\text{-}\mathbf{158}]^{2-}$. The difference between the two uranium ions in each dinuclear subunit results from the dissymmetric ligation mode of these two bridging Schiff bases $[H\text{-}\mathbf{158}]^{2-}$, each being linked to one uranium(IV) ion via its two oxygen atoms, and to the other uranium ion via one oxygen atom only. Each of the six Schiff base ligands has one non-coordinated oxygen atom, two coordinated to one metal ion and one bridging [179].Treatment of UCl_4 with one equivalent of H_2-**157** in tetrahydrofuran leads to $[U(\mathbf{157})(Cl)_2(THF)]$, alternatively synthesized by reaction of UCl_4 with an excess of $[U(\mathbf{157})_2]$. In pyridine $[U(\mathbf{157})(Cl)_2(py)_2]$ was obtained, where the uranium(IV) ion adopts a distorted dodecahedral configuration, while in $[U(\mathbf{L})(Cl)_2(THF)]$ it is seven coordinate in a quite perfect pentagonal bipyramidal environment with the two chlorine atoms in apical positions. On the contrary, none of the reactions of UCl_4 and H_4-**155**, H_4-**156**, H_4-**158** in tetrahydrofuran or pyridine affords the mononuclear complexes $[U(H_2\text{-}\mathbf{L})(Cl)_2(solv)_x]$, but polynuclear species as found for $[Hpy]_2$ $[U_4(\mathbf{155})_2(H_2\text{-}\mathbf{155})(Cl)_6]\cdot 2HpyCl\cdot 2py$. The cation $[U_4(\mathbf{155})_2(H_2\text{-}\mathbf{154})_2(Cl)_6]^{2-}$ is built up from two dinuclear subunits which are bridged by two elongated Schiff bases. One distorted square antiprismatic uranium(IV) ion of each submit is bound to the four atoms of the inner N_2O_2 site of Schiff base $[\mathbf{155}]^{4-}$. One of the bridging Schiff bases $[H_2\text{-}\mathbf{154}]^{2-}$ coordinates to this uranium ion through one oxygen atoms which is also bound to the other uranium(IV) ion, which is in a distorted dodecahedral environment. The other Schiff base $[H_2\text{-}\mathbf{154}]^{2-}$ is coordinated to this uranium(IV) ion via non-bridging two oxygen atoms one of this oxygen atoms is protonated. The outer O_4 cavity of the Schiff base $[\mathbf{155}]^{2-}$ is occupied by the other uranium(IV) ion, which is further bound to two chloride ions and to the bridging and terminal oxygen atoms of a Schiff base $[H_2\text{-}\mathbf{154}]^{2-}$; again one oxygen atom is protonated [180].The transmetalation of $[Zn(H_2\text{-}\mathbf{155})]$ by UCl_4 in pyridine affords $[U_4(\mathbf{155})_2(H_2\text{-}\mathbf{155})_2(Cl)_4(py)_2]$, with a structure very similar to that of $[U_4(\mathbf{155})_2(H_2\text{-}\mathbf{155})_2(Cl)_6]^{2-}$, the major difference being the substitution of one chloride anion bound to one uranium(IV) ion with a pyridine molecule. When H_4-**155** was replaced with H_4-**158** in its reaction with UCl_4, $\{[Hpy]_2$ $[U_4(\mathbf{158})_2(H_2\text{-}\mathbf{158})_2(Cl)_6]$ $[U_4(\mathbf{158})_2(H_2\text{-}\mathbf{158})_2(Cl)_4(py)_2]\}\cdot 16py$ was obtained [180].The similar treatment of $[Cu(H_2\text{-}\mathbf{156})]$ with UCl_4 in pyridine affords $[Hpy]_2$ $[U_6(\mathbf{156})_4(Cl)_{10}(py)_4]\,6py$, where again two terminal and two bridging Schiff base ligands occur. Two uranium(IV) ions occupy respectively the inner N_2O_2 and outer O_2O_2 sites of each terminal Schiff base ligand which adopts a strongly curved umbrella shape. The two bridging Schiff-base ligands contribute three oxygen donor atoms to one of these uranium ions and only one to oxygen atom the other uranium ion. This shift of each bridging Schiff base ligand with respect to terminal one is related to its further coordination to a third uranium ion via one oxygen and two nitrogen donor atoms, and to its symmetric uranium ion via two oxygen atoms. As a result, the hexanuclear species is stretched, the longest U(U distance bearing 19.699 Å (13.57 Å in $[U_4(\mathbf{155})_2(H_2\text{-}\mathbf{155})_2(Cl)_4(py)_2]$). Two uranium ions complete their eight coordination sphere with three chloride ions, other two metal ions with two chloride ions. Two of these metal ions adopt a distorted square antiprismatic configuration, while the other two uranium ions are found in a distorted dodecahedral environmental. Two pyridine molecules are bound to the remaining two uranium ions which are nine coordinate in a distorted tricapped trigonal prismatic environment [180].Also $[M_2U(\mathbf{L})_2(py)_n]$ ($H_4\text{-}\mathbf{L} = H_4\text{-}\mathbf{141}$, $H_4\text{-}\mathbf{153}$, $H_4\text{-}\mathbf{158}\cdots H_4\text{-}\mathbf{161}$; (M=Cu,Zn) and $[Cu_2Th(\mathbf{L})_2]$ ($H_4\text{-}\mathbf{L} = H_4\text{-}\mathbf{153}$, $H_4\text{-}\mathbf{156}$) have been prepared by the reaction of $[M(H_2\text{-}\mathbf{L})]$ with $[An(acac)_4]$ in a 2:1 molar ratio in refluxing pyridine [180], their structure resembling that of $[M_2An(\mathbf{154})_2(py)_n]$ (n = 1, 2) above reported [176]. The trinuclear entities may be considered to be magnetically isolated. For the complexes of $[\mathbf{141}]^{4-}$, $[\mathbf{153}]^{4-}$, $[\mathbf{156}]^{4-}$, $[\mathbf{161}]^{4-}$, $[\mathbf{159}]^{4-}$ with the smallest Cu···U distances, the Cu^{II}–U^{IV} and the Cu^{II}–Cu^{II} coupling is antiferromagnetic and weak antiferromagnetic, respectively while for, the complexes of $[\mathbf{154}]^{4-}$, $[\mathbf{155}]^{4-}$, $[\mathbf{158}]^{4-}$and $[\mathbf{160}]^{4-}$ with the largest Cu···U distances, the Cu^{II}–U^{IV} coupling is ferromagnetic and no interaction is

observed between the copper(II) ions. The magnetic behavior of the $[Cu_2Th(\mathbf{L})_2]$ compounds ($\mathbf{L} = [\mathbf{153}]^{4-}$, $[\mathbf{156}]^{4-}$) in which the thorium(IV) ion is diamagnetic confirms the presence of weak intramolecular antiferromagnetic coupling between the copper(II) ions [180].

Reactions of $[M(H_2\text{-}\mathbf{L})]$ ($M = Cu^{II}$, Zn^{II}; $H_4\text{-}\mathbf{L} = H_4\text{-}\mathbf{141}$, $H_4\text{-}\mathbf{152}$, $H_4\text{-}\mathbf{154}$, $H_4\text{-}\mathbf{155}$, $H_4\text{-}\mathbf{161}$) with one equivalent of UCl_4 in refluxing pyridine afford $[MU(\mathbf{L})(Cl)_2(py)_3]$ and/or $[Hpy][MU(\mathbf{L})(Cl)_3(py)]$ [180]. In all the CuU complexes the copper(II) and uranium(IV) ions occupy, respectively, the N_2O_2 and O_2O_2 cavities of the Schiff base ligand and are bridged by the two oxygen atoms of the salicylidene fragments; the copper(II) ion adopts a square pyramidal coordination mode. In $[CuU(\mathbf{L})(Cl)_2(py)_3]$ ($\mathbf{L} = [\mathbf{141}]^{4-}$, $[\mathbf{161}]^{4-}$), the uranium(IV) ion is in a dodecahedral environment (Fig. 111c), while in $[CuU(\mathbf{L})(Cl)_3(py)]^-$ ($\mathbf{L} = [\mathbf{152}]^{4-}$, $[\mathbf{154}]^{4-}$, $[\mathbf{155}]^{4-}$) the displacement of two pyridine ligands with a chloride ion occurs, and the seven coordinate uranium(IV) ion is in a pentagonal bipyramidal configuration (Fig. 111d) [180].

In $[Hpy]_2[NiU(\mathbf{152})(Cl)_3(py)_2][NiU(\mathbf{152})(Cl)_3(py)]$ two different anionic complexes occur with two and one pyridine molecules coordinated to an octahedral and a square pyramidal nickel(II) ion, respectively. Comparison of the related $Cu^{II}U^{IV}$ and $Ni^{II}U^{IV}$ complexes indicate that the coordination geometry of the uranium(IV) ion is quite identical in all the complexes [180].

In the presence of three equivalents of $AgNO_3$ in pyridine at 20 °C, $[Cu_2U^{IV}(\mathbf{155})_2(py)_2]$ was partially transformed into $[Cu_2U^{V}(\mathbf{155})_2(py)_2](NO_3)$, which was sensitive to heat, being converted back into the uranium(IV) congener. Crystals of $[Cu_2U^{IV}(\mathbf{155})_2(py)_2]$ $[Cu_2U^{V}(\mathbf{155})_2(py)_2](NO_3)\cdot 4py$ were deposited from a pyridine solution at 80 °C. The synthesis of $[Zn_2U^{V}(\mathbf{155})_2(py)_2](NO_3)$ was easier than that of the copper(II) analogue, not requiring an excess of $AgNO_3$; this $Zn_2^{II}U^{V}$ complex proved to be stable up to 80 °C towards the $U^V \rightarrow U^{IV}$ reduction. A refluxing pyridine solution of the complex deposited $[Zn_2U^{IV}(\mathbf{155})_2(py)_2][Zn_2U^{V}(\mathbf{155})_2(py)_2](NO_3)\cdot 4py$. In contrast, oxidation of $[Zn_2U^{IV}(\mathbf{160})_2(py)_2]$ was totally achieved upon addition of one equivalent of $AgNO_3$ in pyridine, and $[Zn_2U^{V}(\mathbf{160})_2(py)_2](NO_3)\cdot py$ was isolated in high yield. Treatment of $[Zn(H_2\text{-}\mathbf{155})]$ with $U(CF_3SO_3)_3$ in pyridine afforded a mixture of $[ZnU^{IV}(\mathbf{155})(CF_3SO_3)_2(py)_x]$ and $[Zn_2U^{IV}(\mathbf{155})_2(py)_x]$. Heating the mixture under reflux gave $[Hpy][Zn_2U^{IV}(\mathbf{155})_2(py)_2](CF_3SO_3)$ together with a few crystals of $[Zn_2U^{V}(\mathbf{155})_2(py)_2](CF_3SO_3)\cdot THF$, this uranium(V) complex likely resulting from oxidation by adventitious traces of air [180].

The crystals of $[M_2U^{IV}(\mathbf{155})_2(py)_2]$ $[M_2U^{V}(\mathbf{155})_2(py)_2](NO_3)\cdot 4py$, isomorphous for $M{=}Zn^{II}$ and Cu^{II} contain discrete neutral and cationic trinuclear complexes $[M_2U(\mathbf{155})_2(py)_2]^{0,+1}$. The attribution of the uranium oxidation state is unambiguous in view of the U^V–O distances, shorter then the U^{IV}–O ones [180].

The condensation of diethylenetriamine and 3-methoxy-2-hydroxybenzaldehyde affords H_2-**161a**, which reacts with $Ln(NO_3)_3\cdot 6H_2O$ ($Ln{=}La^{III}$, Nd^{III}, Eu^{III}, Tb^{III}) to form the isostructural complexes $[Ln(H_2\text{-}\mathbf{161a})(NO_3)_3]$ with the lanthanide(III) ion ten coordinate with four oxygen atoms from H_2-**161a** and six oxygen atoms from three bidentate nitrato anions. The phenol oxygen atoms are deprotonated, the hydrogen protons being migrated to the two iminic nitrogen atoms (Fig. 112a) [181].

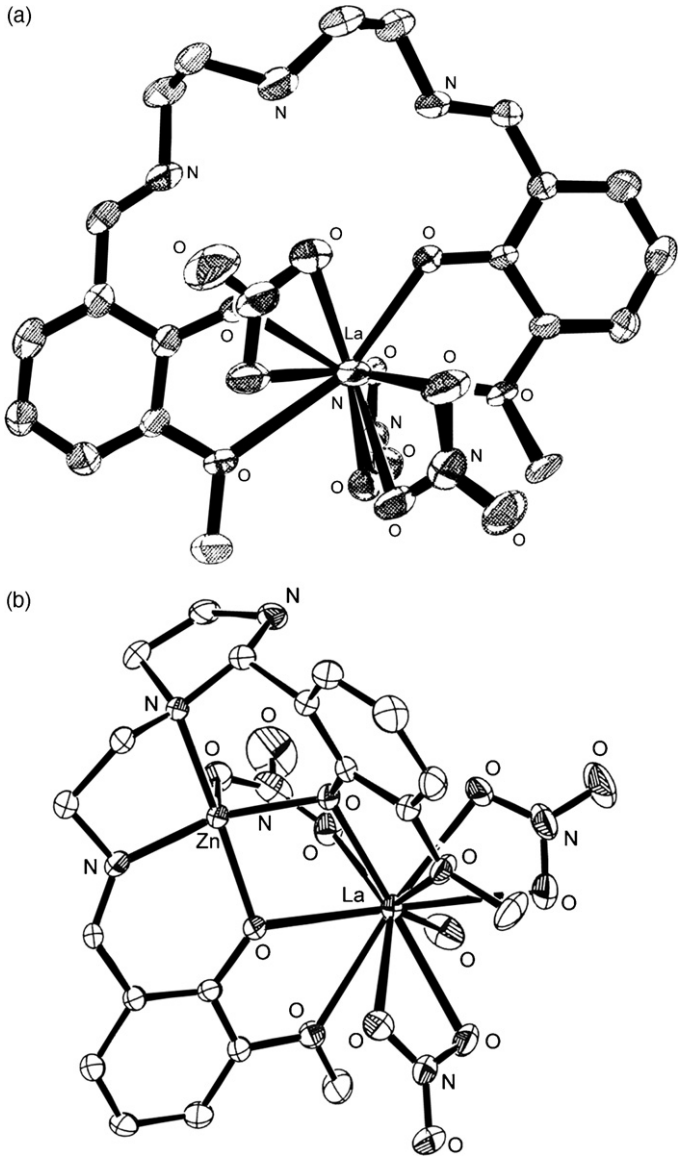

Fig. 112. Structure of $[La(H_3\text{-}\mathbf{161a})(NO_3)_3]$ (a) and $[LaZn(H\text{-}\mathbf{161b})(\mu\text{-}NO_3)(NO_3)_2(H_2O)]^+$ (b).

The terbium(III) complex shows strong emission when excited with 340 nm in the solid state, indicating that H_2-**161a** is a good antenna to absorb energy and transfer it to the terbium(III) ion. The luminescence intensities for the terbium complex, weaker on going from acetonitrile, dioxane, methanol to dimethylformamide solution, may be due to the coordinating effects of solvents. On the contrary, in the solutions of the europium(III) complex, the luminescence characteristic emission wavelengths of the europium ion were not observed [181].

As already observed for the [2 + 2] macrocyclic ligands derived from the [2 + 2] condensation of 2,6-diformyl-4-substituted phenol and 1,5-diamino-3-azapentane [10,18], a ring contraction of the coordination cavity of H_2-**161a** occurs with

the consequent formation of H_2-**161b**, as proved for [LaZn(H-**161b**)(μ-NO_3)(NO_3)$_2$(L)](NO_3) (L = H_2O, C_2H_5OH), obtained by the condensation the appropriate formyl- and amine-precursors in the presence of $Zn(CH_3COO)_2{\cdot}H_2O$, followed by reacting the resulting mononuclear zinc(II) complex with $La(NO_3)_3{\cdot}6H_2O$. The five coordinate zinc(II) ion resides into the inner N_2O_2 site of the Schiff base while the ten coordinate lanthanum(III) ion resides into the outer O_2O_2 site. The non-coordinating nitrogen atom of the Schiff base is protonated (Fig. 112b) [181].

The similar reaction with copper(II) acetate and lanthanum(III) nitrate affords {[Cu_2(H-**161a**)$_2$]$_2$[$La(NO_3)_6$](NO_3)}, where an aggregation of two dinuclear entities [Cu_2(H-**161a**)$_2$]$^{2+}$, one [$La(NO_3)_6$]$^{3-}$ anionic complex and a free nitrate anion occurs. In [Cu_2(H-**161a**)$_2$]$^{2+}$ the copper(II) ions are tetracoordinate in a N_2O_2 environment, formed by one phenoxy oxygen and one iminic nitrogen of two different Schiff bases [H-**161a**]$^-$ while the methoxy oxygen remains uncoordinated. The central amine nitrogen of both the Schiff bases is not coordinated and protonated [181].

The search for neutral ditopic receptors capable of simultaneous complexation of both of the counter ions in a target salt is a subject of great current interest in the general field of molecular recognition. Recognition of hard anions is ensured by strong binding to the hard Lewis acidic uranyl(IV) center in the equatorial plane of the uranium, whereas cation-π interactions are established between the aromatic sidearms and the cation partner of the ion pair [182].

[UO_2(**162a**)(CH_3OH)], [UO_2(**162b**)(CH_3OH)] and [UO_2(**162c**)(CH_3OH)], used as ditopic receptors towards tetralkylammonium and larger alkali metal halides, form strong complexes with [$N(CH_3)_4$](Cl) and [$N(C_4H_9)_4$](Cl). The affinities of both salts towards [UO_2(**162b**)(CH_3OH)] are much higher than towards [UO_2(**162a**)(CH_3OH)]. Binding constants of salts with bromide or iodide are lower by one to two orders of magnitude than those of the chloride analogue. The strong interaction of chloride with the metal centre is responsible for a major contribution to the driving force for complexation; a smaller, yet significant contribution to the stability of complexes with [UO_2(**162b**)(CH_3OH)] arises from cation–π interactions of the cations with the aromatic pendants [183].

RbCl, CsCl, and CsF form the isomorphous complexes {M[UO_2(**162b**)(Cl)]}$_2$, where each uranyl(VI) ion strongly coordinates a chloride ion in its equatorial plane. Two [UO_2(**162b**)(Cl)]$^-$ anions are connected through coordination to alkali metal cations which are placed above the aromatic sidearms similarly to the analogous uranyl(VI) complex with [$N(CH_3)_4$](Cl). Rubidium and cesium cations are similarly coordinated to six oxygen atoms, three from each receptor, thus creating a pseudo-crown ether-like environment for the cation. Additionally, each metal ion in the dimeric unit is linked to both halide ions and, most importantly, to two aromatic sidearms, one from each of the receptors (Fig. 113) [183].

[UO_2(**162a**)(CH_3OH)] does not act as receptor of various alkali metal salts; however, it shows successful 4:2 complexation with CsCl forming different structure, in which one uranyl(VI) complex binds to chloride and the other to a solvent methanol molecule, and both participate in cesium complexation. Four {UO_2(**162c**)} units are assembled in a capsule-like arrangement in which a {CsCl}$_2$ moiety is enclosed. Similarly, in {Cs[UO_2(**162d**)(F)]·$CHCl_3$}, obtained by slow evaporation of a solution of [UO_2(**162d**)·(CH_3OH)] and CsF, two [UO_2(**162d**)(F)]$^-$ anions form a [2 + 2] arrangement with two cesium cations. The fluoride anions are bound in the equatorial plane of the uranyl(VI) centers, and the negatively charged receptor-fluoride units are connected via coordination to metal cations situated in close proximity to the aromatic side arms. Whereas both side arms of [UO_2(**162b**)(CH_3OH)] establish cation–π interactions with the cesium ion, only one side arm of [UO_2(**162d**)(CH_3OH)] interacts with the cesium ion. The contribution of the side arms in the intramolecular assembly with the less preorganized complex [UO_2(**162d**)(CH_3OH)] is significantly lessened, which renders the cesium ion accessible to ligation of a competing donor, even as weak as chloroform [183].

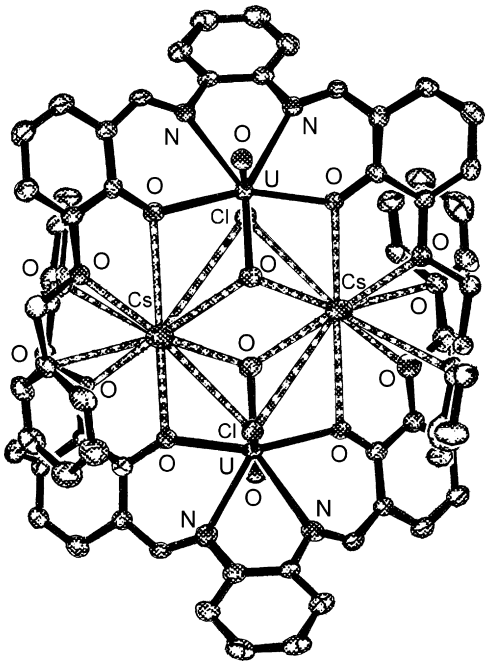

Fig. 113. Structure of {Cs[UO_2(**162b**)(Cl)]}$_2$.

The less ordered structure of the uranyl(VI) complex of [**162d**]$^{2-}$ compared to that of [**162b**]$^{2-}$ is proved in the crystal structures of [UO_2(**162b**)(CH_3OH)] where the side arms are turned inward in a quasimacrocyclic arrangement capable of enclosing the methanol guest through CH···π interactions. [UO_2(**162b**)(CH_3OH)] is rigid enough to retain essentially the same concave shape in different complexes, regardless of the guest coordinated to the uranyl center. In contrast the [**162d**]$^{2-}$ unit in [UO_2(**162d**)(CH_3OH)] adopts a less regular, more open conformation, in which the side arms are completely turned away from the core of the receptor, do not form CH···π connection with the complexed methanol [183].

The condensation of 4,4′-diaminodiphenylmethane and 3-methoxy- or 3-ethoxysalicylaldehyde produces H_2-**162e** and H_2-**162f**, which give rise to $[Cu_2(\mathbf{L})_2]$ when mixed with $Cu(NO_3)_2{\cdot}H_2O$. These copper(II) precursors react with $Gd(NO_3)_3{\cdot}6H_2O$ to form $[Cu_2Gd_2(\mathbf{L})_2(NO_3)_6]$ whose tetranuclear nature was inferred by FAB mass spectra. The magnetic data shows that the Cu_2Gd_2 complexes behave as two independent CuGd pairs, each presenting a ferromagnetic interaction ($J = 4.78$ and $4.6\,cm^{-1}$). Very weak additional antiferromagnetic interactions, probably originating from intra- and/or intermolecular π stacking, have been suggested below 8 K. The field dependence of the magnetization for $[Cu_2Gd_2(\mathbf{162f})_2(NO_3)_6]$ at 2.0 K confirms the ferromagnetic nature of the Cu–Gd interactions and the assembling of the corresponding entities as two independent pairs [184].

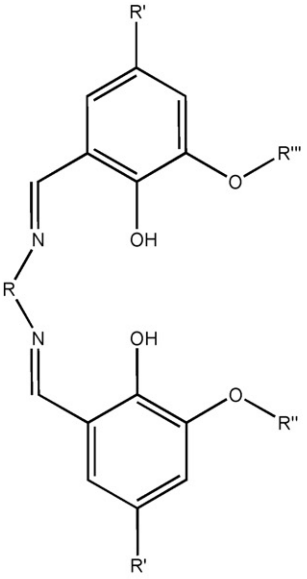

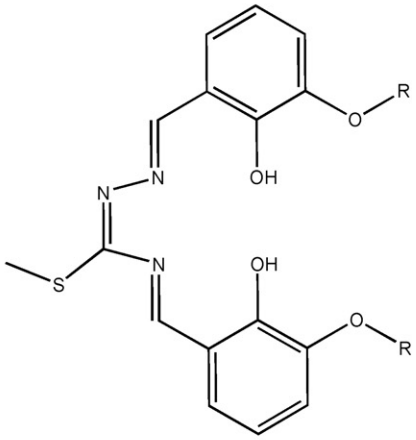

	R
H_2-**151**	CH_3
H_2-**152**	C_2H_5

	R	R'	R''	R'''
H_2-**137**	$(CH_2)_2$	H	CH_3	CH_3
H_2-**138**	$(CH_2)_2$	Br	CH_3	CH_3
H_2-**138a**	$(CH_2)_3$	Br	CH_3	CH_3
H_2-**139**	$(CH_2)_2$	p-$CH_3C_6H_4$	CH_3	CH_3
H_2-**140**	o-C_6H_4	Br	CH_3	CH_3
H_4-**141**	o-C_6H_4	H	H	H
H_2-**142**	$(CH_2)_3$	H	CH_3	CH_3
H_2-**143**	o-C_6H_4	H	CH_3	CH_3
H_2-**143a**	o-C_6H_4	p-$CH_3C_6H_4$	CH_3	CH_3
H_2-**144**	$CH_2C(CH_3)_2CH_2$	H	CH_3	CH_3
H_2-**145**	$C(CH_3)_2CH_2$	H	CH_3	CH_3
H_2-**146**	$(CH_2)_2$	H	C_2H_5	C_2H_5
H_2-**147**	$(CH_2)_3$	H	C_2H_5	C_2H_5
H_2-**148**	$C(CH_3)_2CH_2$	H	C_2H_5	C_2H_5
H_2-**149**	o-C_6H_{10}	H	C_2H_5	C_2H_5
H_2-**150**	o-C_6H_4	H	C_2H_5	C_2H_5
H_4-**153**	$(CH_2)_2$	H	OH	OH
H_4-**154**	$CH_2C(CH_3)_2CH_2$	H	OH	OH
H_4-**155**	$(CH_2)_3$	H	OH	OH
H_4-**156**	$C(CH_3)_2CH_2$	H	OH	OH
H_2-**157**	o-$CH_2C_6H_4$	H	C_2H_5	C_2H_5
H_4-**158**	o-$C_6H_4CH_2$	H	OH	OH
H_4-**159**	3,4-$(CH_3)_2C_6H_2$	H	OH	OH
H_4-**160**	$(CH_2)_4$	H	OH	OH
H_4-**161**	o-C_6H_{10}	H	OH	OH
H_2-**162a**	o-C_6H_4	H	H	H
H_2-**162b**	o-C_6H_4	H	$OCH_2C_6H_5$	$OCH_2C_6H_5$
H_2-**162c**	o-C_6H_4	H	$OCH_2C_6H_5$	H
H_2-**162d**	C_2H_4	H	$OCH_2C_6H_5$	$OCH_2C_6H_5$
H_2-**162e**	$C_6H_4CH_2C_6H_4$	H	OCH_3	OCH_3
H_2-**162f**	$C_6H_4CH_2C_6H_4$	H	OC_2H_5	OC_2H_5

The formyl- or keto-precursors H_2-**163** react with $[TiO(acac)_2]$ and Li_2CO_3 to form $Li_2[Ti(\mathbf{163})_3]$ which can coordinate lithium ions in a second recognition event, giving the triply bridged dinuclear helicate-type complexes $Li[Li_3Ti_2(\mathbf{163})_6)]$. According to NMR and mass spectroscopy data both the mononuclear and the polynuclear complexes are observed in solution as well as in the gas phase. In the crystal, however, only $Li[Li_3Ti_2(\mathbf{163})_6)]$ was found. In $Li[Li_3Ti_2(\mathbf{163})_6]$ (R = H, C_2H_5), two triscatecholate titanium(IV) units $[Ti(\mathbf{163})_3]^{2-}$ are formed with the aldehydes all oriented in the same direction. Three pseudo-tetrahedrally coordinated lithium cations are bridging two $[Ti(\mathbf{163})_3]^{2-}$ moieties by binding to an internal catecholate oxygen and a carbonyl oxygen atom of each Ti-complex moiety giving rise to $[Li_3Ti_2(\mathbf{163})_6]^-$. The formation of $[Li_3Ti_2(\mathbf{163})_6]^-$ is highly specific for lithium counter ions. Sodium and potassium ions did not mediate polynuclear formation [185].

In $Na_4[Ti_2(\mathbf{163a})_3]\cdot 7DMF\cdot H_2O$ the two pseudo-octahedral titanium(IV) ions are bridged by three $[\mathbf{163a}]^-$ ligands. One of these triscatecholate units has the nitrogen atoms oriented to the outside of the helicate cavity, while the two other azine units have one nitrogen atom oriented to the inside and one to the outside of the cavity. Two distorted octahedral sodium ions are bound to two internal catechol oxygen atoms of one of the complex units and to a nitrogen atom. In addition one dimethylformamide molecule is binding from the outside of the cavity to each of the sodium ions and one water and one dimethylformamide molecule are bridging the two cations. Two additional sodium ions are bound to external oxygen atoms of the helicates and are bridged by dimethylformamide molecules to lead to the polymeric chain $\{[Na_2(DMF)_3][Ti_2Na_2(\mathbf{163a})_3(DMF)_3(H_2O)]\}_n$ in the solid state (Fig. 114a) [185].

H_4-**163b**···H_4-**163q**, similarly prepared by condensation of 2,3-dihydroxybenzaldehyde and diamine containing appropriate spacers, undergo tautomerisation and show thermochromic and photochromic behavior: when these solids are cooled in liquid nitrogen, a fading of the intense color was observed. At low temperature the hydroxy-imine form is the preferred tautomer, while at higher temperature the more

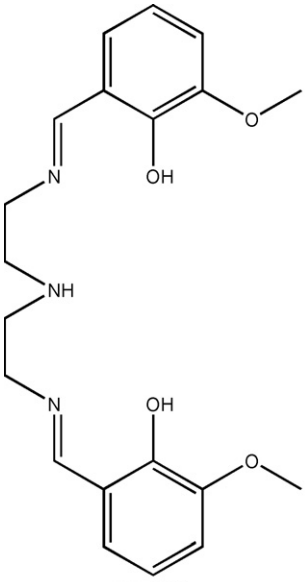

H_2-**161a**

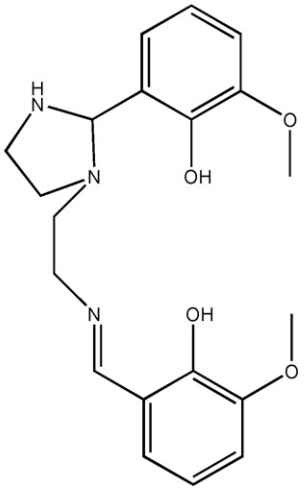

H_2-**161b**

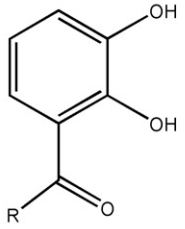

H_2-**163** R= H, CH_3, C_2H_5, n-C_3H_7, n-C_4H_9, n-C_5H_{11}, n-C_6H_{13}, n-C_7H_{15}, n-C_8H_{17}, n-$C_{10}H_{21}$, n-$C_{11}H_{23}$, i-C_3H_7, C_6H_5

The azine-bridged dicatechol H_4-**163a**, prepared by condensation of 2,3-dihydroxybenzaldehyde and hydrazine hydrate, forms the triple-stranded dinuclear helicates $M_4[Ti_2(\mathbf{163a})_3]$ with $[TiO(acac)_2]$ in the presence of M_2CO_3 ($M = Li^I$, Na^I, K^I) [185].

colored keto-amine form is favored. The structure at 223 K of H_4-**163e** shows that the aliphatic–$(CH_2)_4$-spacer adopts a zigzag conformation and connects the two catechol-imine units in the keto-amine tautomeric form where the proton of the 2-hydroxygroup is transferred to the nitrogen [186].

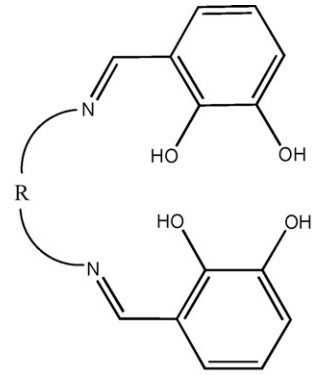

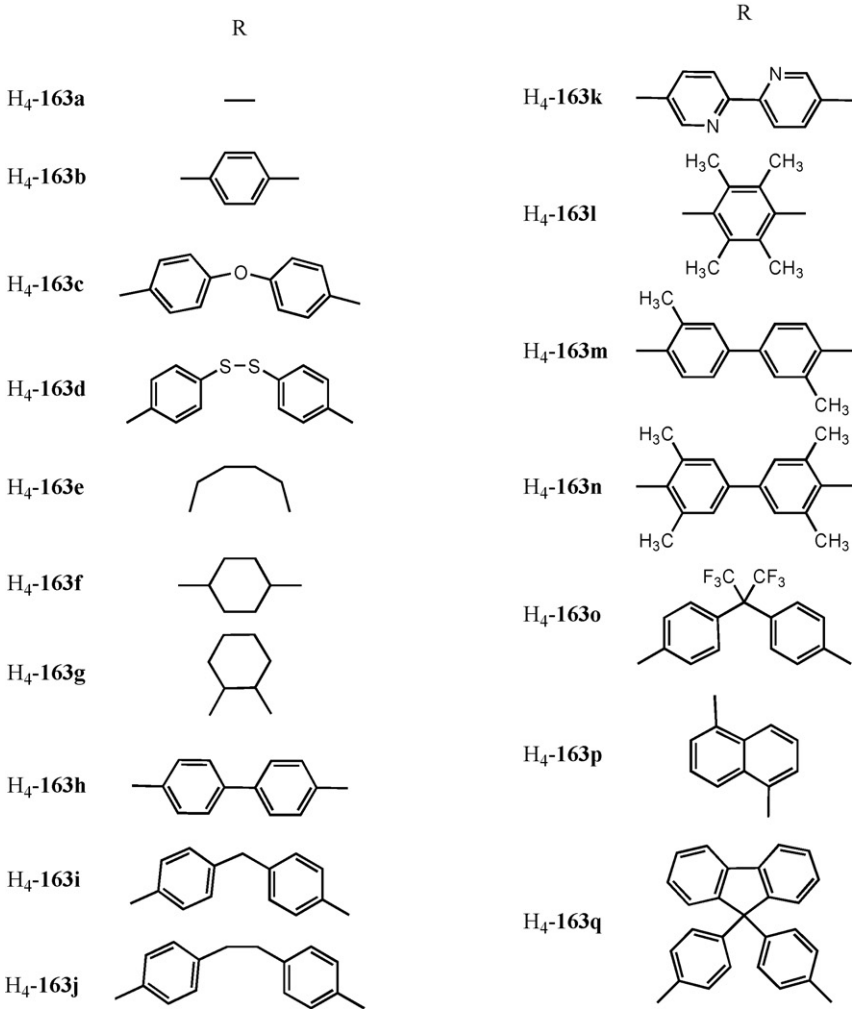

The synthetic procedure above reported for $M_4[Ti_2(\mathbf{163a})_3]$ affords also the triple stranded dinuclear helicates $M_4[Ti_2(\mathbf{L})_3]$ (H_4-**L** = H_4-**163b**···H_4-**163j**) with each imine moiety directed towards the outside of the cavity of the helicate. However, an inward orientation of the imine can be observed, if coordination to an internal alkali metal cation takes place. In solution a dynamic exchange between encapsulated and free countercations takes place and therefore a conformation with the C=N double bonds directed outside the cavity should be the preferred one [186].

Due to the rigidity of the spacer, the Schiff base ligands in $K_2[K_2Ti_2(\mathbf{163b})_3(DMF)_6(H_2O)]$ wrap around the two titanium ions, possessing only a slight helical twist. The geometry at the titanium(IV) centers, 12.547 Å apart, is in between a distorted octahedron and a distorted trigonal prism. Two potassium ions are encapsulated in the large internal cavity, binding to the

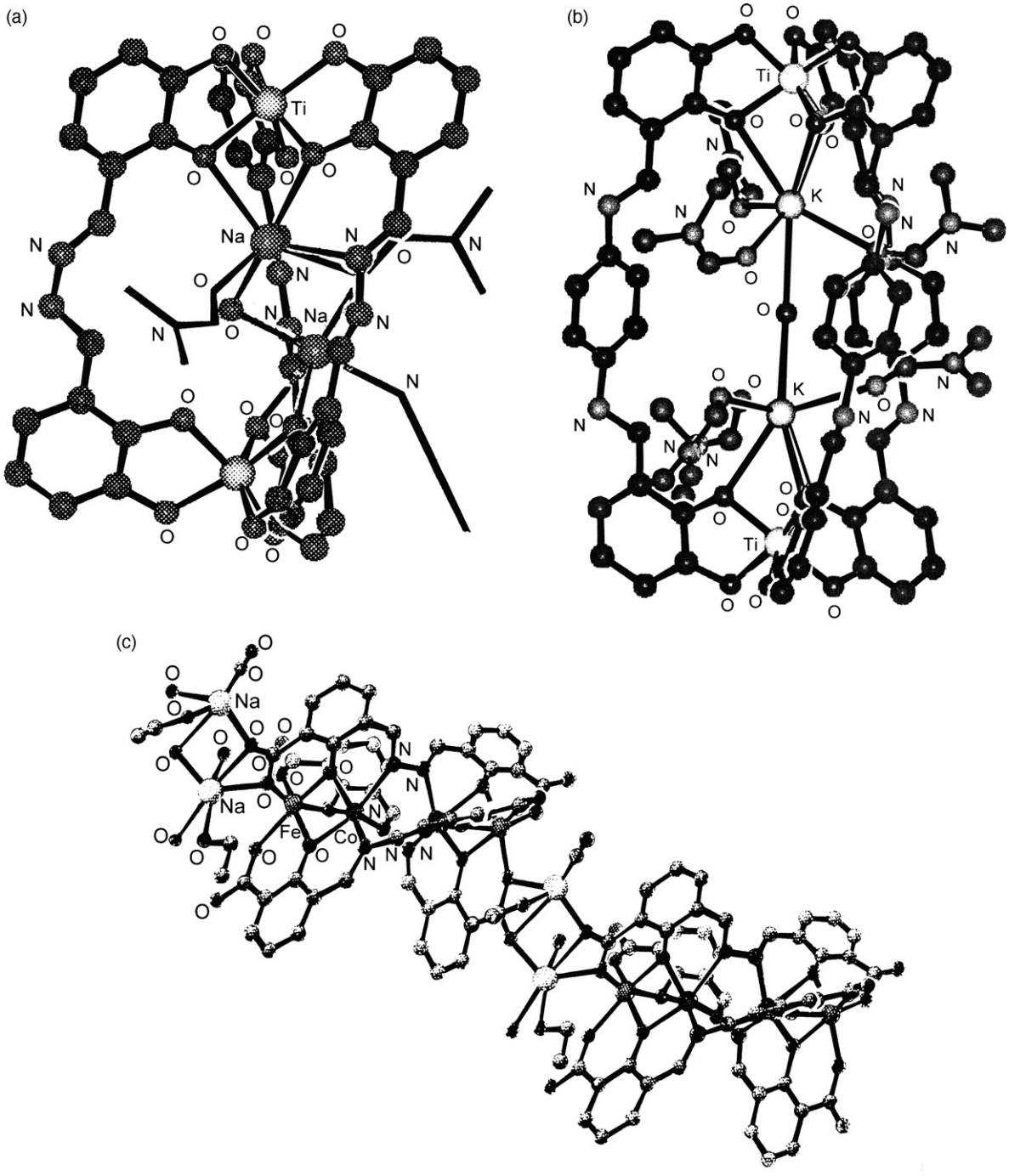

Fig. 114. Structure of $[Ti_2Na_2(\mathbf{163a})_3(DMF)_3(H_2O)]^{2-}$ (a), $[Ti_2K_2(\mathbf{163b})_3(DMF)_6(H_2O)]^{2-}$ (b) and $[Co_2^{II}Fe_2^{III}Na_2^{I}(\mathbf{163'})_3(H_2O)_4(C_2H_5OH)_2]_\infty$ (c).

internal oxygen atoms of the catecholate ligands. Their coordination sphere is saturated by three dimethylformamide molecules and by a water molecule, bridging the two encapsulated cations (Fig. 114b) [186].

Also in $Na_2[Na_2Ti_2(\mathbf{L})_3]\cdot$nDMF ($\mathbf{L} = [\mathbf{163f}]^{4-}$, $[\mathbf{163h}]^{4-}$, $[\mathbf{163i}]^{4-}$, $[\mathbf{163j}]^{4-}$) two sodium cations are encapsulated in the helicate and additionally bound to two water and to three dimethylformamide molecules. Again, the three $[\mathbf{L}]^{4-}$ ligands slightly wrap around the titanium(IV) ions. In $Na_2[Na_2Ti_2(\mathbf{163f})_3]$ the cyclohexyl rings adopt a chair-type conformation. The two titanium ions, 12.475 Å apart, and the ligands lead to a helix with a somewhat more pronounced helical twist compared to the phenyl bridged derivative. In $Na_2[Na_2Ti_2(\mathbf{163h})_3]\cdot$13DMF the two titanium ions are at a distance of 16.946 Å. The total length of the cylindrical complex is approximately 2.1 nm. The $[\mathbf{163h}]^{4-}$ ligands adopt a conformation with the imine hydrogen atoms pointing into the cavity, directed towards the catecholate oxygen atoms. In $Na_2[Na_2Ti_2(\mathbf{163i})_3]\cdot$10DMF, 2.05 nm long, the titanium(IV) ions are 14.84 Å apart. In addition to the interaction with two

internal catecholate oxygen atoms and two or three dimethylformamide molecules, respectively, the two sodium ions also bind to the imine nitrogen atoms of one of the three [**163i**]$^{4-}$ ligands, enforcing an "inward" orientation of the imines of this strand [186,187]. Finally, in $Na_2[Na_2Ti_2(\mathbf{163j})_3]\cdot 13DMF$ the obtained supramolecular cylinder is 2.25 nm long with a Ti···Ti separation of 19.06 Å. Each internal sodium cation also binds to three internal catecholate oxygen atoms [187].

In $Na_2[Na_2Ti_2(\mathbf{163k})_3]$, the three [**163k**]$^{4-}$ ligands and two titanium(IV) ions, 16.980 Å apart, form a cylinder of approximately 2.1 nm length, with the linear rigid ligands slightly twisting around the metal–metal axis. Surprisingly, one of the bipyridine units of the spacers possesses the nitrogen atoms oriented *s-trans* to each other, while the others are *s-cis* configured. Two sodium cations, encapsulated in the interior of the helicate and separated by 10.603 Å solely bind to the internal oxygen atoms of the catecholates. Three molecules of dimethylformamide complete the six coordination about these cations. Two further sodium cations bind to the termini of the helicate and through dimethylformamide-bridging lead to an infinite polymer in the solid state with alternating helicity of the helices in the polymer strand [188].

Attempt to bind metal complex units to the outside of the triple-stranded helicate $[Ti_2(\mathbf{163k})_3]^{4-}$, by reaction with $K_2[Pd(C1)_4]$ resulted in the hydrolysis products [Pd(L)(Cl_2)], where L is 5,5′-diamino-2,2′-dipyridine, and $[Ti(3\text{-formylcatecholate})_3]^{2-}$ [188].

When the bulky ligands H$_4$-**163l**···H$_4$-**163n** are used with potassium as the counter cation, oligomeric or polymeric side products are also observed; H$_4$-**163p** quantitatively forms $M_4[Ti_2(\mathbf{163p})_3]$. NMR investigations at variable temperature show that H$_4$-**163q**, which possesses a spiro fluorenyl group at the central unit of the spacer, forms the meso-helicate $M_4[Ti_2(\mathbf{163q})_3]$ [188].

The above reaction using $[VO(acac)_2]$ instead of $[TiO(acac)_2]$ affords $M_4[V_2(\mathbf{L})_3]$ (H$_4$-**L** = H$_4$-**163a**, H$_4$-**163h**·H$_4$-**163j**). In $Na_4[V_2(\mathbf{163a})_3]$ one [**163a**]$^{4-}$ spacer adopts an *s-cis* orientation, with the nitrogen lone pairs pointing away from the cavity of the helicate and the imine hydrogen atoms pointing inwards, while the other two [**163a**]$^{4-}$ spacers adopt an s-*trans* conformation, with one lone pair of one nitrogen atom pointing outwards and the other inwards. The latter conformation is enforced by encapsulation of two sodium ions in the interior of the helicate $[V_2(\mathbf{163a})_3]^{4-}$. Each of the sodium ions binds to two internal catecholate oxygen atoms and one of the internal nitrogen atoms and to two methanol oxygen while further methanol oxygen bridges these two cations. The coordination at the vanadium centers is distorted octahedral with a V···V separation of 8.339 Å [187].

Similarly, the reaction of 3-formylsalicyclic acid and hydrazine hydrate affords H$_4$-**163′**, with one inner N_2O_2 and one outer O_2O_2 site capable of interacting with two different metal ions. Moreover, the oxygen atoms from the carboxylato groups allow the propagation of the helical motif through subsequent coordination to a third metal ion as shown in $\{[Co_2Fe_2Na_2(\mathbf{163'})_3(H_2O)_4(C_2H_5OH)_2]\ 3H_2O\}_\infty$, resulting from the reaction of H$_4$-**163′** with $Na_2CO_3\cdot H_2O$, followed by addition of $Fe(ClO_4)_3\cdot 6H_2O$ and $Co(ClO_4)_2\cdot 6H_2O$. The $Co_2^{II}Fe_2^{III}Na_2$ polymer consists of tetranuclear triple-stranded dianionic helicates connected through sodium ions. In each anionic entity $\{Co_2^{II}Fe_2^{III}(\mathbf{163'})_3\}^{2-}$, two cobalt(II) and two iron(III) ions are accommodated into the resulting triple helicate architecture. The N_3O_3 distorted octahedral cobalt(II) ions are coordinated by the inner pockets of the helicand while the iron(III) ions are coordinated by the peripheral pockets of the helicand. Within the tetranuclear helicate the Co···Co and Co···Fe distances are 3.620 Å and 2.926 Å, respectively. Homochiral $[Co_2^{II}Fe_2^{III}(\mathbf{163'})_3]^{2-}$ anions are connected by pairs of sodium ions, resulting in a chiral 1-D coordination polymer (Fig. 114c). Each site of the tetranuclear anion interacts with two six coordinate sodium ions through one carboxylato group. The bridging mode of the carboxylato group is quite unusual, connecting one iron and two sodium ions [189].

In $\{[Co_2Fe_2Na_2(\mathbf{163'})_3(H_2O)_4(C_2H_5OH)_2]\cdot 3H_2O\}_\infty$ an antiferromagnetic coupling operates ($J_1 = -44.5\ cm^{-1}$), resulting from a stronger exchange pathway between the iron(III) and cobalt(II) ions connected by three phenoxo bridges, and a second weak antiferromagnetic interaction ($J_2 = -2.8\ cm^{-}1$) between the two central cobalt(II) ions through the three $\mu_{1,2}$-diazino bridges [189].

H$_2$-**164a** was prepared by the reaction of 3-methoxy-2-hydroxybenzaldehyde with 1,2-bis(aminoxy)ethane. The diamine precursor was obtained by treatment of 1,2-diaminoethane with *N*-hydroxyphtalimide followed by hydrazinolysis. H$_2$-**164a**, whose structure reveals all-anti conformation of the ethylenebis(oxynitrilo) bridge, resulting in a planar structure with two salicylaldoxime units apart from each other, reacts with nickel(II) or copper(II) acetate to form [Ni(**164a**)(H_2O)$_2$] or [Cu(**164a**)] with the copper(II) ion in a distorted square planar geometry [190].

In $[Zn_3(\mathbf{164a})_2(CH_3COO)_2]$, originating from a 2:3 mixture of H$_2$-**164a** and zinc(II) acetate and containing the central distorted octahedral zinc(II) ion in an O_6 environment and the other two zinc(II) ions in a trigonal bipyramidal in a N_2O_3 environment (Fig. 115a), partially transmetalates with lutetium(III) or lanthanum(III) salts to form $[ZnLu(\mathbf{164a})(CH_3COO)_3]$ and $[Zn_2La(\mathbf{164a})_2(CH_3COO)_2](NO_3)$, respectively. In the ZnLu complex (Fig. 115b) the five coordinate square pyramidal zinc(II) ion in the N_2O_2 site and the lutetium(III) ion in the external O_2O_2 donor set of [**164a**]$^{2-}$ are bridged by an acetate ion. Thus, the central zinc ion in the initial trinuclear zinc(II) complex is replaced by the lutetium(III) ion, and the trinuclear assembly dissociates. In the Zn_2La complex the two zinc(II) ions reside into the N_2O_2 moieties of two [**164a**]$^{2-}$ ligand and the resulting units {Zn(**164a**)} further coordinate to the ten coordinate lanthanum(III) in an η^2-fashion. Two acetate ions coordinate to the trinuclear Zn-La-Zn core from the same side of the complex (Fig. 115c). Probably, the structure of the complex in solution is essentially the same as that in the crystalline state [190,191].

In $[CuGd(\mathbf{164a})(CH_3COO)_3]$ and $[CuGd(\mathbf{164a})(NO_3)_3]$, obtained from an equimolar mixture of H$_2$-**164a**, $Cu(CH_3COO)\cdot H_2O$ and the appropriate gadolinium(III) salt, the five coordinate square pyramidal or square planar copper(II) ion, respectively, is located in the N_2O_2 site of

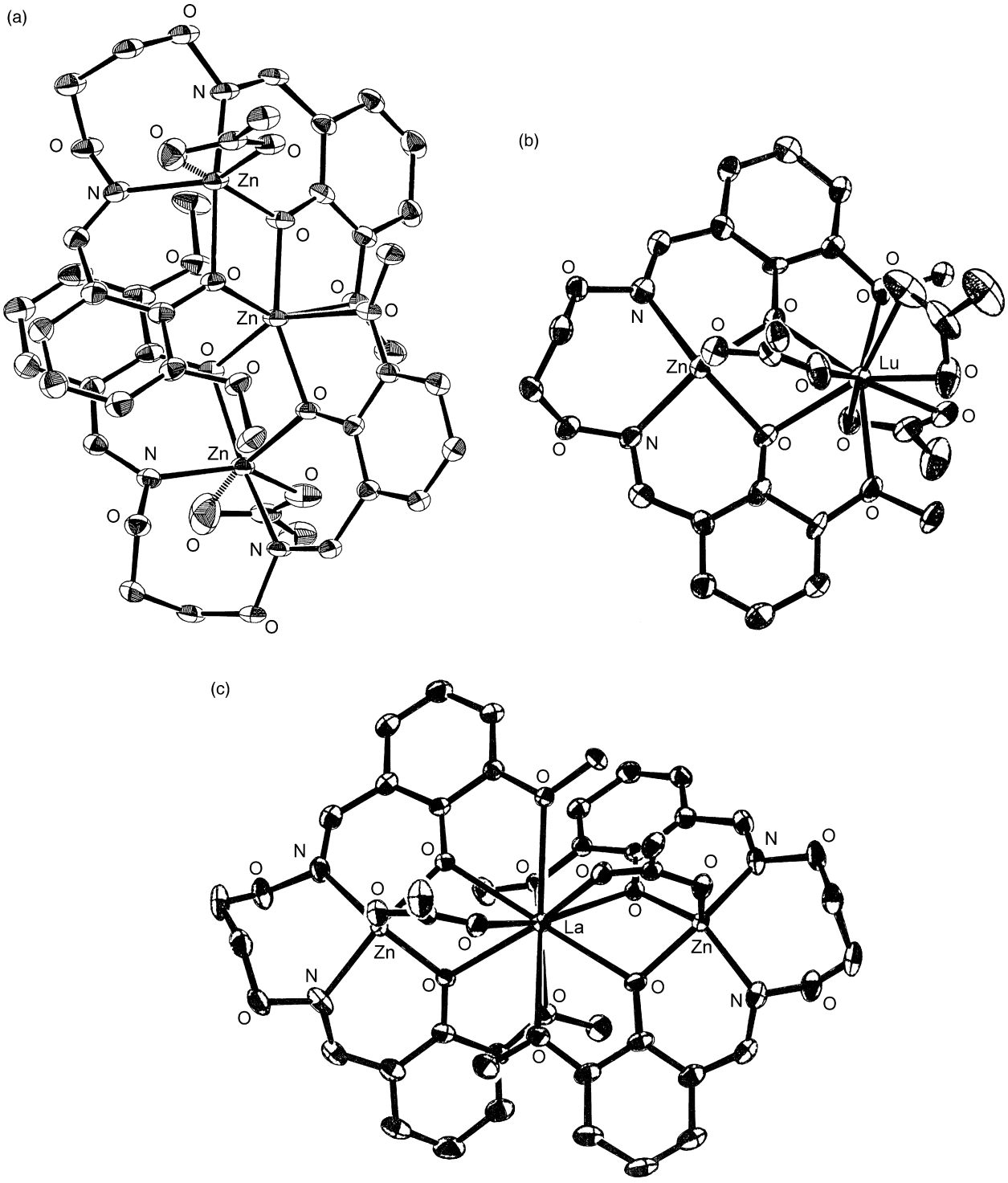

Fig. 115. Structure of $[Zn_3(\mathbf{164a})_2(CH_3COO)_2]$ (a), $[ZnLu(\mathbf{164a})(CH_3COO)_3]$ (b) and $[Zn_2La(\mathbf{164a})_2(CH_3COO)_2]^+$ (c).

$[\mathbf{164a}]^{4-}$ while the nine coordinate gadolinium(III) ion resides in the outer O_2O_2 site. One acetate bridges the two metal ions; the other two acetates coordinate only to the gadolinium(III) ion in a bidentate fashion. In $[CuGd(\mathbf{164a})(NO_3)_3]$ the coordination environment about the gadolinium(III) ion is completed by three bidentate nitrato ligands. The Cu···Gd distance are 3.497 Å and 3.433 Å, respectively [191]. H_4-**164b** and $Zn(CH_3COO)_2{\cdot}2H_2O$ form $[Zn_3(\mathbf{164b})(CH_3COO)_2(C_2H_5OH)]$, with the three zinc ions in a trigonal bipyramidal geometry. The two 1,2-bis(salicylideneaminooxy)ethane moieties provide the N_2O_2 donor set to the two outer zinc ions, while the oxygen atoms of the central catechol moiety coordinate to all three zinc ions. In addition, the two acetato ligands act as bridging groups between two zinc(II) ions (Fig. 116) [191].

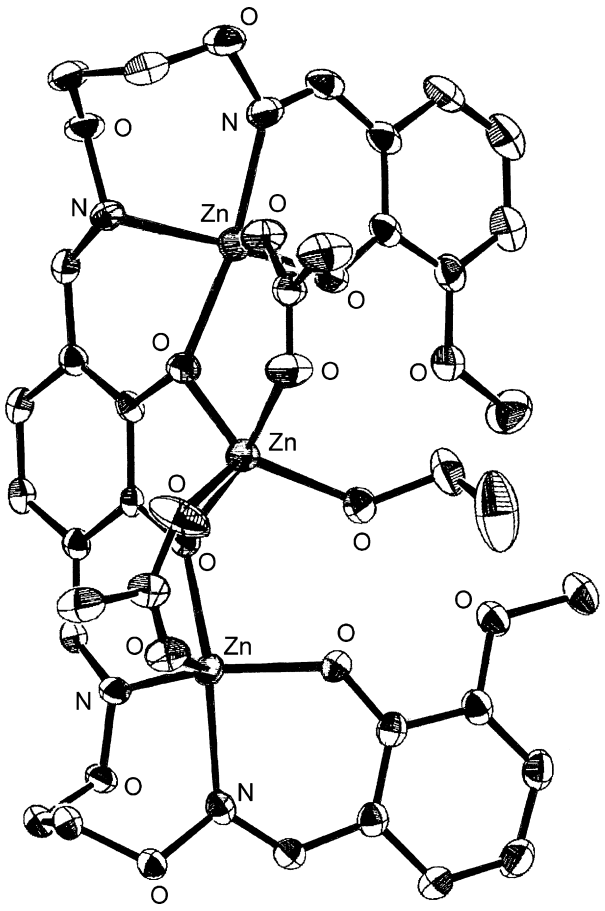

Fig. 116. Structure of $[Zn_3(\mathbf{164b})(CH_3COO)_2(C_2H_5OH)]$.

$[Zn_3(\mathbf{164b})(CH_3COO)_2(C_2H_5OH)]$ liberates one zinc(II) ion when treated with $Eu(NO_3)_3{\cdot}6H_2O$, forming the helical complex $[Zn_2Eu(\mathbf{164b})(CH_3COO)_2(NO_3)(H_2O)]$ where the trinuclear Zn-Eu-Zn core is bridged by the phenolate oxygen atoms of $[\mathbf{164b}]^{4-}$ and the acetato anions. The two zinc ions in a octahedral and a square pyramidal environment, respectively, fill the N_2O_2 donor sets of $[\mathbf{164b}]^{4-}$. Six oxygen atoms of $[\mathbf{164b}]^{4-}$ wrap around the nine coordinate europium(III) ion (Fig. 117a). Interestingly, a mixture of H_4-**164b** with excess zinc(II) and europium(III) salts gave complexes identical to $[Zn_2Eu(\mathbf{164b})(CH_3COO)_2]^+$: the zinc(II) ions, thus, bind selectively to the two N_2O_2 moieties of $[\mathbf{164b}]^{4-}$ while the europium(III) ion prefers the central cavity. Hence, the heterotrinuclear Zn_2Eu complex is stabilized to a greater extent than the Zn_3 homotrinuclear one. As a result, only the central zinc ion of the homotrinuclear complex, initially formed, is transmetalated quantitatively by the lanthanide(III) ion [191].

NMR, X-ray diffractometry and ESI mass spectrometry indicate that $[Zn_3(\mathbf{164b})(CH_3COO)_2(C_2H_5OH)]$ recognizes the calcium(II) ion with the formation of $[Zn_2Ca(\mathbf{164b})(ClO_4)_2(CH_3OH)_2]$, where the $\{Zn_2(\mathbf{164b})\}$ moiety forms a one-turn helix surrounding the calcium(II) ion. All the six oxygen atoms of the inner recognition site of the $\{Zn_2(\mathbf{164b})\}$ moiety coordinate to the calcium(II) ion (Fig. 118). Also, these investigations show that $[Zn_3(\mathbf{164b})]^{2+}$

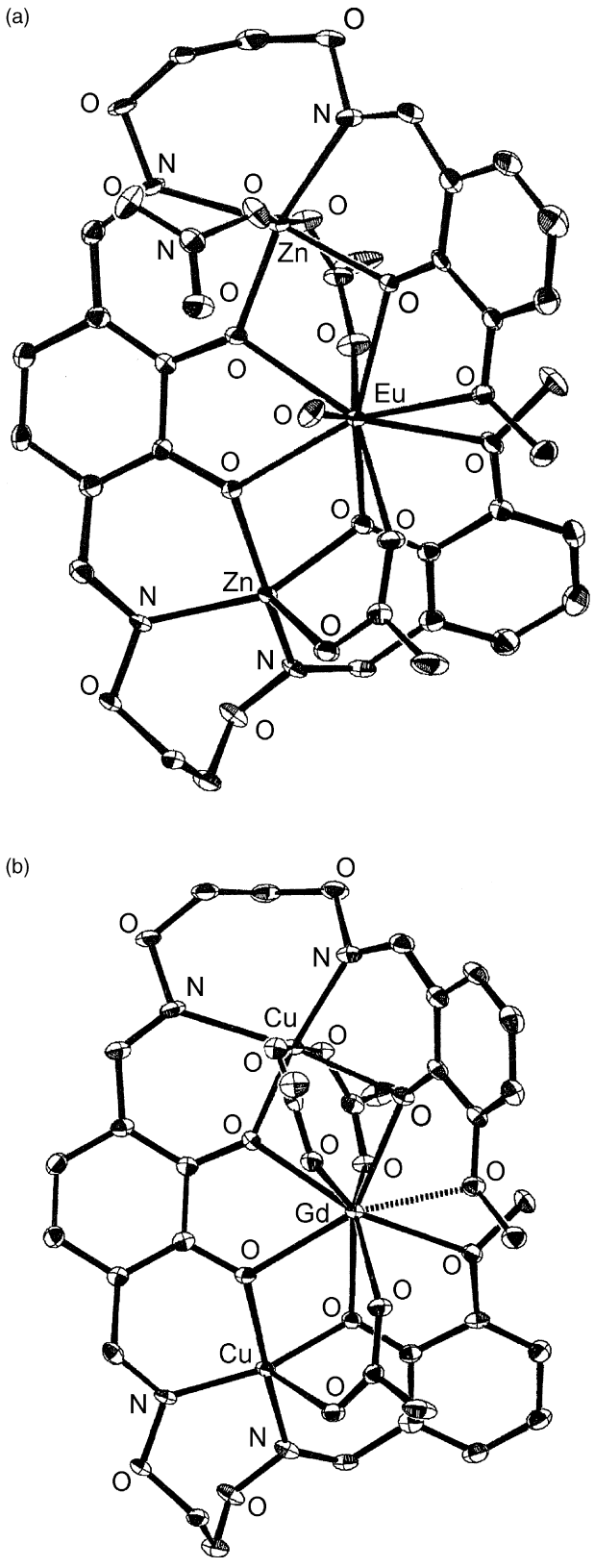

Fig. 117. Structure of $[Zn_2Eu(\mathbf{164b})(CH_3COO)_2(NO_3)(H_2O)]$ (a) and $[Cu_2Gd(\mathbf{164b})(CH_3COO)_3]$ (b).

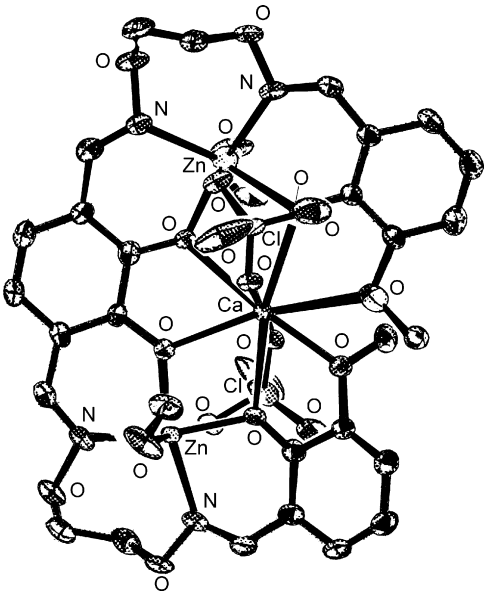

Fig. 118. Structure of $[Zn_2Ca(\mathbf{164b})(ClO_4)_2(CH_3OH)_2]$.

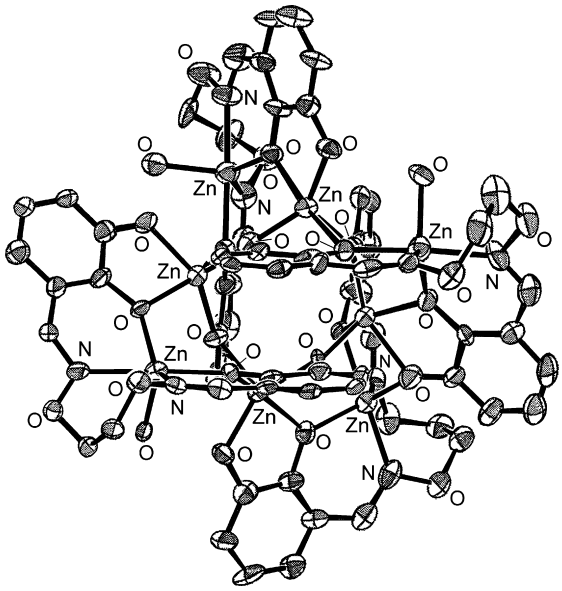

Fig. 119. Structure of $[Zn_8(\mathbf{164c})_4(H_2O)_3]$.

recognize the calcium(II) ion much easier than barium(II) ion (the binding is ≅200 time stronger for Ca^{II} with respect to Ba^{II}). Under similar conditions the magnesium(II) ion does not cause the transmetalation even when 1000 equivalent of Mg^{II} is used. Furthermore, $[Zn_3(\mathbf{164b})(CH_3COO)_2(C_2H_5OH)]$ does not show affinity for alkali metal ions (Na^I, K^I, Rb^I, Cs^I) [192].

In $[Cu_2Gd(\mathbf{164b})(CH_3COO)_3]$, synthesized by one-pot reaction of H_4-**164b** with 2 equivalents of $Cu(CH_3COO)_2{\cdot}H_2O$ and one of $Gd(CH_3COO)_3$, the two copper ions are octahedrally and square pyramidally located at the N_2O_2 moieties of $[\mathbf{164b}]^{4-}$ while the four phenoxy oxygen atoms of the $[\mathbf{164b}]^{4-}$ coordinate to the nine coordinate gadolinium(III) ion, which is weakly coordinated to the methoxy groups. The Gd···Cu and Cu···Cu distances are 3.309 Å and 6.079 Å, respectively (Fig. 117b). The ferromagnetic interaction among the Cu^{II}–Gd^{III}–Cu^{II} triad in $[Cu_2Gd(\mathbf{164b})(CH_3COO)_3]$ ($J_{CuGd} = 5.0\,cm^{-1}$), comparable to that of the corresponding dinuclear complexes $[CuGd(\mathbf{164a})(X)_3]$ ($J = 4.5\,cm^{-1}$ for $X = CH_3COO$ and $7.6\,cm^{-1}$ for $X = NO_3^-$), indicates that the $S = 9/2$ ground state of $[Cu_2Gd(\mathbf{164b})(CH_3COO)_3]$, in which the three local spins are aligned in a parallel fashion, is significantly populated at low temperatures [191].

H_4-**164c**, prepared by the condensation of 1,2-bis(aminooxy)ethane with two equivalents of 2,3-dihydroxybenzaldehyde, adopts an extended conformation where the two salicylaldoxime moieties are apart from each other [193]. When mixed with $Zn(CH_3COO)_2{\cdot}H_2O$, it forms $[Zn_8(\mathbf{164c})_4(H_2O)_3]$, where the N_2O_2 sites of the ligands $[\mathbf{164c}]^{4-}$ are occupied by the four outer zinc ions while the other four inner zinc ions connect a $\{Zn(\mathbf{164c})\}$ unit to the adjacent one in such a way that it binds two catecholato moieties. Phenolate oxygen atoms of the catechol moieties also coordinate in a μ_2-fashion to the four inner zinc(II) ion. The two types of $[\mathbf{164c}]^{4-}$–$[\mathbf{164c}]^{4-}$ linkage with four inner zinc ions resulted in the formation of a cyclic tetramer. Each of the inner zinc ions in O_2O_2 chamber is five coordinate, with catechol phenolate oxygen donors occupying all five sites: one inner zinc(II) ion adopts a trigonal bipyramidal geometry, whereas the other three zinc ions have a square pyramidal structure. In the center of the octanuclear cluster, there is a Zn_4O_4 eight-membered ring, which adopts a chair–chair conformation and the four inner Zn···Zn distances are in the range of 3.32–3.45 Å. The outer zinc ions have a similar trigonal bipyramidal geometry. The four outer zinc ions contribute to the formation of four Zn_3O_3 six-membered rings outside of the inner eight-membered Zn_4O_4 ring. In addition, there is a

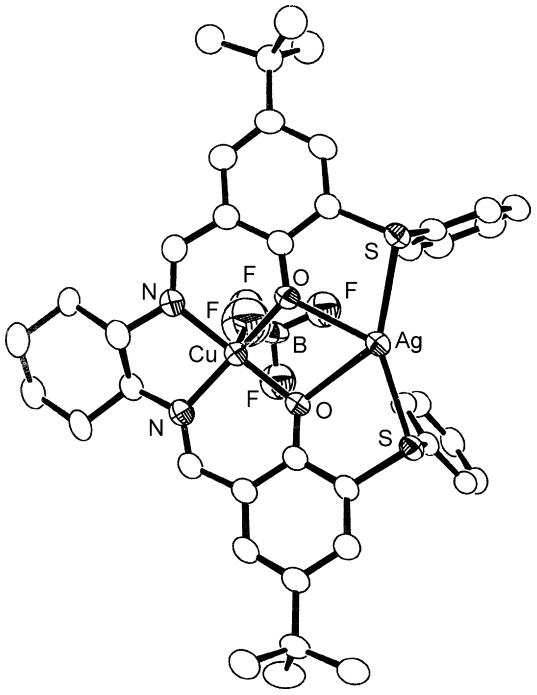

Fig. 120. Structure of $[CuAg(\mathbf{166b})]^+$.

Zn_2O_2 four-membered ring. One outer Zn···Zn interatomic distance (6.180 Å) is considerably shorter than the other three (7.161 Å, 7.328 Å and 7.294 Å) (Fig. 119). $[Zn_8(\mathbf{164c})_4(H_2O)_3]$ also exists in solution and maintains a similar octanuclear conformation, although exchange of the coordinating water molecules presumably takes place [193].

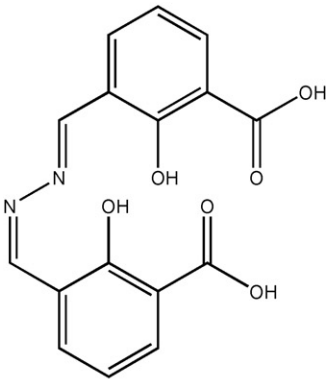

H_4-**163'**

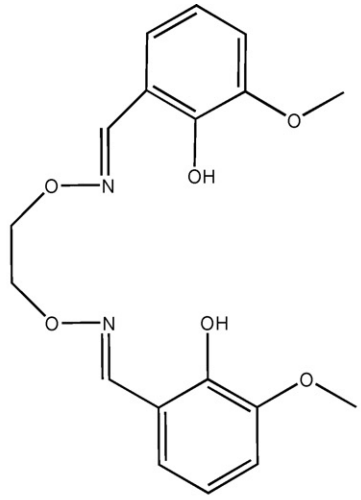

H_2-**164a**

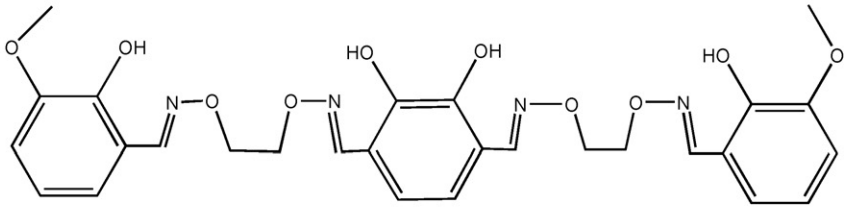

H_4-**164b**

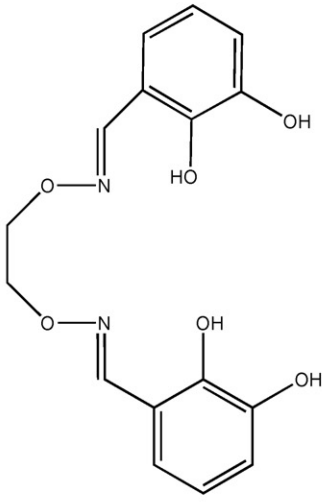

H_4-**164c**

Similarly, H_4-**164c** and cobalt(II) acetate gives $[Co_8(\mathbf{164c})_4(C_2H_5OH)_3]\cdot 2C_2H_5OH\cdot 0.5CHCl_3$ with the eight five coordinate cobalt(II) ions in an assembly of the $[\mathbf{164c}]^{4-}$ ligands similar to that of the zinc(II) analogue. Again, the discrete octanuclear structure occurs also in solution, as confirmed by ESI mass spectra. An antiferromagnetic interaction among the cobalt(II) ions was found [193].

The larger derivative H_6-**164d** reacts with four equivalents of $Zn(CH_3COO)_2\cdot 2H_2O$ to give $[Zn_4(\mathbf{164d})(CH_3COO)_2]$, together with other isomers. The further addition of barium(II) ions turns the mixture of isomers into the sole $[Zn_3Ba(\mathbf{164a})(CH_3COO)_2]^{2+}$, where a binding of barium(II) ion in the helical cavity and simultaneous release of a zinc(II) ion

occurs. The [Zn_4(**164d**)$(CH_3COO)_2$] isomers did not change into a single component when an alkali or alkaline-earth metal ion (M = K^I, Cs^I, Mg^{II}, Ca^{II}) was added, as supported by the ESI mass spectrometry. Thus, [Zn_4(**164d**)$(CH_3COO)_2$] was found to act as a barium(II)-selective metalloreceptor [193].

The formyl precursors H-**165a** and H-**165b**, prepared by a two-step procedure involving the insertion of a –SR group at the position −2 of 4-*tert*-butylphenol followed by the introduction of a formyl group at the −6 position, were converted into H_2-**166a** or H-**166b** by condensation with rac-*trans*-1,2-diaminohexane and into H_2-**167a** and H_2-**167b** by subsequent reduction**.** Both the Schiff bases and the corresponding polyamines afford [Cu(**L**)], when reacted with $Cu(CH_3COO)_2{\cdot}H_2O$: ESI mass spectra show dimer peaks in addition to the expected molecular ions, implying that significant association of the compounds takes place [194]. These complexes with $AgBF_4$ give [CuAg(**L**)](BF_4). In [CuAg(**166b**)]$(BF_4){\cdot}1.45CH_3CN$, the {Cu(**166b**)} moiety acts as a ligand toward the silver(I) ion through the two thioether sulfur atoms and, by bridging interactions, through the phenoxide oxygen donors. The copper(II) ion is four coordinate square planar as in the mononuclear analogue (Fig. 120). EPR spectra in frozen CH_2Cl_2 show that [CuAg(**166b**)](BF_4) retains its integrity in solution while [CuAg(**166a**)](BF_4) dimerizes [194].

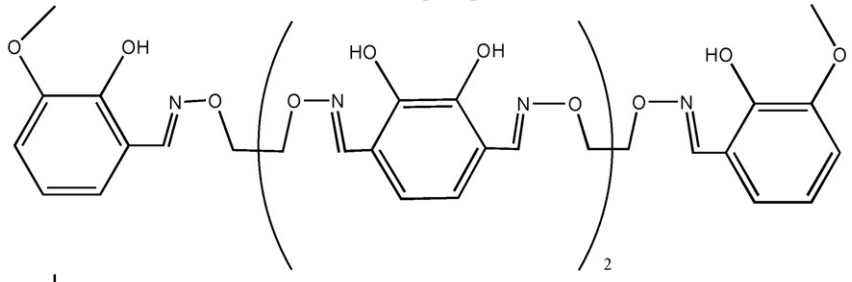

H_6-**164d**

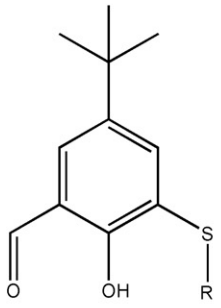

	R
H-**165a**	CH_3
H-**165b**	C_6H_5

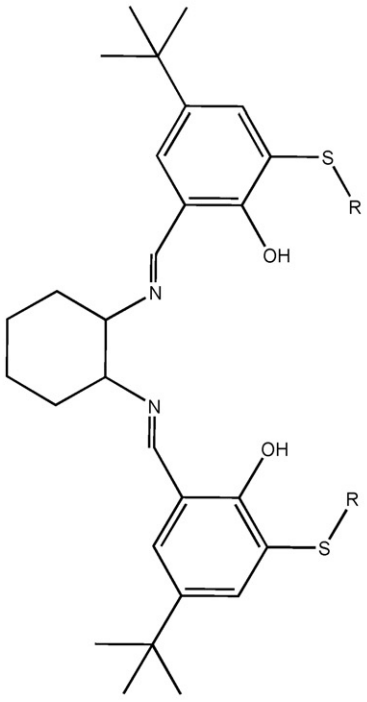

	R
H_2-**166a**	CH_3
H_2-**166b**	C_6H_5

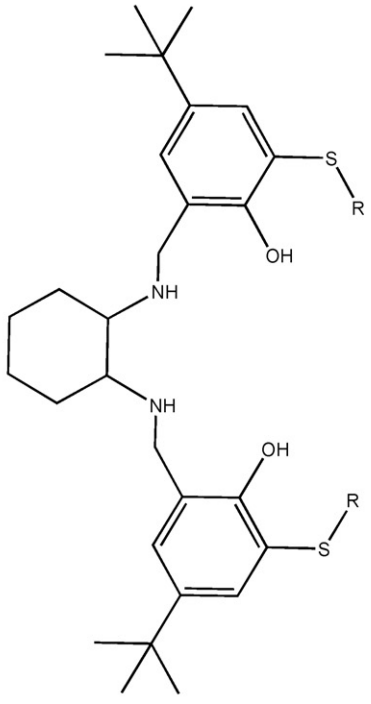

	R
H_2-**167a**	CH_3
H_2-**167b**	C_6H_5

The viability of using the simple inexpensive Schiff base derivatives to extract both metal cations and their attendant anions from aqueous solutions was recently reviewed [19]. Appending appropriate tertiary amine groups to the Schiff base framework allows the metal salt to be transported in a zwitterionic form of the ligand. In a solvent-extraction based process this leaves the pH of the aqueous feed unchanged and removes the need for inter-stage neutralization in a metal recovery circuit. Direct addition of nickel(II) or copper(II) sulfate to the ditopic ligands H_2-**168a**···H_2-**168d** in methanol yields [M(H_2-**168a**···**d**)(SO_4)]. The availability of [M(**168a**···**d**] from the reaction of the appropriate Schiff base with the desired metal(II) acetate, allowed to study the uptake of sulfuric acid by these complexes in solvent extraction experiments, e.g. $[M(\mathbf{168a}\cdots\mathbf{d})]_{(org)} + H_2SO_{4(aq)} \rightleftharpoons [M(H_2\text{-}\mathbf{168a}\cdots\mathbf{d})(SO_4)]_{(org)}$ as a function of pH, and to determine how this depends on preorganization of the ligands. The free ligands H_2-**168a**···H_2-**168d** and the related complexes show a good solubility in chloroform [195].

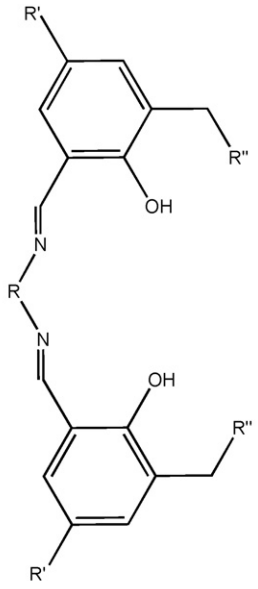

	R	R'	R''
H_2-**168a**		$C(CH_3)_3$	$N(n\text{-}C_6H_{13})_2$
H_2-**168b**	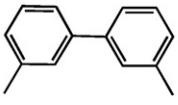	$C(CH_3)_3$	$N(n\text{-}C_6H_{13})_2$
H_2-**168c**		$C(CH_3)_3$	$N(n\text{-}C_6H_{13})_2$
H_2-**168d**	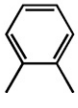	$C(CH_3)_3$	$N(n\text{-}C_6H_{13})_2$

Very little transfer of sulfate to the organic phase is observed at pH > 2.0. As the pH is dropped to values <0.5 the uptake increases rapidly, owing to the extraction of two mono-charged HSO_4^- anions which are present in the aqueous phase in an excess at pH < 1. In contrast, [Cu(**168d**] loads sulfate at pH < 4.5 and the loading curve suggests that [Cu(H_2-**168d**)(SO_4)] predominates in the pH range 1.5–3.5. An important feature of this loading behavior is that the copper complex of H_2-**168d** is effectively selective for SO_4^{2-} over HSO_4^-; in contact with an aqueous sulfate solution at pH 1.92 where the SO_4^{2-}:HSO_4^- ratio is 1:1 the organic phase contains only [Cu(H_2-**168d**)(SO_4)] [195].

The insertion of pendant piperidine or morpholine groups leads to an increase in solubility in non-polar solvents of the resulting ligands (H_2-**168e**···H_2-**168m**), a property of great importance to the solvent extraction studies. H_2-**168e** and H_2-**168f** have an extended configuration with the pendant morpholine groups not well arranged for encapsulation of a sulfate ion. On the contrary, incorporation of a metal ion into the Schiff bases binding site of these ligands significantly changes the disposition of the pendant amine groups aligning them more effectively for sulfate binding. Ligands with a planar N_2O_2 donor set form very stable copper(II) complexes. In order to facilitate the removal of the copper(II) ion from these binding sites, rigid bridging units could be incorporated which alter the disposition of the N_2O_2 coordination planes to generate distortions from square planarity. In order to generate distortion from planarity, a 2,2′-biphenylene moiety was inserted in order to encourage the formation of pseudo-tetrahedral N_2O_2 donor set. A strong deviation from planarity was observed in H_2-**168i** and H_2-**168l**. The structure of the free ligands shows that considerable strain energy would be required to define a planar N_2O_2 donor set; this destabilizes copper-binding and hence enhances metal ion recovery from the loaded ligand [196].

	R	R'	R''
H_2-**168e**		$C(CH_3)_3$	
H_2-**168f**		$C(CH_3)_3$	
H_2-**168g**		C_9H_{19}	
H_2-**168h**		$C(CH_3)_3$	
H_2-**168i**	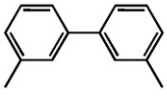	$C(CH_3)_3$	
H_2-**168l**	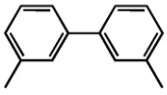	C_9H_{19}	
H_2-**168m**		CH_3	

The formation of [M(H_2-**L**)(SO_4)] (H_2-**L** = H_2-**168e**···H_2-**168m**) occurs almost immediately upon mixing in alcoholic solution of the appropriate metal(II) sulfate and H_2-**L**. Imposition of a different coordination geometry upon the metal ion does not effect the ability of H_2-**168i** to form discrete metal sulfate complexes although in the case of nickel(II) the mode of metal salt binding is shown to be different as determined by the structure of [Ni(H_2-**168i**)(SO_4)]. Noticeably, the formation of [Zn(H_2-**168i**)(SO_4)] indicates that metal salt complexes can also be formed with other metal ions. Furthermore, [Cu(**168h**)] and [Cu(**168i**)], can also be formed by using copper acetate as the metal source: the isolation of either [Cu_2(H_2-**168h**)(SO_4)] or [Cu_2(H_2-**168i**)(SO_4)] and [Cu(**168h**)] or [Cu(**168i**)] depends on the relative basicities of the anion and the pendant tertiary amine and on the solvent [196].

The structure of [Cu(**168h**)] confirms the absence of any associated anions. The complex is approximately planar with the copper(II) ion into the N_2O_2 Schiff base site. This aligns the pendant piperidine groups such that a piperidine N···N separation of 5.789 Å occurs, compared with 12.158 Å and 12.170 Å in the related ethane-bridged free ligand H_2-**168e**, and 16.22 Å in H_2-**168m** [196].

The structure of {[Cu(H_2-**168e**)](SO_4)} (Fig. 121a) demonstrates the capability of the copper(II) complex to incorporate the sulfate anion between the morpholinium groups by a combination of direct electrostatic interaction as well hydrogen bonds to the ammonium nitrogen atoms. Protonation of the morpholine units together with sulfate-incorporation causes only minor changes in the copper(II) geometry [196].

In [Ni(H_2-**168e**)(SO_4)] the sulfate anion is bound by two separate bifurcated hydrogen bonds as opposed to two single H-bonds in the copper structure, but the morpholinium N···N distances are very similar. The sulfate is slightly closer to the metal centre than in the copper structure.

The non-availability of the structure of copper(II) complexes of H_2-**168i** and H_2-**168l** does not allow defining the coordination geometry imposed by the biphenylene bridge which destabilizes extracted copper species. However, [Ni(H_2-**168i**)(SO_4)]·4CH_2Cl_2 crystallizes readily and has a pseudo-octahedral structure. The unusual presence of the bidentate sulfate anion in the nickel(II) coordination sphere appears to be favoured by the proximity of the piperidinium nitrogen atoms, which provide both electrostatic attraction and hydrogen bond. The other protonated nitrogen atom is arranged too far from the sulfate oxygen atoms to form any hydrogen bonds (Fig. 121b) [196].

The extraction studies and the electronic spectra of [Cu(**168i**)] and [Cu(H_2-**168i**)(SO_4)] suggest that sulfate is only weakly coordinated to the copper centre in solution, presumably owing to the displacement of the N_2O_2 donor set from planarity [196].

As nickel(II) extraction by H_2-**168e**···H_2-**168l** requires very long equilibration times, experiments for the loading/stripping process were undertaken with copper(II) using the same ligands. Whilst the *o*-phenylene bridged ligand H_2-**168g** gives >95% of the theoretical copper-loading when contacted with an excess of aqueous copper(II) sulfate solution, it proved impossible to strip copper(II) with 5 M sulfuric acid. With H_2-**168l**, copper(II) was

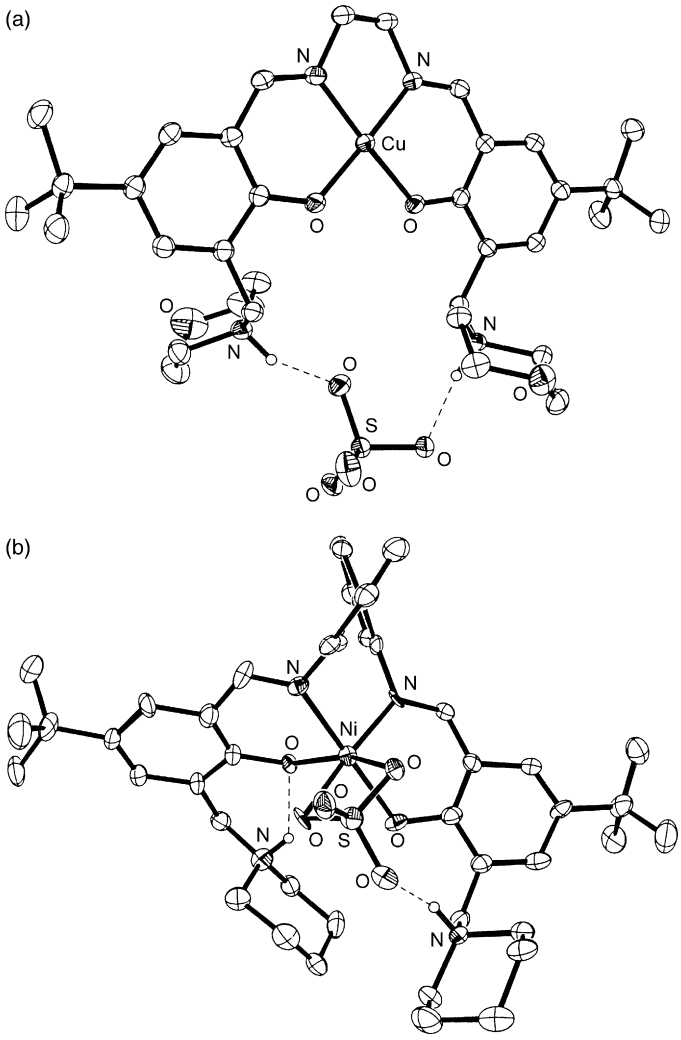

Fig. 121. Structure of {[Cu(H_2-**168e**)](SO_4)} (a) and [Ni(H_2-**168i**)(SO_4)] (b).

loaded to >95% of extractant capacity when a 0.01 M chloroform solution was contacted with an excess of $CuSO_4$ in a feed solution of pH 4.5 (no significant change in pH of the aqueous feed was observed); the loaded organic phase was stripped to <5% of copper capacity when contacted with sulfuric acid to give an equilibrium pH 0; the sulfate content of the organic phase falls to <1% of the theoretical capacity when the Cu-stripped organic is contacted with aqueous ammonia at an equilibrium pH ≥ 11.0. After one cycle of loading and stripping the extractant H_2-**168l** was reloaded to the same (>95%) level with copper(II) sulfate, indicating that it is robust and stable to hydrolysis, oxidation and *trans*-imination when contacted with either high or low pH aqueous solutions for 24 h at room temperature [196].

Competitive cobalt(II), copper(II), zinc(II) and cadmium(II) mixed metal ion transport experiments (H_2O/$CHCl_3$/H_2O), using H_2-**168l** as ionophore in the $CHCl_3$ phase with pH 2.3 for the aqueous source and pH 1.3 for the receiving one, prove the sole selective transport of copper(II) over the other metal ions present in the source phase. This is consistent with the $CuSO_4$ complex of H_2-**168l** being thermodynamically favored in the organic phase [196].

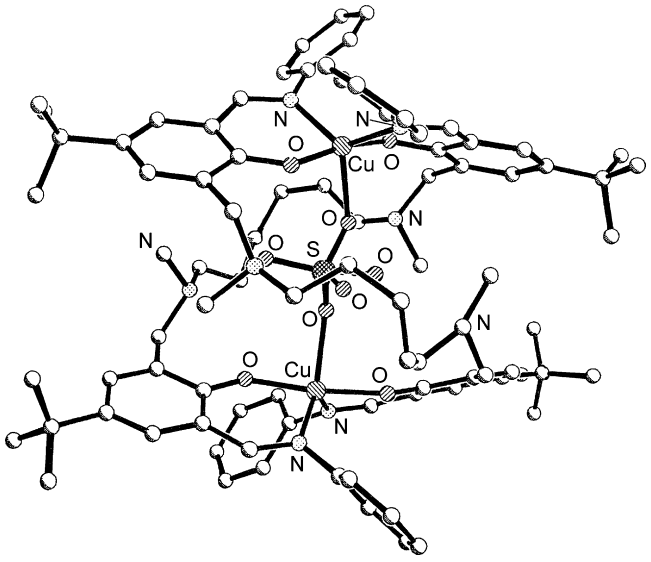

Fig. 122. Structure of $[Cu_2(H_2\text{-}\mathbf{169})_2(SO_4)]^{2+}$.

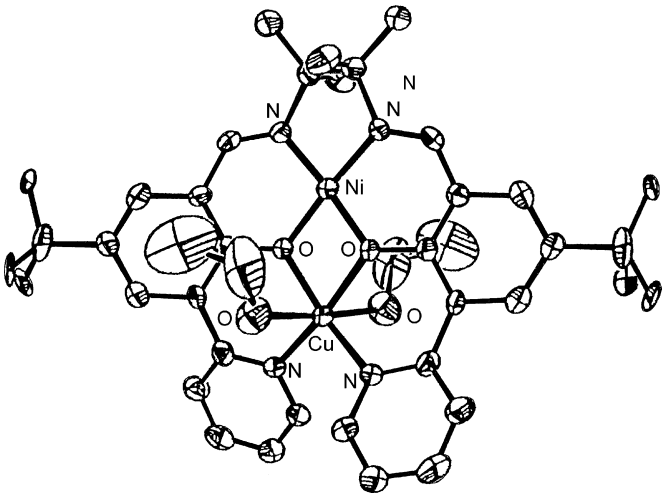

Fig. 123. Structure of $[NiCu(\mathbf{171a})(C_2H_5OH)_2]^{2+}$.

In order to increase the cation and anion selectivity, synthetic approaches have been followed involving the introduction of a strap, as in H_2-**169**, between the pendant amino groups which, on protonation, bind the sulfate ion. Straps between the aminomethyl substituents of the salicylaldehyde units are readily incorporated using a Mannich condensation of the appropriate long chain secondary diamine. The resulting functionalized dialdehyde precursor can be converted to the desires Schiff base by reaction with appropriate amine. $[Cu_2(H_2\text{-}\mathbf{169})_2(SO_4)](SO_4)$, readily isolated by mixing copper(II) sulfate and H_2-**169**, is made up of two ligands in their zwitterionic forms (deprotonated phenols and protonated amines), two copper(II) metal centers, 6.4 Å apart, and two SO_4^{2-} anions, one of which is encapsulated inside the complex. Each copper(II) ion is in a distorted trigonal bipyramidal environment. The four trialkylammonium N–H groups form medium to strong H-bonds with one encapsulated SO_4^{2-} anion (Fig. 122). A similar ligand architecture was found in $[Cu_2(H_2\text{-}\mathbf{169})_2(BF_4)](BF_4)_3$ where the encapsulated BF_4^- is not coordinated to the distorted square planar N_2O_2 copper ions but forms weaker H-bonds with the alkyl ammonium protons. UV/vis and FAB mass spectrometry results indicate that $[Cu_2(H_2\text{-}\mathbf{169})_2(SO_4)](SO_4)$ maintains the same assembly in solution [197].

H_2-**170**, possessing contiguous tetra- and hexadentate coordination sites, has been synthesized by condensation of 2-formyl-4-methyl-6[4-methyl-6-(4-methylpiperazin-1-yl)methyl]phenol with 1,8-diaminonaphthalene. $[M(H\text{-}\mathbf{170})](ClO_4)$ and $[M_2(\mathbf{170})](ClO_4)_2$ have been prepared by reaction of H_2-**170** with $M(ClO_4)_2{\cdot}6H_2O$ ($M = Cu^{II}$, Ni^{II}), respectively in a 1:1 or 1:2 molar ratio. ^1H NMR data show that the nickel(II) ion is square planar in the N_2O_2 compartment in the mononuclear complex. Electrochemical studies show for $[Cu(H\text{-}\mathbf{170})](ClO_4)$ a single quasireversible one electron wave and at −0.83 V (E_{pc}) and two quasireversible one electron reduction waves for $[Cu_2(\mathbf{170})](ClO_4)$, at −0.68 V ($E_{pc}{}^1$) and −1.35 V ($E_{pc}{}^2$) in the cathodic region. $[Ni(H\text{-}\mathbf{170})](ClO_4)$ shows one quasireversible reduction potential at −0.80 V (E_{pc}) and $[Ni_2(\mathbf{170})](ClO_4)_2$ shows two irreversible reduction potentials at −1.10 V ($E_{pc}{}^1$) and −1.40 V ($E_{pc}{}^2$) in the cathodic region. Kinetic studies on the oxidation of catechol to *o*-quinone using the copper(II) complexes of H_2-**170** and hydrolysis of 4-nitrophenyl phosphate using the similar nickel(II) complexes as catalysts show that the dinuclear complexes have higher rate constant values than these of the corresponding mononuclear complexes [198].

Bromination of 5-*tert*-butyl salicylaldehyde gives 3-bromo-5-*tert*-butylsalicyaldehyde which, by palladium-catalyzed cross coupling with 2-(tri-n-butylstannyl)pyridine in tetrahydrofuran, produces the formyl precursor H-**171**. Condensation of this aldehyde with 2,3-diamino-2,3-dimethylbutane affords H_2-**171a** [199]; the Schiff base, by addition of $Ni(CH_3COO)_2{\cdot}4H_2O$ gives rise to [Ni(**171a**)]. Further addition of $Ni(CH_3COO)_2{\cdot}4H_2O$ or $Cu(CH_3COO)_2{\cdot}2H_2O$, followed by anion exchange with ammonium hexafluorophosphate, produces the isomorphous complexes $[Ni_2(\mathbf{171a})(C_2H_5OH)_2](PF_6)_2$ and $[NiCu(\mathbf{171a})(C_2H_5OH)_2](PF_6)_2$ (Fig. 123), where one square planar nickel(II) ion is located in the inner N_2O_2 cavity while the second axially elongated octahedral metal ion (nickel(II) or copper(II)) occupies the outer O_2N_2 binding site. The two metal ions are bridged by two phenolate oxygen atoms at a Ni···Cu and Ni···Ni separation of 2.898 Å and 2.950 Å, respectively [200].

The enantiomeric chiral ligands H_2-**171b** and H_2-**171c**, prepared by the condensation of H-**171** with either (*R*,*R*)- and (*S*,*S*)-1,2-diaminocyclohexane in the form of mono(+)-tartrates, form mononuclear, homo- and hetero-dinuclear complexes with copper and nickel salts [199].

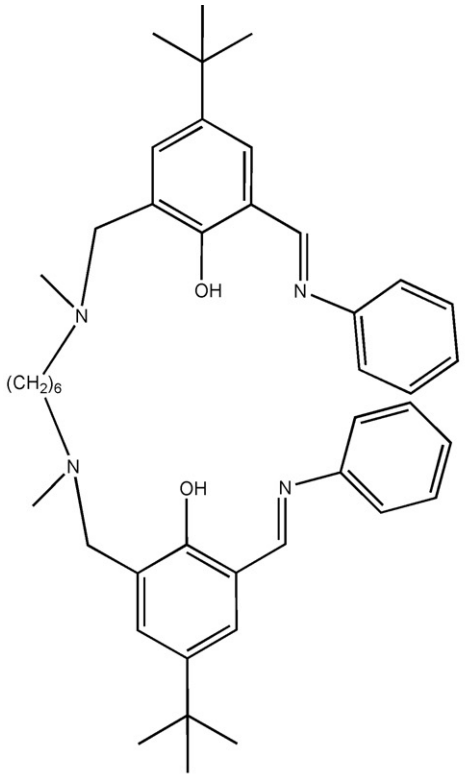

H_2-**169**

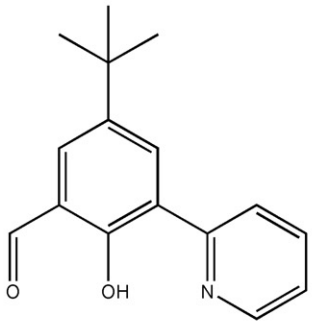

H-**171**

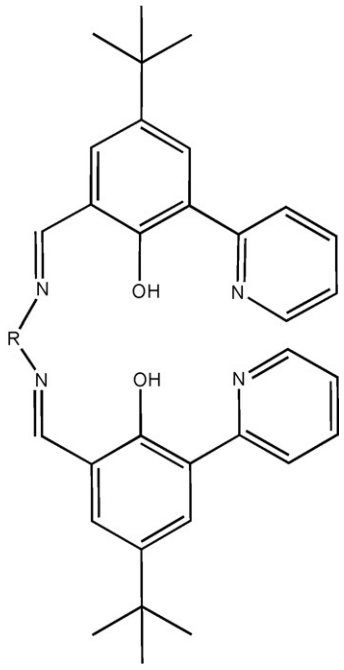

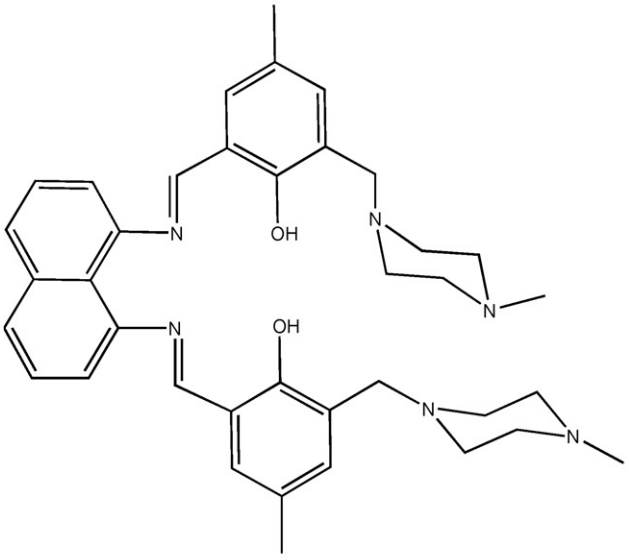

H_2-**170**

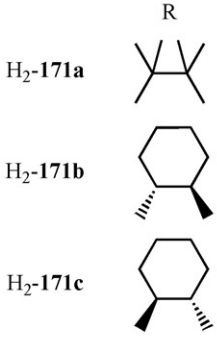

H_2-**171a**

H_2-**171b**

H_2-**171c**

The ruthenium, chromium, titanium, and zinc complexes of H_2-**172a** and H_2-**172b**, containing two quinoline bases linked to a tetradentate N_2O_2 Schiff base core, have been prepared and tested as bifunctional catalysts. The structure of the μ-oxo-titanium dimer $[Ti_2(\mathbf{172a})_2(\mu\text{-}O)\{OC_6H_4C(CH_3)_3\}_2]$ shows a typical Schiff base coordination pattern and illustrates that the nitrogen atoms of the quinoline groups participate in neither intra- nor intermolecular coordination. In addition, the quinoline groups are probably oriented to act as bases toward substrates coordinated at the apical positions of these complexes. The quinolines are oriented toward the titanium centers such that replacement of the μ-oxo ligand with a ketone ligand places the quinoline nitrogen atoms close to the ketone α-proton, as would be required for the quinoline to mediate deprotonation. As an indication that the quinoline bases can alter the activity of these Schiff base complexes, the addition of dialkylzinc to aldehydes in the catalytic formation of the related alcohols was shown to be accelerated by the complexes with H_2-**172a** or H_2-**172b** relative to the similar Schiff base lacking the quinoline groups [201].

8. [1 + 2] Side off systems

The [1 + 2] side off ligands derive from the condensation of one equivalent of the appropriate diformyl precursor H_2-**173a**, H_2-**173b** or H_2-**173c** with two equivalents of a monoamines H_2N– which quite often contain additional donor groups (Scheme 7). These Schiff bases can be reduced to the amine analogues by reaction with BH_4^-.

[Zn(**173a**)] or [Co(**173a**)], derived from the reaction of [Li_2(**173a**)] with the appropriate metal(II) salt, are converted into [Zn(H_2-**174a**)]$(PF_6)_2$ or [Co(H-**174a**)]$(PF_6)_2$ by condensation with aniline. ^{1}H NMR spectra of [Zn(H_2-**174a**)]$(PF_6)_2$ indicate the presence of two protons in the N_2O_2 cavity. In the corresponding amine complexes [M(**174b**)] (M=Co^{II}, Zn^{II}) prepared by reduction of the imine complexes, the presence of these protons was not detected. [Co^{II}(**174b**)] can be oxidized to [Co^{III}(**174b**)] by ferricinium ion; the same complexes can be obtained by oxidation [Co^{II}(H_2-**174a**)]$(PF_6)_2$ with ferricinium ion to [Co^{III}(H_2-**174a**)]$(PF_6)_3$ followed by reduction of the imine groups. In [Zn(H_2-**174a**)]$(PF_6)_2$ the six coordinate pseudo-octahedral zinc(II) ion coordinates two amine nitrogen atoms, two phenolic oxygen atoms, and two *trans*-pyridine nitrogen atoms. The structure is C_2 symmetric; the absolute configuration about the zinc(II) ion is Δ, Δ, Λ, and the configuration about the nitrogen atoms of the amine group are R, R. The imine groups are tilted above and below of the N_2O_2 plane; the zinc(II) ion is located in this plane. The open-site cavity defined by two phenolic oxygen atoms and the two imine nitrogen atoms is too large to accommodate a metal ion of the first transition series [202].

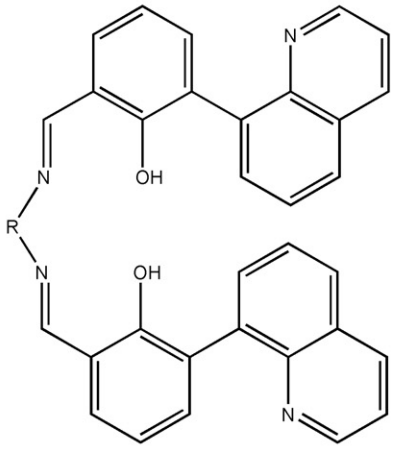

	R
H_2-**172a**	$(CH_2)_2$
H_2-**172b**	o-C_6H_{10}

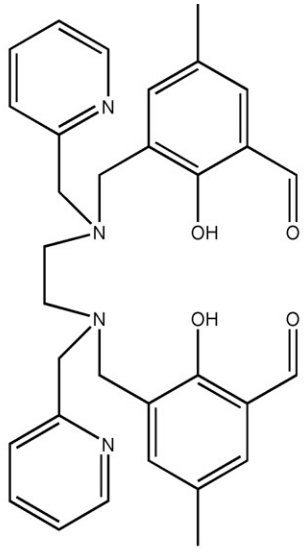

H_2-**173a**

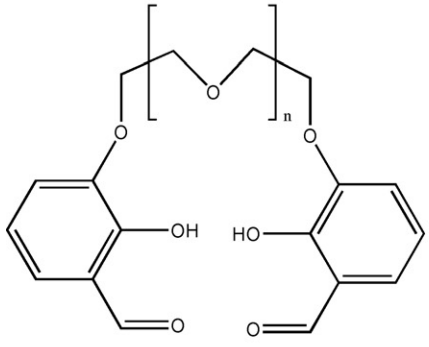

	n
H_2-**173b**	1
H_2-**173c**	2

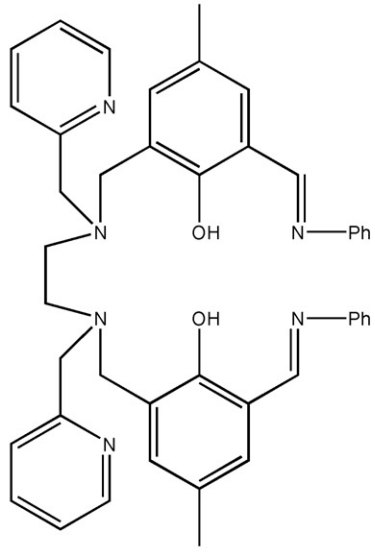

H_2-**174a**

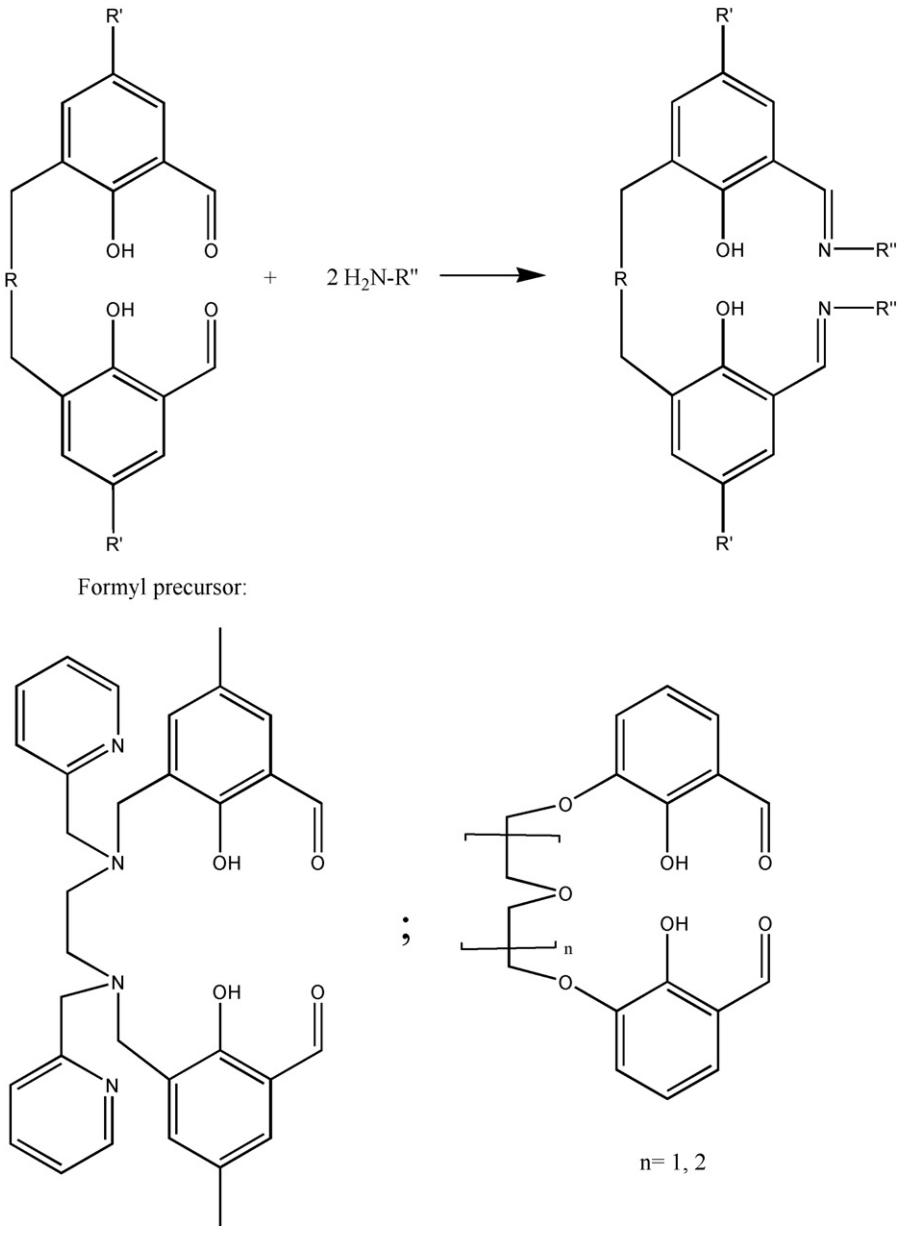

Scheme 7. Synthesis of the [1 + 2] side-off ligands.

The condensation of H_2-**173b**, H_2-**173c**, [Na_2(**173b**)] or [Na_2(**173c**)] with $NH_2(CH_2)_nC_6H_4N$ ($n = 1$, 2) and H_2NCH_2COOH gives rise to H_2-**175a**, [Na(H-**175a**)(H_2O)], H_2-**175b** and [Na(H_3-**175c**)(H_2O)], which contains one inner O_2O_3 or O_2O_4 and one outer $N_2N_2O_2$ or $N_2O_2O_2$ adjacent coordination site. The formation of [1 + 2] entities for these compounds was proved by ESI-mass and ^{1}H NMR spectra. [Ni(**175a**)] and [Cu(**175a**)] have been synthesized by reaction of H_2-**175a** with the appropriate metal acetate while [NiNa(**L**)(CH_3COO)]·nH_2O (H_2-**L** = H_2-**175a**, H_2-**175b**) derived from the reaction of the preformed ligand with nickel(II) acetate in the presence of NaOH; the same complexes have been obtained by template procedure. An octahedral coordination about the nickel(II) ion was proposed. Similarly, [MNa(H-**175c**)(H_2O)] (M=Cu^{II}, Ni^{II}) was prepared by the reaction of [Na(H_3-**173c**)(H_2O)] with the appropriate metal acetate; again an octahedral coordination about the nickel(II) ion was proposed [203].

The reduction of H_2-**175a** and H_2-**175b** to H_2-**176a** and H_2-**176b** was monitored by ^{1}H NMR and FAB or ESI-mass spectra. The related complexes [MNa(**L**)(CH_3COO)]·nH_2O or [MnNa(**L**)($CH_3COO)_2$]·nH_2O (M = Cu,Ni) were synthesized by reaction of H_2-**176a** or H_2-**176b** with the appropriate metal acetate hydrate in the presence of NaOH. Solid state electronic spectra and magnetic measurements indicate that the copper(II) ion is square pyramidal while nickel(II) ion is octahedral [203].

In [NiBa(**177**)]$(CF_3SO_3)_2$·$4H_2O$, obtained by H_2-**177**, $Ni(CH_3COO)_2$·$4H_2O$ and $Ba(CF_3COO)_2$, in spite of the open diimine structure in [**177**]$^{2-}$ the nickel(II) ion accepts intramolecular double chelation from the two salicylidene imine groups in a head-to-head manner. Thus, the polyether group forms a loop-like crown-ethers. The nickel(II) ion has an

octahedral geometry while the barium(II) ion is nine coordinate. The oxime oxygen atoms were coordinated to the adjacent barium(II) ions in a head-to-tail manner. Consequently, the neighboring nickel(II) ions are pressed closely to form a four-membered Ni_2O_2 ring (Fig. 124), this inducing a ferromagnetic Ni···Ni coupling. The complex releases the barium(II) ion with the consequent formation of [Ni(**177**)], when treated with guanidinium sulfate [204].

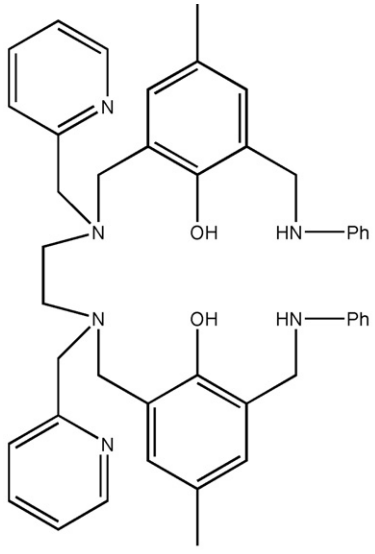

H_2-**174b**

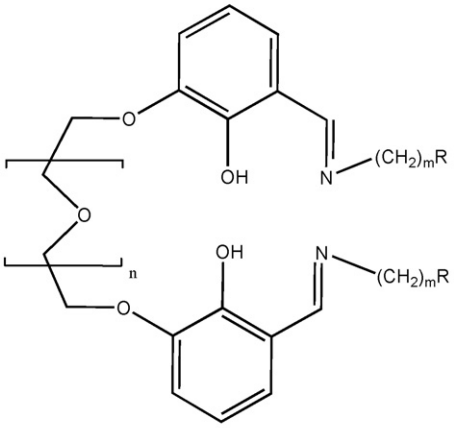

	R	n	m
H_2-**175a**	C_5H_4N	1	1
H_2-**175b**	C_5H_4N	2	2
H_4-**175c**	COOH	1	1

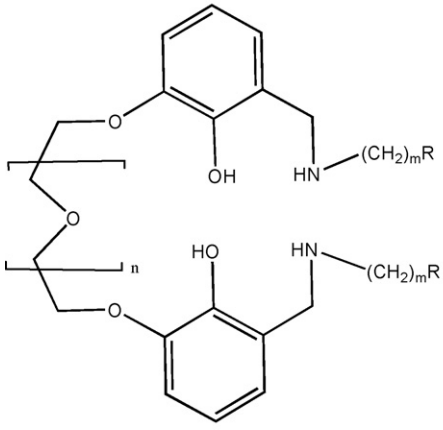

	R	n	m
H_2-**176a**	C_5H_4N	1	1
H_2-**176b**	C_5H_4N	2	2

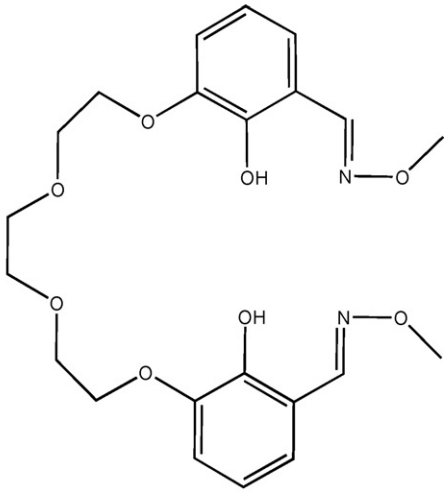

H_2-**177**

H_2-**178a**···H_2-**178d** were prepared by condensation of the appropriate diformyl derivative with methyl- or *n*-propylamines. H_2-**178d** and $Ni(CH_3COO)_2{\cdot}4H_2O$ yield the helical complex $[Ni_2(\mathbf{178d})_2]{\cdot}CHCl_3$, where each nickel(II) ion is linked in a *trans* square planar geometry by NO-coordination sites from two different ligands, winding in a helical loop from one nickel(II) to the other nickel(II) ion. The nickel ions and chelating groups lie approximately on two parallel planes, with a Ni···Ni distance of 3.554 Å (Fig. 125). The ^{1}H NMR spectrum of the complex confirms the persistence in solution of the helical arrangement. Reaction of H_2-**178d** with $Cu(CH_3COO)_2{\cdot}H_2O$ yields a complex which, according to ESI mass spectrometry data, was suggested to be $[Cu_2(\mathbf{178d})_2]$ like the nickel(II) complex [205].

9. Asymmetric side-off systems

The asymmetric side-off compartmental ligands have been prepared by condensation of 3-methoxy- or 3-ethoxy-2-hydroxybenzaldehyde, salicylaldehyde or 3-formyl-2-hydroxybenzoic acid with the amine precursors, derived from the reaction of the esters of 3-methoxy-2-hydroxobenzoic acid or salicylic acid with the appropriate diamine $H_2N–R–NH_2$. They contain an inner N_2O_2 site, with one amide and one amine nitrogen and two phenolic functions, and an outer O_2O_2 or O_2O site, involving again the two phenolic functions and one or two oxygen atoms of the methoxy-, ethoxy-, or carboxylic group. In addition, the Schiff base H-**179a**, synthesized by the [1 + 1]

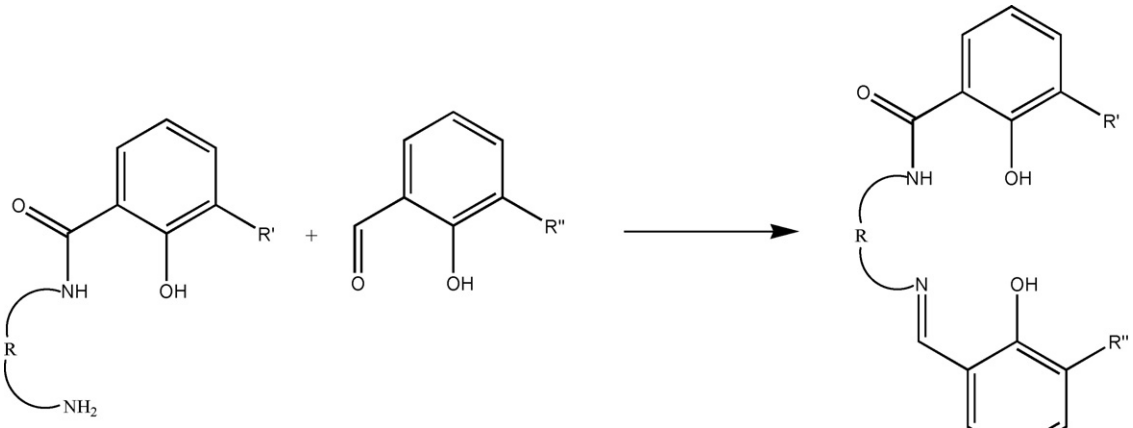

R = $(CH_2)_2$; $C(CH_3)_2CH_2$; $CH_2C(CH_3)_2CH_2$
R' = OCH_3; OC_2H_5; H
R"= OCH_3; H; COOH

Scheme 8. Synthesis of asymmetric side-off ligands.

condensation of salicylaldehyde with an excess of ethylenediamine, by further reaction with 3-formyl-2-hydroxybenzoic acid, forms, H_3-**179** which also contains an inner N_2O_2 site and an outer O_2O site (Scheme 8).

The reaction of H_3-**179** with $Cu(CH_3COO)_2{\cdot}H_2O$ or the condensation of [Cu(H-**179a**)(OH)]·$2H_2O$ with 3-formyl-2-hydroxybenzoic acid afford [Cu(H-**179**)], which forms $[Cu_2Co(\mathbf{179})_2(H_2O)]{\cdot}H_2O{\cdot}CH_3OH$ or $[Cu_2Ni(\mathbf{179})_2(H_2O)]{\cdot}2H_2O$ with the appropriate metal(II) perchlorate in the presence of NaOH. In both the complexes the central metal(II) ion is in an O_6 distorted octahedral geometry, formed by four phenolato and two carboxylate oxygen atoms from two terminal {Cu(**179**)} moieties. In $[Cu_2Co(\mathbf{179})_2(H_2O)]{\cdot}H_2O{\cdot}CH_3OH$ one terminal square planar copper(II) ion lies in a N_2O_2 site and the other copper(II) ion is square pyramidal in a N_2O_3 environment (Fig. 126) while in $[Cu_2Ni(\mathbf{179})_2(H_2O)]{\cdot}2H_2O$ the two terminal copper(II) ions are in a N_2O_2 square planar environment. The magnetic properties of these two heterotrinuclear complexes indicate an antiferromagnetic interaction between the central cobalt(II) or nickel(II) ion and the outer copper(II) ion ($J = -26.2\,cm^{-1}$ for Cu_2Co complex and $-50.6\,cm^{-1}$ for the Cu_2Ni one) [206].

The amine-amide precursors H-**180a** and H-**180b** derive from the reaction of ethylsalicylate and NH_2RNH_2 (R=CH_2CH_2, $C(CH_3)_2CH_2$). H_2-**180a** reacts with 3-formylsalicyclic acid to form H_4-**180** which affords $K_2[Cu(\mathbf{180})]{\cdot}1.5H_2O$ when mixed with KOH and $Cu(CH_3COO)_2{\cdot}H_2O$. The subsequent addition of $Cu(CH_3COO)_2{\cdot}H_2O$ forms $\{[Cu_4(\mathbf{180})_2(H_2O)]{\cdot}H_2O\}_n$, where the two neutral dinuclear units $\{Cu_2(\mathbf{180})(H_2O)\}$ and $\{Cu_2(\mathbf{180})\}$ are held together by a carboxylic group of the $\{Cu_2(\mathbf{180})(H_2O)\}$ moiety. In the $\{Cu_2(\mathbf{180})(H_2O)\}$ unit the inner copper(II) ion has a square planar N_2O_2 coordination, while the outer five coordinate copper(II) ion is in a O_5 trigonal bipyramidal geometry. Two $\{Cu_2(\mathbf{180})(H_2O)\}$ units are bridged together to form a tetranuclear structure. Each $\{Cu_2(\mathbf{180})\}$ units contains an inner square planar copper(II) ion in the N_2O_2 coordination set and an outer copper(II) ion coordinated by two bridged phenoxo atoms, one carboxylic oxygen atom, one carboxylic oxygen atom from the $\{Cu_2(\mathbf{180})(H_2O)\}$ moiety of the another adjacent unit. Again a tetranuclear structure $\{Cu_2(\mathbf{180})\}_2$ is formed. The two different tetranuclear assembles are held together to form a 1D $\{Cu_4(\mathbf{180})_2(H_2O)_2\}\{Cu_4(\mathbf{180})_2\}$ $\{Cu_4(\mathbf{180})_2(H_2O)_2\}\{Cu_4(\mathbf{180})_2\}$ chain. This complex shows is dominated by the antiferromagnetic interactions between the two copper(II) ions bridged by two phenoxo groups ($J = -130.5\,cm^{-1}$) with additional weak antiferromagnetic interactions between adjacent dinuclear systems ($J = -1.18\,cm^{-1}$) [207].

H_3-**181a**, H_3-**181b**, H_3-**182a**, H_3-**182b**, H_3-**182c**, H_3-**181d** and H_3-**183**, derived from the [1 + 1] condensation of H_2-**180a**, H_2-**180b**, H_2-**182e**, H_2-**182f**, H_2-**182g** with

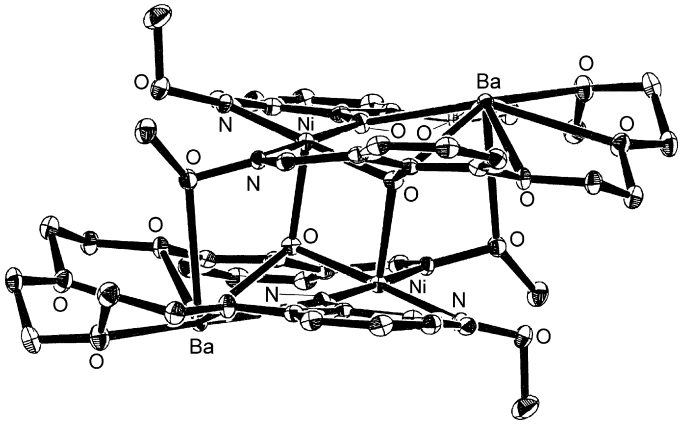

Fig. 124. Structure of $[NiBa(\mathbf{177})]_2^{4+}$.

the related formyl derivative, react with the appropriate metal(II) acetate in the presence of potassium hydroxide or *tert*-butoxide to form [MK(**L**)] (M=Cu^{II}, Ni^{II}), with a N_2O_2 square planar metal(II) ion and a O_5 five coordinate potassium ion bound to the outer O_2O_2 site and to a methanol molecule. The simple mixing of [MK(**181a**)] with $[Ln(hfacac)_3(H_2O)_2]$ or $Tb(NO_3)_3{\cdot}H_2O$ (Ln^{III} = Eu^{III}, Gd^{III}, Tb^{III}, Dy^{III}) gave $[M_2Ln_2(\mathbf{181a})_2(hfacac)_4]$ (H-hfacac = hexafluoroacetylacetone) or $[Cu_2Tb_2(\mathbf{181a})_2(NO_3)_4]$ as indicated by FAB-mass spectra [208]. Under the same conditions $[M(hfacac)_2]$ (M=Zn^{II}, Cu^{II}, Ni^{II}, Co^{II}, Mn^{II}) or $[Mn(acac)_2]$ form $[Cu_2^{II}M_2^{II}(\mathbf{181a})_2(hfacac)_2]$ and $[Cu_2^{II}Mn_2^{II}(\mathbf{181a})_2(acac)_2]$, (H-facac = hexafluoroacetylacetone; H-acac = acetylacetone) [209]. The powder X-ray diffraction patterns showed that the $Cu_2^{II}Ln_2^{III}$ complexes are isomorphous to each other; the $Ni_2^{II}Ln_2^{III}$ complexes, also isomorphous to each other, are not isomorphous to the $Cu_2^{II}Ln_2^{III}$ complexes [208,210].

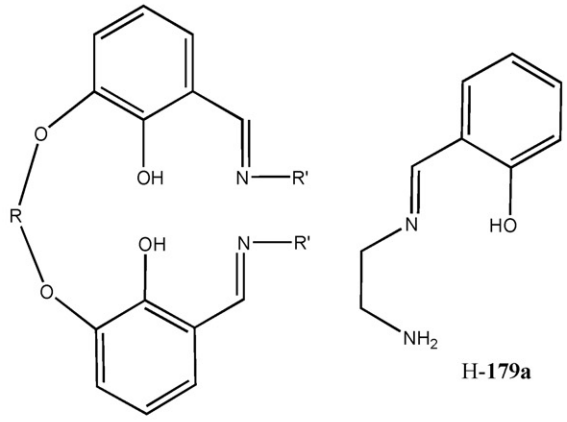

H-**179a**

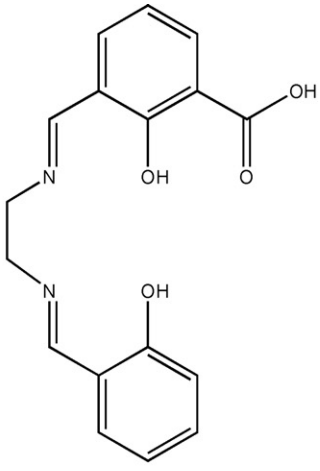

H_3-**179**

	R	R'
H_2-**178a**	$(CH_2)_4$	n-C_3H_7
H_2-**178b**	$(CH_2)_8$	n-C_3H_7
H_2-**178c**	$(CH_2)_{12}$	n-C_3H_7
H_2-**178d**	o-C_6H_4	CH_3

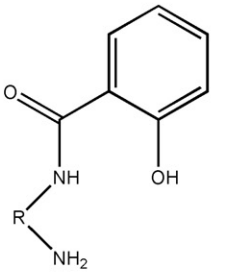

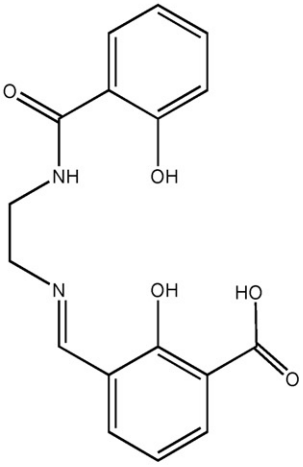

H_4-**180**

	R
H_2-**180a**	$(CH_2)_2$
H_2-**180b**	$C(CH_3)_2CH_2$

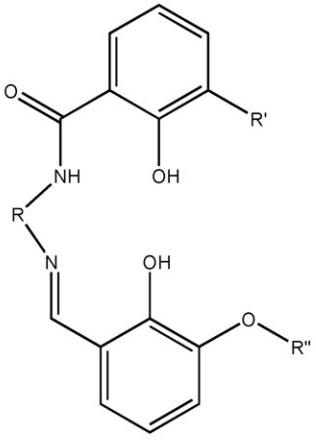

	R	R'	R''
H_3-**181a**	$(CH_2)_2$	H	CH_3
H_3-**181a**	$C(CH_3)_2CH_2$	H	CH_3
H_3-**182a**	$C(CH_3)_2CH_2$	OCH_3	CH_3
H_3-**182b**	$(CH_2)_2$	OCH_3	CH_3
H_3-**182c**	$(CH_2)_2$	OCH_3	C_2H_5
H_3-**182d**	$CH_2C(CH_3)_2CH_2$	OCH_3	CH_3

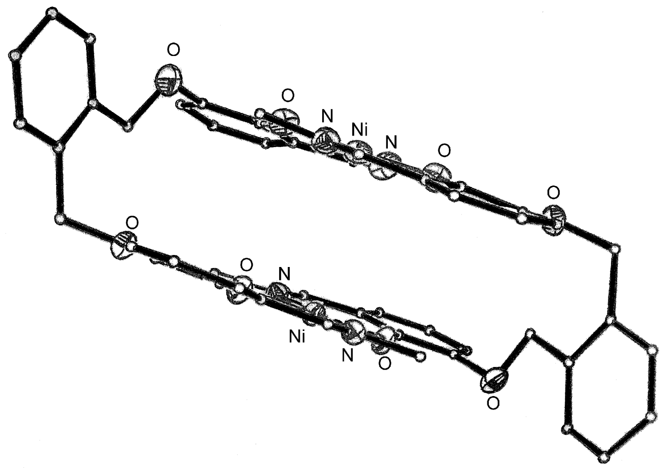

Fig. 125. Structure of $[Ni_2(\mathbf{178d})_2]$.

In the cyclic structure of $[Cu_2Gd_2(\mathbf{181a})_2(hfacac)_4]$, each square planar $[Cu(\mathbf{181a})]^{3-}$ functions as a mononegative bridging ligand-complex to the two eight coordinate gadolinium(III) ions. The two phenoxo and the methoxy atoms at one side of the copper(II) complex coordinate to a gadolinium(III) ion as a tridentate ligand with a Cu···Gd distance of 3.432 Å while the amido oxygen atom on the opposite side of the copper(II) complex coordinates to another gadolinium(III) ion as a monodentate ligand with a Cu···Gd distance of 5.620 Å. The Cu···Cu and Gd···Gd distances are 4.953 and 7.886 Å, respectively (Fig. 127a) [208].

$[Cu_2Mn_2(\mathbf{181a})_2(acac)_2]$ (Fig. 127b) has a cyclic $Cu_2^{II}Mn_2^{II}$ tetranuclear structure, which resembles the above $Cu_2^{II}Ln_2^{III}$ ones, the major difference being the hexacoordinate O_6 environment about the manganese(II) ions instead of the O_8 eight coordinate lanthanide(III) ion. Furthermore, each copper(II) ion is square planar in a N_2O_2 donor set [209].

Also the structures of $[Cu_2Tb_2(\mathbf{182a})_2(NO_3)_4]·2CH_2OH$ and $[Cu_2Tb_2(\mathbf{183})_2(NO_3)_4(DMF)_2]$ (Fig. 128) resemble those of the Cu_2Ln_2 ones containing β-diketonates. The copper(II) ions adopt a square planar coordination in the inner N_2O_2 site, while the nine coordinate terbium(III) ions are in the outer (O_2O_2 or O_2O) sites. The two ions are doubly bridged one to the other by two phenoxo oxygen atoms belonging to $[\mathbf{182a}]^{3-}$ or $[\mathbf{183}]^{3-}$ with Cu···Tb separations of 3.400 and 3.417 Å, respectively. In $[Cu_2Tb_2(\mathbf{183})_2(NO_3)_4(DMF)_2]$ and $[Cu_2Tb_2(\mathbf{182a})_2(NO_3)_4]$, the copper···copper separations are 5.001 and 5.232 Å, respectively while the separations between the copper(II) and terbium(III) ions, bound to each other through the amido oxygen, are 5.535 and 5.730 Å, respectively. The intermolecular metal···metal separations are larger than 6.8 Å for $[Cu_2Tb_2(\mathbf{183})_2(NO_3)_4(DMF)_2]$ and 7.2 Å for $[Cu_2Tb_2(\mathbf{182a})_2(NO_3)_4]$ [210].

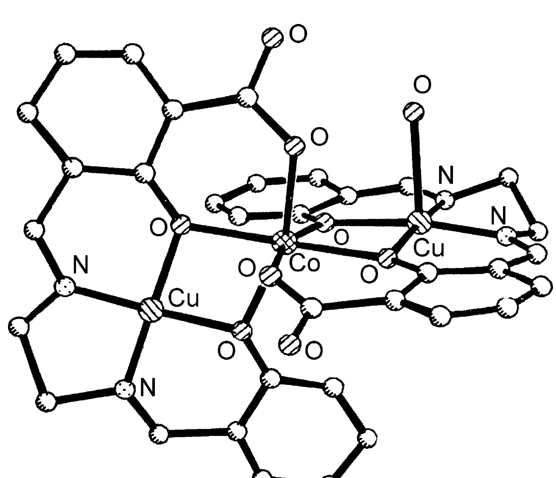

Fig. 126. Structure of $[Cu_2Co(\mathbf{179})_2(H_2O)]$.

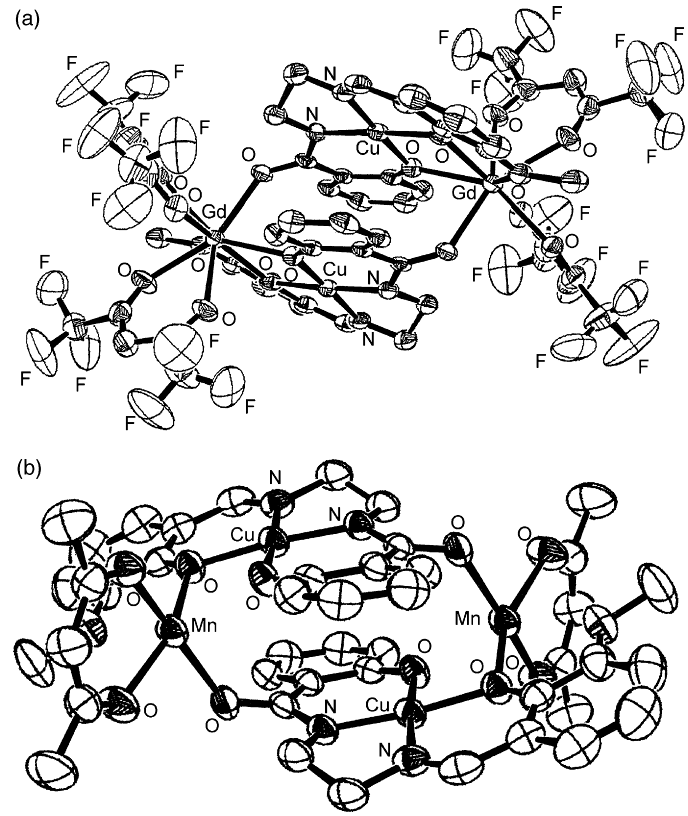

Fig. 127. Structure of $[Cu_2Gd_2(\mathbf{181a})_2(hfacac)_4]$ (a) and $[Cu_2Mn_2(\mathbf{181a})_2(acac)_2]$ (b).

The magnetic interaction between the Cu^{II} and Eu^{III} ions has been estimated to be small positive or nearly zero. The Cu_2Gd_2 complex with $[\mathbf{181a}]^{3-}$ has an $S = 8$ spin ground state resulting from the Cu^{II}-Gd^{III} ferromagnetic coupling within the cyclic $Cu_2^{II}Gd_2^{III}$ tetramer ($J_1 = +3.1\ cm^{-1}$ and $J_2 = +1.2\ cm^{-1}$) while the intra- and intermolecular Gd^{III}-Gd^{III} magnetic interaction is negligible. A ferromagnetic interaction between the copper(II) and terbium(III) ions and between the copper(II) and dysprosium(III) ions was proposed to occur in the related Cu_2Ln_2 complexes with $[\mathbf{181a}]^{3-}$. The field dependence on the magnetization of these complexes confirms the ferromagnetic nature of the interaction between copper(II) and dysprosium(III) ions [208]. In the Cu_2Gd_2 complexes with $[\mathbf{182a}]^{3-}$ and $[\mathbf{183}]^{3-}$ there are two different ferromagnetic Cu–Gd interactions: the stronger one

($J = 7.09$–$2.56\,cm^{-1}$) is supported by the double phenoxo bridge while the weaker one ($J = 0.53$–$0.07\,cm^{-1}$) corresponds to the single amido bridge (Cu–N–C–O–Gd). Replacement of the gadolinium(III) ions with the anisotropic terbium(III) ions yields tetranuclear entities showing slow relaxation of magnetization and magnetization hysteresis. Detailed relaxation and hysteresis loop studies establish single-molecule magnet (SMM) behavior, which is influenced by weak intermolecular interactions [210]. For the tetranuclear $Cu_2^{II}M_2^{II}$ complexes the intramolecular Cu^{II}–Cu^{II} and M^{II}–M^{II} magnetic interactions have been both neglected, because no Cu^{II}–Cu^{II} magnetic interaction was detected in $[Cu_2^{II}Zn_2^{II}(\mathbf{181c})_2(hfacac)]_2$ and the M^{II}–M^{II} distance is even longer than the Cu^{II}–Cu^{II} one. The calculated coupling constants were $J_1 = -13.3\,cm^{-1}$, and $J_2 = -13.3\,cm^{-1}$ for $[Cu_4^{II}(\mathbf{181a})_2(hfacac)_2]$, $J_1 = -15.8\,cm^{-1}$, $J_2 = -15.8\,cm^{-1}$, for $[Cu_2^{II}Ni_2^{II}(\mathbf{181a})_2(hfacac)_2]$; $J_1 = -10.9\,cm^{-1}$, $J_2 = -3.7\,cm^{-1}$, and $zJ' = -0.09\,cm^{-1}$ for $[Cu_2^{II}Fe_2^{II}(\mathbf{181a})_2(hfacac)_2]$; $J_1 = -11.0\,cm^{-1}$, $J_2 = -3.8\,cm^{-1}$, and $zJ' = -0.06\,cm^{-1}$ for $[Cu_2^{II}Mn_2^{II}(\mathbf{181a})_2(hfacac)_2]$ and $J_1 = -20.2\,cm^{-1}$ and $J_2 = -0.3\,cm^{-1}$ for $[Cu_2^{II}Co_2^{II}(\mathbf{181a})_2(hfacac)_2]$ (J' is the coupling constant between tetranuclear units) [209].

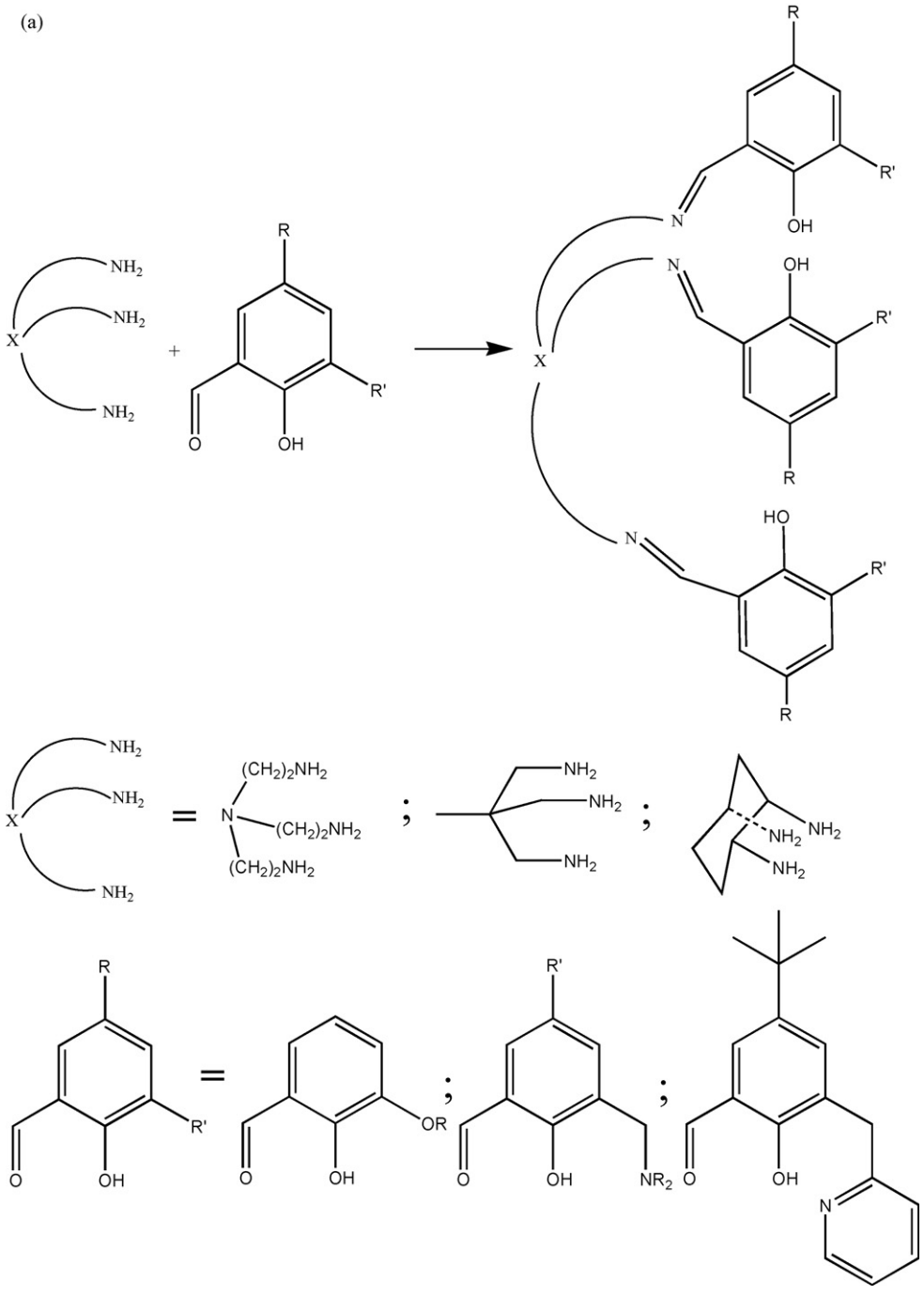

Scheme 9. Synthesis of [3 + 1] (a) or [1 + 3] (b) ligands .

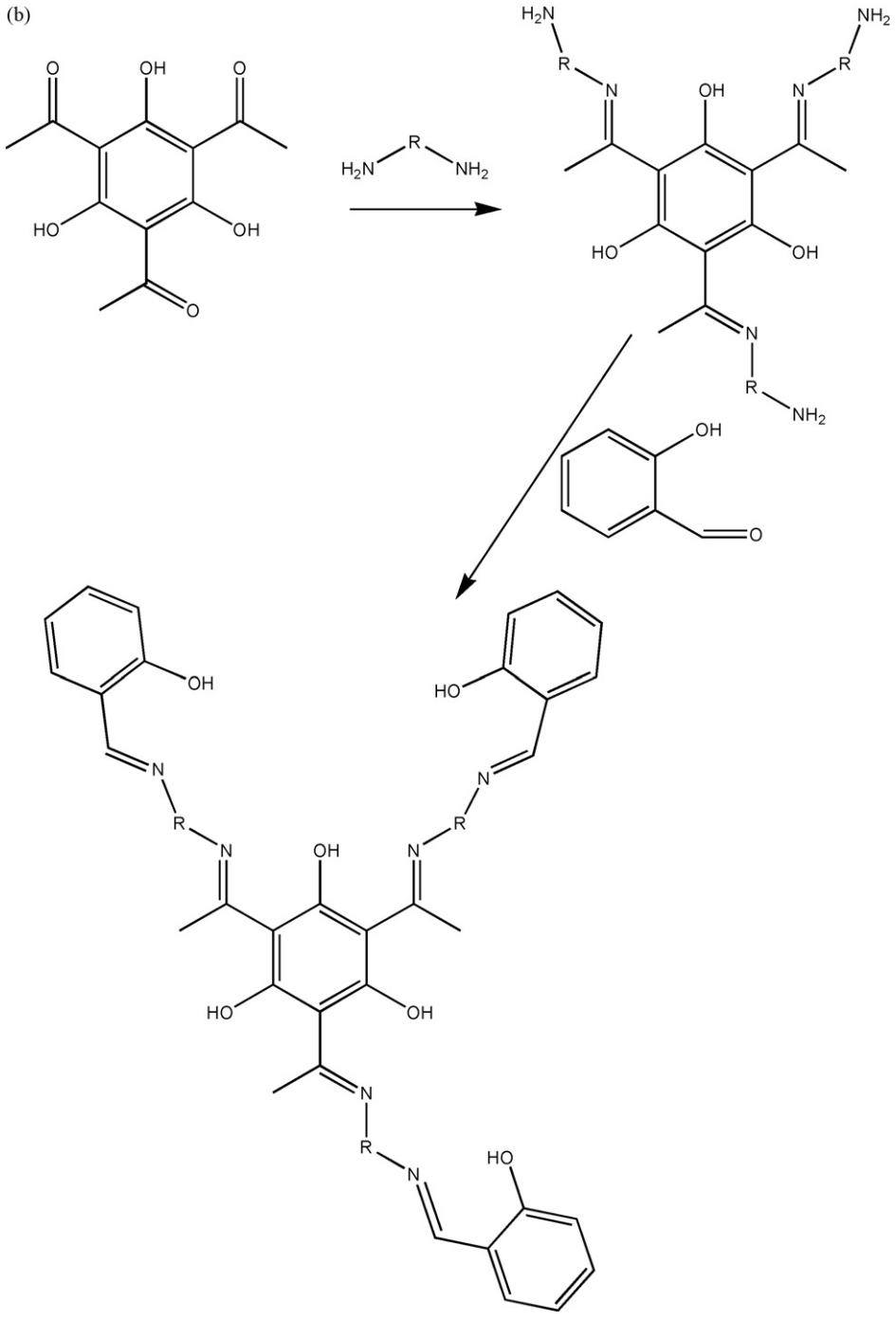

Scheme 9. (*Continued*).

10. [3 + 1] and [1 + 3] Polypodal systems

The synthesis and the coordination chemistry of tripodal polyamines have been successfully tested in the formation of the related Schiff bases by [3 + 1] condensation with the appropriate formyl-derivatives, according to Scheme 9a. Furthermore, the keto-derivative 1,3,5-trihydroxy-2,4,6-triacetylbenzene forms [1 + 3] polynucleating ligands by a step by step reaction with the diamine $H_2NC(CH_3)_2CH_2NH_2$ in a 1:3 molar ratio followed by condensation of the resulting Schiff base with three equivalents of salicylaldehyde or 3,5-substituted salicylaldehyde, according to Scheme 9b.

The complexation of the heptadentate ligands, derived from ring-substituted salicylaldehydes and tris(2-aminoethyl)amine (tren) with lanthanide(III) ions was known to be dominated by the sensitivity of these ligands to hydrolysis which prevented isolation of the expected neutral lanthanide complexes [211]. Mixing of H_3-**184**, derived from

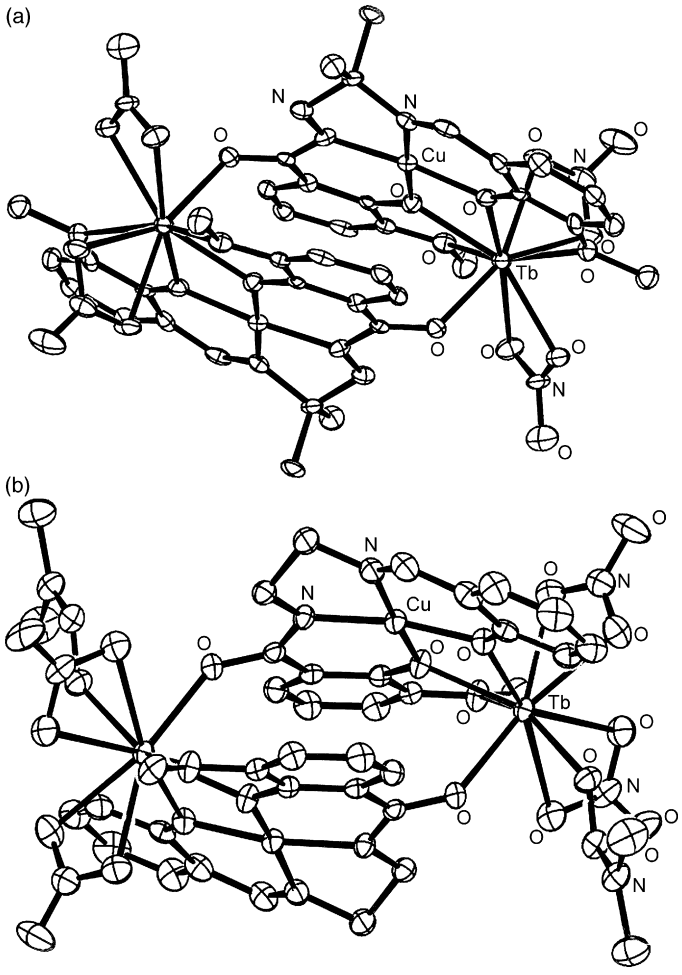

Fig. 128. Structure of $[Cu_2Tb_2(\mathbf{183})_2(NO_3)_4(DMF)_2]$.

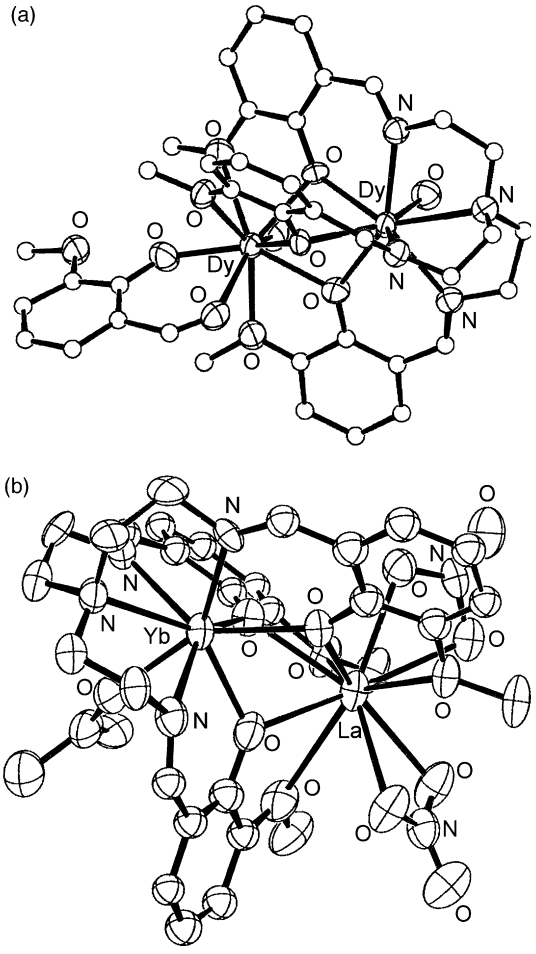

Fig. 130. Structure of $[Dy_2(\mathbf{184})(o\text{-vanillinato})(H_2O)_2]^{2+}$ (a) and $[YbLa(\mathbf{184})(NO_3)_2(CH_3COCH_3)]^{+}$ (b).

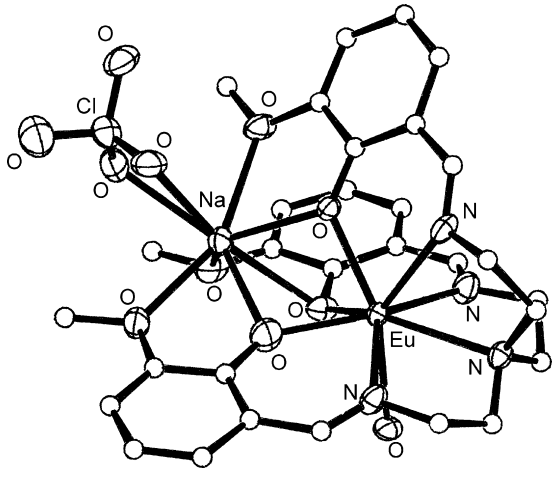

Fig. 129. Structure of $[EuNa(\mathbf{184})(H_2O)(ClO_4)]$.

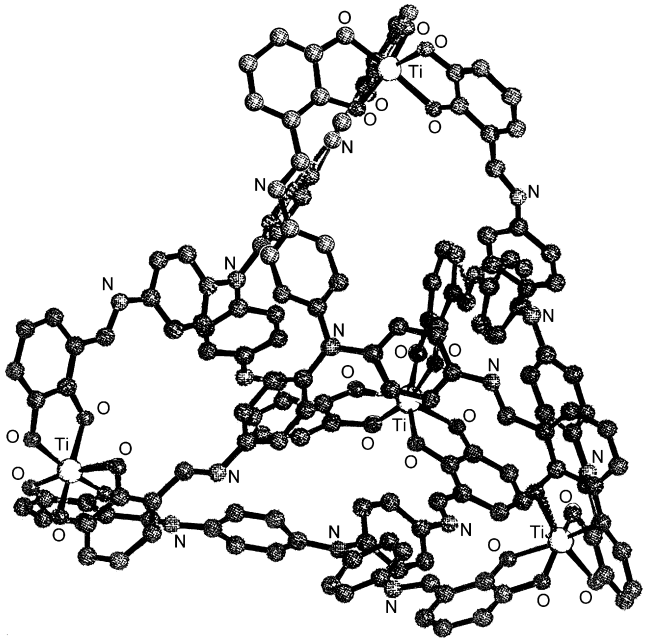

Fig. 131. Structure of $[Ti_4(\mathbf{185a})_4]^{4-}$.

3-methoxy-2-hydroxybenzaldehyde instead of salicylaldehyde, with $Ln(NO_3)_3{\cdot}6H_2O$ (Ln = Y, La, Eu, Tb, Dy) does not cause hydrolysis of the ligand, but proton migration from the phenol to the imine function and the coordination of the lanthanide(III) ion at the outer O_3O_3 site, as confirmed by ^1H NMR. Addition of base (especially CsOH) to [Ln(H_3-**184**)$(NO_3)_3(H_2O)_2$] induces a color change and precipitation of [Ln(**184**)(H_2O)] (Ln = Y, Eu,Tb,Dy), with a migration of the lanthanide ion from the O_3O_3 to the inner N_4O_3 chamber. The same complexes have been obtained by direct synthesis with H_3-**184**, $LnCl_3{\cdot}nH_2O$ and CsOH [213]. These complexes, when mixed with $NaClO_4$, give rise to [LnNa(**184**)$(ClO_4)(H_2O)$] where, according to NMR and X-ray data, the europium(III) and the sodium ions, 3.504 Å, apart, are eight coordinate in the inner N_4O_3 site and in the outer O_3O_3 coordination site of $[\mathbf{184}]^{3-}$, respectively. The shortest intermolecular Eu···Eu distance is 5.817 Å (Fig. 129) [212,213].

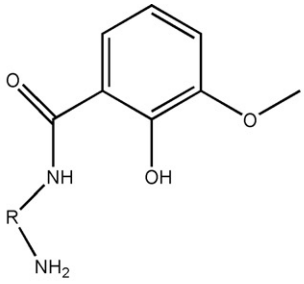

	R
H_2-**182e**	$C(CH_3)_2CH_2$
H_2-**182f**	$(CH_2)_2$
H_2-**182g**	$CH_2C(CH_3)_2CH_2$

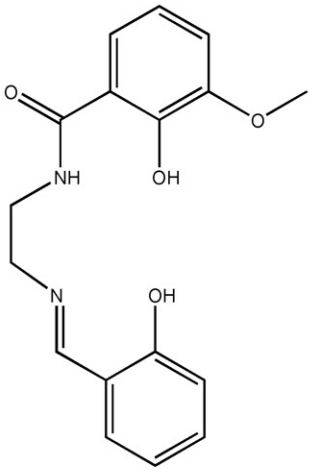

H_3-**183**

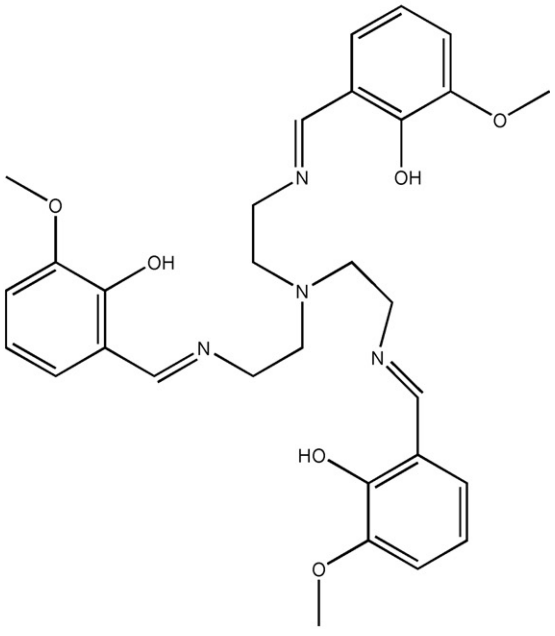

H_3-**184**

Also, it is possible to introduce a second identical or different lanthanide(III) ion into the outer O_3O_3 chamber through the reaction of [Ln(**184**)(H_2O)] with $Ln(NO_3)_3{\cdot}6H_2O$ or $Ln'(NO_3)_3{\cdot}6H_2O$ which gives rise to $[Ln_2(\mathbf{184})(NO_3)_2(H_2O)_2](NO_3)$ or $[LnLn'(\mathbf{184})(NO_3)_2(H_2O)_2](NO_3)$ respectively; FAB-mass spectra indicate the exclusive formation of heterodinuclear species, without any trace of signals coming form scrambling of the two lanthanide ions, especially when the lanthanide(III) ion (Ln′) in the outer site has a larger ionic radius than the lanthanide(III) ion (Ln) in the inner site. A magnetic study shows a weak ferromagnetic interaction in the GdNd, GdCe, and YbGd complexes with $[\mathbf{184}]^{3-}$. In contrast, an antiferromagnetic interaction occurs in the DyGd and ErGd complexes. Such magnetic behaviour provides additional support to the existence of heterodinuclear complexes [212]. $[Gd_2(\mathbf{184})(NO_3)_3]{\cdot}3H_2O$ shows an antiferromagnetic behavior ($J = -1.04\,cm^{-1}$) [68,213].

The introduction of *o*-vanillinato $[van]^-$ in a methanol solution of [Dy(**184**)(H_2O)] and $Dy(NO_3)_3{\cdot}5H_2O$ affords $[Dy_2(\mathbf{184})(van)(H_2O)_2](NO_3)_2{\cdot}2H_2O$ (Fig. 130a), with a core unit built up from two dysprosium(III) ions, one nine coordinate in the inner N_4O_3 coordination site and the other eight coordinate in the outer O_3O_3 coordination site, triply bridged by three phenolate oxygen atoms of $[\mathbf{184}]^{3-}$ [68].

In $[YbLa(\mathbf{184})(NO_3)_2(CH_3COCH_3)]_2[La(NO_3)_5(H_2O)]$, obtained from [Yb(**184**)] and an excess of $La(NO_3)_3{\cdot}5H_2O$, the eight coordinate ytterbium(III) and ten coordinate lanthanum(III) ions, 3.633 Å apart, are encapsulated by the N_4O_3 inner coordination chamber and the outer O_3O_3 chamber of $[\mathbf{184}]^{3-}$, respectively (Fig. 130b) [213].

The use of appropriate triamines in the [1 + 3] condensation reaction with 3-formyl-2 hydroxy phenol affords the triscatechol derivatives H_6-**185a**, H_6-**185b** and H_6-**185c** which, analogously to the related dicatechol ligands H_4-**163a**···H_4-**163q** and H_4-**163**, can adopt the catechol imine or the keto-enamine structure. The equilibrium between the two different structures is temperature dependent and therefore thermochromic behavior can be observed for the catechol imines. The more intense color at high temperatures is due to the keto-enamine structure, while the slightly yellow color at low temperatures corresponds to the catechol imine. In H_6-**185c** hydrogen bonding with transfer of the hydrogen from the internal hydroxo group to the imine nitrogen atoms is observed in the solid state but only at two of the three catechol units. Here, two keto-enamine and one catechol imine moieties are present in the solid state.

H_6-**185a** or H_6-**185b** react with $TiO(acac)_2$ and alkali metal carbonate to form the highly symmetric tetranuclear

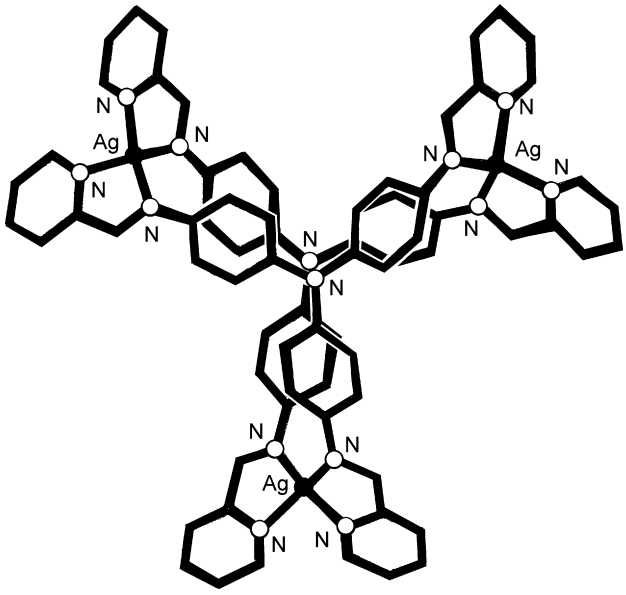

Fig. 132. Structure of $[Ag_3(\mathbf{186})_2]^{3+}$.

complexes $M_8[Ti_4(\mathbf{L})_4]$ (M = Li, Na, K), as indicated by NMR and FT-ICR MS measurements and confirmed by the structure of $K_8[Ti_4(\mathbf{185a})_4]{\cdot}23DMF$ (Fig. 131) which contains four titanium(IV) ions located on the corners of slightly distorted tetrahedron with all four complex units having the same configuration. The triangular faces are blocked by the four ligands $[\mathbf{185a}]^{6-}$, which each coordinate to three

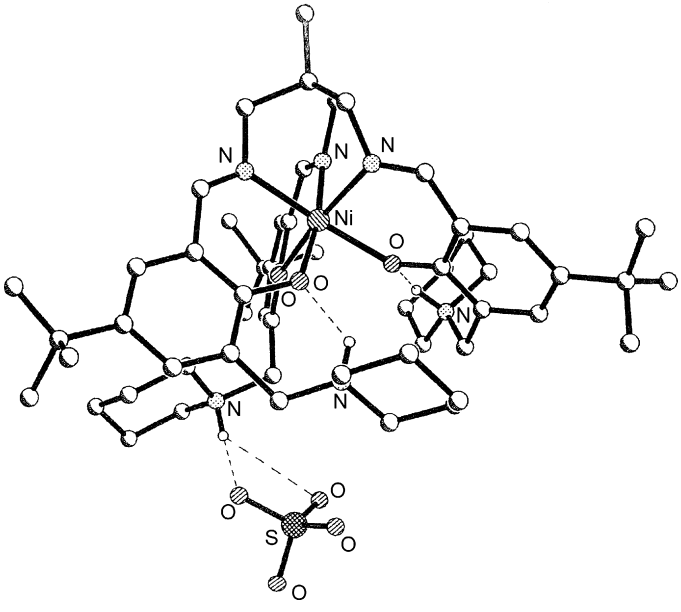

Fig. 133. Structure of {[Ni(H_3-**188**)](SO_4)}.

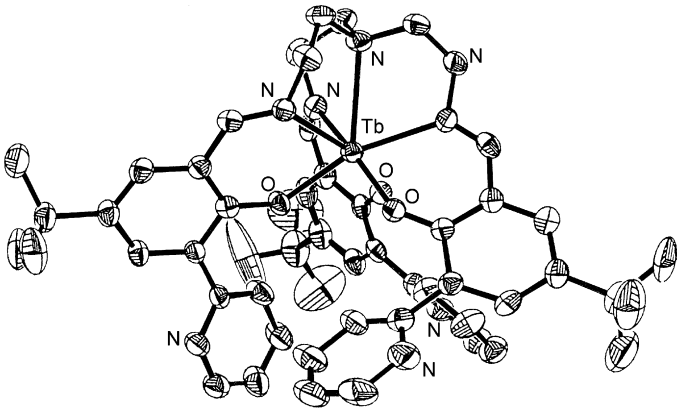

Fig. 134. Structure of [Tb(**190**)].

of the metal centers. Four potassium ions lay in the interior of a huge cavity, each binding to the three oxygen atoms of the four titanium tris(catecholate) units. Additionally each potassium ion binds three dimethylformamide molecules. The Ti···Ti distances are in the range 16.7–17.1 Å [214].

The similar reaction of H_6-**185c** with titanium(IV) ions and sodium salts leads to Na[NaTi(**185c**)] in which the sodium ion acts as a template and stabilizes the mononuclear titanium(IV) complex. One sodium ion coordinates to the internal catecholate oxygen atoms and the nitrogen atoms of $[\mathbf{185c}]^{6-}$. The potassium ion, bigger than the sodium ion, cannot act in a similar fashion and give rise to a mixture of oligomers whose crystallization results in a few crystals of $K_2[K_2(Ti_3O_2)(\mathbf{185c})_2]$ where $[\mathbf{185c}]^{6-}$ encapsulates a Ti_3O_2 cluster. One of the ligands is approaching from the top, the other from the bottom forming two cavities for the binding of two potassium cations. Finally, the oligomeric mixture of coordination compounds of $[\mathbf{185c}]^{6-}$, when dissolved in dimethylsulfoxide, forms the tetranuclear complex $[Ti_4(\mathbf{185c})]^{8-}$ as indicated by NMR and ESI –mass spectra [214].

The C_3-symmetry tris-bidentate ligand **186**, synthesized in two steps via N_2H_4–Pd/C mediated reduction of tris-4-nitrotriphenylamine followed by condensation of the resulting triamine with 2-formylpyridine, reacts with $AgPF_6$ in the presence of $[NH_4](PF_6)$ to form $[Ag_3(\mathbf{186})_2](PF_6)_3$ (Fig. 132) which maintains its trinuclear structure also in solution. ^{1}H NMR complexometric titration of a $CD_3CN/CDCl_3$ solution of **186** with successive addition of $AgPF_6$ firstly leads to $[Ag_2(\mathbf{186})_2]^{2+}$, which by further addition of the silver(I) salt, turns into non-fluxional helicate complex $[Ag_3(\mathbf{186})_2]^{3+}$, stable also in the presence of excess silver(I) ion [215].

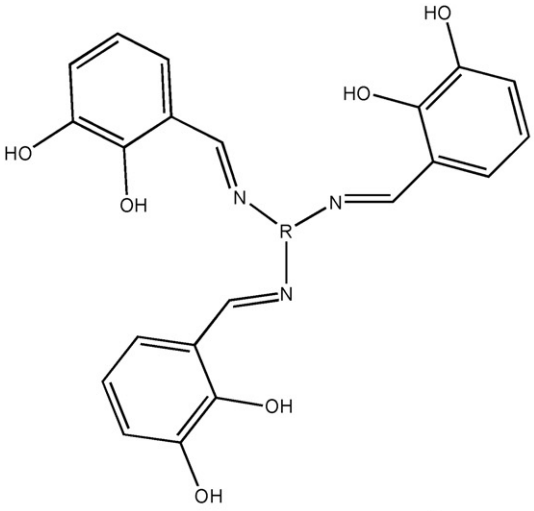

H_6-**185a**

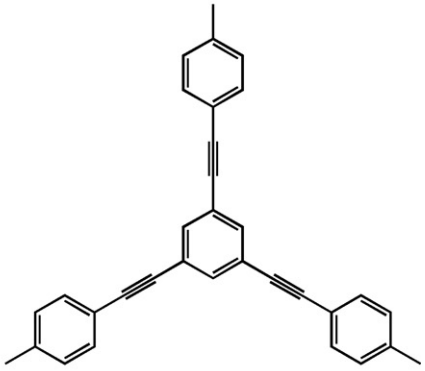

H_6-**185b**

H_6-**185c**

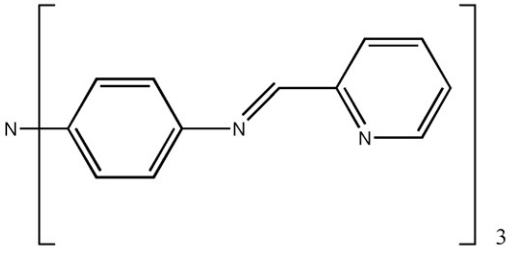

186

H_3-**187a**, H_3-**187b**, H_3-**187c**, H_3-**188** and H_3-**189**, prepared by [3 + 1] condensation of the appropriate precursors, act as ditopic ligands for $NiSO_4$ or $NiCl_2$. Zwitterionic form of these ligands has a trianionic N_3O_3 Ni-binding site and a

tricationic trialkylammonium sulfate binding site and gives an overall neutral $NiSO_4$-complex which is needed to achieve high solubility in non-polar water-immiscible solvents. The formation of the Schiff bases was confirmed by the X-ray structure of H_3-**187a**, which is very expanded with the tertiary amine groups more than 5.2 Å from their centroid [216].

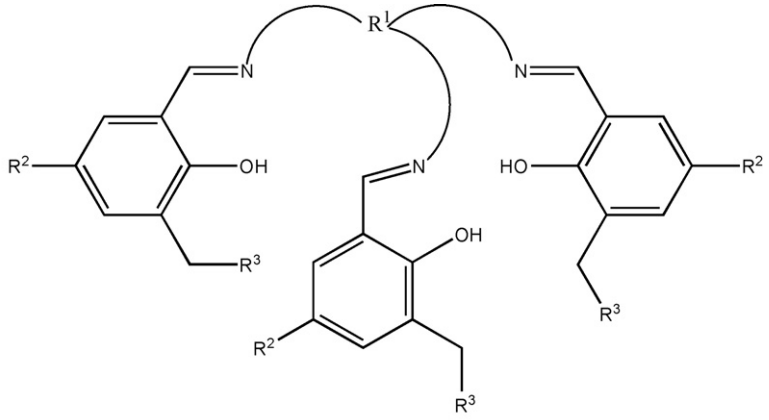

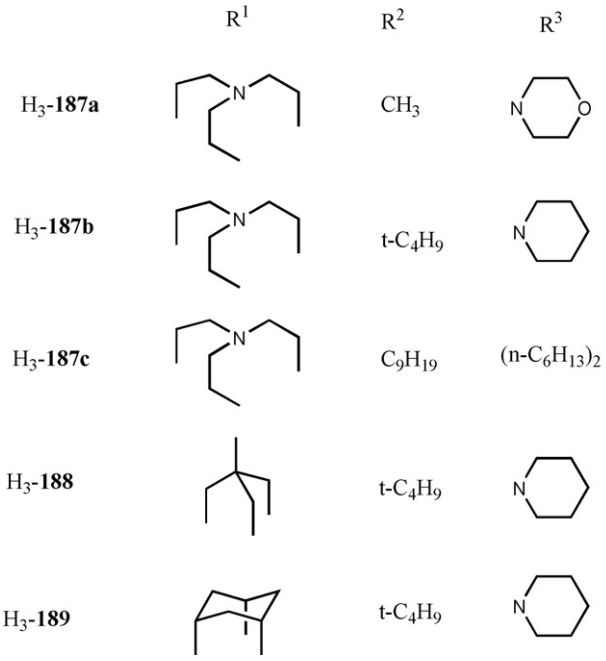

Incorporation of the nickel(II) ion into the N_3O_3 donor set influences the disposition of the pendant tertiary amine groups, and hence the efficacy of anion binding as observed for {[Ni(H_3-**188**)(SO_4)]} (Fig. 133) and {[Ni(H_3-**188**)](Cl)}(Cl), obtained by reaction of H_3-**188** with $NiSO_4{\cdot}6H_2O$ or $NiCl_2{\cdot}6H_2O$ in a 1:1 molar ratio in methanol. Formation of these complexes results in a pseudo-octahedral coordination geometry about the metal ion. One of the piperidinium protons forms a bifurcated H-bond to two oxygen atoms of the sulfate ion. Two of the piperidinium protons make close contacts to the phenolate oxygen atoms in the same arms of the ligand. In [Ni(H_3-**188**)](Cl)}(Cl) all the piperidine nitrogen atoms make fairly close contacts to their neighboring phenolate oxygen atoms. One of the chloride ions lies close to the pseudo-threefold axis and is bonded strongly to one piperidinium group and weakly to another [216].

The kerosene-soluble ligand H_3-**188** is a good extractant for nickel salts, showing high selectivity for recovery of $NiCl_2$ over $NiSO_4$. This reagent can be stripped and recycled directly using aqueous ammonia or by first displacing the nickel(II) ion with acid and then neutralizing the pendant alkylammonium groups. The acid-stripping, however, is accompanied by hydrolytic degradation of the reagent [216].

The condensation of 5-*tert*-butyl-2-2-hydroxy-3-(2′pyridyl)benzaldehyde with tris-(2-aminoethyl)amine in the presence of lanthanide(III) nitrate gives the remarkably stable isomorphous complexes [Ln(**190**)], where the seven coordinate monocapped octahedron lanthanide(III) ion encapsulates within the N_4O_3 cavity of $[\mathbf{190}]^{3-}$; all the pyridyl groups remain uncoordinated (Fig. 134). The ^{1}H NMR spectrum of [Lu(**190**)] in CD_3OD proves the presence of only one species with a structure similar to that in solid-state. Furthermore, luminescent studies of the europium(III) and terbium(III)

complexes indicate the coordination of two methanol molecules to the lanthanide ions [217].

H_6-**191a**, H_6-**191b** and H_6-**191c**, derived from the [1 + 3] condensation of 1,3,5-trihydroxy-2,4,6-triacetylbenzene with $NH_2C(CH_3)_2CH_2NH_2$ followed by the further [1 + 3] condensation of the resulting tris-imine derivative with three equivalents of salicylaldehyde, 3,5-di-*tert*-butyl-2-hydroxybenzaldehyde or 5-nitro-2-hydroxybenzaldehyde [218-220], when mixed with $Ni(CH_3COO)_2{\cdot}4H_2O$ forms [Ni_3(**L**)] where the three square planar diamagnetic metal ions are coordinated by two phenolato donors and two imine nitrogen donors, as confirmed by ^1H and ^{13}C NMR spectra and X-ray structure. Whereas the overall structure of [Ni_3(**191c**)] is nearly planar, the structures of [Ni_3(**191a**)] and [Ni_3(**191b**)] are bowl-shaped as a result of ligand folding. The Ni···Ni distances are 7.00 Å, 7.17 Å and 7.13 Å, respectively. There is a remarkable enhancement of the electronic absorptions on going from H_2-salen to H_6-**191a** and from [Ni(salen)] to [Ni_3(**191a**)], attributable to a strong electronic communication between the three Schiff base units involving π molecular orbitals [218]. Similarly, the reaction of H_6-**191a** with $Cu(CH_3COO)_2{\cdot}2H_2O$ affords [Cu_3(**191a**)]·$CHCl_3{\cdot}0.5C_6H_5CH_3$ where three {Cu(salen)}-like units are bridged in a m-phenylene arrangement. Each copper ion is in a distorted square planar coordination environment [219,220].

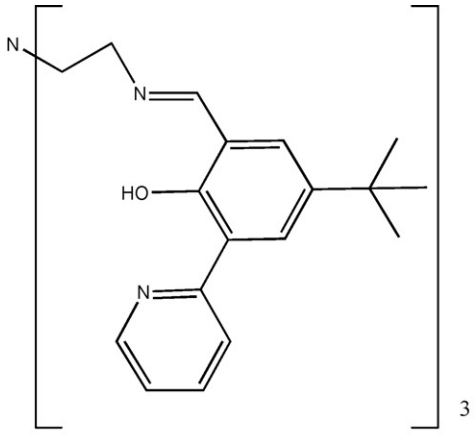

H_3-**190**

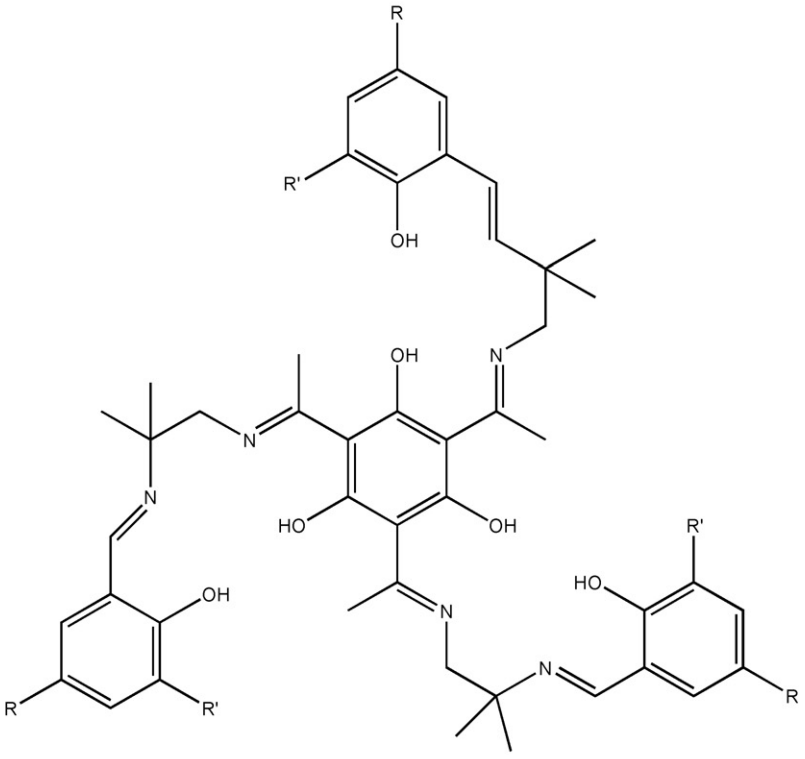

	R	R'
H_6-**191a**	H	H
H_6-**191b**	$C(CH_3)_3$	$C(CH_3)_3$
H_6-**191c**	NO_2	H

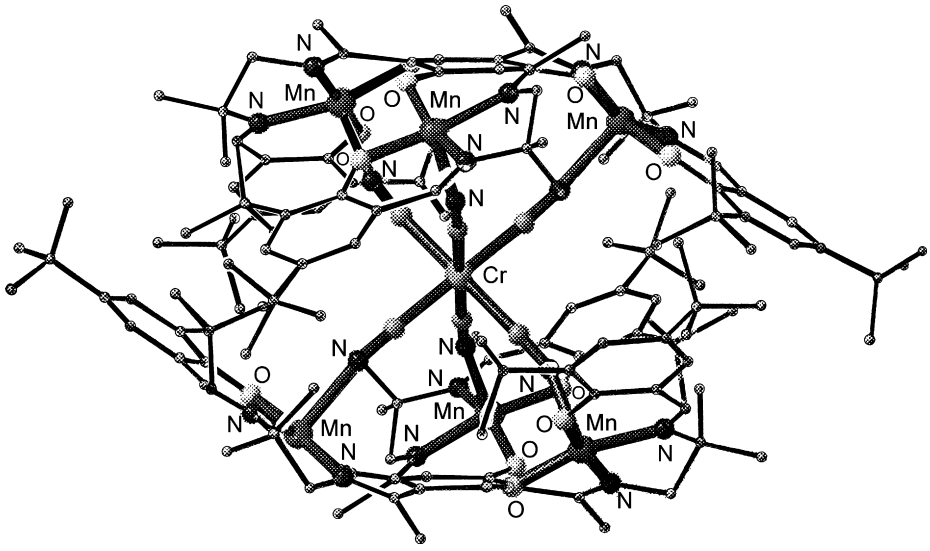

Fig. 135. Structure of $[\{Mn_3(\mathbf{191b})\}_2\{Cr(CN)_6\}(CH_3OH)_3(CH_3CN)_2\}^{3+}$.

Magnetic susceptibility and EPR measurement show that in $[Cu_3(\mathbf{185a})]$ the three copper(II) ions are non interacting at room temperature but ferromagnetically coupled ($J = 1.52\,cm^{-1}$) with decreasing temperature with an $S_t = 3/2$ spin ground state. In particular, the EPR spectrum of $[Cu_3(\mathbf{191a})]$ exhibits a pattern of 10 hyperfine lines due to the coupling of three copper(II) ions. Resonances around $g = 4$ in both perpendicular and parallel mode EPR spectra demonstrate a zero-field splitting of $D \sim 74 \times 10^{-4}\,cm^{-1}$ arising from anisotropic/antisymmetric exchange interactions. The DFT calculations show an alternation in the sign of the spin densities of the central benzene ring corroborating the spin-polarization mechanism as origin for the ferromagnetic coupling. Experimental and density functional theory calculations support that the ferromagnetic coupling observed in $[Cu_3(\mathbf{191a})]$ derives from a spin-polarization mechanism [219].

The three {Ni(salen)}-like subunits are electronically interacting via the π system of the bridging chloroglucinol backbone. The strength of this interaction is mediated by two opposing effects: the electron density at the terminal phenolates and the folding of the ligand at the central phenolates. $[Ni_3(\mathbf{191a})]$ is irreversibly oxidized at 0.32 V versus ferrocenium/ferrocene (Fc^+/Fc), whereas $[Ni_3(\mathbf{191b})]$ and $[Ni_3(\mathbf{191c})]$ exhibit reversible oxidations at 0.22 V versus Fc^+/Fc and 0.52 V versus Fc^+/Fc respectively. The oxidized species $[Ni_3^{III}(\mathbf{191b})]^+$ and $[Ni_3^{III}(\mathbf{191c})]^+$ undergo a valence–tautomeric transformation, involving a nickel(III) ion and a phenoxyl radical species, as observed by EPR spectroscopy. Thus, these oxidized forms exhibit the phenomena of valence tautomerism and mixed valence simultaneously. The oxidized trinuclear complexes are intrinsically mixed valence because of three {Ni(salen)}-like subunits. Additionally, the oxidized species exhibit a valence tautomerism between a metal-centered oxidation to the nickel(III) species and a ligand-centered oxidation to a phenoxyl radical. The comparison between $[Ni_3^{II}(\mathbf{191b})]^+$ and $[Ni_3^{II}(\mathbf{191c})]^+$ establishes that the ligand-centered oxidation occurs at the central benzene ring. The delocalization of this phenoxyl radical over three {Ni(salen)}-like units stabilizes this radical compared to the analogous phenoxyl radical of a mononuclear $[Ni^{III}(salen)]^+$. This delocalization proves the strong electronic communication of the three {Ni-(salen)} subunits through the central chloroglucinol unit [220].

The reaction of H_6-**191b**, $Mn(CH_3COO)_2{\cdot}4H_2O$, $K_3[Cr(CN)_6]$ and $NaBPh_4$ in CH_3OH/H_2O yields, $[\{(Mn_3\mathbf{191b})\}_2\{Cr(CN)_6\}(CH_3OH)_3(CH_3CN)_2](BPh_4)_3{\cdot}4CH_3CN{\cdot}2(C_2H_5)_2O$, as indicated by MALDI-TOF and ESI mass spectra and confirmed by the X-ray structure, which consists of two $[Mn_3(\mathbf{191b})]$ complexes bridged by a central $[Cr(CN)_6]^{3-}$ ion as a sixfold connector (Fig. 135). The manganese ions are in a N_3O_2 square pyramidal coordination geometry in which the nitrogen atoms of $[Cr(CN)_6]^{3-}$ units occupy apical positions. The analysis of the magnetic properties reveals that this complex is indeed a single-molecule magnet [220].

11. Conclusion and future perspectives

A remarkable number of papers has been published in the period of time covered by the present review (2002–2006), regarding the acyclic Schiff base compartmental ligands, their reduced polyamine derivatives and the related homo- and/or hetero-polynuclear complexes.

The different typologies of symmetric or asymmetric ligands, i.e. [1 + 1] acyclic, [1 + 1], [1 + 2] or [2 + 1] end-off, [2 + 1] or [1 + 2] side-off and [3 + 1] or [1 + 3] polypodal systems, have been considered, emphasizing their ability to recognize selectively specific species (especially metal ions in a particular oxidation state) at the two adjacent similar or dissimilar coordination sites. Generally, the two coordination sites of these ligands have been designed to give rise to dinuclear complexes, where the two metal ions complete their coordination environment with the related counter anions and/or solvent molecules.

When the ligand design favors the occurrence of coordinative instauration at the metal ions, owing to the lack of a suitable donor atom at least in one of the two coordination chambers, polynuclear or polymeric species are obtained via the formation of bridges between neighboring complexes (i.e., $–O^-$, $–S^-$, CH_3COO^-, NCS^-, N_3^-, etc.).

Special efforts have been devoted in these last years to the preparation of suitable asymmetric ligands, capable of assuring, thanks to their quite dissimilar coordination chambers in close proximity, the coordination of a specific metal ion exclusively in one of the two chambers with the consequent formation of pure heteronuclear isomers.

The best conditions for the acquisition of the designed ligands have been reported, together with those which give rise to systems different from the designed ones. In particular, the role of the formyl- and amine-precursors in directing the reactions, especially in the presence of metal ions as templating agents, the role of the solvent and of the temperature have been evaluated. Also, the site occupancy of the different metal ions, the site migration and the transmetalation processes have been estimated especially by X-ray diffractometric, magnetic, ESR, IR, UV–vis, NMR and electrochemical measurements. Cyclic voltammetry data allowed defining the occurrence and the stability of mixed-valent complexes, together with their physico-chemical properties.

In the present review compartmental ligands have been considered, with adjacent similar or dissimilar coordination chambers connect by appropriate endogenous bridging groups as hydroxo, phenolate, thiophenolate, or pyridazine, capable of holding together two metal ions, giving rise to quite peculiar physico-chemical properties (i.e. magnetic, optical, electrochemical, etc.), to enhanced or unusual reactivity and catalysis (hydrolysis of phosphoric esters, oxidation of organic substrates, polymerization of appropriate monomers, etc.).

Recently the immobilization of some quite promising systems on appropriate surfaces or polymeric platforms has successfully been pursued. Different synthetic strategies were proposed for grafting or bonding compartmental Schiff bases and/or their related complexes to silica gel as follows:

- one step grafting of a compartmental ligand, previously modified with a peripheral arm bearing a terminal $–Si(OR)_3$ grafting group, to samples of activated silicas;
- grafting on to silica of a primary diamine already functionalized with a $Si(OR)_3$ group, and later formation of a grafted compartmental ligand via suitable condensation reactions;
- bonding of mononuclear or heterodinuclear Schiff base complexes to silica gel samples previously functionalized with organic compounds bearing terminal coordinating groups.

In all these synthetic pathways, condensation of appropriately chosen or designed amine and formyl-precursors was employed to yield acyclic systems capable of recognizing d- and/or f-metal ion selectively. A rapid growing of basic and applied studies of this solid-state chemistry can easily be foreseen.

Very recently a quite interesting synthetic strategy was proposed for the preparation of 2D immobilized complexes in the form of densely packed self-assembled monolayer (SAM) on atomically planar Au(1 1 1) surface: it consists in the use of the disulfide diacid HOOC-$(CH_2)_2$-S_2-$(CH_2)_2$COOH (H_2-L′) as a suitable exogenous bonding linker between two dinuclear cobalt(II) complexes with 2,6-bis(*N*,*N*′-bis(-2-pyrolyl)amino)-methyl)-4-*tert*-butylphenolato) (H_3-**L**); the resulting tetranuclear disulfide complex $[Co_4(\mathbf{L})_2(L')]$, cleaved at the gold surface, generates two dinuclear complexes $[Co_2(\mathbf{L})(L'')]$ (H-L″ = HOOC$(CH_2)_2$SAu), each bound to the surface by a covalent Au-thiolate bond. This SAM system is capable of reversible O_2 binding, its affinity toward O_2 being much higher compared to the dicobalt(II) solution precursor [221].

The anchorage of similar systems, bearing suitable functionalizations at the periphery of their coordinating moiety, on to molecular platforms (biopolymers or molecules of biological relevance) originates quite important systems to be employed in medicine or biology (both in diagnosis and therapy).

The evolution of the dinuclear systems into the polynuclear ones is another promising goal recently pursued by different synthetic strategies, i.e.:

- The design of appropriate precursors which give rise to more sophisticated systems capable of selective multiple recognition processes.
- The use of specific metal ions suitable to form polynuclear systems instead of the dinuclear ones.
- The use of bifunctional ligands which link two or more dinuclear species into a unique entity containing tetranuclear or ordered polymeric complexes. The particular compartmental ligands, used to form the dinuclear unit, address the systems toward the formation of homo- or hetero-polynuclear systems.

This has favored the growth of a chemical engineering aimed at giving rise to new network topologies, controlled by appropriately designed synthetic routes, capable of turning well defined heterodinuclear or heterotrinuclear complexes into oligomeric, 1D, 2D or 3D coordination species by the use of suitable spacers. Useful functionalities as molecular magnetic materials, conducting solids, zeolite-like materials, catalysts, environment materials, etc. are deriving from this synthetic strategy.

Self-organization of single organic or inorganic components into sophisticated architectures with peculiar optical and/or magnetic properties is another goal of these researches, currently pursued with great interest. Several of these systems, containing homo- or hetero-polymetallic clusters, are under scrutiny owing to their ability to act as single molecule magnets.

This last synthetic strategy has been pursued quite recently also with different dinucleating ligands as 1,3- or 1,4-substituted phenylene-bis-β-diketonates. Under suitable experimental conditions they form the planar homodinuclear $[M_2$(1,3-bis-β-dike)$_2]$ or homotrinuclear complexes $[M_3$(1,4-bis-β-dike)$_3]$ which, by subsequent reaction with difunctional linkers (L = 4,4′-bipyridine, pyrazine, 1,4-diazabiciclo [2.2.2]-octane 4,4′-dipyridylsulfide, 4,4-(1,3-xylylene)-bis(3,5-dimethylpyrazole), hexamethylenetetramine etc.) capable of coordinating the metal ions in their axial positions, evolve

into the polymeric species $[M_2(1,3\text{-bis-}\beta\text{-dike})_2(L)]_\infty$ or $[M_3(1,4\text{-bis-}\beta\text{-dike})_3(L)]_\infty$. Similar systems, under the same experimental conditions, do not evolve into the polymeric ones but form only coordination compounds $[M_2(1,3\text{-bis-}\beta\text{-dike})_2(L)_2]$ or dimerize to the tetranuclear species $[M_4(1,3\text{-bis-}\beta\text{-dike})_4(L)_2]$. Thus, the use of specific chelating moieties (i.e. bis-β-diketonates), metal ions (i.e. Cu^{II}, Fe^{III}) or bridging linkers can address selectivity the synthesis towards a unique complex with a well defined complexity [222]. Using similar polynucleating bis-β-diketonates with additional coordinating functionalities, the synthesis of homo-dinuclear, -tetranuclear or -octanuclear complexes can be tuned [223].

The design of acyclic compartmental ligands as anion receptors is another increasing area of interest. In order to propose efficient systems, appropriate precursors have been synthesized, capable of forming complexes with ideal environment for selective binding of anions, since the size of the encapsulation cavity could be modulated by the choice of the metal ion. For instance, quite recently Schiff base complexes have been prepared with an outer chamber containing four phenol groups into a tetrahedral array that tightly binds fluoride ion though four OH···F hydrogen bonding interactions [224].

As further evolution of this concept the design of compartmental ligands suitable to recognize a cation in one chamber and the related anion in the adjacent one in order to transport selectively a specific salt across an appropriate membrane, was successfully carried out. The efficiency of a number of side-off ligands capable of transferring transition metal sulfate from one water solution into another across an organic membrane was tested and proposed for the solution of problems of relevance in hydrometallurgy.

The insertion of appropriate spacers between the coordinating moieties, i.e. the use of appropriate diamine of the type $H_2N\text{-spacer-}NH_2$ allowed the formation of quite interesting polynuclear helicate complexes capable of including different metal ions (i.e. Ti^{IV} and K^I or Na^I). The synthesis of metallohelicates, by twisting multidentate organic ligands, through interaction with appropriate metal ions, plays a key role in the development of supramolecular chemistry. Homo- and hetero-polynuclear species arise from these syntheses with unique structural features and peculiar optical or magnetic properties.

All these examples and the continuously growing publications demonstrate that many efforts are currently carried out and the related results under adequate scrutiny in order to apply the acyclic compartmental ligands and/or the related complexes to different, quite important fields which range from the preparation of molecular- or nano-systems, to the set up of probes, sensors and devices for analytical, medical or biological applications of supramolecular arrays for new or more efficient catalytic processes, the storage and/or activation of small molecules, the encapsulation of dangerous species, the selective transport and recovery of salts or organic compounds. The great interest devoted to these fields by different, highly esteemed groups all over the world will lead to new, quite exciting results both in basic and applied chemistry.

Acknowledgments

We thank Mrs. G. Bonato and Mr. A. Aguiari, for the valuable assistance in the collecting and classifying the data and in preparing drawings and the manuscript. Also we thank Progetto FIRB RBNE019H9K-MIUR for financial support.

References

[1] S. Brooker, Coord. Chem. Rev. 222 (2001) 33.
[2] W. Huang, H.-B. Zhu, S.-H. Goiu, Coord. Chem. Rev. 250 (2006) 414.
[3] A.L. Gavrilova, B. Bonish, Chem. Rev. 104 (2004) 349.
[4] D. Brooker, Eur. J. Inorg. Chem. (2002) 2535.
[5] P.A. Gale, Coord. Chem. Rev. 240 (2003) 191.
[6] P.D. Beer, E.J. Hayes, Coord. Chem. Rev. 240 (2003) 167.
[7] V. McKee, J. Nelson, R.M. Town, Chem. Soc. Rev. 32 (2003) 309.
[8] C. Suksai, T. Tuntulani, Chem. Soc. Rev. 32 (2003) 192.
[9] R. Ziessel, Coord. Chem. Rev. 216/217 (2001) 195.
[10] C. Liu, M. Wang, T. Zhang, H. Sun, Coord. Chem. Rev. 248 (2004) 147.
[11] P. Molenveld, J.F.J. Engbersen, D.N. Reinhoudt, Chem. Soc. Rev. 29 (2000) 75.
[12] V. Alexander, Chem. Rev. 95 (1995) 273.
[13] H. Okawa, H. Furutacki, D.E. Fenton, Coord. Chem. Rev. 174 (1998) 51.
[14] A. Martell, J. Penitka, D. Kong, Coord. Chem. Rev. 216 (2001) 55.
[15] J. Nelson, V. McKee, G. Morgan, in: K.D. Karlin (Ed.), Progress in Inorganic Chemistry, vol. 47, 1998, p. 167.
[16] S.R. Collinson, D.E. Fenton, Coord. Chem. Rev. 148 (1996) 19.
[17] W. Radecka, V. Paryzek, J. Patroniak, Lisowski, Coord. Chem. Rev. 249 (2005) 2156.
[18] (a) P.A. Vigato, S. Tamburini, Coord. Chem. Rev. 248 (2004) 1717;
(b) P. Guerriero, S. Tamburini, P.A. Vigato, Coord. Chem. Rev. 139 (1995) 17.
[19] P.A. Vigato, S. Tamburini, L. Bertolo, Coord. Chem. Rev. 251 (2007) 1311.
[20] (a) P. Gomez-Romero, C. Sanchez, Functional Hybrid Materials, Wiley–VCH, Weinheim (D), 2004;
(b) L.N.H. Arakaki, J.G.P. Espinola, M.G. da Fonseca, S.F. de Oliveira, A.N. de Sousa, T. Arakaki, C. Airoldi, J. Colloid Interface Sci. 273 (2004) 211;
(c) J.A.A. Sales, F.P. Faira, A.G.S. Prado, C. Airoldi, Polyhedron 23 (2004) 719;
(d) A.R. Cestari, E.F.S. Viera, E.C.N. Lopes, R.G. da Silva, J. Colloid Interface Sci. 272 (2004) 271;
(e) A.G.S. Prado, A.H. Tosta, C. Airoldi, J. Colloid Interface Sci. 269 (2004) 259;
(f) J.A. Sales, C. Airoldi, J. Non-Crist. Solids 330 (2003) 142.
[21] P. Sutra, D. Brunel, Chem. Commun. (1996) 2485.
[22] E.F. Murphy, L. Schmidt, T. Burgi, M. Maciejewski, A. Baiker, D. Grunther, M. Schneider, Chem. Mater. 13 (2001) 1296.
[23] I. Bar-Nahum, H. Cohen, R. Newmann, Inorg. Chem. 42 (2003) 3677.
[24] C.D. Nunes, M. Pillinger, A.A. Valente, A.D. Lopes, I.C. GonÇalves, Inorg. Chem. Commun. 6 (2003) 1228.
[25] R.J.P. Corriu, E. Lancelle-Beltran, A. Mehdi, C. Reyé, S. Brandès, R. Gillard, Chem. Mater. 15 (2003) 3152.
[26] P. Di Bernardo, P.L. Zanonato, S. Tamburini, P.A. Vigato, Inrog. Chim. Acta 360 (2007) 1083.
[27] Z.-Y. Zhang, C. Brouca-Cabarrecq, C. Hemmert, F. Dahan, J.P. Tuchagues, J. Chem. Soc., Dalton Trans. (1995) 1453.
[28] (a) X. Xia, M. Verelst, J.-C. Daran, J.-P. Tuchagues, J. Chem. Soc., Chem. Commun. (1995) 2155;
(b) Y. Xie, W. Bu, X. Xu, H. Jiang, Q. Liu, Y. Xue, Y. Fan, Inorg. Chem. Commun. 4 (2001) 558.
[29] S. Theil, R. Yerande, R. Chikate, F. Dahan, A. Brousseksou, S. Padhye, J.-P. Tuchagues, Inorg. Chem. 36 (1997) 6279.

[30] V. Patroniak, A.R. Stefankiewicz, J.-M. Lehn, M. Kubicki, M. Hoffmann, Eur. J. Inorg. Chem. (2006) 144.
[31] H. Asada, K. Hayashi, S. Negoro, M. Fujiwara, T. Matsushita, Inorg. Chem. Commun. 6 (2003) 193.
[32] N. Reddig, M.U. Triller, D. Pursche, A. Rompel, B. Krebs, Z. Anorg. Allg. Chem. 628 (2002) 2458.
[33] P. de Hoog, L. Durán Pachón, P. Gamez, M. Lutz, A.L. Spek, J. Reedijk, Dalton Trans. (2004) 2614.
[34] H.-D. Bian, W. Gu, J.-Y. Xu, F. Bian, S.-P. Yan, D.-Z. Liao, Z.-H. Jang, P. Cheng, Inorg. Chem. 42 (2003) 4265.
[35] S.K. Dey, M.S. El Fallah, J. Ribas, T. Matsushita, V. Gramlich, S. Mityra, Inorg. Chim. Acta 357 (2004) 1517.
[36] J.P. Costes, F. Dahan, J.-P. Laurent, Inorg. Chem. 25 (1986) 413.
[37] H.-D. Bian, J.-Y. Xu, W. Gu, S.-P. Yan, P. Cheng, D.-Z. Liao, Z.-H. Jiang, Polyhedron 22 (2003) 2927.
[38] Y.-B. Jiang, H.-Z. Kou, R.-J. Wang, A.-L. Cui, Eur. J. Inorg. Chem. (2004) 4608.
[39] (a) M.S. Ray, S. Chattopadhyay, M.G.B. Drew, A. Figuerola, J. Ribas, C. Siaz, A. Ghosh, Eur. J. Inorg. Chem. (2005) 4562;
(b) B. Sarkar, M.S. Ray, M.G.B. Drew, A. Figuerola, C. Diaz, A. Ghosh, Polyhedron 25 (2006) 3084;
(c) W.J. Jones, S. Gupta, L.J. Theriot, F.T. Helm, W.A. Baker Jr., Inorg. Chem. 17 (1978) 87;
(d) L. Menz, W. Haase, Z. Naturforch. A 31 (1976) 177;
(e) C. Aronica, G. Pilet, G. Chastanet, W. Wernsdorfer, J.-F. Jaquot, D. Lineau, Angew. Chem. Int. Ed. 45 (2006) 4659.
[40] M.K. Saha, I. Bernal, F.R. Fronczek, Chem. Commun. (2004) 84.
[41] M.F. Iskander, L. El-Sayed, N.M.H. Salem, W. Haase, H.J. Linder, S. Foro, Polyhedron 23 (2004) 23.
[42] R. Srinivasan, I. Sougandi, K. Velavan, R. Venkatesan, B. Verghese, P. Sambasiva Rao, Polyhedron 23 (2004) 1115.
[43] S. Mukherjee, T. Weyhermuller, E. Bill, P. Chaudhuri, Eur. J. Inorg. Chem. (2004) 4209.
[44] M. Koikawa, M. Ohba, T. Tokii, Polyhedron 24 (2005) 2257.
[45] J.B. Vincent, H.-R. Chang, K. Folting, J.C. Huffman, G. Christon, D.N. Hendrickson, J. Am. Chem. Soc. 109 (1987) 5703.
[46] Y.-G. Li, L. Lecren, W. Wernsdorfer, R. Clérac, Inorg. Chem. Commun. 7 (2004) 1281.
[47] W.-H. Gu, X.-Y. Chen, L.-H. Yin, A. Yu, X.-Q. Fu, P. Cheng, Inorg. Chim. Acta 357 (2004) 4085.
[48] (a) C. Boskovic, E. Rusanov, H. Stoeckli-Evans, H.U. Güdel, Inorg. Chem. Commun. 5 (2002) 881;
(b) A. Sieber, C. Boskovic, R. Bircher, O. Waldmann, S.T. Ochsenbein, G. Chaboussant, H.U. Güdel, N. Kirchner, J. van Slageren, W. Wernsdorfer, A. Neels, H. Stoeckli-Evans, S. Janssen, F. Juranyl, H. Mutka, Inorg. Chem. 44 (2005) 4315.
[49] N. Hoshino, T. Ito, M. Nihei, H. Oshio, Inorg. Chem. Commun. 6 (2003) 377.
[50] N. Hoshino, T. Ito, M. Nihei, H. Oshio, Chem. Lett. (2002) 844.
[51] H. Oshio, M. Nihei, A. Hiroyuki, H. Nojiri, M. Nakano, A. Yamaguchi, Y. Karaki, H. Ishimoto, Chem. Eur. J. 11 (2005) 843.
[52] C. Boskovic, A. Sieber, G. Chaboussant, H.U. Güdel, J. Ensling, W. Wernsdorfer, A. Neels, G. Labat, H. Stoeckli-Evans, S. Janssen, Inorg. Chem. 43 (2004) 5053.
[53] M. Dey, C.P. Rao, P.K. Saaenketo, K. Rissanen, Inorg. Chem. Commun. 5 (2002) 380.
[54] M. Dey, C.P. Rao, P.K. Saarenketo, K. Rissanen, Inorg. Chem. Commun. 5 (2002) 924.
[55] M.S. Ray, G. Mukhopadhyay, M.G.B. Drew, T.-H. Lu, S. Chaudhuri, A. Ghosh, Inorg. Chem. Commun. 6 (2003) 961.
[56] Y. Xie, H. Jiang, A.S.-C. Chan, Q. Liu, X. Xu, C. Du, Y. Zhu, Inorg. Chim. Acta 333 (2002) 138.
[57] A. Valent, M. Melník, D. Hudecová, B. Dudová, R. Kivekäs, M.R. Sundberg, Inorg. Chim. Acta 340 (2002) 15.
[58] Z. Lü, D. Zhang, S. Gao, D. Zhu, Inorg. Chem. Commun. 8 (2005) 746.
[59] C.-T. Yang, M. Vetrichelvan, X. Yang, B. Moubaraki, K.S. Murray, J.J. Vittal, Dalton Trans. (2004) 113.
[60] Y. Zou, W.-L. Liu, S. Gao, J. Xie, Q.-J. Meng, Chem. Commun. (2003) 2946.
[61] Y. Zou, W.-L. Liu, S. Gao, C.-S. Lu, D.-B. Dang, Q.-J. Meng, Polyhedron 23 (2004) 2253.
[62] Y. Zou, W.-L. Liu, C.-S. Lu, J.-L. Xie, C.-L. Ni, Q.-J. Meng, Inorg. Chem. Commun. 6 (2003) 1217.
[63] W. Liu, Y. Song, Y. Li, Y. Zou, D. Dang, C. Ni, Q.-J. Meng, Chem. Commun. (2004) 2348.
[64] W.-L. Liu, Y. Zou, C.-L. Ni, Z.-P. Ni, Y.-Z. Li, Y.-G. Yao, Q.-J. Meng, Polyhedron 23 (2004) 849.
[65] X. Wang, J.J. Vittal, Inorg. Chem. 42 (2003) 5135.
[66] S.K. Dey, N. Mondal, M.S. El Fallah, R. Vicente, A. Escuer, X. Solans, M.F. Bardía, T. Matsushita, V. Gramlich, S. Mitra, Inorg. Chem. 43 (2004) 2427.
[67] S. Sen, P. Talukder, S.K. Dey, S. Mitra, G. Rosair, D.L. Hughes, G.P.A. Yap, G. Pilet, V. Gramlich, T. Matsushita, Dalton Trans. (2006) 1758.
[68] J.P. Costes, F. Dahan, F. Nisodeme, Inorg. Chem. 42 (2003) 6556.
[69] R. Kannappan, D.M. Tooke, A.L. Spek, J. Reedijk, Inorg. Chim. Acta 359 (2006) 334.
[70] I.J. Hewitt, J.-K. Tang, N.T. Madhu, R. Clerac, G. Buth, C.F. Anson, A.K. Powell, Chem. Commun. (2006) 2650.
[71] Y. Zou, W.-L. Liu, C.-S. Lu, L.-L. Wen, Q.-J. Meng, Inorg. Chem. Commun. 7 (2004) 985.
[72] F. a), G.I. Tuna, J.-P. Pascu, M. Sutter, S. Andruh, J. Golhen, H. Guillevic, Pritzkow, Inorg. Chim. Acta 342 (2003) 131.
[73] F. Tuna, L. Patron, M. Andruh, Inorg. Chem. Commun. 6 (2003) 30.
[74] N. Sengottuvelan, D. Saravanakumar, M. Kandaswamy, Inorg. Chem. Commun. 8 (2005) 297.
[75] H. Adams, D.E. Fenton, P.E. McHugh, Inorg. Chem. Commun. 7 (2004) 880.
[76] H. Adams, D.E. Fenton, L.R. Cummings, P.E. McHugh, M. Ohba, H. Okawa, H. Sakiyama, T. Shiga, Inorg. Chim. Acta 357 (2004) 3648.
[77] J. Hermann, D. Schumacher, A. Erxleben, Eur. J. Inorg. Chem. (2002) 2276.
[78] H. Adams, S. Clunas, D.E. Fenton, T.J. Gregson, P.E. McHugh, S.E. Spey, Inorg. Chem. Commun. 5 (2002) 211.
[79] H. Adams, S. Clunas, D.E. Fenton, D.N. Towers, J. Chem. Soc., Dalton Trans. (2002) 3933.
[80] H. Adams, S. Clunas, D.E. Fenton, Inorg. Chem. Commun. 5 (2002) 1063.
[81] H. Adams, S. Clunas, D.E. Fenton, S.E. Spey, J. Chem. Soc., Dalton Trans. (2002) 441.
[82] H. Adams, S. Clunas, D.E. Fenton, G. Handley, P.E. McHugh, Inorg. Chem. Commun. 5 (2002) 1044.
[83] H. Adams, L.R. Cummings, D.E. Fenton, P.E. McHugh, Inorg. Chem. Commun. 6 (2003) 19.
[84] (a) D.E. Fenton, Inorg. Chem. Commun. 5 (2002) 537;
(b) D.E. Fenton, H. Okawa, Chem. Ber. Recueil. 130 (1997) 433.
[85] H. Adams, S. Clunas, L.R. Cummings, A.E. Fenton, P.E. McHugh, Inrog. Chem. Commun. 6 (2003) 837.
[86] H. Adams, S. Clunas, D.E. Fenton, T.J. Gregson, P.E. McHugh, S.E. Spey, Inorg. Chim. Acta 346 (2003) 239.
[87] P. Amudha, M. Kansaswamy, L. Govindasamy, D. Velmurugan, Inorg. Chem. 37 (1998) 4486.
[88] H. Adams, S. Clunas, D.E. Fenton, S.E. Spey, Dalton Trans. (2003) 625.
[89] D. Saravanakumar, N. Sengottuvelan, G. Priyadarchni, M. Kandaswamy, H. Okawa, Polyhedron 23 (2004) 665.
[90] (a) P. Merkel, N. Möller, M. Piacenza, S. Grimme, A. Rompel, B. Krebs, Chem. Eur. J. 11 (2005) 1201;
(b) C.P. Pradeep, P.S. Zacharias, S.K. Das, Inorg. Chem. Commun. 9 (2006) 1071.
[91] I.A. Koval, D. Pursche, A.F. Stassen, P. Gamez, B. Krebs, J. Reedijk, Eur. J. Inorg. Chem. (2003) 1669.
[92] (a) H. Adams, D.E. Fenton, S.R. Haque, S.L. Heath, M. Ohba, H. Okawa, S.E. Spey, J. Chem. Soc., Dalton Trans. (2000) 1849;
(b) H. Adams, S. Clunas, E. D:, Fenton, Inorg. Chem. Commun. 4 (2001) 667.
[93] M.C.B. de Oliveira, M. Scalpellini, A. Neves, H. Terenzi, A.J. Bortoluzzi, B. Szpoganics, A. Greatti, A.S. Mangrich, E.M. de

Souza, P.M. Fernandez, M.R. Soares, Inorg. Chem. 44 (2005) 921.
[94] I.A. Koval, M. Huisman, A.F. Stassen, P. Gamez, M. Lutz, A.L. Speck, J. Reedijk, Eur. J. Inorg. Chem. (2004) 591.
[95] (a) I.A. Koval, M. Huisman, A.F. Stassen, P. Gamez, M. Lutz, A.L. Spek, D. Pursche, B. Krebs, J. Reedijk, Inorg. Chim. Acta 357 (2004) 294;
(b) J.A. Koval, M. Sgobba, M. Huisman, M. Lüken, E. Saint-Aman, P. Gamez, B. Krebs, J. Reedijk, Inorg. Chim. Acta 359 (2006) 4071;
(c) M. Huisman, I.A. Koval, P. Gamez, J. Reedijk, Inorg. Chem. Acta 359 (2006) 1786.
[96] H. Adams, D.E. Fenton, P.E. McHugh, Inorg. Chem. Commun. 7 (2004) 147.
[97] H. Machinaga, K. Matsufuji, M. Ohba, M. Kodera, H. Okawa, Chem. Lett. (2002) 716.
[98] K. Abe, K. Matsufuji, M. Ohba, H. Okawa, Inorg. Chem. 41 (2002) 4461.
[99] H. Adams, D.E. Fenton, P.E. McHugh, T.J. Potter, Inorg. Chim. Acta 331 (2002) 117.
[100] H. Adams, D.E. Fenton, P.E. McHugh, Polyhedron 22 (2003) 75.
[101] R. Jovito, A. Neves, A.J. Bortoluzzi, M. Lanznaster, V. Drago, W. Haase, Inorg. Chem. Commun. 8 (2005) 323.
[102] S. Aime, L. Calabi, C. Cavallotti, E. Gianolio, G.B. Giovenzana, P. Losi, A. Maiocci, G. Palmisano, M. Sisti, Inorg. Chem. 43 (2004) 7588.
[103] R.A. Peralta, A. Neves, A.J. Bortoluzzi, A. Cesellato, A. dos Anjos, A. Greatti, F.R. Xavier, B. Szpoganicz, Inorg. Chem. 44 (2005) 7690.
[104] L. Li, A.A. Narducci Sarjeant, K.K. Karlin, Inorg. Chem. (2006) 7160.
[105] (a) D. Ghosh, S. Mukhopadhyay, S. Samanta, K.-Y. Choi, A. Endo, M. Chaudhury, Inorg. Chem. 42 (2003) 7189;
(b) D. Ghosh, N. Kundu, G. Maity, K.-Y. Choi, A. Caneschi, A. Endo, M. Chaudhury, Inorg. Chem. 43 (2004) 6015.
[106] S. Brooker, S.S. Iremonger, P.G. Plieger, Polyhedron 22 (2003) 665.
[107] (a) Y. Lan, D.K. Kennepohl, B. Moubaraki, K.S. Murray, J.D. Cashion, G.B. Jameson, S. Brooker, Chem. Eur. 9 (2003) 3772;
(b) J.R. Price, Y. Lan, G.B. Jameson, S. Brooker, Dalton Trans. (2006) 1491.
[108] (a) P.G. Plieger, A.J. Downard, B. Moubaraki, K.S. Murray, S. Brooker, Dalton Trans. (2004) 2157;
(b) J.C. Roder, F. Meyer, H. Pritzkov, Chem. Commun. (2001) 2176;
(c) D.J. de Geest, A. Noble, B. Moubaraki, K.S. Murray, D.S. Larsen, S. Brooker, Dalton Trans. (2007) 467.
[109] M. Prabhakar, P.S. Zacharias, S.K. Das, Inorg. Chem. 44 (2005) 2585.
[110] N.A. Rey, A. Neves, A.J. Bortoluzzi, C.T. Pich, H. Terenzi, Inorg. Chem. (2007) 348.
[111] K. Matsufuji, H. Shiraishi, Y. Miyasato, T. Shiga, M. Ohba, T. Yokoyama, H. Okawa, Bull. Chem. Soc. Jpn. 78 (2005) 851.
[112] (a) B.-H. Ye, X.-Y. Li, I.D. Williams, X.M. Chen, Inorg. Chem. 41 (2002) 6426;
(b) J. Mauzur, A.M. Gercia, A. Vegas, A. Ibañez, Polyhedron 26 (2007) 115.
[113] D. Visinescu, M. Andruh, A. Müller, M. Schmidtmann, Y. Journaux, Inorg. Chem. Commun. 5 (2002) 42.
[114] (a) S.M. Haddad, D.N. Hendrickson, J.P. Cannady, R.S. Drugo, D.S. Bieksza, J. Am. Chem. Soc. 101 (1979) 898;
(b) M. Julve, M. Verdaguer, J. Faus, F. Tinti, J. Moratal, A. Monge, E. Gutiérrez-Publa, Inorg. Chem. 26 (1987) 3520;
(c) V. Tudor, V. Kravtsov, M. Julve, F. Lloret, Y.A. Simonov, J. Lipkowski, V. Buculei, M. Andruh, Polyhedron 20 (2001) 3033.
[115] D. Visinescu, G.I. Pascu, M. Andruh, J. Magull, H.W. Roesky, Inorg. Chim Acta 340 (2002) 201.
[116] (a) G.S. Papaefstathiou, Z. Zhong, L. Geng, L.R. MacGillivray, J. Am. Chem. Soc. 126 (2004) 9158;
(b) G.S. Papaefstathiou, I.G. Georgiev, T. Friscic, L.R. MacGillivray, Chem. Commun. (2005) 3974.
[117] (a) T. Glaser, I. Liratzis, R. Fröhlich, T. Weyhermüller, Chem. Commun. (2007) 356;
(b) T. Glaser, I. Liratzis, Synlett (2004) 735.
[118] H. Demirelli, M. Tümer, A. Gölcü, Bull. Chem. Soc. Jpn. 79 (2006) 867.
[119] (a) S. Mukherjee, T. Weyhermüller, E. Bothe, K. Wieghardt, P. Chaudhuri, Eur. J. Inorg. Chem. (2003) 863;
(b) S. Mukherjee, T. Weyhermüller, E. Bothe, P. Chaudhuri, Eur. J. Chem. (2003) 1956.
[120] (a) K.K. Nanda, A.W. Addison, N. Paterson, E. Sinn, L.K. Thompson, U. Sakaguchi, Inorg. Chem. 37 (1998) 1028;
(b) D. Black, A.J. Blake, K.P. Dancey, A. Harison, M. McPartlin, S. Parsons, P.A. Tasker, G. Whittaker, M. Schröder, J. Chem. Soc. Dalton Trans. (1998) 3953;
(c) C. Krebs, M. Winter, T. Weyhermüller, E. Bill, K. Wieghardt, P. Chaudhuri, J. Chem. Soc., Chem. Commun. (1995) 1913;
(d) S. Kharna, T. Weyhermüller, E. Bill, P. Chandhuri, Inorg. Chem. 45 (2006) 5911;
(e) P. Chandhuri, Coord. Chem. Rev. 243 (2003) 143.
[121] (a) S.P. Foxon, D. Utz, J. Astner, S. Schindler, F. Thaler, F.W. Heinemann, G. Liehr, J. Mukherjee, V. Balamurugan, D. Ghosh, R. Mukherjee, Dalton Trans (2004) 2321;
(b) H. Adams, D.E. Fenton, P.E. McHugh, Inorg. Chem. Commun. 7 (2004) 140.
[122] S. Schindler, H. Elias, H. Paulus, Z. Naturforshung. B 45 (1990) 607.
[123] K.D. Karlin, A. Farooq, Y. Gulneth, J.C. Hayes, J. Zubieta, Inorg. Chim. Acta 153 (1988) 73.
[124] T. Shiga, K. Maruyama, L. Han, H. Oshio, Chem. Lett. 34 (2005) 1648.
[125] C. Higuchi, H. Sakiyama, H. Okawa, D.E. Fenton, J. Chem. Soc., Dalton Trans. (1995) 4015.
[126] C.K. Williams, N.R. Brooks, M.A. Hillmyer, W.B. Tolman, Chem. Commun. (2002) 2132.
[127] (a) N.V. Kaminskaia, B. Spingler, S.J. Lippard, J. Am. Chem. Soc. 122 (2000) 6411;
(b) N.V. Kaminskaia, B. Spingler, S.J. Lippard, J. Am. Chem. Soc. 123 (2001) 6555.
[128] K.S. Bharatli, A.K. Rahiman, V. Rajesh, S. Seedaran, P.G. Aravidan, D. Velmurugan, V. Narayanan, Polyhedron 25 (2006) 2859.
[129] (a) G. Siedle, B. Kersting, Dalton Trans. (2006) 2114;
(b) G. Siedle, P.-G. Lassahn, V. Lozan, C. Janiak, B. Kersting, Dalton Trans. (2007) 52.
[130] (a) S.-F. Huang, Y.-C. Chou, P. Misra, C.-J. Lee, S. Mohanta, H-.H. Wei, Inorg. Chim. Acta 357 (2004) 1627;
(b) Y.-C. Chou, S.-F. Huang, R. Koner, G.-H. Lee, Y. Wang, S. Mohanta, H-.H. Wei, Inorg. Chem. 43 (2004) 2759.
[131] A. Mukherjee, M.K. Saha, M. Nethaji, A.R. Chakravarty, Chem. Commun. (2004) 716.
[132] S. Gupta, A. Mukherjee, M. Nethaji, A.R. Chakravarty, Polyhedron 24 (2005) 1922.
[133] A. Mukherjee, M.K. Saba, I. Rudra, S. Ramasesha, M. Nethaji, A.R. Chakravarty, Inorg. Chim. Acta 357 (2004) 1077.
[134] Y. Song, C. Massera, O. Roubean, P. Gamez, A.M. Manotti Lanfredi, J. Reedijk, Inorg. Chem. 43 (2004) 6842.
[135] A. Mukherjee, I. Rudra, S.G. Naik, S. Ramasesha, M. Nethaji, A.R. Chakravarty, Inorg. Chem. 42 (2003) 5660.
[136] (a) S. Gupta, A. Mukherjee, M. Nethaji, A.R. Chakravarty, Polyhedron 23 (2004) 643;
(b) S.G. Naik, A. Mukherjee, R. Raghunathan, M. Nethaji, S. Ramasesha, A.R. Chakravarty, Polyhedron 25 (2006) 2135.
[137] R. Bagai, K.A. Abboud, G. Christou, Dalton Trans. (2006) 3306.
[138] (a) C.-H. Weng, S.-C. Cheng, H.-M. Wei, H.-H. Wei, C.-J. Lee, Inorg. Chim. Acta 359 (2006) 2029;
(b) M. Tsuchimoto, T. Ishii, T. Imaoka, K. Yamamoto, N. Yoshioka, Y. Sunatsuki, Bull. Chem. Soc. Jpn. 79 (2006) 1393;
(c) M. Tsuchimoto, T. Ishii, T. Imaoka, K. Yamamoto, Bull. Chem. Soc. Jpn. 77 (2004) 1849.
[139] (a) S.-F. Huang, Y.-C. Chou, P. Misra, C.-J. Lee, S. Mohanta, H.-H. Wie, Inorg. Chim. Acta 357 (2004) 1627;
(b) Y.-C. Chu, S.-F. Huang, R. Koner, G.-H. Lee, Y. Wang, S. Mohamda, H.-H. Wie, Inorg. Chem. 43 (2004) 2759.
[140] (a) C.J. Lee, S.C. Cheng, H.H. Lin, H.H. Wie, Inorg. Chem. Commun. 8 (2005) 235;
(b) D. Moreno, C. Palopoli, V. Daier, S. Shova, L. Vendier, M. Gouzoles-Sierra, Dalton Trans. (2006) 5156.

[141] S. Pal, A.K. Barik, S. Gupta, A. Hazra, S.K. Kar, S.-M. Peng, G.-H. Lee, R.J. Butcher, M.S. El Fallah, J. Ribas, Inorg. Chem. 44 (2005) 3880.
[142] Y. Song, P. Gamez, O. Roubeau, M. Lutz, A.L. Spek, J. Reedijk, Eur. J. Inorg. Chem. (2003) 2924.
[143] U.F. Song, G.A. Van Albada, M. Quesada, I. Mutikainen, U. Turpeinen, J. Reedijk, Inorg. Chem. Commun. 8 (2005) 975.
[144] Y. Xie, X. Liu, Q. Liu, H. Jiang, J. Ni, K. Wei, Inorg. Chim. Acta 357 (2004) 4297.
[145] Y.S. Xie, X.T. Liu, M. Zhang, K.-J. Wei, Q.-L. Liu, Polyhedron 24 (2005) 165.
[146] T. Gajda, A. Jancsó, S. Mikkola, H. Lönnberg, H. Sirges, J. Chem. Soc. Dalton Trans. (2002) 1757.
[147] S. Striegler, M. Dittel, Inorg. Chem. 44 (2005) 2728.
[148] J.-P. Costes, F. Dahan, F. Nicodème, Inorg. Chem. 40 (2001) 5285.
[149] J. Tang, I. Hewitt, M.T. Madhu, G. Chastanet, W. Wernsdorfer, C.E. Ansor, C. Benelli, R. Sessoli, A.K. Powell, Angew. Chem. Int. Ed. 45 (2006) 1729.
[150] (a) X. Yang, R.A. Jones, M.J. Wiester, Dalton Trans. (2004) 1878;
(b) X. Yang, B.P. Hahn, A. Jones, K.J. Stevenson, J.S. Swinnea, Q. Wu, Chem. Commun. (2006) 3827.
[151] (a) T. Glaser, J. Liratzis, R. Fröhlich, Dalton Trans. (2005) 2892;
(b) T. Glaser, J. Liratzis, O. Kataeva, R. Fröhlich, M. Paicenza, S. Grimme, Chem. Commun. (2006) 1024.
[152] T. Glaser, H. Theil, I. Liratzis, T. Weyhermüller, E. Bill, Inorg. Chem. 45 (2006) 4889.
[153] X. Yang, R.A. Jones, R.J. Lai, A. Waheed, M.M. Oye, A.L. Holmes, Polyhedron 25 (2006) 881.
[154] W.-K. Lo, W.-K. Wong, W.-Y. Wong, J. Guo, Eur J. Inorg. Chem. (2005) 2950.
[155] X. Yang, R.A. Jones, V. Lynch, M.M. Oye, A.L. Holmes, Dalton Trans. (2005) 849.
[156] J.-P. Costes, J.-P. Laussac, F. Nicodeme, J. Chem. Soc. Dalton Trans. (2002) 2731.
[157] X. Yang, R.A. Jones, J. Am. Chem. Soc. 127 (2005) 7686.
[158] L. Salmon, P. Thuéry, M. Ephritikhine, Polyhedron 23 (2004) 623.
[159] J.H. Thurston, G.-Z. Tang, D.W. Trahan, K.H. Whitmire, Inorg. Chem. 43 (2004) 2708.
[160] (a) A. Elmail, Y. Elerman, Z. Naturforsch. 58b (2003) 639;
(b) A. Elmail, Y. Elerman, Z. Naturforsch. 59b (2004) 530;
(c) A. Elmail, Y. Elerman, Z. Naturforsch. 58b (2004) 535;
(d) A. Elmail, Y. Elerman, J. Mol. Struct. 737 (2005) 29.
[161] R. Gheorghe, P. Cucos, M. Andruh, J.-P. Costes, B. Donnadieu, S. Shova, Chem. Eur J. 11 (2005) 1.
[162] W.-K. Lo, W.-K. Wong, J. Guo, W.-Y. Wong, K.-F. Li, K.-W. Cheah, Inorg. Chim. Acta 357 (2004) 4510.
[163] (a) W.-K. Wong, X. Yang, R.A. Jones, J.H. Rivers, V. Lynch, W.-K. Lo, D. Xiao, M.M. Oye, A.L. Holmes, Inorg. Chem. 45 (2006) 4340;
(b) W.-K. Lo, W.-K. Wong, W.-Y. Wong, J. Guo, K.-T. Yeung, Y.-K. Cheng, X. Yang, R.A. Jones, Inorg. Chem. 45 (2006) 9315.
[164] X.P. Yang, R.A. Jones, W.-K. Wong, V. Lynch, M.M. Oye, A.L. Homes, Chem. Commun. (2006) 1836.
[165] J.-P. Costes, J.M. Clemente-Juan, F. Dahan, F. Dumestre, J.-P. Tuchagues, Inorg. Chem. 41 (2002) 2886.
[166] S. Mohanta, H.-H. Lin, C.-J. Lee, H.-H. Wie, Inorg. Chem. Commun. 5 (2002) 585.
[167] J.-P. Costes, G. Novitchi, S. Shova, F. Dahan, B. Donnadieu, J.-P. Tuchagues, Inorg. Chem. 43 (2004) 7792.
[168] G. Novitchi, S. Shova, A. Caneschi, J.-P. Costes, M. Gdaniec, N. Stanica, Dalton Trans. (2004) 1194.
[169] R. Koner, G.-H. Lee, Y. Wang, H.-H. Wie, S. Mohanta, Eur. J. Inorg. Chem. (2005) 1500.
[170] R. Gheorghe, P. Cucos, M. Andruh, J.-P. Costes, B. Donnadieu, S. Shova, Chem. Eur. J. 12 (2005) 187.
[171] R. Gheorghe, M. Andruh, A. Muller, M. Schmidtmann, Inorg. Chem. 41 (2002) 5314.
[172] (a) J.-P. Costes, F. Dahan, A. Dupuis, J.-P. Laurent, Inorg. Chem. 36 (1997) 3429;
(b) J.-P. Costes, F. Dahan, J.-P. Laurent, Inorg. Chem. 33 (1994) 2738;
(c) J.-P. Costes, R. Gheorghe, M. Andruh, S. Shova, J.-M.C. Juan, New J. Chem. 30 (2006) 572.
[173] M. Nayak, R. Koner, H.-H. Lin, U. Flörke, M.-H. Wie, S. Mohanta, Inorg. Chem. (2006) 10764.
[174] J.-P. Costes, F. Dahan, G. Novitchi, V. Arion, S. Shova, J. Lipkowski, Eur. J. Inorg. Chem. (2004) 1530.
[175] T. Le Borgne, E. Rivière, J. Marrot, P. Thuéry, J.-J. Girerd, M. Ephritikhine, Chem. Eur. J. (2002) 773.
[176] L. Salmon, P. Thuéry, E. Rivière, J.-J. Gired, M. Ephritikhine, Dalton Trans. (2003) 2872.
[177] (a) L. Salmon, P. Thuéry, M. Ephritikhine, Polyhedron 26 (2007) 645;
(b) L. Salmon, P. Thuéry, M. Ephritikhine, Polyhedron 26 (2007) 631.
[178] (a) L. Salmon, P. Thuéry, M. Ephritikhine, Polyhedron 25 (2006) 1537;
(b) L. Salmon, P. Thuéry, M. Ephritikhine, Dalton Trans. (2004) 1635.
[179] L. Salomon, P. Thuéry, M. Ephritikhine, Acta Cryst. C 59 (2003) m246.
[180] (a) L. Salmon, P. Thuéry, M. Ephritikhine, Dalton Trans. (2004) 4139;
(b) L. Salmon, P. Thuéry, E. Rivière, M. Ephritikhine, Inorg. Chem. 45 (2006) 83.
[181] (a) W. Dou, J.-N. Yao, W.-S. Liu, Y.-W. Wang, J.-R. Zheng, D.-Q. Wang, Inorg. Chem. Commun. 10 (2007) 105;
(b) P. Di Bernardo, F. Benetollo, S. Tamburini, P.A. Vigato, P. Zanonato, Inorg. Chem. Commun., in press.
[182] (a) M.T. Reetz, in: J.L. Atwood, J.E. Davies, D.D. McNicol, F. Vogtle (Eds.), Comprenhensive Supramolecular Chemistry, vol. 2, Pergamon, Oxford, 1996, p. 553;
(b) M.M.G. Antonisse, D.N. Reinhoudt, Chem. Commun. (1998) 443;
(c) P.D. Beer, J.B. Cooper, in: L. Mandolini, R. Ungaro (Eds.), Calixarenes in Action, Imperial College Press, London, 2000, p. 111;
(d) P.D. Beer, P.A. Gale, Angew. Chem. Int. Ed. 40 (2001) 486;
(e) G.J. Kirkovits, J.A. Shriver, P.A. Gale, J.L. Sessler, J. Incl. Phenom. Macrocyclic Chem. 41 (2001) 69;
(f) J.M. Mahoney, A. M: Beatty, B.D. Smoth, J. Am. Chem. Soc. 123 (2001) 5847;
(g) J.M. Mahoney, R.A. Marshall, A.M. Beatty, B.D. Smith, S. Camiolo, P.A. Gale, J. Supramol. Chem. 1 (2001) 289;
(h) J.M. Mahoney, G.U. Nawaratna, A.M. Beatty, P.J. Duggan, B.D. Smith, Inorg. Chem. 43 (2004) 5902.
[183] (a) M. Cametti, M. Nissinen, A. Dalla Cort, L. Mandolini, K. Rissanen, Chem. Commun. (2003) 2420;
(b) M. Cametti, M. Nissinen, A. Dalla Cort, L. Mandolini, K. Rissanen, J. Am. Chem. Soc. 127 (2005) 3831;
(c) M. Cametti, M. Nissinen, A. Dalla Corte, K. Rissanen, L. Mandolini, Inorg. Chem. 45 (2006) 6099.
[184] G. Novitchi, J.-P. Costes, J.-P. Tuchagues, Dalton Trans. (2004) 1735.
[185] (a) M. Albrecht, S. Mirtschim, M. de Groot, I. Janser, J. Runsink, G. Raabe, M. Kogej, C.A. Schalley, R. Fröhlich, J. Am. Chem. Soc. 127 (2005) 10371;
(b) M. Albrecht, S. Kamptmann, R. Fröhlich, Polyhedron 22 (2003) 643.
[186] M. Albrecht, I. Janser, S. Kamptmann, P. Weis, B. Wibbeling, R. Fröhlich, Dalton Trans. (2004) 37.
[187] M. Albrecht, I. Janser, H. Houjou, R. Fröhlich, Chem. Eur. J. 10 (2004) 2839.
[188] (a) M. Albrecht, I. Janser, A. Lützen, M. Hapke, R. Fröhlich, P. Weis, Chem. Eur. J. 11 (2005) 5742;
(b) I. Janser, M. Albrecht, K. Hunger, S. Burk, K. Rissanen, Eur. J. Inorg. Chem. (2006) 244.
[189] P. Cucos, M. Pascu, R. Sessoli, M. Avarvari, F. Pontillart, Inorg. Chem. 45 (2006) 7035.
[190] (a) S. Akine, T. Taniguchi, T. Nabeshima, Chem. Lett. 30 (2001) 682;
(b) S. Akine, T. Taniguchi, T. Nabeshima, Inorg. Chem. 43 (2004) 6142;
(c) S. Akine, T. Taniguchi, T. Nabeshima, Chem. Lett. 35 (2006) 604.
[191] (a) S. Akine, T. Taniguchi, T. Nabeshima, Angew. Chem. Int. Ed. 41 (2002) 4670;
(b) S. Akine, T. Matsumoto, T. Taniguchi, T. Nabeshima, Inorg. Chem. 44 (2005) 3270.

[192] S. Akine, T. Taniguchi, T. Saiki, T. Nabeshima, J. Am. Chem. Soc. 127 (2005) 540.
[193] S. Akine, W. Dong, T. Nabeshima, Inorg. Chem. 45 (2006) 4677.
[194] I. Sylvestre, J. Wolowska, C.A. Kilner, E.J.L. McInnes, A. Malcolm, Halcrow, Dalton Trans. 19 (2005) 3241.
[195] S.G. Galbraith, P.G. Plieger, P.A. Tasker, Chem. Commun. (2002) 2662.
[196] (a) R.A. Coxall, L.F. Lindoy, H.A. Miller, A. Parkin, S. Parsons, P.A. Tasker, D.J. White, Dalton Trans. (2003) 55;
(b) M. Prabhakar, P.S. Zacharias, S.K. Das, Inorg. Chim. Commun. 9 (2006) 899.
[197] P.G. Plieger, S. Parsons, A. Parkin, P.A. Tasker, J. Chem. Soc., Dalton Trans. (2002) 3928.
[198] K.R. Krishnapriya, M. Kandaswamy, Polyhedron (2005) 113.
[199] F. Lam, J.-X. Xu, K.S. Chan, J. Org. Chem. 61 (1996) 8414.
[200] F. Lam, R.-J. Wang, T.C.W. Mak, K.S. Chan, J. Chem. Soc., Chem. Commun. (1994) 2439.
[201] E.F. DiMauro, A. Mamai, M.C. Kozlowski, Orgnaometallic 22 (2003) 850.
[202] A.N. Rahnama, H. Golchoubian, R. Pritchard, Bull. Chem. Soc. Jpn. 78 (2005) 1047.
[203] U. Casellato, S. Tamburini, P. Tomasin, P.A. Vigato, Inorg. Chim. Acta 357 (2004) 4191.
[204] T. Nakabayashi, T. Ishida, T. Nogami, Inorg. Chem. Commun. 7 (2004) 1221.
[205] M. Isola, V. Liuzzo, F. Marchetti, A. Raffaelli, Eur. J. Inorg. Chem. (2002) 1588.
[206] R.-J. Tao, C.-Z. Mei, S.-Q. Zang, Q.-L. Wang, J.-Y. Niu, D.-Z. Liao, Inorg. Chim. Acta 357 (2004) 1985.
[207] R.-J. Tao, F.-A. Li, Y.-X. Cheng, S.-Q. Zang, Q.-L. Wang, J.-Y. Niu, D.-Z. Liao, Inorg. Chim. Acta 359 (2006) 2053.
[208] T. Kido, Y. Ikuta, Y. Sunatsuki, Y. Ogawa, N. Matsumoto, N. Re, Inorg. Chem,. 42 (2003) 398.
[209] S. Osa, Y. Sunatsuki, Y. Yamamoto, M. Nakamura, T. Shimamoto, N. Matsumoto, N. Re, Inorg. Chem. 42 (2003) 5507.
[210] J.-P. Costes, M. Auchel, F. Dahan, V. Peyrou, S. Shova, W. Wernsdorfer, Inorg. Chem. 45 (2006) 1924.
[211] E.C. Alyea, A. Malek, A.E. Vongioukas, Can. J. Chem. 60 (1982) 667.
[212] J.-P. Costes, F. Nicodème, Chem. Eur. J. 8 (2005) 3442.
[213] J.-P. Costes, F. Dahan, A. Dupuis, S. Lagrave, J.-P. Laurent, Inorg. Chem. 37 (1998) 153.
[214] (a) M. Albrecht, I. Janser, S. Meyer, P. Weis, R. Fröhlich, Chem. Commun. (2003) 2854;
(b) M. Albrecht, I. Janser, R. Fröhlich, Chem. Commun. (2005) 157;
(c) M. Albrecht, I. Janser, S. Burk, P. Weis, Dalton Trans. (2006) 2875.
[215] B. Conerney, P. Jensen, P.E. Kruger, C. MacGloinn, Chem. Commun. (2003) 1274.
[216] N. Akkus, J.C. Campbell, J. Davidson, D.K. Henderson, H.A. Miller, A. Parkin, S. Parsons, P.G. Plieger, R.M. Swart, P.A. Tasker, L.C. West, Dalton Trans. 20039 (1932).
[217] W.-K. Wong, H. Liang, J. Guo, W.-Y. Wong, W.-K. Lo, K.-F. Li, K.W. Cheah, Z. Zhou, W.-T. Wong, Eur. J. Inorg. Chem. (2004) 829.
[218] T. Glaser, M. Heidemeier, T. Lügger, Dalton Trans. (2003) 2381.
[219] T. Glaser, M. Heidemeier, S. Grimme, E. Bill, Inorg. Chem. 43 (2004) 5192.
[220] T. Glaser, M. Heidemeier, R. Fröhlich, P. Hildebrandt, E. Bothe, E. Bill, Inorg. Chem. 44 (2005) 5467.
[221] H. Wackerbarth, F.B. Larsen, A.G. Hansen, C.J. McKenzie, J. Ulstrup, Dalton Trans. (2006) 3438.
[222] (a) J.K. Clegg, K. Gloe, M.J. Hayter, O. Kataeva, L.F. Lindoy, B. Moubaraki, J.C. McMurtrie, K. S: Murray, D. Schilter, Dalton Trans. (2006) 3977;
(b) J.K. Clegg, L.F. Lindoy, J.C. McMurtrie, D. Schilter, Dalton Trans. (2005) 857;
(c) J.K. Clegg, L.F. Lindoy, B. Moubaraki, K.S. Murray, J.C. McMurtrie, Dalton Trans. (2004) 2417;
(d) J.K. Clegg, L.F. Lindoy, J.C. McMurtrie, D. Schilter, Dalton Trans. (2006) 3114.
[223] (a) G. Aromí, C. Boldron, P. Gamez, O. Roubeau, H. Kooijman, A.L. Spek, H. Stoecki-Evans, J. Ribas, J. Reedijk, Dalton Trans. (2004) 3586;
(b) G. Aromí, P. Gamez, C. Boldron, H. Kooijman, A.L. Spek, J. Reedijk, Eur. J. Inorg. Chem. (2006) 1940;
(c) G. Aromí, J. Ribas, P. Gamez, O. Roubeau, H. Kooijman, A.L. Spek, S. Teat, E. MacLean, H. Stoeckli-Evans, J. Reedijk, Chem. Eur. J. 10 (2004) 6476.
[224] (a) A. Cottone III, D. Morales, J.L. Lecuivre, M.J. Scott, Organometallics 21 (2002) 418;
(b) E.R. Libra, M.J. Scott, Chem. Commun. (2006) 1485.